SCHOOL OF CHEMISTRY

CARDIFF UNIVERSITY

Novel polymers of intrinsic microporosity

Thesis submitted for the degree of Doctor of Philosophy by:

Mohammed Hashem

Supervisor: Neil B. McKeown   **2011**

UMI Number: U567051

UMI®

Dissertation Publishing

ProQuest®

DECLARATION

This work has not previously been accepted in substance for any degree and is not concurrently submitted in candidature for any degree.

Signed .... (candidate)   Date .....06.05..201\

STATEMENT 1

This thesis is being submitted in partial fulfillment of the requirements for the degree of Doctor of Philosophy.

Signed .... (candidate)   Date ...06.05..2011

STATEMENT 2

This thesis is the result of my own independent work/investigation, except where otherwise stated. Other sources are acknowledged by explicit references.

Signed ......06..05..2011.......... (candidate)   Date ....

STATEMENT 3

I hereby give consent for my thesis, if accepted, to be available for photocopying and for inter-library loan, and for the title and summary to be made available to outside organisations.

Signed .... (candidate)   Date 06.05.2011

Acknowledgement

Abstract

The research in this thesis is concerned with the synthesis of novel microporous polymeric materials starting from different functionalised monomers. After an introduction to organic microporous materials, the description of the research begins by focusing on the synthesis of network and ladder polymers derived from triptycene compounds with different groups on the bridgehead carbons and aromatic units. In particular, the effect of such substitution on the porosity of the resulting polymers is assessed.

The range of polymeric porous materials is extended by the use of the biphenyl unit as a building block. Also, a series of microporous polymers were synthesised based on the hexaazatrinapthylene unit (HATN). A modified HATN monomer was used to prepare co-polymer membranes and study the effects of such additive on gas permeability and selectivity.

Some macrocyclic compounds, such as phthalocyanine, with unique geometry are used to prepare novel polymer of intrinsic microporosity taking advantage of the rigid non-planar structure of these compounds.

The work concludes by applying Yamamoto coupling polymerisation to some brominated rigid monomers to synthesise novel microporous polymers that consists merely of hydrogen and carbon. The prepared polymers is characterised by their elemental analysis, thermogravimetric analysis and nitrogen sorption analysis.

Abbreviations

Å	Angstrom
aq	Aqueous
b	Broad
bpy	2,2'-bipyridyl
calc.	Calculated
CI	Chemical ionisation
DCM	Dichloromethane
DMAc	N,N-Dimethylacetamide
DMF	N,N–Dimethylformamide
DMSO	Dimethyl sulphoxide
EI	Electron Impact
ES	Electrospray
Et	Ethyl
g	Grams
GPC	Gel Permeation Chromatography
HATN(F)$_6$	2,3,8,9,14,15-hexafluoro-5,6,11,12,17,18-hexaazatrinapthylene
HATN	5,6,11,12,17,18- hexaazatrinapthylene
h	Hour/s
HRMS	High Resolution Mass Spectrometry
Hz	Hertz
IUPAC	International Union of Pure and Applied Chemistry
J	Coupling constant (in Hz)
LRMS	Low Resolution Mass Spectrometry
m	Multiplet
MALDI	Matrix-assisted laser desorption/ionisation
Me	Methyl
MeOH	Methanol
mL	Millilitre(s)
mmol	Millimole(s)
Mn	Unit number average
Mw	Molecular weight
Mp	Melting point
nm	Nanometers
NMR	Nuclear Magnetic Resonance
p/p°	Partial (relative) pressure
Pc	Phthalocyanine
Ph	Phenyl
PIM	Polymers of Intrinsic Microporosity
q	quartet
RT	room temperature

R	undefined group
s	singlet
S_NAr	Nucleophilic aromatic substitution
STP	Standard Temperature and Pressure
t	triplet
t-Bu	tert Butyl
Triptycene	9,10-Dihydro-9,10-o-benzenoanthracene
TGA	Thermogravimetric Analysis
THF	Tetrahydrofuran
TLC	Thin Layer Chromatography
TOF	Time of flight
UV	Ultraviolet
vis	Visible
Wt.%	Weight percent
XRD	X-ray diffraction

Table of Contents

INTRODUCTION

Chapter 1. Introduction

Porous materials are continuously connected structures with porosity in at least one dimension, according to International Union of Pure and Applied Chemistry (IUPAC), the definition of porosity is 'having cavities, channels, or interstices, which are deeper than they are wide'.[1] IUPAC classifies porous solids according to the width of pores and channels in the material: microporous (<2 nm), mesoporous (2-50 nm), and macroporous (>50 nm). Generally, the synthesis process and the interaction between the building blocks of a material determine the porosity of a particular type the material. In addition to conventional porous materials such as activated carbon and zeolites, extensive research has been performed recently with polymeric materials exhibiting different levels of porosity; the attractiveness of porous polymers is due to their unique properties such as high surface area that leads to other phenomena arising from the spatial dimensions of the material known as adsorption.

Adsorption is of great technological importance, some adsorbents are used on a large scale as desiccants, catalysts or catalyst supports; others are used for the separation of gases, liquids purification and pollution control or for respiratory protection[2]. In addition, adsorption phenomena play a vital role in many solid state reactions and biological mechanisms.[3]

1.1 Adsorption phenomena and isotherms

When a gas (adsorbate) is confined in a closed space in the presence of a porous solid (adsorbent), the solid begins to adsorb the gas onto its surface and into its pores, the gas molecules are transferred and accumulated on and in the solid material as a result of the forces between the solid surface and the adsorbate. Two kinds of forces give rise to adsorption: physical and chemical, these types of adsorption are termed (physisorption) and (chemisorptions) respectively. Physical adsorption includes weak *Van der Waals* interactions with no bond formation or breaking and often reversible, while in chemisorptions, the adsorbate molecules can be attached to the adsorbent surface through the formation of chemical bonds (often covalent).

The amount adsorbed on a solid surface will depend upon the temperature, pressure and the interaction potential between the vapor and the surface. Therefore, at the same equilibrium pressure and temperature, a plot of adsorbed gas volume per unit weight of adsorbent versus pressure is referred to as the sorption isotherm of a particular vapor-solid interface.

Solid/gas systems have been shown to exhibit characteristic adsorption isotherms with the first systematic attempt to classify adsorption isotherms for solid-gas equilibria being proposed in 1940 by Braunauer, Deming, Deming and Teller (BDDT)[4], in which they interpreted five types of isotherms, the same classification reported again in 1982 by IUPAC[5] with an additional isotherm identified by Sing.
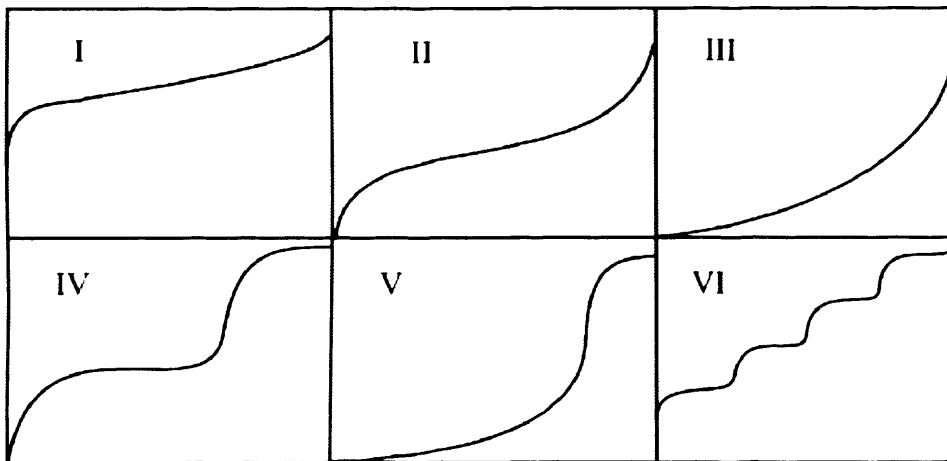
Figure 1.1. Schematic representations of different types of adsorption isotherm.

Type I adsorption isotherm is related to adsorption limited to one molecular layer and indicates that the pores are microporous where pore filling occurs significantly at relatively low partial pressure and characterised by a plateau which may cut the p/p° axis sharply or show a tail as saturation pressure is approached. Most adsorption occurs at low pressure due to high adsorption in pores resulting from a strong interaction between pore walls and adsorbate with the adsorption process being essentially complete at 0.5 p/p°. The incidence of hysteresis varies: many of (Type I) isotherms usually have no hysteresis loops at all, while others display a definite loop. Type I isotherm is most commonly observed with microporous solid materials, in which the micropores in the solid are no more than a few molecular diameters in

width, therefore the potential fields from neighbouring walls will overlap and the interaction energy of the solid with the gas molecule will be correspondingly enhanced resulting in increased adsorption. Type I isotherm is the only kind that is reported in the results section of this thesis, although the amount of hysteresis associated with adsorption at higher pressure varies and it origin is discussed. Types II-VI isotherms are found for mesoporous, macroporous and non-porous solids.

1.2 Porosity assessments

A key element of the assessment of porous media is surface area determination but the accurate measurement of the surface area of porous solids presented a significant problem in early studies of adsorption. If the physical adsorption capacity were limited to a close packed monolayer, the determination of the saturation limit from an experimental isotherm with a known size molecule would be straightforward leading to the specific surface area. However, this is not so as physisorption generally involves multilayer adsorption. In multilayer adsorption, molecular layering commences at pressures well below that required for completion of the monolayer which leads to uncertainties as to how to extract the monolayer capacity from the experimental isotherm.

Two methods are widely used to calculate the experimental data and estimate the surface area: Langmuir and Brunauer, Emmett and Teller (BET), which are both routinely used to calculate the specific surface area of microporous materials from nitrogen adsorption measurements

1.2.1 Langmuir Theory of Adsorption.

Langmuir[6] describes the simplest isotherm (Type I) based on monolayer coverage using a derived equation based on the following assumptions:

(1) Adsorption is a dynamic process.

(2) Adsorption of gas molecules on a surface cannot exceed monolayer coverage.

(3) All sites are equivalent and the surface is uniform.

(4) The ability of a molecule to adsorb at a given site is independent of the surrounding sites, assuming no interactions between adsorbed molecules.

Since adsorption is considered dynamic, the rate of adsorption equals the rate of desorption at equilibrium:

$$A\,(g) + M\,(surface) \rightleftharpoons AM\,(surface)$$
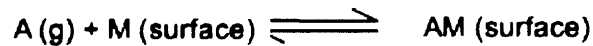
Based on these assumptions, Langmuir used a direct kinetic derivation to describe the adsorption in terms of an equation:

$$\frac{P}{V} = \frac{1}{V_m\,b} + \frac{P}{V_m}$$

where P= pressure of gas; V= equilibrium amount of gas adsorbed per unit mass of adsorbent at relative pressure p/p° (mmol g^{-1}); V_m = amount of gas required for monolayer coverage of adsorbent (mmol g^{-1}); b= adsorption coefficient, dependent on temperature but independent of surface coverage and describing in some way the energetic of the surface; The plot of $\frac{P}{V}$ against P will yield a straight line with a slope of 1/V_m, the specific surface area S can be calculated using the following equation: $S_{Langmuir} = V_m\,A_m\,N_A$

The Langmuir theory of adsorption is useful to describe (Type I) adsorption isotherms but has limitations based on the original assumption, one of which is that it only applies to monolayer formation and does not take into account adsorption past this level.

1.2.2. The Brunauer, Emmett and Teller (BET) Theory

The BET[7] model extends the monolayer Langmuir model to multilayer adsorption, although derived over seventy years ago, the BET theory continues to be almost universally used because of its simplicity, and its ability to accommodate each of the five isotherm types. It assumes that the surface is homogeneous and that the different layers of molecules do not interact. Each adsorbed molecule in the

monolayer is assumed to be adsorption site for second layer of molecules, and so on as the relative pressure increases, until bulk condensation occurs.

In the region of relative pressures near the completion of monolayer, the BET theory and experimental isotherms do agree very well leading to a powerful and extremely useful method for the estimation of surface areas of various porous materials. The BET model in the final form is given as:

$$\frac{P}{V[P^o - P]} = \frac{1}{V_m\,C} + \frac{C-1}{V_m\,C}\frac{P}{P^o}$$

Where; V and V_m are molar volume adsorbed at the relative equilibrium pressure (p/p^o) and the monolayer capacity respectively, C is a constant, which is related exponentially to the heat of adsorption at the first and subsequent layers.

The determination of surface areas from the BET theory is a straightforward application of the equation: a plot of $P/V(P^o-P)$ versus P/P^o, will yield a straight line usually in the range of $0.05 < P/P^o < 0.35$. The slope (S) and the intercept of (I) of a BET plot will give: $S = \frac{[C-1]}{V_m\,C}$ and $I = \frac{1}{V_m\,C}$
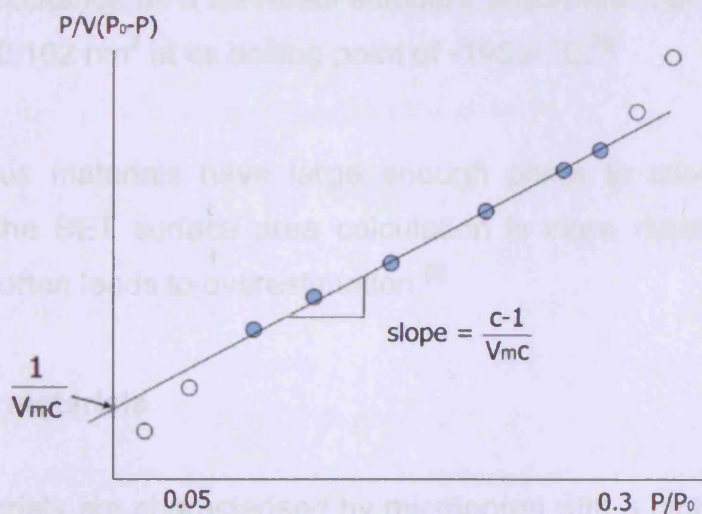
Figure 1.2. Typical BET model plot.

Solving the preceding equation for V_m and C gives: $V_m = \dfrac{1}{V_m \, C} + I$ and $C = S + \dfrac{1}{I}$

The BET equation usually gives a good representation within the range of relative pressures 0.05-0.3, and this range is generally used in practice for surface area measurement. At higher relative pressures, the BET equation is usually inaccurate because of capillary condensation effect. The total specific surface area is calculated from the equation:

$$S_{BET} = \frac{V_m \, N_A \, A_m}{V_{mol}}$$

In which; V_m is the volume of monolayer, N_A is Avagadro's constant and V_{mol} is the molar volume of the gas; A_m is the cross-sectional area occupied by one molecule of adsorbate gas.

For surface area determinations, nitrogen as being the ideal adsorbate, exhibits the unusual property that on almost all surfaces, its C value is sufficiently small to prevent localized adsorption and yet adequately large to prevent the adsorbed layer from behaving as a two dimensional gas. Thus, the unique properties of nitrogen have led to its acceptance as a universal standard adsorbate with an assigned cross sectional area of 0.162 nm² at its boiling point of -195.6 °C.[8]

Since most porous materials have large enough pores to allow more than one adsorbed layer, the BET surface area calculation is more reliable than Langmuir surface area that often leads to overestimation.[9]

1.3 Microporous materials

Microporous materials are characterised by micropores with a high surface area and a specific pore structure that defines the accessibility to the pore cavities via pore diameters of less than 2 nm. They can be classified by the nature of their structure: crystalline (e.g. zeolites or Metal-Organic-Frameworks) where the dimensions of the

micropores are determined by the crystal framework, therefore, there is very little or no distribution of pore size and amorphous such as activated carbons and hypercrosslinked polymers where the structure does not have long-range order and they are considered amorphous or disordered and therefore can possess a broad pore size distribution.

1.3.1 Zeolites

Zeolites comprise a large family of microporous crystalline aluminosilicates or silicates, the structure of zeolites are usually based on tetrahedral SiO_4 and AlO_4 units linked together by oxygen to form an ordered crystalline framework with well-defined surface chemistry and relatively high surface areas between 300-600 $m^2 g^{-1}$, The general formula of zeolite is $M^{n+}[Si_x Al_y O_z].mH_2O$ where M^{n+} are extra-framework cations and mH_2O are sorbed water molecules.[10]

Also due to their ordered crystalline lattice and well-defined pore structure, the micropores of these materials can adsorb selectively depending upon the molecular size and shape of the potential adsorbents, which makes them highly useful in a number of industrial applications e.g. as ion exchangers for water softening, as drying agents or absorbents for organic vapours, as molecular sieves and separation membranes or as catalysts for the production of petrochemicals, fluid cracking catalysts and sorbents in volatile organic removal.[11]

1.3.2 Metal-organic and covalent-organic frameworks

Metal organic frameworks (MOFs) are crystalline inorganic-organic hybrid materials comprising metals, or metal clusters, which are interconnected by organic linkers.[12] The organic ligands can act as nodes to direct framework topology and ligand geometries are typically linear, trigonal, or tetrahedral rigid polydentate. Common organic linkers to prepare porous (MOFs) are based on carboxylate or pyridyl donors are used to coordinate metal ions or higher-nuclearity metal clusters, often referred to as 'secondary building units'.[13]

The most important property of (MOFs) is their high porosity (fraction of void volume to total volume) and high specific surface area, which has led to many potential

applications concerned with applications in gas storage,[14] molecular separation,[15] heterogeneous catalysis[16] and drug delivery.[17]

Recently, an ultra-porous metal framework named MOF-210 was prepared with the highest BET surface area of 6240 $m^2 g^{-1}$ (Langmuir surface area = 10400 $m^2 g^{-1}$), yet reported,[18] by joining the octahedral $Zn_4O(CO_2)_6$ with 4,4',4"-[benzene-1,3,5-triyl-tris(ethyne-2,1-diyl)]tribenzoate and biphenyl-4,4'-dicarboxylate.
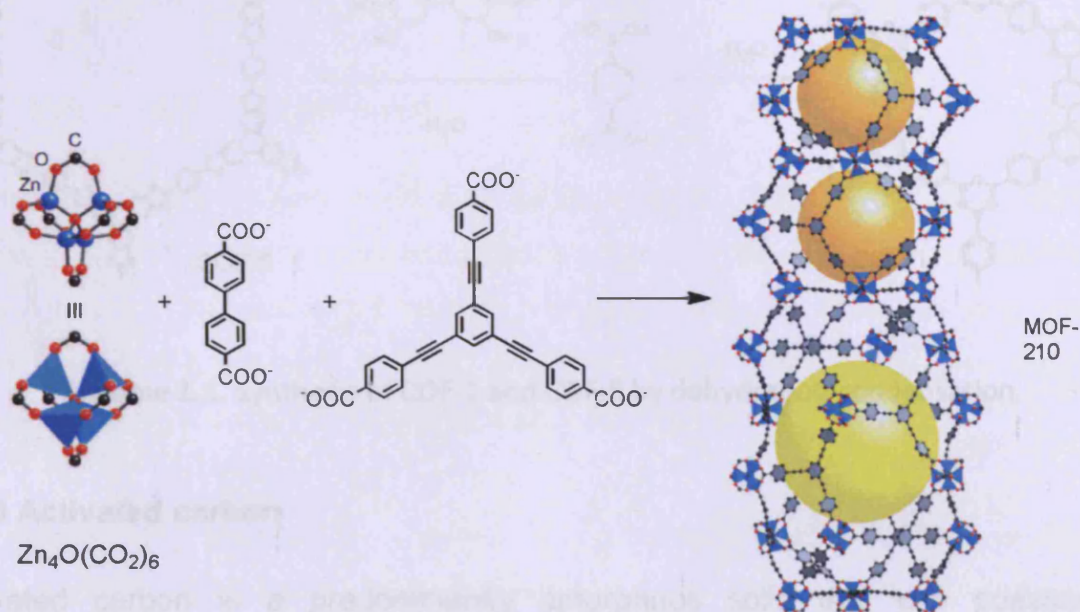
Figure 1.4. Connecting $Zn_4O(CO_2)_6$ unit (left) with organic linkers to form MOF-210 (yellow ball indicates void space in the structure).

Covalent-organic frameworks (COFs) are similar (MOFs) but do not incorporate metal cations and they merely consist of light elements (B, C, O, H) held together by strong covalent bonds. COFs are generally prepared either by water elimination from boronic acid building blocks to form planar six-membered B_3O_3 (boroxine) or by dehydration condensation between boronic acid molecules and catechol building blocks to form a five-membered BO_2C_2 ring.[19] The bonding generated from dehydration is reversible but the stable overall structure favours the formation of the framework. An example of COF synthesis is the dehydration of 1,4-benzenediboronic acid to give COF-1 with a BET surface area of 711 $m^2 g^{-1}$ and the

dehydration condensation reaction between 1,4-benzenediboronic acid and 2,3,6,7,10,11-hexahydroxytriphenylene to produce COF-5 with a BET surface area of 1590 m^2 g^{-1}.[19]
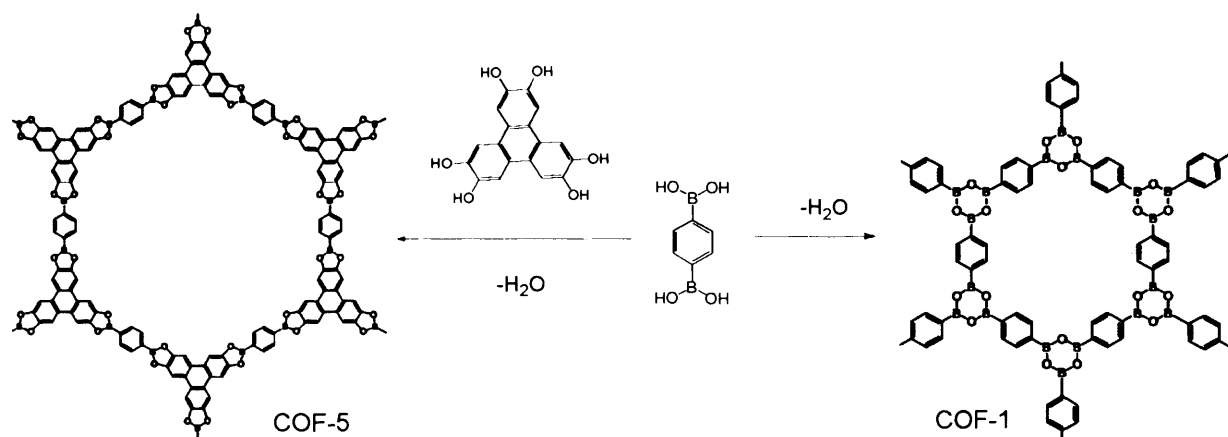
Scheme 1.1. Synthesis of COF-1 and COF-5 by dehydration condensation.

1.3.3 Activated carbon

Activated carbon is a predominantly amorphous solid that can possess an extraordinary large internal surface area and pore volume, which is responsible for its adsorptive properties, which are exploited in many different liquid- and gas-phase applications.[20] Activated carbons are produced by the carbonisation of different natural or synthetic materials followed by chemical and/or physical activation. During carbonisation, nanoporosity is created from the random arrangement of planar hexagonal graphene sheets that are cross-linked by non-graphitised aliphatic units to create a polymer network that cannot fill space efficiently. The spaces between the twisted network of defective carbon layers of activated carbon constitute the microporous, mesoporous and macroporous structures offering a large internal surface area up to 2500 m^2/g.
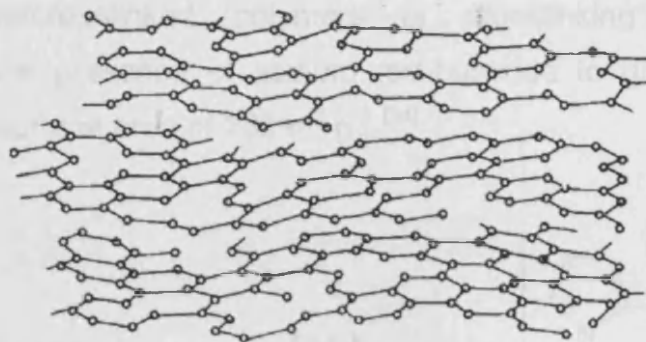
Figure 1.5. Schematic representation of activated carbon structure.

1.3.4 Hypercrosslinked polymers

Hypercrosslinked polymers were first synthesised by Davankov[21] and represent another class of predominantly microporous organic materials that can exhibit high surface areas. The permanent porosity in hypercrosslinked materials is a result of the formation of extensive chemical crosslinks within a solvent-swollen state that prevent the polymer chains from collapsing into a dense nonporous state.[22]

Hypercrosslinking involves the swelling of a polymer to create a distance between polymer chains followed by "immobilization" of the pores in their solvated state through a secondary cross-linking process such as Friedel-Crafts alkylation using a Lewis acid, which makes polymer chains locked in a state that resembles closely its solvated state, when the solvent is removed, the space that it leaves behind becomes the pores.[23]
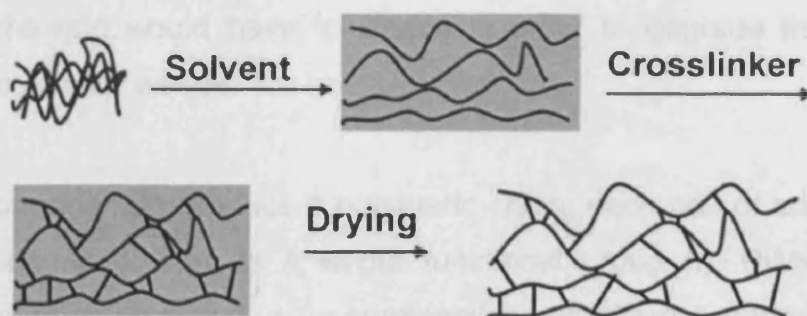
Figure 1.6. Schematic representation of the hypercrosslinking process.[23]

Example of Hypercrosslinked polymers is crosslinking polypyrroles with diiodomethane in the presence of sodium *tert*-butoxide to give hypercrosslinked materials with BET surface area of 732 m^2 g^{-1}.[24]
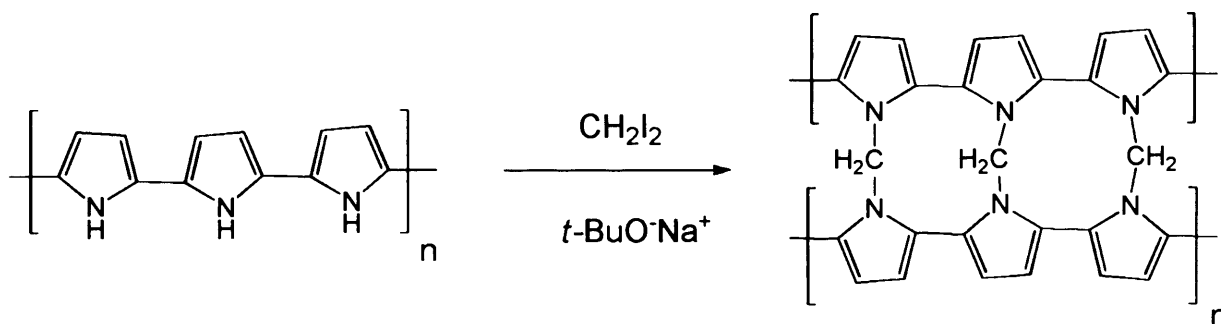
Scheme 1.2. Preparation of nanoporous hypercrosslinked polypyrroles.

1.3.5 Polymers of intrinsic microporosity (PIMs)

Another class of microporous materials was first reported by McKeown et al[25] and are of interest because of their ease of synthesis, wide potential applications and high thermal and chemical stability. PIMs are prepared using a dioxane-forming reaction between aromatic catechol and activated ortho-halogen containing aromatic monomers. The resulting polymer chains consists of fused aromatic rings joined using double strand linkage in way that prevents efficient packing of polymer chains, thus large void space is obtained. The 'intrinsic' microporosity originates directly from the polymer's highly rigid and contorted molecular structure and is not dependent on the history or processing of the material. The stability of these polymers originated from their double strand structure, where two covalent bonds within the same ring would have to cleave in order to degrade the polymer and decrease its molecular weight.

For dioxane formation, to produce a polymeric chain, each pair of adjacent hydroxyl groups or halogens counts as a single functional group (*f*). PIMs with different structures have been prepared using combinations of different monomers containing two or more functionalities (*f*) or active dioxane-forming sites. For the formation of a microporous structure, at least one of the monomers must contain a site of contortion

12

(e.g. A1 and A2), which may be a spiro-centre (e.g. A2) or non-planar molecular structure (e.g. A4). [25]
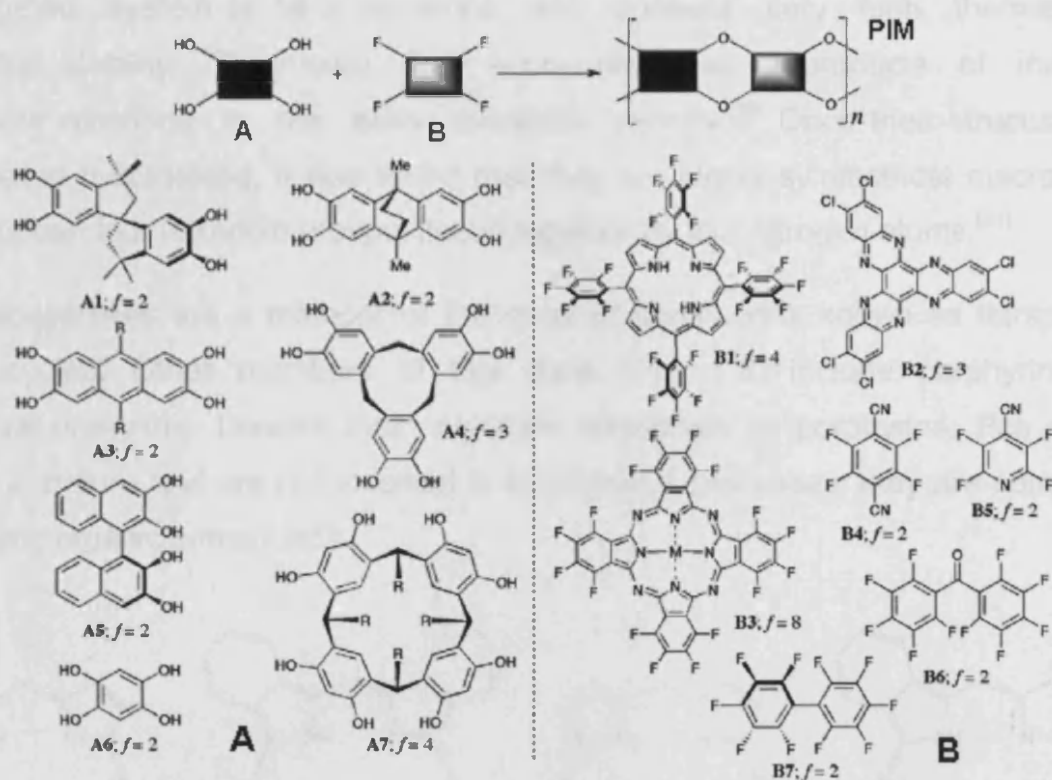
Figure 1.7. Various monomer combinations used for PIM synthesis.

The insoluble network polymers are obtained using monomer combinations with an average functionality (*f*) greater than two (e.g. A1 and B2). Non-network polymers prepared from various combinations of the bifunctional monomers (e.g. A1 and B4), are referred to as ladder polymers and some are soluble in common organic solvents and are thus solution-processable.

The advantage of PIMs over other microporous materials is the ability to engineer materials according to the desired application including gas separation polymers,[26] adsorption and separation of organic compounds, heterogeneous catalyst[27] based on hexaazatrinapthylene monomer (B2) or porphyrin monomer (B1) and potential hydrogen storage media.[28-29]

1.4 Phthalocyanine

Phthalocyanines (Pcs) are aromatic macrocyclic compounds, which have a conjugated system of 18 π electrons and possess very high thermal and chemical stability. They were first encountered as byproducts of industrial chemical reactions in the early twentieth century.[30] Once their structure was elucidated by Linstead, it was found that they are highly symmetrical macrocycles that contain four isoindole groups, linked together by four nitrogen atoms.[31]

Phthalocyanines are a member of the class of compounds known as tetrapyrrolic macrocycles. Other members of this class (Fig. **1.8**) include porphyrins and tetraazaporphyrins. Despite their structural similarities to porphyrins, Pcs do not occur in nature and are not involved in biochemical processes; they are completely synthetic organic compounds.

Porphyrin   Tetrabenzoporphyrin   Tetraazaporphyrin   Tetrabenzotetraazaporphyrin
                                                                                              (Phthalocyanine)
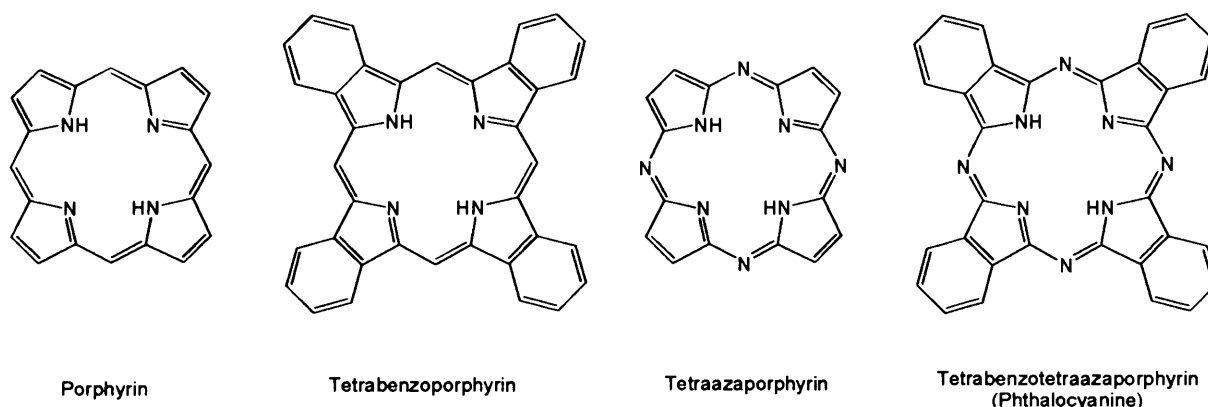
Figure 1.8. A family of four tetrapyrrolic macrocycles

The central cavity of the Pc dianion (Pc^{2-}) can accommodate a wide variety of metal ions by coordinate-covalent bonding between the metals and the nitrogen atoms to form a metallophthalocyanine (MPc).[32] However, because the central cavity is too small, some large metal ions such as, Ge^{2+}, Sn^{2+} and Pb^{2+} do not perfectly fit into the Pc cavity. [33]

Synthesis of Pcs can be achieved using different routes that typically involve the

refluxing of a suitable building block (such as a phthalonitrile) in a high boiling solvent (such as pentanol, DMAc, quinoline). A metal cation is often used as template. The reaction is oxidative; therefore reaction intermediates are highly unstable, and not readily isolable for the pursuit of stepwise syntheses.
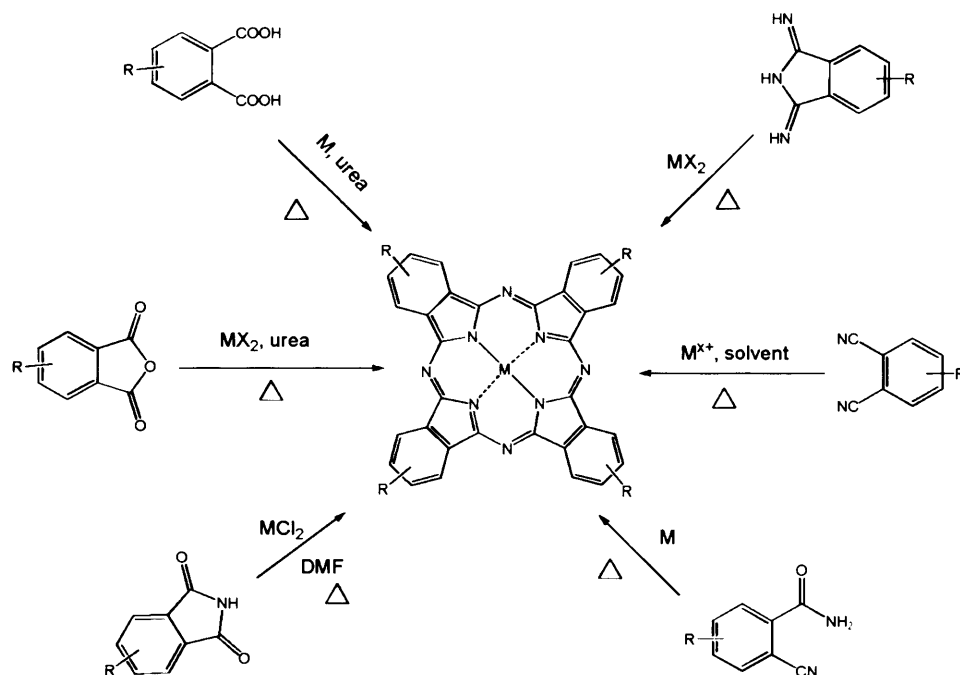
Scheme 1.3. Synthesis of MPcs from typical starting materials.[30]

A number of polymers based on repeating units containing phthalocyanine moieties have been synthesized. Most efforts at preparing phthalocyanine polymers have utilized the phthalocyanine macrocyclisation reaction as the material-forming step, with bridged or bilateral building blocks such as 1,2,4,5-tetracyanobenzene,[34] tetracarboxcylic acid[35] or dicyanobenzenes linked by alkyl chains or other intermediary groups.[36-37] This strategy often results in two-dimensional sheets of fused or linked pigments. Generally, phthalocyanine network polymers show a strong tendency for the aromatic components to aggregate into columnar stacks, resulting in nonporous solids.[38]

McKeown *et al.* reported the synthesis of microporous phthalocyanine network polymer constructed using a highly rigid spirocyclic linker (5,5',6,6'-tetrahydroxy-3,3,3',3'-tetramethyl-1,1'-spirobisindane) that would ensure a space-inefficient packing of the macrocycles and enforce an orthogonal orientation of adjacent phthalocyanine units to prevent cofacial intermolecular interactions (e.g. π–π interactions) and induce porosity.[39]
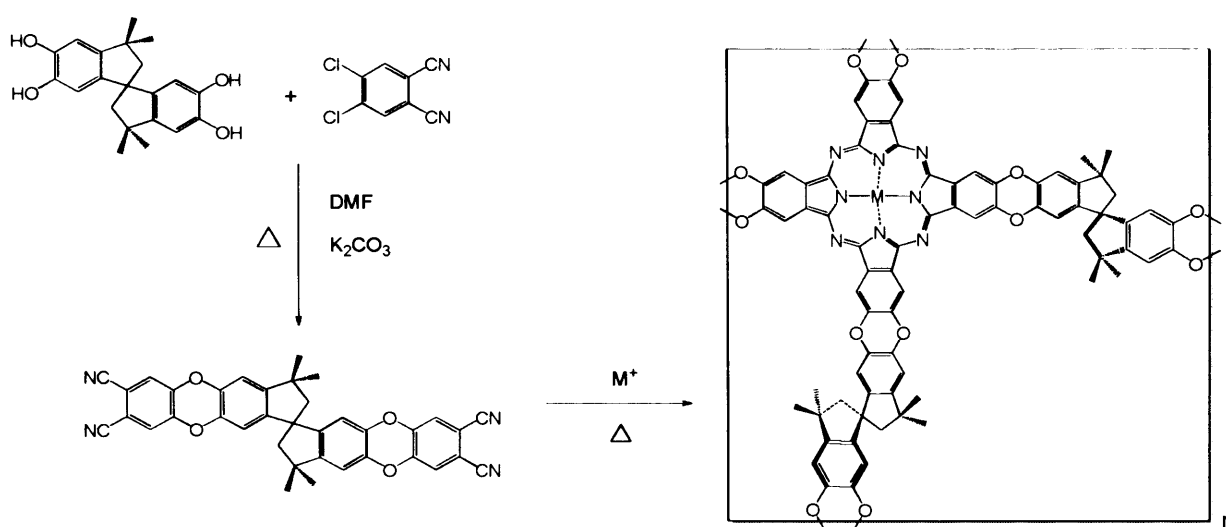
Scheme 1.4. Synthesis of microporous MPcs.

Phthalocyanine network polymers have high surface areas (500-1000 m^2 g^{-1}) with micropores of diameter in the range 0.6-0.8 nm.[39]

1.5 Conjugated microporous polymers

A chemically conjugated system is a system of atoms covalently bonded with alternating single and double or even triple bonds. This system results in a general delocalization of the electrons across all of the adjacent parallel aligned p-orbitals of the atoms.

The first conjugated polymer synthesis by oxidative coupling polymerization method, which was reported first in the 1960s by Kovacic,[40] developed later by Yoshino

and co-workers[41] for the large-scale synthesis of polythiophenes and polyfluorenes using Lewis acids catalysts, such as $FeCl_3$, $MoCl_3$, and $RuCl_3$. In this approach, the 3-alkylthiophene monomer is dissolved in a suspension of $FeCl_3$ in $CHCl_3$ or other appropriate solvents. $FeCl_3$ oxidizes the 3-alkylthiophene monomer to produce radical centers, predominantly in the 2- and 5- positions of the thiophene, which propagates to form a black polythiophenes precipitate
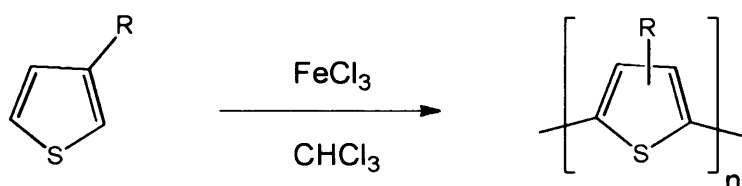
Scheme 1.5. Synthesis of regio-random poly(3-alkylthiophene) using oxidative coupling.

The molecular weights of polythiophenes are reasonably high, but have structural defect due to reactions occurring at both the 2,5- and the 3,4-positions.[42]

The quest for well-defined, high molecular weight, defect free polymers became the driving force for developing new techniques to synthesis high molecular weight conjugated homo or co-polymers including Yamamoto,[43] Suzuki[44] and Stille[45] coupling methods.

Microporous conjugated polymers were first reported by Cooper et al.[46] with BET surface areas up to 834 m^2 g^{-1} using Sonogashira–Hagihara coupling[47] between 1,4-diiodobenzene and 1,3,5-triethynylbenzene mediated by palladium catalyst. The same research group also demonstrated the possibility to tune the micropore size distribution and surface area by varying the length of the rigid organic linkers used.[46]
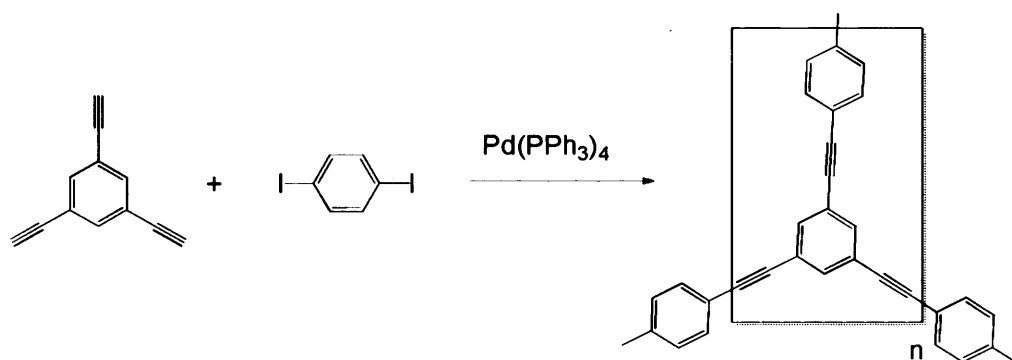
Scheme 1.7. Synthesis of conjugated microporous polymer using Sonogashira–Hagihara coupling.[46]

1.6 Yamamoto Coupling Polymerisation

A convenient and efficient approach to synthesize conjugated polymers was first reported by Yamamoto in 1977.[43] Yamamoto coupling is similar to oxidative coupling in that it produces a regio-random polymer.[48] The Ni-promoted synthetic method was developed by using the polycondensation of halo-aromatic compounds. When the polymerization is carried out using Ni(0)Lm, the polymerization is considered to proceed through the following fundamental reactions, as illustrated in scheme 1.1.[49]
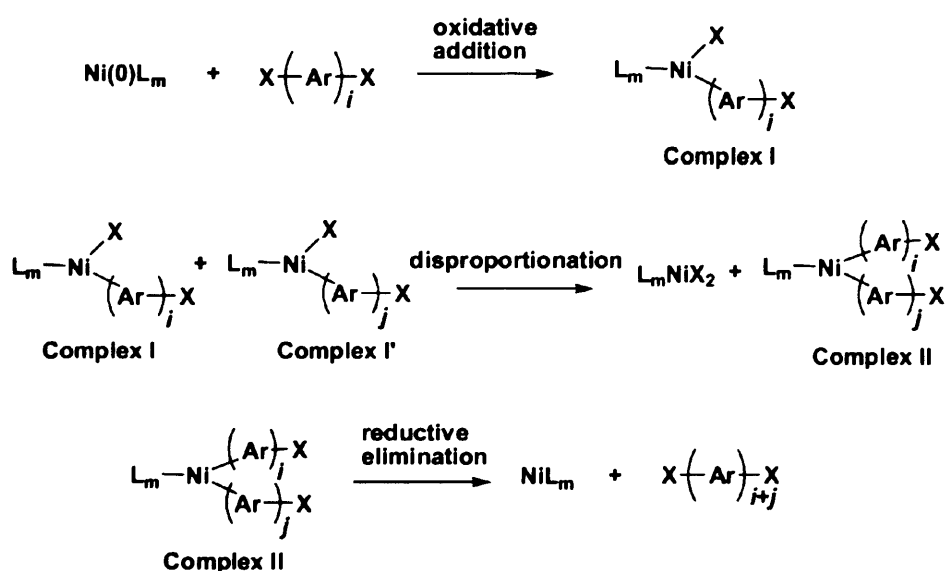
Scheme 1.8. The mechanism of Yamamoto coupling polymerization.

18

The first step is oxidative addition of C-X to Ni(0)Lm. The second step is disproportionation, thirdly, diorganonickel (II) complexes NiR_2L_m undergo reductive coupling (or reductive elimination) reactions to give a coordination of molecules (R-R), the last step is facilitated by the back-donation from the central metal.

Thus, the mechanism of Yamamoto coupling polymerization for organometallic polycondensation is summarized[49] as:

i)   Oxidative addition
ii)   Back-donation
iii)   Reductive elimination.

The zero valence nickel catalyst used in stoichiometric amount to the bromine factor (number of bromines) on monomers, the acidic workup or reaction gives H-termination for the engaged catalyst complexes as shown in scheme 1.9.

$$(X)NiL_m\text{———}(Ar)_i\text{———}X \ + \ H^+ \ \longrightarrow \ H\text{———}(Ar)_i\text{———}X$$

Complex I

$$L_mNi(X)\text{———}(Ar)_i\text{———}(X)NiL_m \ + \ H^+ \ \longrightarrow \ H\text{———}(Ar)_i\text{———}H$$
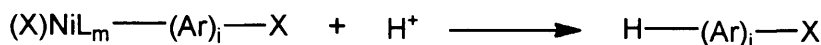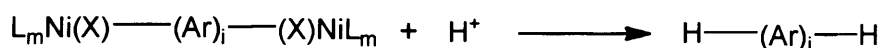
Complex III

Scheme 1.9. Acidic termination of Yamamoto polymerization.

The highly efficient Yamamoto coupling polymerization has proven recently to be an effective method to prepare microporous polymeric materials[50-52], for example, highly porous crystalline porous aromatic framework termed (PAF) with highest surface area yet reported for purely organic material (BET 5640 m^2 g^{-1}, Langmuir 7000 m^2 g^{-1}) were prepared by self-coupling tetrakis(4-bromophenyl)methane using stoichiometric amount of bis(cyclooctadiene)Ni(0) in DMF.[51]
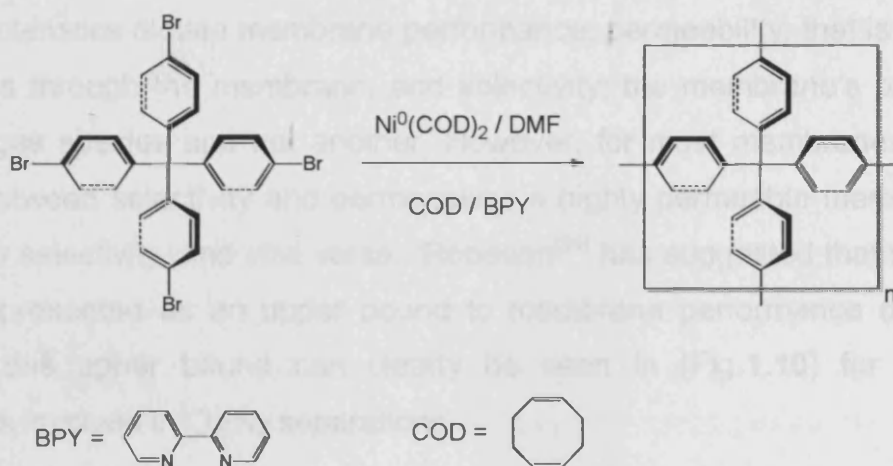
Scheme 1.10. Synthesis of porous aromatic framework via Yamamoto coupling.

1.7 Membranes

Thin layer of polymeric material acts as a semi-permeable barrier by the obstruction of gross mass movement between two phases but permits passage of certain species from one phase to the other with various degrees of restriction. Separation occurs when the membrane controls the rate of movement of various molecules between two liquid phases, two gas phases, or a liquid and gas phase.[53]

The action of a membrane between two gas phases is often referred to as a gas separation membrane, which behaves as a selective filter to separate one or more gases from a feed mixture and generate a specific gas rich permeate, as shown in figure (**1.9**).
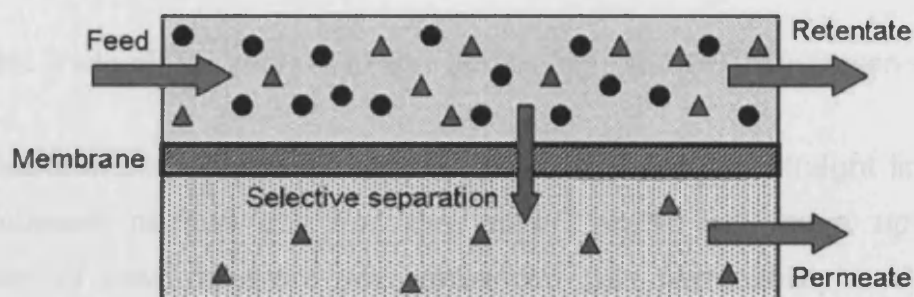
Figure 1.9. Schematic of membrane gas separation.

Two characteristics dictate membrane performance, permeability; that is the flux of a specific gas through the membrane, and selectivity; the membrane's preference to pass one gas species and not another. However, for most membranes, there is a trade-off between selectivity and permeability; a highly permeable membrane tends to have low selectivity, and *visa versa*. Robeson[54] has suggested that this trade-off may be represented as an upper bound to membrane performance composed of polymers, this upper bound can clearly be seen in (Fig.**1.10**) for a range of membranes involved in O_2/N_2 separations.
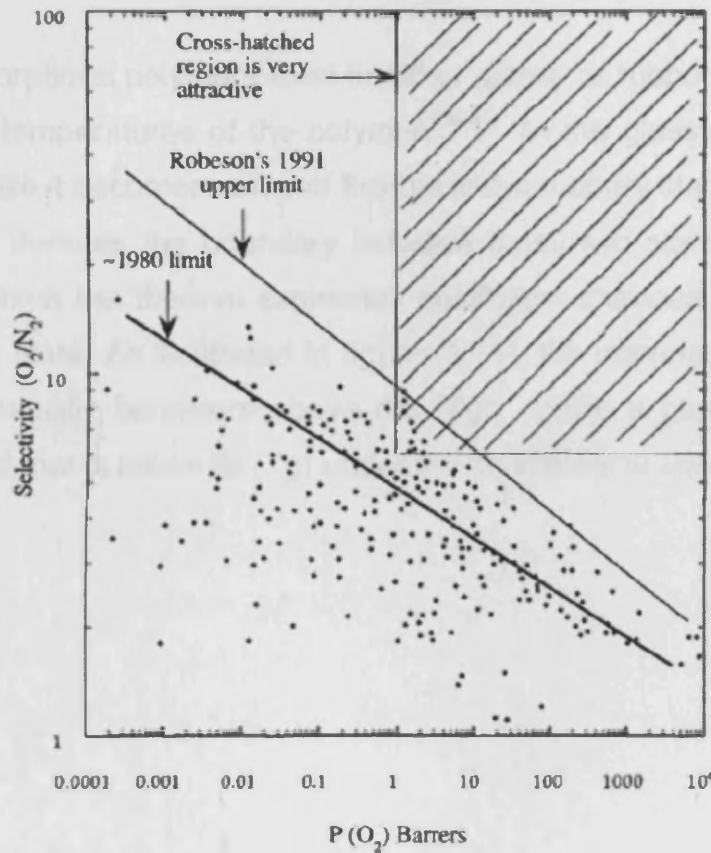
Figure 1.10. Trade-off line curve of oxygen permeability and oxygen/nitrogen selectivity.

All polymeric materials are empirically lying on or below the straight line of upper bound, Robeson pointed out that the upper bound will move upwards with development of new polymers with enhanced gas permeability and selectivity. Indeed, the development of new polymers such as PIMs has resulted in Robeson updating his upper bound for a number of gas pairs in 2008.[55] The cutting edge of

polymeric membrane research takes place when materials are found that can break this upper limit, achieving both high selectivity and high permeability.

One of the dominant materials in the membrane separation technology is polymer membranes; they are amorphous polymeric material, which is cost-effective with sufficient selectivity and good processability. Gas transport through membrane materials and the intrinsic permeation characteristic of polymers are significantly influenced by polymeric chain structures.

Basically, the amorphous polymers exist in either glassy or rubbery state depending on the operating temperatures of the polymer.[56-57] In the glassy state, polymer is hard and rigid, while it becomes soft and flexible in the rubbery state. Glass transition temperature (Tg) denotes the boundary between these two states, where it is the temperature at which the thermal expansion coefficient changes in going from the rubbery to glassy state. As illustrated in figure (1.11), the material is rubbery, which exhibits the viscoelastic behaviors above the (Tg). While a glassy polymer is an polymeric material that is below its (Tg) under the conditions of use.[58]
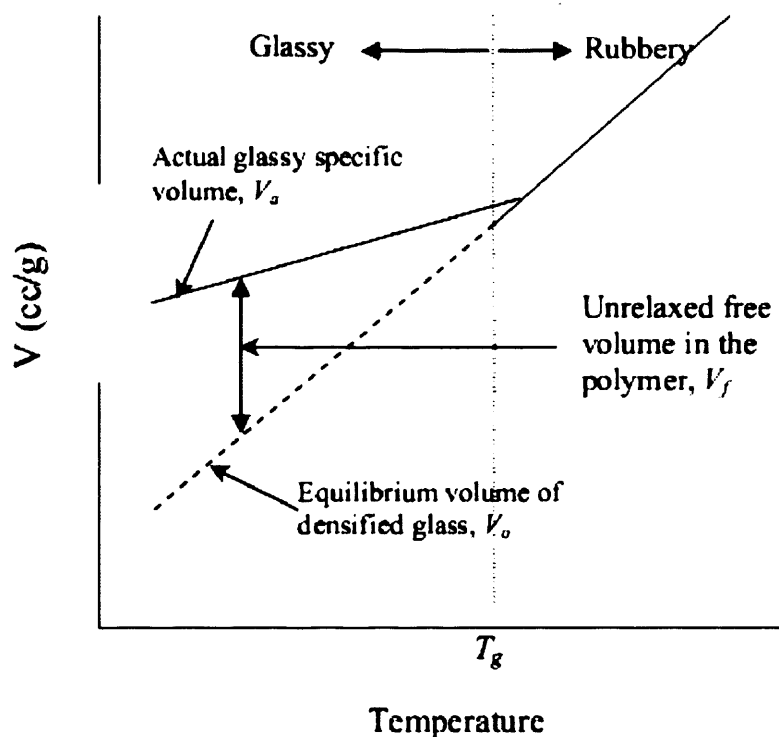
Figur 1.11. Schematic representation of the relationship between the polymer specific volume and temperature in an amorphous polymer[58]

Rubbery membranes are able to rearrange on a meaningful time scale and are usually in thermodynamic equilibrium. Therefore, gas solubility within the polymer matrix follows Henry's Law and is linearly proportional to the partial pressure. For most gases, rubbery membranes generally exhibit higher diffusivity and resulted in higher permeability as compared to glassy membranes. However, lower separation efficiency is often achieved by rubbery materials as a consequence of their small diffusivity selectivity.[59]

Conversely, glassy membranes operate below the glass transition temperature and therefore polymer rearrangement is on a long time scale meaning the membrane never reaches thermodynamic equilibrium. Hence, the polymer chains are packed imperfectly, leading to excess free volume in the form of microscopic voids in the polymeric matrix. Within these voids Langmuir adsorption of gases occurs that increases the solubility,[60] glassy materials may also characterised by a low intra-segmental mobility and long relaxation time.[57] Accordingly, glassy materials are

inherently more size and shape selective, resulting in higher selectivity and mechanical stability relative to rubbery materials. Thus, glassy polymers are more commonly used in membrane separation processes.

1.7.1 Transport mechanisms through polymeric film/membrane

Gas permeation through a dense polymer membrane is most often described with five possible mechanisms[56, 61] for membrane separation: Knudson diffusion, molecular sieving, solution-diffusion separation, surface diffusion and capillary condensation, molecular sieving and solution-diffusion are the main mechanisms for nearly all gases.
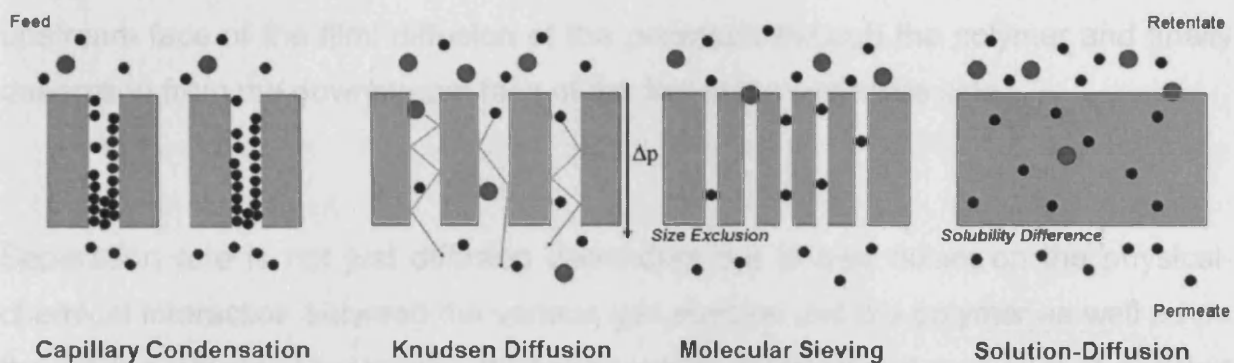
Figure 1.12. Schematic representation of the different mechanisms for membrane gas separation.

Knudson separation is based on gas molecules passing through membrane pores small enough to prevent bulk diffusion, separation is based on the difference in the mean path of the gas molecules due to collisions with the pore walls, which is related to the molecular weight of separating membranes.

Molecular sieving relies on size exclusion to separate gas mixtures, pores within the membrane are of a carefully controlled size relative to the kinetic (sieving) diameter of the gas molecule, this allows diffusion of smaller gases at a much faster rate than larger gas molecules.

Surface diffusion is the migration of adsorbed gases along the pore walls of porous membranes,[62] the rate of surface diffusion is determined by the level of interaction

between the adsorbed gases and pore surface. Thus, molecules diffuse along the pore walls relative to the strength of this interaction, and separation is mainly achieved by the difference in the degree of this interaction for the individual gases.

Capillary condensation is an extension of surface diffusion; when the vapour pressure becomes low, adsorbed gas can undergo partial condensation within the pores, this condensed component diffuses more rapidly through the pore than gases, causing more separation of the condensable gas.[63-64]

Transport of gases through a dense polymeric film or the selective layer of an integral membrane occurs *via* solution-diffusion mechanism,[56] this is based on the solubility of specific gases within the membrane and their diffusion through the dense membrane matrix. It is believed to occur in three steps: sorption of penetrant on the upstream face of the film; diffusion of the penetrant through the polymer and finally desorption from the downstream face of the film at the permeate side.

Separation rate is not just diffusion dependent but is also reliant on the physical-chemical interaction between the various gas species and the polymer as well as on the driving force and membrane thickness, which determines the amount of gas that can accumulate in the membrane polymeric matrix. The solution-diffusion model describes gas permeation through a dense polymer membrane with the equation:

$$P = DS$$

Where, P is the permeability coefficient routinely expressed in Barrers (10^{-10} $cm^3_{(gas)}$ (STP) $cm^{-2}_{(membrane)}$ s^{-1} $cmHg^{-1}$); D is the diffusion coefficient, often given in units of cm^2/s; S is the solubility coefficient in units of $cm^3_{(gas)}$ $cm^{-3}_{(polymer)}$ $cmHg^{-1}$.

The preferential ability of a polymer membrane to permeate one gas (A) over another gas (B) is referred to as the ideal selectivity ($\alpha_{A/B}$),[26] which can be obtained by the following equation:

$$\alpha_{A/B} = \frac{P_A}{P_B} = \frac{D_A}{D_B}\frac{S_A}{S_B}$$

The selectivity can also be defined as the product of the diffusivity selectivity and the solubility selectivity of gases (A) and (B). The diffusivity selectivity (D_A/D_B) is governed by the size difference of penetrant gases and the size-sieving ability of a polymer material.

An important factor that influences the diffusivity selectivity is the available free volume (i.e. voids) not occupied by polymer chains at nanoscale dimensions through which penetrant gases migrate. In a polymer possessing relatively little free volume, as in the case of most glassy polymers, only gas molecules able to fit within existing void regions can diffuse through the membrane. Solubility selectivity (S_A/S_B), on the other hand, is governed by the solubility of gas (A) relative to the solubility of gas (B) in the polymer.

Materials that perform close to the upper bound in the separation of simple gases are generally glassy polymers, which are dominated by diffusivity selectivity and thus are often employed to remove lighter gases such as H_2, whereas rubbery polymers are dominated by solubility selectivity and are therefore often used to remove heavier gases like CO_2.[26]

1.7.2 Polymer of intrinsic microporosity (PIM) membranes

PIM membranes prepared from ladder polymers with ridged backbone incorporate "sites of contortion" that force the backbone to twist and turn erratically, creating polymer chains that cannot pack efficiently in the solid state. Recently, two examples of polymers of intrinsic microporosity referred to as (PIM-1 and PIM-7) were reported to possess good characteristics for making gas separation membranes providing a combination of high permeability and good selectivity that places them well above the Robeson's upper-bound for many gas pairs.[26] The backbone structure of both PIM-1 and PIM-7 is based on the 3,3,3',3'-tetramethyl-1,1'-spirobisindane unit in which the spiro-centre (a tetrahedral carbon atom that is part of two five-membered rings) acts as a "site of contortion".
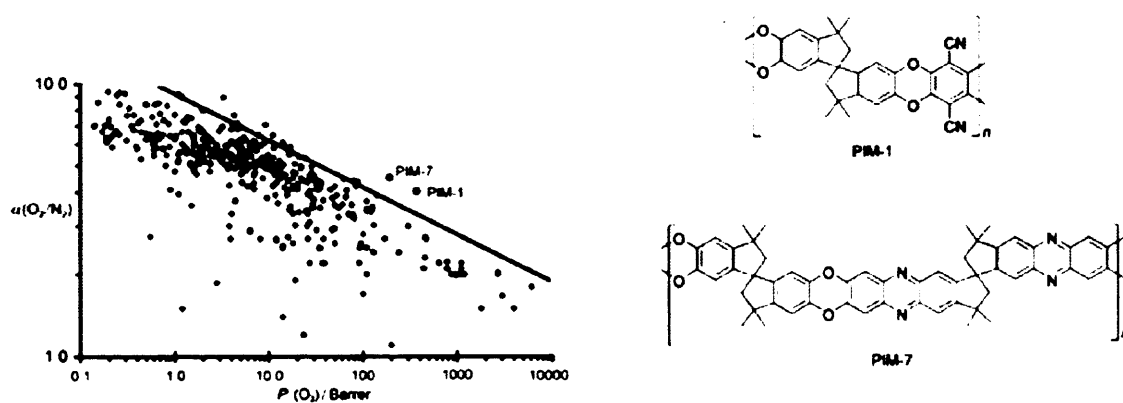
Figure 1.13. O_2/N_2 selectivity vs. O_2 permeability trade-off for PIM1 and PIM-7.

For O_2/N_2 separation study, Polymers PIM-1 and PIM-7 show substantially higher selectivity than other polymers of similar permeability, the solubility values of these membranes are extraordinarily high but solubility selectivity is relatively small, O_2/N_2 separation for the PIMs is dominated by the diffusivity selectivity (smaller gas molecules diffuse faster) as expected for glassy polymers.

PIMs also lie above or near to the upper bound line for several other commercially important gas combinations, including CO_2/CH_4, H_2/N_2 and H_2/CH_4, The improved permeability and selectivity data of PIM membranes over Robeson's (1991) line has contributed to revision of the upper bound in 2008.[55]

The high apparent solubility of gases in PIMs may be attributed in part to their microporous character,[65] which provides a high capacity for gas uptake, therefore boosting permeability. It has been noted[66] that polymers that lie on or close to Robeson's upper bound line all possess very rigid molecular structures.

This behavior indicates that these PIMs are inherently different to the many polymers that have been investigated previously for gas permeability and the concept of PIMs is an excellent one for designing highly rigid but solution-processible polymers, which combine high selectivity with high permeability making them interesting candidates for applications such as efficient gas separation membranes, selective reactant supply and selective product removal for increased conversion.

27

1.8 General characterisation of polymers

Polymer characterisation is an important step in materials engineering to evaluate the morphology, physical and chemical structure, as well as the characteristics of bulk membranes. The characterisation instrumentation include: Infra-red absorption, Differential Scanning Calorimetry (DSC), X-ray Scattering/Diffraction, Scanning Electron Microscopy (SEM), Thermogravimetric analysis (TGA) and some other techniques to reveal the properties of materials formed. Moreover, Gel Permeation Chromatography (GPC) and Nuclear Magnetic Resonance (NMR) are obtainable for soluble polymers. For microporous polymers, nitrogen adsorption using a Surface Area Analyzer is also important.

1.8.2 Gel permeation chromatography

Size exclusion chromatography is a chromatographic method in which particles are separated based on their size or more specifically, hydrodynamic volume. The technique is called Gel Permeation Chromatography (GPC)[67] when the column is packed with particles that swell in the presence of solvent and form a gel in which the space between cross-links in the gel surface generates pores of varying diameter.[68] The principle of this method is that particle of different sizes will elute through the column at different rates, smaller particles enter the smaller pores and "explore" the narrow pore space in the column. However, larger particles cannot enter the narrow pores and therefore pass through the column more quickly. Therefore, smaller particles take a longer time to elute than larger particles. A UV-vis or refractive index detector monitors the eluent absorption as it exits the column, generating a plot of absorbance vs. time. The equipment is generally calibrated using polymers of known molecular mass. Weight average (M_w) and number average molecular weights (M_n) are calculated using:

$$M_w = \sum_i \frac{n_i\, M_i^2}{n_i\, M_i} \quad \text{and} \quad M_n = \frac{\Sigma_i\, n_i\, M_i}{\Sigma_i\, n_i} \quad \text{respectively.}$$

Where n_i is the number of molecules of molecular weight M_i

The ratio of molecular weight and molecular number, which is defined as the Polydispersity Index (PDI) is calculated from:

$$PDI = \frac{M_w}{M_n}$$

1.8.3 Thermogravimetric Analysis

Thermogravimetric analysis (TGA) is used to determine the thermal stability of materials and the fraction of volatile components. TGA measurements monitor the mass change of a specimen when the sample is heated. The measurement is carried out in an inert atmosphere (nitrogen) and the sample weight is recorded as a function of increasing temperature. The onset temperature of decomposition of the sample is estimated from the point of intersection of two lines: one extrapolated from the slope of the curve just prior to the loss in mass and the second from the steepest part of the curve.
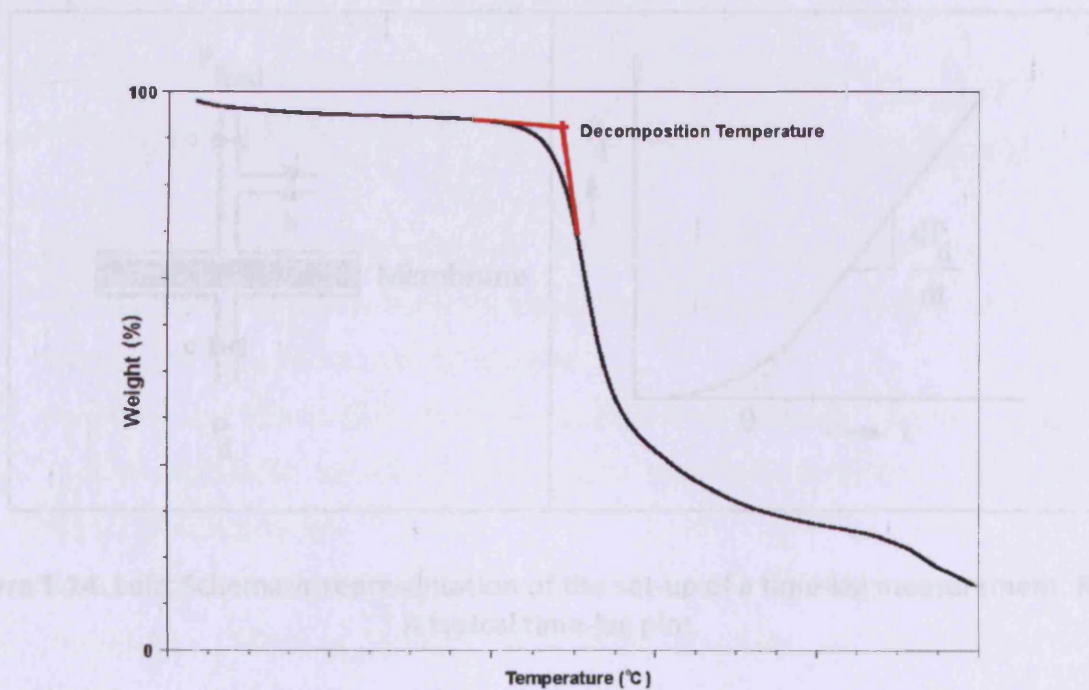
Figure 1.15. Example of TGA plot

This technique is broadly used to study thermal degradation of polymers. The thermal degradation on polymeric materials varies greatly with the nature of the polymer[69]. For example, natural polymers like Cellulose decompose below 100 °C,

whereas polyimides are stable up to 400 °C. There are other factors that affect the changes greatly like the presence of additives and the atmosphere used.

1.8.1 Permeability experimental measurement.

The simplest method to experimentally measure both the permeability coefficient P and the diffusion coefficient D for polymeric membranes is the time-lag method. This method was first proposed by Daynes[70] and refined by Barrer.[71] In this technique the membrane is initially evacuated from any residual gas by applying vacuum to both sides of the membrane for several hours. At time t=0 the upstream side of the membrane is exposed to the desired gas at the desired pressure P_{feed}. From that moment on the pressure on the downstream side (P_d) is measured and plotted. A typical plot of the pressure vs. time is also shown in (Fg. 1.14).
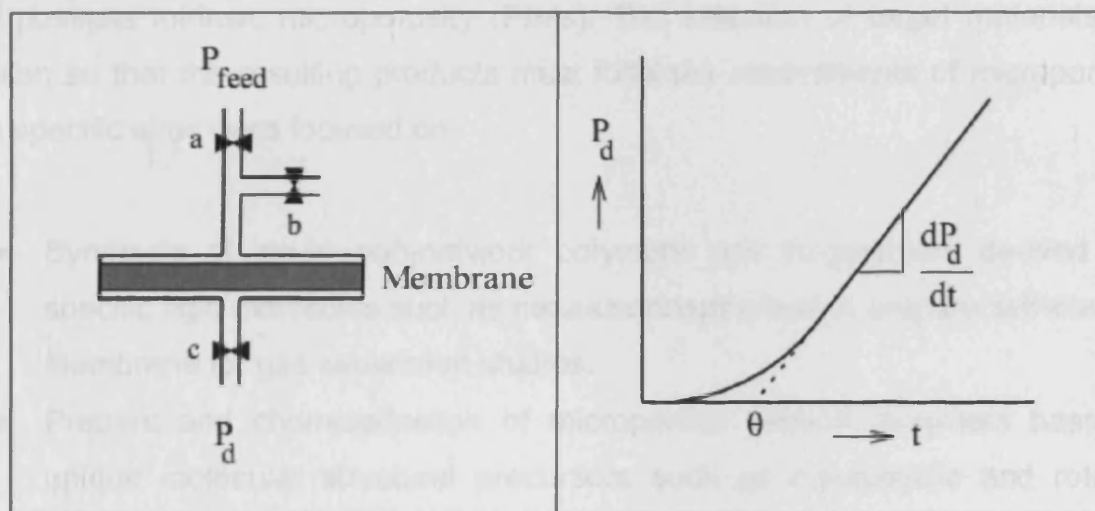
Figure 1.14. Left: Schematic representation of the set-up of a time-lag measurement. Right: A typical time-lag plot.

From the extrapolation of the steady-state part of the curve, the time-lag (θ) is obtained and the diffusion constant can be calculated[72] directly from:

$$D = \frac{l^2}{6\,\theta}$$

Where (*l*) is membrane thickness, the permeation coefficient (P) is calculated from the slope of the straight steady-state part using:

$$P = \frac{1}{P_{feed}} \frac{V_d\, M_{gas}\, l}{\rho\, R\, T\, A} \frac{dP_d}{dt}$$

Where V_d is the downstream compartment volume, M_{gas} the molecular weight of the penetrant gas at density ρ and A is the membrane area. The solubility coefficient S is calculated from the diffusion and the permeability coefficients using: P = DS.

1.9 Aims of project

The general aim of this study is to prepare novel thermally stable polymeric materials that possess intrinsic microporosity (PIMs). The selection of target materials was chosen so that the resulting products must fulfill the requirements of microporosity. The specific aims were focused on:

- Synthesis of novel non-network polymers and co-polymers derived from specific rigid molecules such as hexaazatrinapthylene to prepare self-standing membrane for gas separation studies.

- Prepare and characterization of microporous network polymers based on unique molecular structural precursors such as macrocyclic and rotation-hindered compounds.

- Prepare and characterise of novel PIMs exploring different polymerisation route *via* dehalogenative Yamamoto coupling of halogenated rigid compounds.

RESULTS AND DISCUSSION

Chapter 2. Synthesis and characterisation of triptycene-based polymers

This chapter reports on the synthesis of the required triptycene monomers and the polymers derived from them. Recent work had indicated that triptycene based polymers posses a greater degree of porosity[28] compared to other PIMs. This enhancement appears to originate from the macromolecular shape of the polymer framework, as dictated by the triptycene units, which helps to reduce intermolecular contact between the extended planar struts of the rigid framework and thus reduces the efficiency of packing within the solid. The (R) groups at bridgehead positions have a significant effect on porosity with longer alkyl chains appearing to block the microporosity created by the rigid organic framework.

Triptycene consists of three phenyl ring "panels" joined together by a single "hinge" running through carbons 9 and 10, known as the bridgehead carbons[73]. This unique rigid molecular three-blade geometry hinders efficient packing and produces void spaces in the clefts between the rings termed "Internal molecular free volume".[74]

Triptycene is conveniently prepared by the Diels-Alder reaction between anthracene as diene and benzyne as dienophile. By using anthracene derivative and substituted benzynes, a large number of substituted triptycenes have been produced.
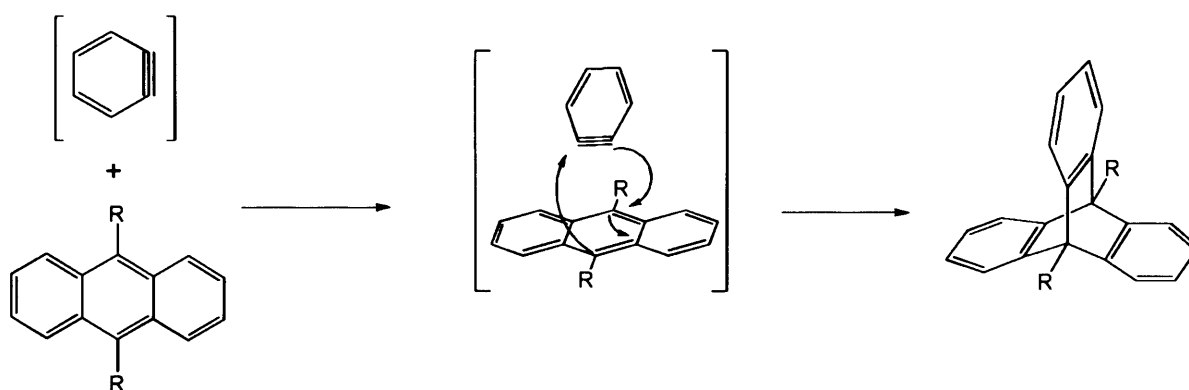
Figure 2.1. Triptycene formation *via* [4+2] cycloaddition (Diels-Alder reaction).

The driving force of the cycloaddition is the electron density of reactants so that, generally, the combination of dienes with electron-donating substitutes and

dienophiles with electron-withdrawing substituents accelerates the reaction (normal electron-demand Diels-Alder reaction).[75] Alternatively, the combination of electron-withdrawing groups in the diene with dienophiles having electron-donation groups can also be successful (inverse electron-demand Diels-Alder reaction).[76]

2.1 Benzyne precursor

Since benzyne is a very reactive species, it has to be generated *in-situ*. One convenient source of benzyne for use in Diels-Alder reactions is the thermal decomposition of benzenediazonium-2-carboxylate, which is prepared as a relatively stable salt using the procedure[77] for converting 2-aminobenzoic acid into its corresponding diazonium salt. Hence, the required benzyne precursor 4,5-dimethoxybenzenediazonium-2-carboxylate was prepare by the reaction of commercially available 2-amino-4,5-dimethoxybenzoic with hydrochloric acid and isoamyl nitrite in excellent yields (> 90 %). The air-dried product (1) is a heat-sensitive precursor and decomposes readily forming the dimethoxybenzyne *in-situ* as a very reactive intermediate (*Fig 2.2*).
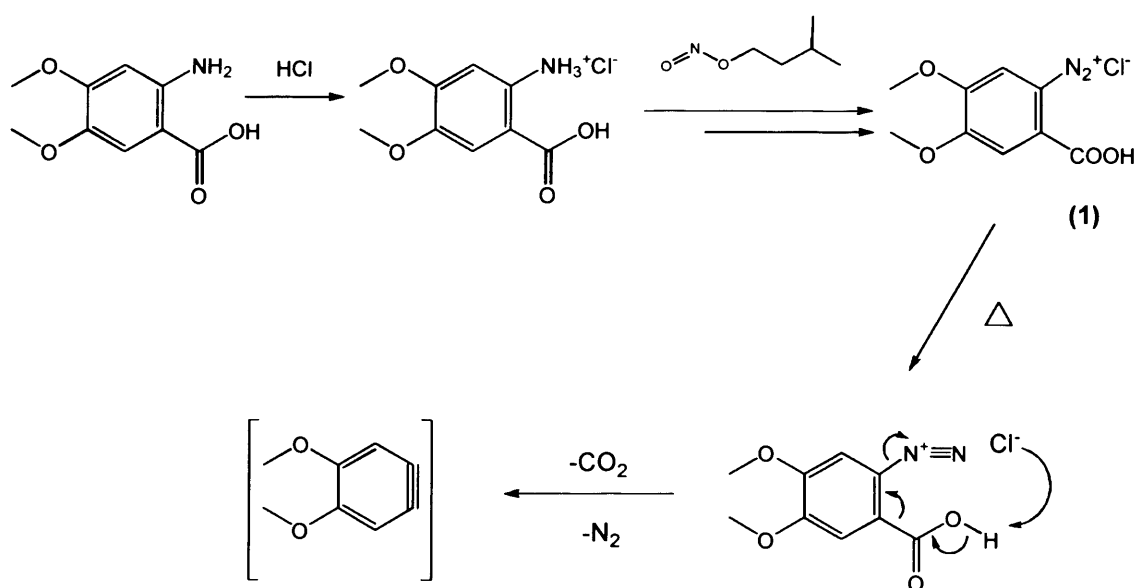
Figure 2.2. Formation of the required benzyne precursor.

The decomposition of diazonium salt is achieved by refluxing in relatively high boiling solvents and the rate of decomposition can be improved by adding small amount of propylene oxide to neutralise the generated HCl.[77]

2.2 Preparation of substituted tetramethoxyanthracenes

As noted, substituted anthracenes serve as the diene in Diels-Alder reactions for triptycenes. For the desired monomers 2,3,6,7-tetramethoxyanthracenes are required with different substituents placed on the 9,10 positions. These anthracenes can readily be prepared by the acid promoted reaction of veratrole with the corresponding aldehyde, by the method of Ostaszewski et al.[78], for which the proposed mechanism of formation is shown in figure (2.3).
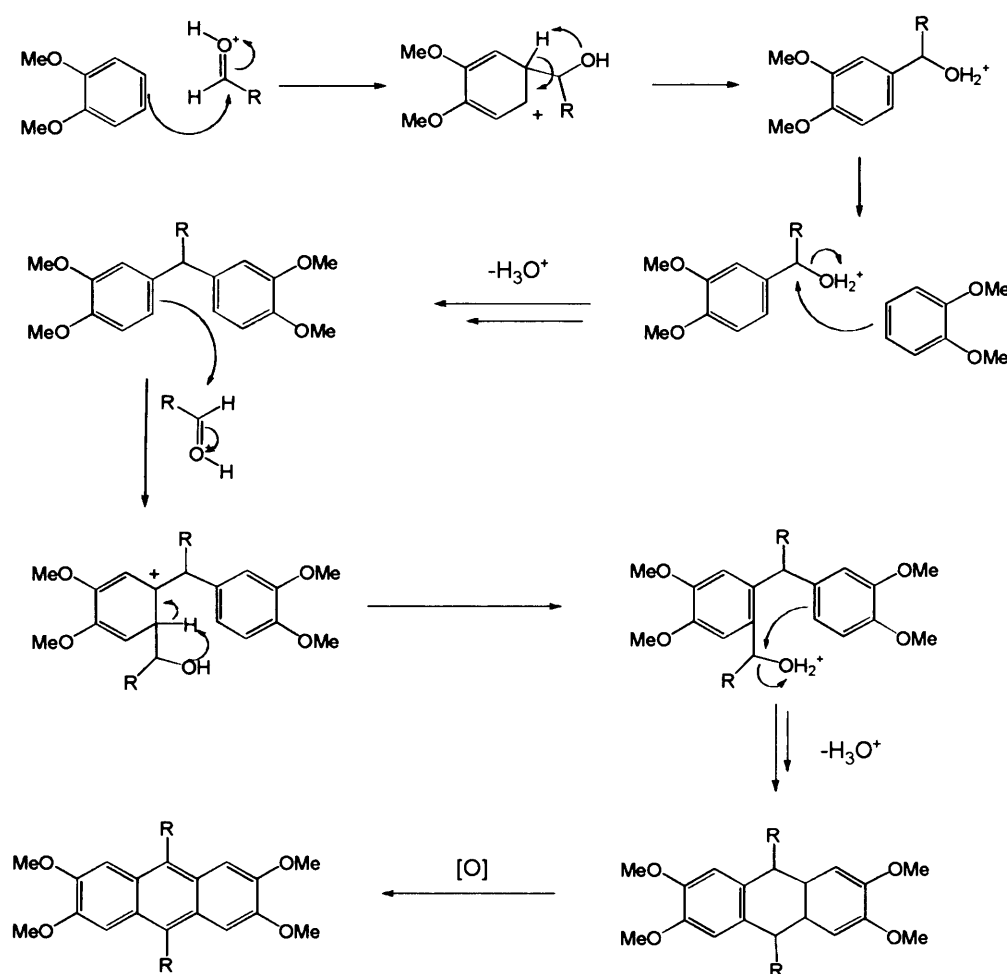
Figure 2.3. Proposed mechanism for formation of anthracene from veratrole and aldehyde[78].

The temperature at which the reaction is carried out is crucial; if the temperature of the very exothermic reaction exceeds 10 °C, the reaction produces an oligomeric solid by-product, which was found to be insoluble in any common organic solvent.

2.3 Dibenzyl-triptycene-based polymer

To investigate further the effect of the bridgehead groups on the porosity of the triptycene networks, a triptycene-based polymer with benzyl groups placed at the bridgehead positions has been prepared starting from phenyl acetaldehyde (Scheme 2.1). The required triptycene monomer was prepared using a multi-step procedure: 9,10-dibenzyl-2,3,6,7-tetramethoxyanthracene (2) was prepared in low yield by condensation of phenyl acetaldehyde with veratrole (1,2-dimethoxybenzene) mediated by concentrated sulphuric acid. In spite of many attempts and systematic changes of reaction conditions (concentration of the starting materials and reaction temperatures) the low yield could not be improved. Nevertheless, sufficient 9,10-dibenzyl tetramethoxyanthracene (2) was obtained to progress.

By refluxing 9,10-dibenzyl tetramethoxyanthracene (2) with an excess of dimethoxy-diazonium salt (1) in a mixture of dichloroethane and 1,2-epoxypropane, the 2,3,6,7,14,15-hexamethoxytriptycene (3) was obtained in a reasonable yield (50 %) based on starting anthracene (Scheme 2.1). Following the very efficient procedure for the cleavage of of aromatic ethers described by McOmie et al.[6] using BBr3 in non-electron donor solvents under dry conditions, the corresponding catechol-based triptycene (4) was obtained in high yield, which was dried and used immediately for polymerisation as it is found to be oxidised rapidly. The structures of compounds 2-4 were confirmed by NMR and mass spectroscopy.
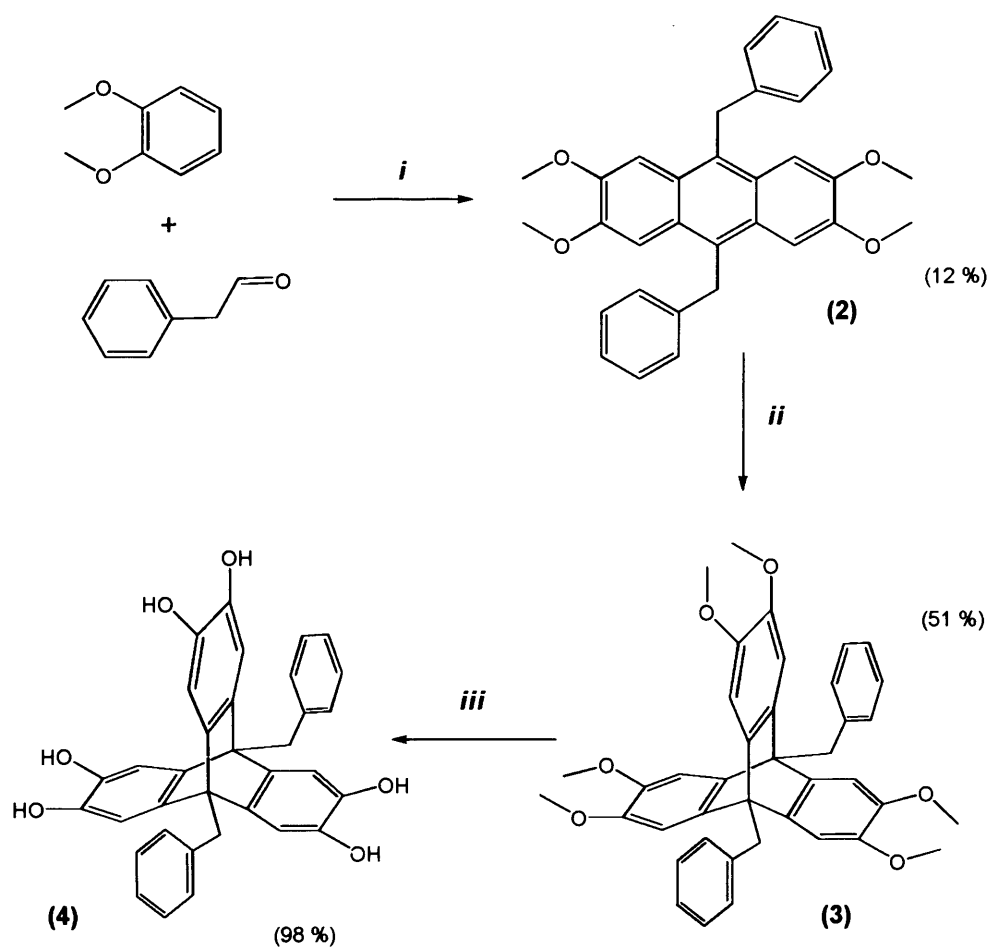
Scheme 2.1. Synthesis of the dibenzyl-triptycene monomer. Reagent and conditions: (*i*) H₂SO₄, 0-5 °C, 2 h; (*ii*) diazonium salt of 4,5-dimethoxy-2-aminobenzoic acid, 1,2-epoxypropane, dichloroethane, reflux, 12 h; (*iii*) v. BBr₃,CH₂Cl₂, RT, 3 h.

The reaction of 9,10-dibenzyl-2,3,6,7,14,15-hexahydroxytriptycene **(4)** with 1.5 molar equivalents of 2,3,5,6-tetrafluoroterephthalonitrile in the presence of K₂CO₃ in DMF in anhydrous conditions at 80 °C gave the di(benzyl)triptycene-based polymer **(5)** in high yield (*Scheme 2.2*).
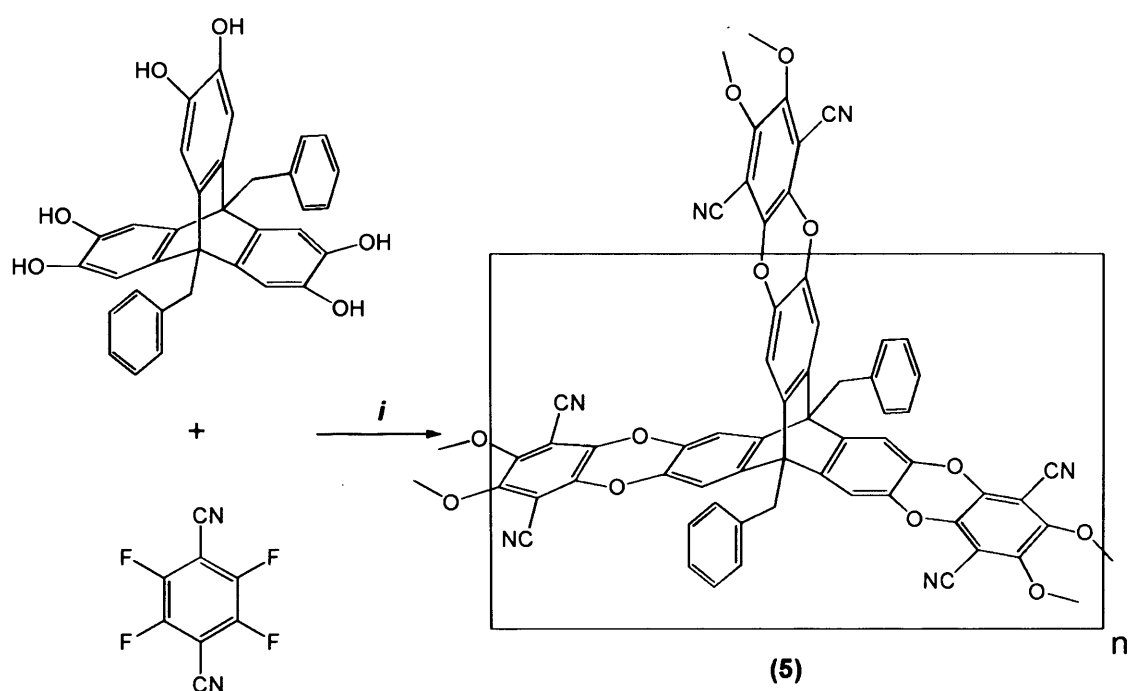
Scheme 2.2. Synthesis of the dibenzyl-triptycene-based polymer. *Reagent and conditions*: (*i*) K_2CO_3, DMF, 80 °C, 24 h.

The crude product was obtained by quenching the reaction with acidified water and simple filtration. It was then washed with copious amounts of hot water to ensure the removal of the residual DMF and the potassium salts. The resulting orange solid was insoluble in all organic solvents tested consistent with the formation of a network polymer. Due to the insolubility of the polymer in cold or boiling solvents, purification was accomplished by refluxing in THF, acetone and finally methanol. The removal of solvent traces was achieved by drying overnight in a vacuum oven at 120 °C. Nitrogen sorption analysis at 77 K confirmed the microporosity of the product, which has an apparent BET surface area of 880 m^2 g^{-1}.

2.4 Di(sec-butyl)triptycene–based polymer

Another triptycene network polymer with sec-butyl bridgehead groups has been prepared from a monomer obtained by following the same three-step reaction scheme as above but starting from 2-methylbutyraldehyde (*Scheme 2.3*).
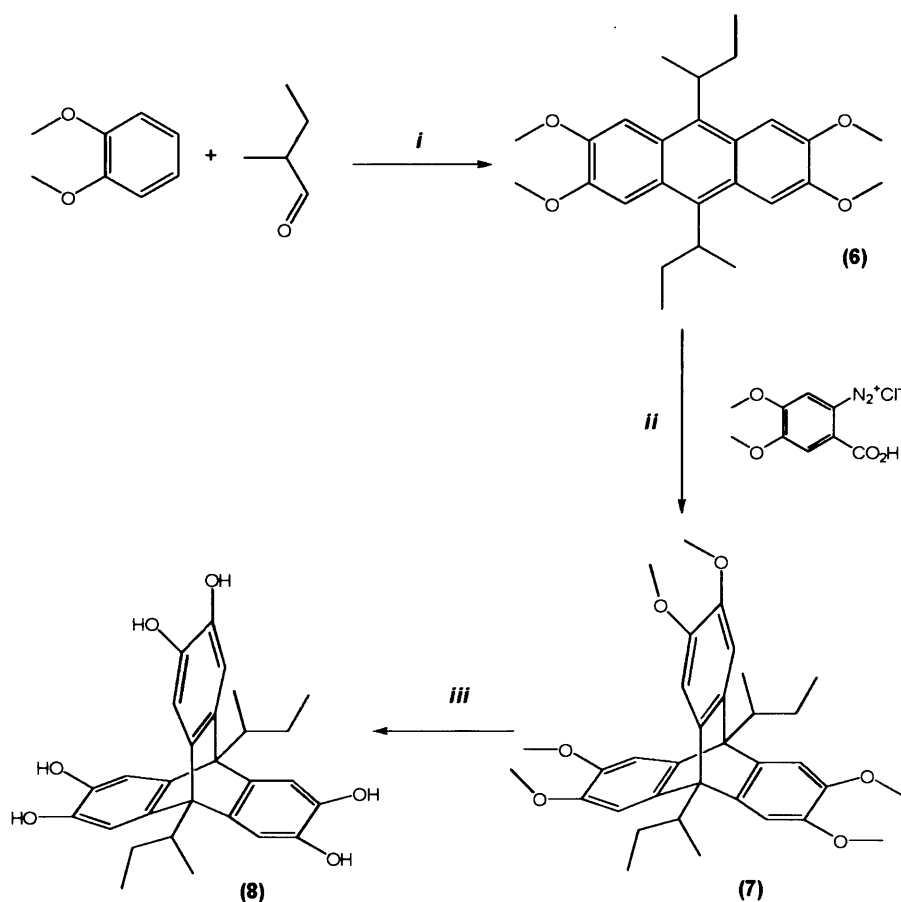
Scheme 2.3. Synthesis of the di(*sec*-butyl)-triptycene monomer. *Reagent and conditions:* (*i*) H_2SO_4, 0-5 °C, 2 h; (*ii*) 1,2-epoxypropane, dichloroethane, reflux, 12 h; (*iii*) BBr_3,CH_2Cl_2, RT, 12 h.

The ^1H NMR spectrum for triptycene **(7)** shows an unexpected pattern of peaks: two sets for CH_3-CH (d, m) with exact ratio of 1:3, two broad multiple sets for CH_2-CH and CH-CH_2-CH_3 (Fig **2.4**). This behaviour must arise due to the hindered rotation of the bridgehead substituent and the stereochemistry of the *sec*-butyl group. It is known that the architecture of triptycene imposes severe steric restrictions on the motion of a short alkyl chain attached to the bridgehead carbon.[28] The peaks associated with the methoxy protons are composed of a doublet and triplet with an exact ratio of 1:3, the compound also give a highly complex set of peaks for the aromatic protons, which cannot be fully interpreted.
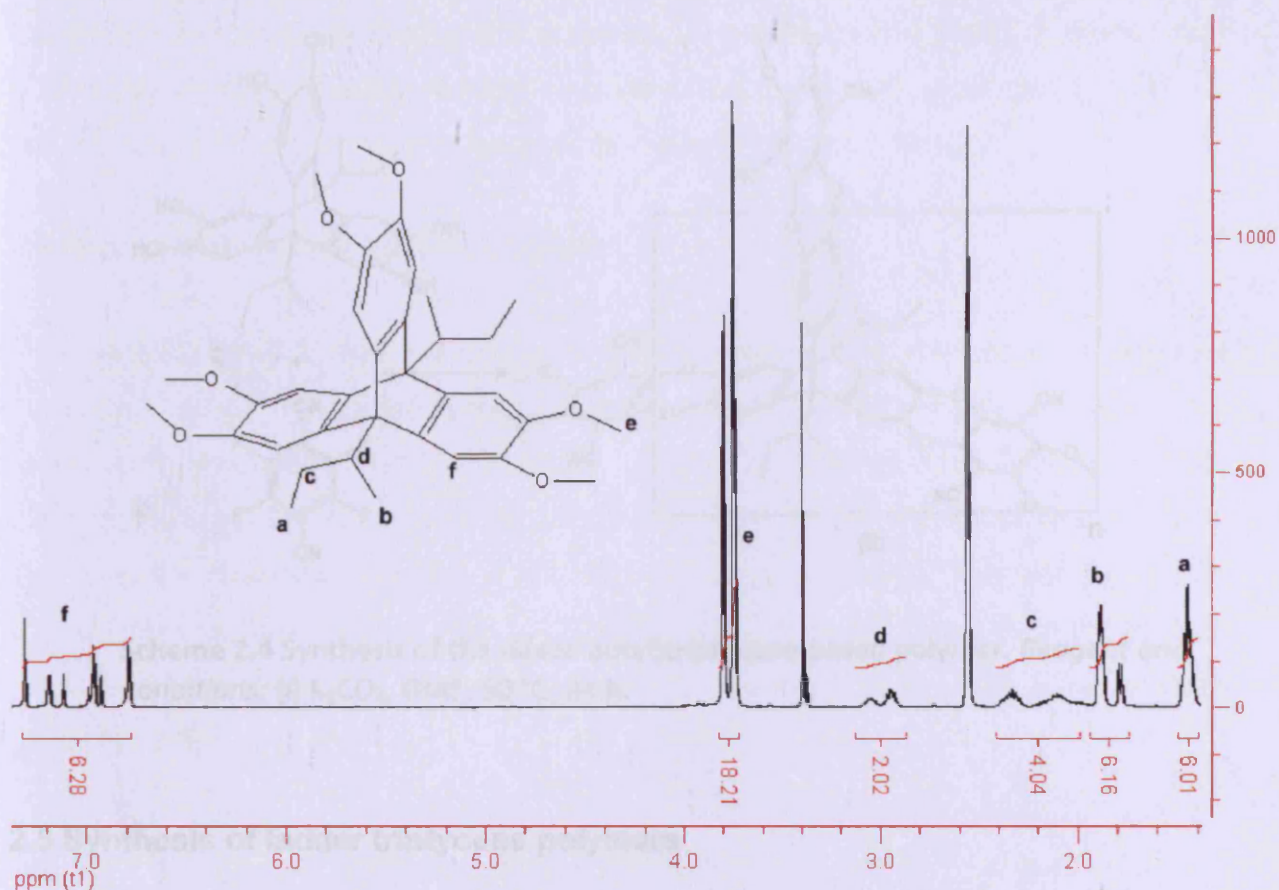
Figure 2.4 ^{1}HNMR spectra of compound **(7)** (DMSO-d6).

The ^{1}H NMR for **(8)** confirmed the removal of methoxy groups but showed the same pattern of peaks for the aliphatic and aromatic protons. The NMR measurements for **(7)** and **(8)** have been repeated at 80 °C and 100 °C with no noticeable change due to peaks coalescence.

The network polymer **(9)** derived from monomer **(8)** was successfully prepared by reaction with 2,3,5,6-tetrafluoroterephthalonitrile in (1:1.5) molar ratio as shown in scheme **(2.4)**, which was purified as described for polymer **(5)**. Nitrogen adsorption measurement at 77 K indicated an apparent BET surface area of 945 m^2 g^{-1} for polymer **(9)**.
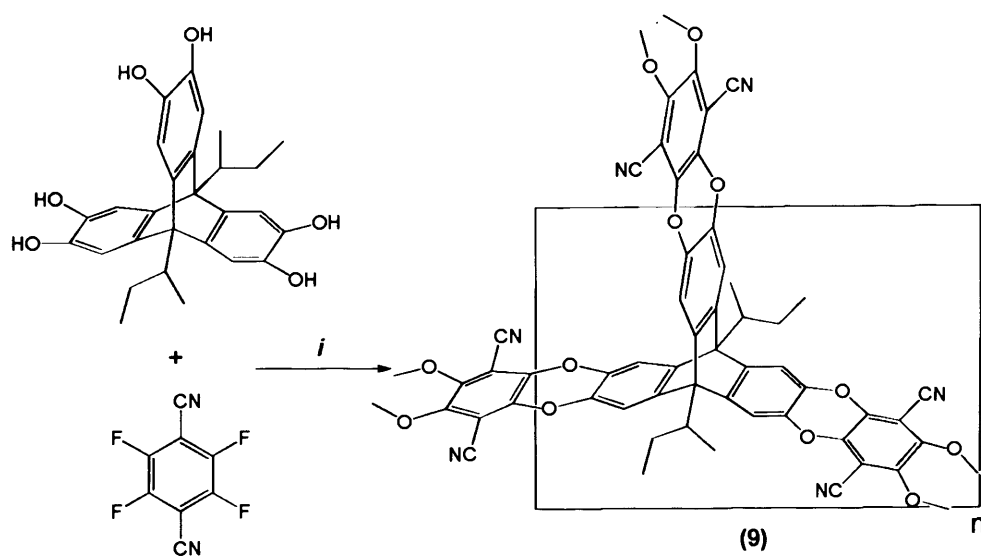
Scheme 2.4 Synthesis of the di(sec-butyl)triptycene-based polymer. *Reagent and conditions:* (*i*) K_2CO_3, DMF, 80 °C, 24 h.

2.5 Synthesis of ladder triptycene polymers

Non-network polymers, designated here as 'ladder polymers', were synthesised by the reaction between triptycene monomers that contains two active functional groups for polymerisation ($f = 2$) and 2,3,5,6-tetrafluoroterephthalonitrile. All triptycene compounds used for this application were prepared using the same benzyne–anthracene Diels-Alder reaction. Another route of generating the reactive benzyne species is by using an organolithium to eliminate bromines from o-dibromo aryls.[79] (*Fig 2.5*).
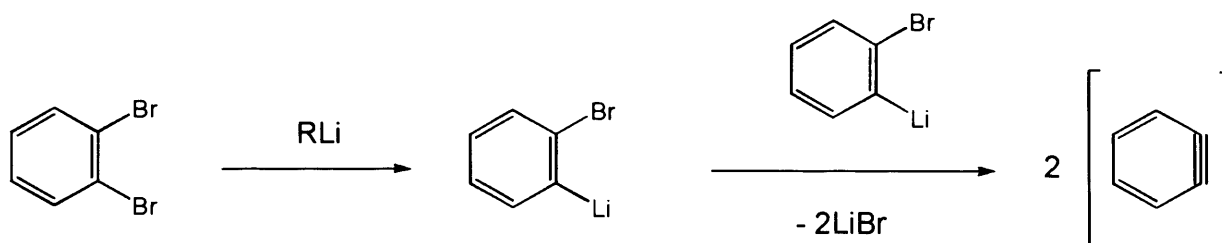
Figure 2.5. Generating benzyne by o-dibromo aryl elimination.

Controlled reaction conditions are required to maximize the yield of Diels-Alder adduct so that very dilute reaction mixtures are used with slow addition of the base[79] and by carrying out the reaction at low temperature (-78 °C).[80]

2.6 Dibromotriptycene-based polymers

By slow addition of a dilute solution of one equivalent of n-butyllithium in hexane to a dilute mixture of 1,2,4,5-tetrabromobenzene and 2,3,6,7-tetramethoxy-9,10-diethyl anthracene in toluene in dry conditions, 2,3,6,7-tetramethoxy-14,15-dibromo-9,10-diethyltriptycene **(10)** is prepared albeit in low yield (~ 15 %). All attempts to improve the yield by changing reaction conditions were unsuccessful. The corresponding 2,3,6,7-tetrahydroxy-14,15-dibromo-9,10-diethyltriptycene **(11)** was obtained in high yield by demethylation of methoxy groups on compound **(10)** using BBr₃ in DCM (*Scheme 2.5*).
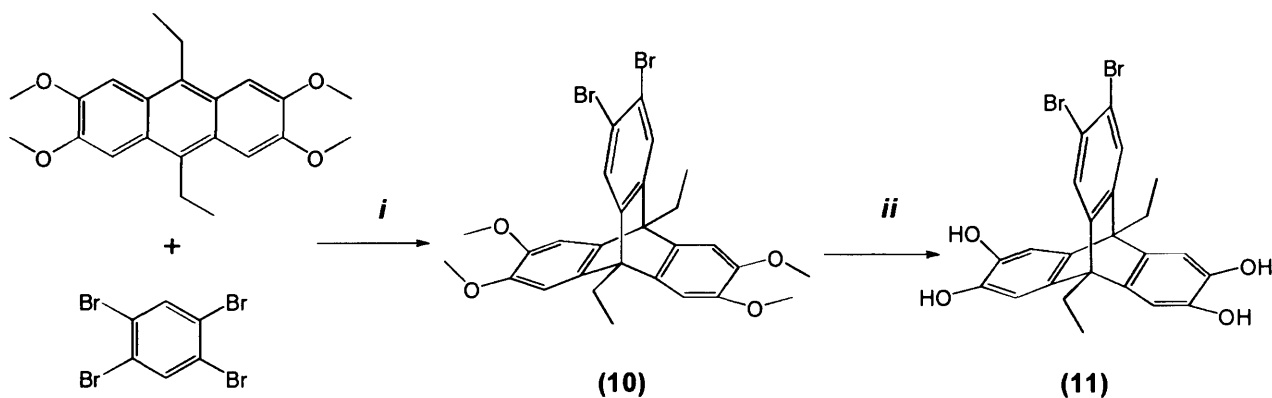
Scheme 2.5. Synthesis of 2,3,6,7-tetrahydroxy-14,15-dibromo-9,10-diethyltriptycene monomer. *Reagent and conditions*: (*i*) Toluene, n-BuLi in hexane, RT. (*ii*) BBr₃, DCM, RT, 12 hours.

The dibromotriptycene-based polymer **(12)** was prepared by the polymerization reaction of 2,3,6,7-tetrahydroxy-14,15-dibromo-9,10-diethyltriptycene **(11)** with a molar equivalent of 2,3,5,6-tetrafluoroterephthalonitrile in anhydrous DMF and in presence of potassium carbonate at 60 °C for 48 hours (*Scheme 2.6*). The

polymerization reaction was carried out with solids content of less than 10 % and performed under nitrogen atmosphere using dry equipment.
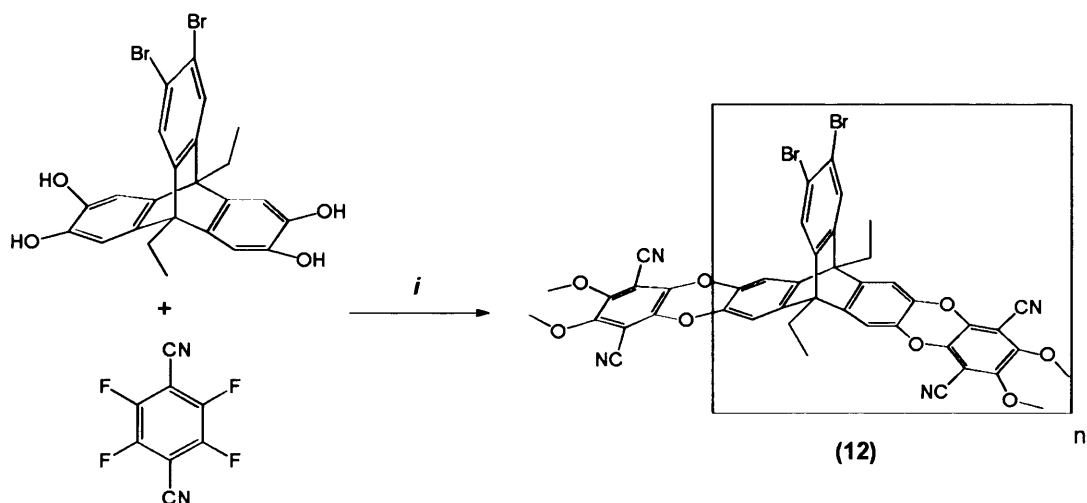
Scheme 2.6. Synthesis of dibromotriptycene-based polymer. *Reagent and conditions*: (*i*) DMF, K_2CO_3, 60 °C, 48 hours.

Quenching the reaction with aqueous acidic solution gave the crude polymer, which was collected by filtration, washed with copious amounts of water and methanol and dried. The polymer shows excellent solubility at room temperature in common organic solvents such as THF and $CHCl_3$. It is likely the bromine presence within polymer backbone reduces the interactions between the polymer chains making them more accessible for organic solvents are responsible for their enhanced solubility.

Purification of **(12)** was achieved using a slightly different approach than used for the insoluble network polymers. The polymer was dissolved in a minimum amount of chloroform, the solution filtered through glass wool then reprecipitated by drop-wise addition of the solution into stirred methanol. This procedure ensured the removal of low molecular weight oligomers.

Although the polymerization reaction was performed under mild conditions (*i.e.* low temperature and low concentration of the monomers) some insoluble products were separated from the crude polymers. This may be due to some cross-linking. The polymerization reaction was sensitive to both reaction temperature and the reactant concentration, when the polymerization was performed at a higher temperature or concentration, a larger amount of insoluble polymer was obtained.

The GPC analysis for **(12)** showed that the soluble polymer has a weight average molecular weight (M_w) of 35800 g mol^{-1} and expected polydispersity for a step-growth polymer $(M_w/M_n = 2.48)$. Due to its excellent solubility, attempts were made to cast the polymer into film from CHCl$_3$ solution using slows evaporation; however, the resulting film was inflexible, brittle and unsuitable for further study as a gas separation membrane, this is possibly due to the relatively low molecular weight of this polymer.

To obtain a more robust and flexible membrane, the monomer **(11)** was incorporated into copolymers prepared with 5,5',6,6'-tetrahydroxy-3,3,3',3'-tetramethyl-1,1'-spirobisindane and 2,3,5,6-tetrafluoroterephthalonitrile, the monomers used for the preparation of the well-studied film-forming ladder polymer PIM-1 using a molar ratio of 1:1:2 (*Scheme* **2.7**).

(13)
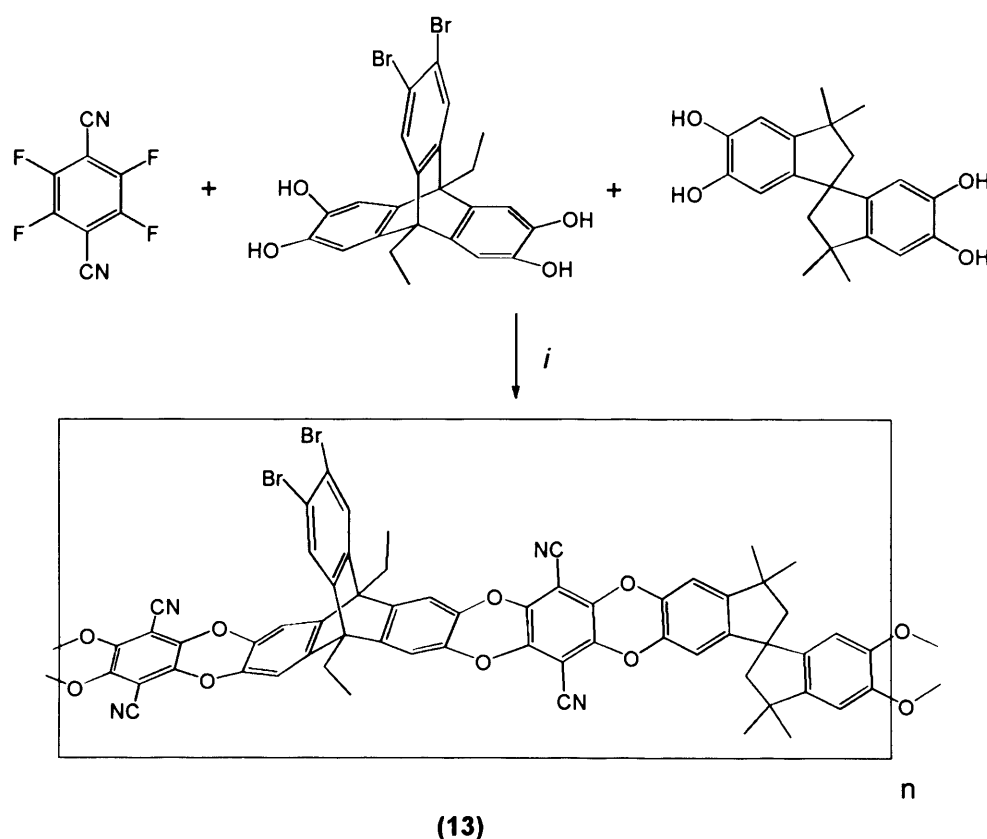
Scheme 2.7 Synthesis of dibromotriptycene-based co-polymer **(13)**. *Reagent and conditions*: (*i*) DMF, K$_2$CO$_3$, 60 °C, 48 h.

The resulting co-polymer **(13)** showed excellent solubility in chloroform and THF. The GPC analysis (THF) indicated an average molecular weight (M_w) of 69700 g mol^{-1}, which was sufficient to obtain a robust, self-standing and flexible film was casted from chloroform solution suitable for gas permeation studies.

The ^{1}H NMR spectroscopy for **(13)** showed broad peaks consistant with the anticipated structure of the copolymer and confirmed the presence of dibromo-triptycene unit in a 1:1 ratio relative to the tetramethyl-1,1'-spirobisindane unit, based on the integration ratio of the methyl groups (*Fig 2.6*).
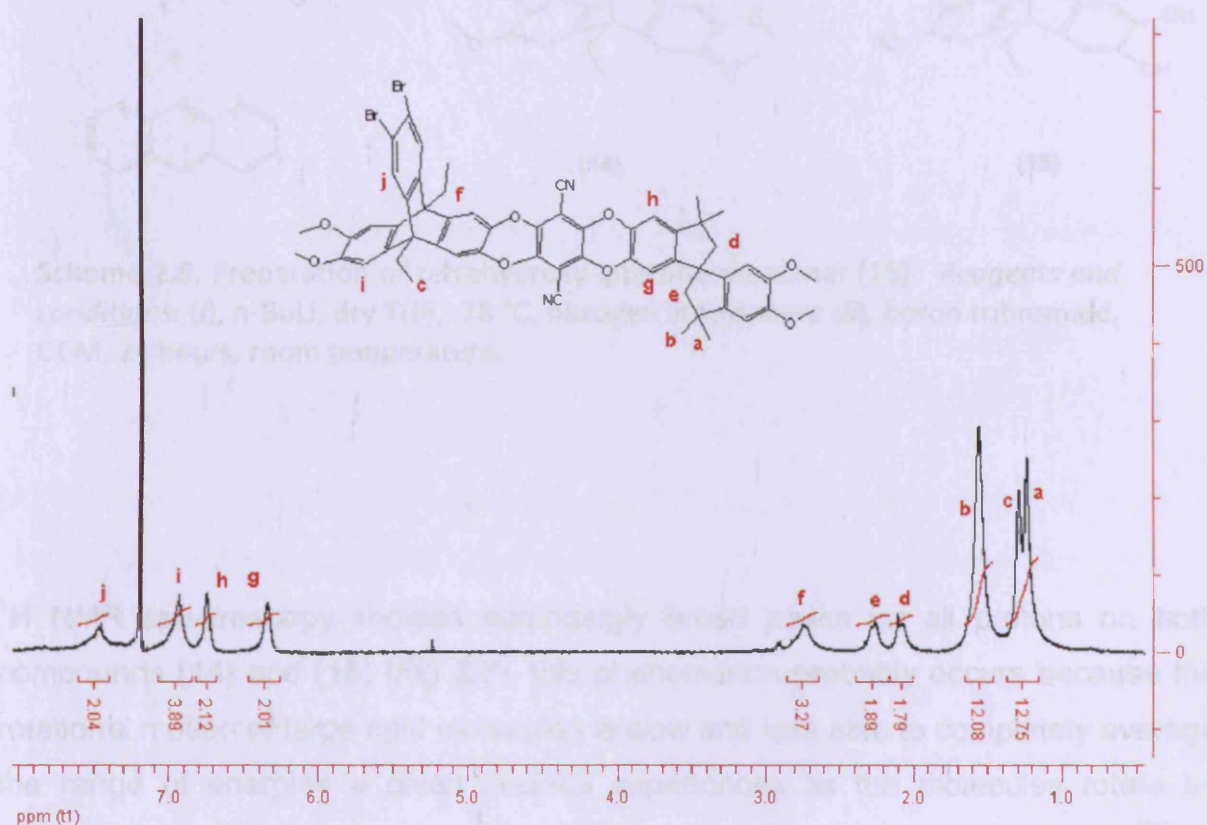
Figure 2.6. ^{1}HNMR spectra of dibromo-triptycene based co-polymer **(13)**.

2.7 Bitriptycene-based polymer

By performing a second Diels-Alder reaction on monomer **(10)**, a larger triptycene (termed *Iptycene*) monomer was obtained, this was achieved by adding one

equivalent of *n*-BuLi in THF to a mixture of **(10)** and an excess of anthracene in dry THF at -78 °C under nitrogen atmosphere to give **(14)** with an average yield of 40%. The demethylation of compound **(14)** using BBr₃ in dry DCM gave the corresponding catechol monomer **(15)** in high yield (95 %), (*Scheme 2.8*).
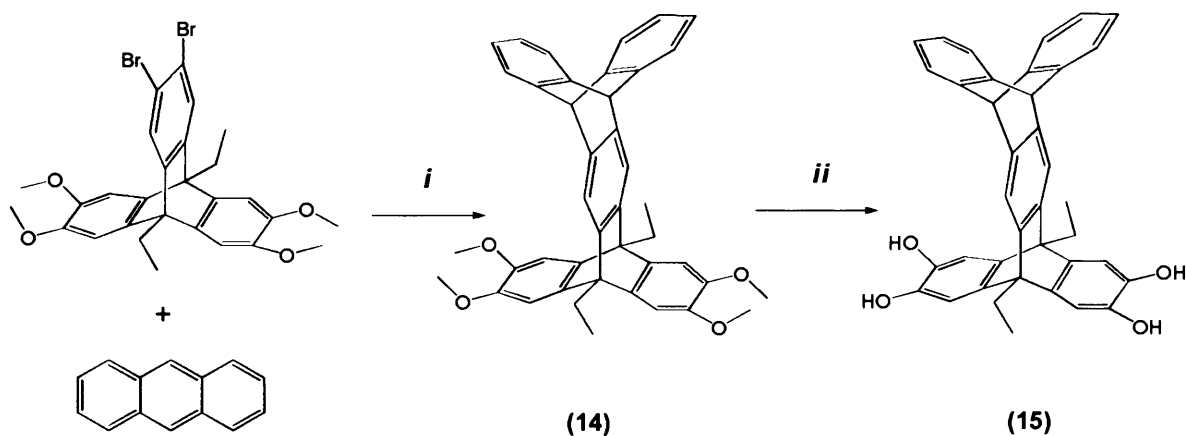
Scheme 2.8. Preparation of tetrahydroxy-iptycene monomer **(15)**. *Reagents and conditions*: (*i*), n-BuLi, dry THF, -78 °C, nitrogen atmosphere (*ii*), boron tribromide, DCM, 24 hours, room temperature.

¹H NMR spectroscopy showed surprisingly broad peaks for all protons on both compounds **(14)** and **(15)** (*Fig 2.7*), this phenomenon probably occurs because the rotational motion of large rigid molecules is slow and less able to completely average the range of energies a given nucleus experiences as the molecules rotate by diffusion through different orientations with respect to the applied magnetic field[81].
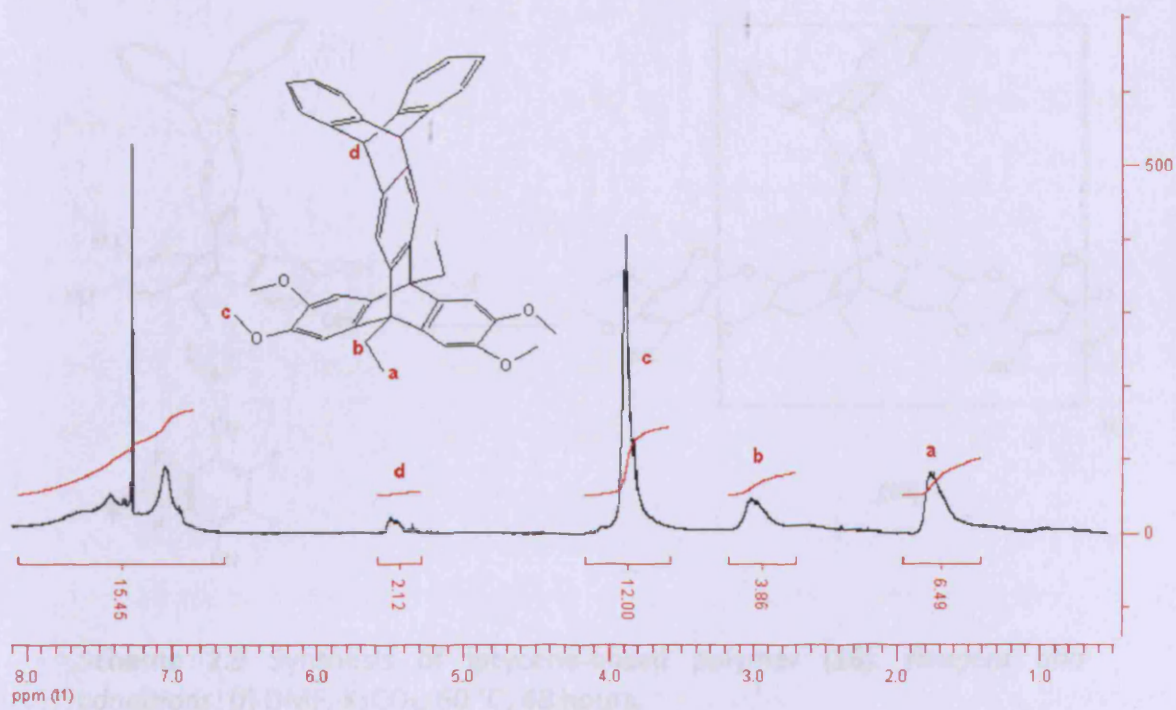
Figure 2.7. ¹H NMR spectra of compound **(14)** showing the unexpected peak broadening.

¹³C NMR spectroscopy failed to show any distinguishable peaks despite all attempts to change sample concentration and number of scans, however, mass spectroscopy confirmed the chemical formula of **(14)** and **(15)**.

The monomer **(15)** was reacted with a molar equivalent of 2,3,5,6-tetrafluoro-terephthalonitrile in the presence of potassium carbonate in DMF in anhydrous conditions, at a temperature of 60 °C to afford polymer **(16)** as an orange powder (*Scheme* **2.9**).

Scheme 2.9 Synthesis of iptycene-based polymer **(16)**. *Reagent and conditions:* (*i*) DMF, K_2CO_3, 60 °C, 48 hours.

The resulting product was found to be insoluble in all common organic solvents tested. Due to its insolubility, characterisation by solution NMR and GPC trace were not possible. The product was purified by refluxing in various organic solvents and was found to have an apparent BET surface area of 726 m^2 g^{-1}.

2.8 Characterisation of the triptycene-based polymers

The chemical structures of the polymers were evaluated by their elemental analysis. In general, the H, and N elemental analysis values agreed in a certain degree with the expected values for the proposed repeat units of the network polymers (*Table 2.1*).

Polymer	Yield %	C % (Calc.) Found	H % (Calc.) Found	N % (Calc.) Found	Br % (Calc.) Found
(5)	93	(76.34) 68.85	(2.71) 2.60	(5.69) 5.42	-
(9)	97	(73.35) 63.68	(3.58) 3.51	(6.26) 5.94	-
(12)	88	(58.92) 55.22	(2.45) 2.64	(4.29) 4.23	(24.98) 24.84
(13)	94	(65.78) 62.45	(3.26) 3.10	(5.03) 4.91	(14.37)17.35
(16)	91	(82.29) 72.63	(3.87) 3.47	(4.18) 3.97	-

Table 2.1. The elemental analyses for the triptycene network polymers

From the elemental analysis data, the percentage of carbon within the polymers is significantly lower than the expected values based on the idealised structures. This appears to be a general feature of PIMs and can be attributed both to the presence of unreacted hydroxyl and fluorine end-groups and to incomplete combustion during analysis (i.e. carbon formation). The microporosity may also play a role as water or solvent molecules (guests) may be trapped within inaccessible cavities or adsorbed prior to analysis.

2.81 Nitrogen adsorption analysis

The porosity of these polymers was assessed from their nitrogen sorption isotherm obtained at 77 K. All the isotherms show significant adsorption at low relative pressure (p/p° < 0.1) characteristic of a microporous material. The apparent BET surface areas were determined to be in the range 500- 940 $m^2 g^{-1}$ using a multi point BET calculation, which shows that these polymers have a significant amount of microporosity. The total pore volume was also determined and calculated from the amount of nitrogen adsorbed at a relative pressure p/p°= 0.98 and was found to be in the range of 0.42-0.58 $cm^3 g^{-1}$ (Table 2.2).

Polymer	BET surface area ($m^2 g^{-1}$)	Pore volume ($cm^3 g^{-1}$)
(5)	899	0.57
(9)	945	0.58
(12)	511	0.48
(13)	536	0.42
(16)	726	0.45

Table 2.2. BET surface area and pore volume values for triptycene polymers.

The desorption curve lies well above the adsorption curve for all samples leading to significant hysteresis extended to low relative pressure ($p/p^o > 0.4$) and is distinct from that associated with mesoporosity, which closes at a high relative pressure ($p/p^o > 0.4$)[82] and may be attributed either to a complex micropore structure incorporating throats and cavities, or to sorbate-induced swelling of a microporous materials[83].

Figure (2.8) represents the adsorption/desorption isotherm of prepared triptycene polymers as a powder sample, the volume of nitrogen adsorbed (V_{ads}) in cm^3 per gram of the adsorbent is plotted versus relative pressure (p/p^o).
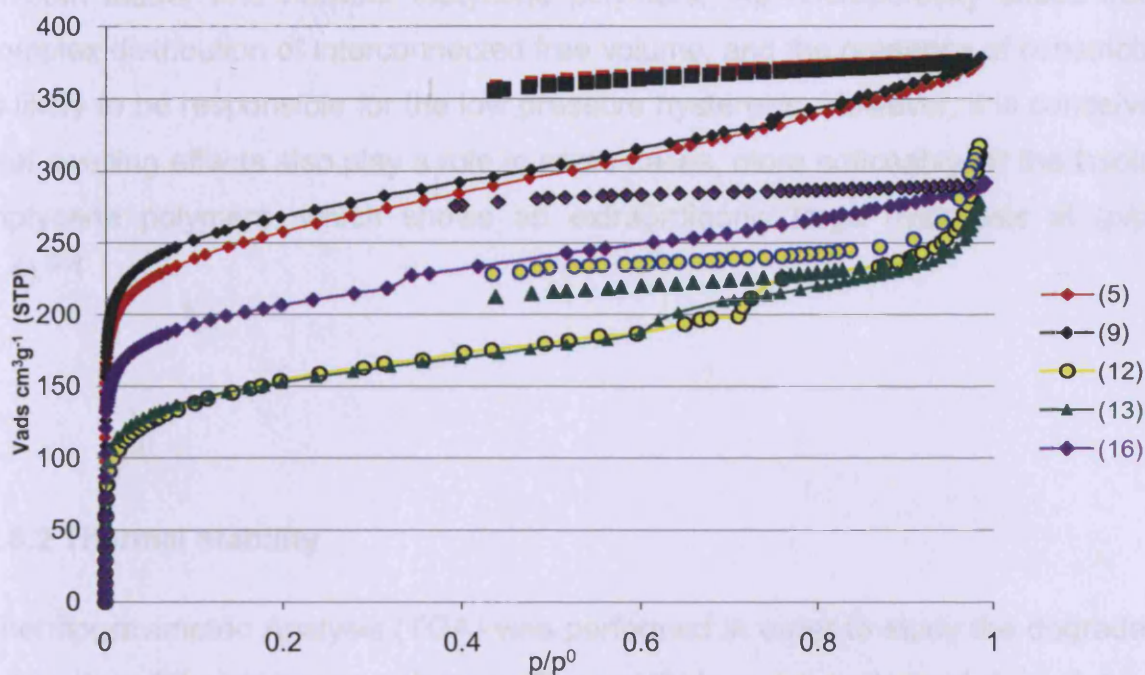
Figure 2.8. Nitrogen adsorption (solid lines)/desorption (dashed lines) isotherms at 77 K for ladder and network triptycene polymers.

Gas adsorption demonstrates that the network polymers possess a greater degree of microporosity relative to ladder polymers. However, the microporosity demonstrated by di(*sec*-but)-triptycene and dibenzyl-triptycene polymer is much lower than that obtained for the methyl or *iso*-propyl triptycene networks previously prepared (BET surface area = 1600-1700 m^2 g^{-1}).[28] This suggests that both the bridged benzyl and (*sec*)-butyl groups have a similar pore blocking effect to that demonstrated for longer chains (e.g. pentyl). It is noticeable that the lack of a network structure combined with the presence of the bromine substituent in polymer **(12)** reduces significantly the amount of N_2 adsorbed at (p/p°= 0.98. although this material is still has significant microporosity (apparent BET surface area > 500 m^2g^{-1}). This effect is also noticeable on the PIM-1/triptycene copolymer **(13)**, which has lower microporosity as compared to PIM-1.[26]

For polymer **(16)**, the second triptycene unit within the backbone of ladder polymer gave a non-network polymer with a relatively high degree of microporosity with an apparent BET surface area similar to that of PIM-1.

In both ladder and network triptycene polymers, the microporosity arises from a complex distribution of interconnected free volume, and the presence of constrictions is likely to be responsible for the low pressure hysteresis. However, it is conceivable that swelling effects also play a role in some cases, more noticeably for the insoluble triptycene polymers, which shows an extraordinarily large hysteresis at ($p/p°$ > 0.4).[28]

2.8.2 Thermal stability

Thermogravimetric Analysis (TGA) was performed in order to study the degradation properties of the triptycene polymers. The weight loss due to thermal degradation for these polymers commences at 400-450 °C; the close thermal degradation temperature range for these polymers is probably attributable to the similar initial mechanism involving the retro Diels-Alder of triptycene that occurs at relatively high temperature.

(TGA) profile showed a small mass loss between (2-5 %) for each polymer at lower temperature up to 250 °C which may be due to entrapped solvent or water. In all cases, thermal degradation in nitrogen results in a loss of mass of only 40-50 % of original weight up to 1000 °C, indicating that carbonization is occurring, which is consistent with the low values for carbon obtained during elemental analysis (*Fig. 2.9*).
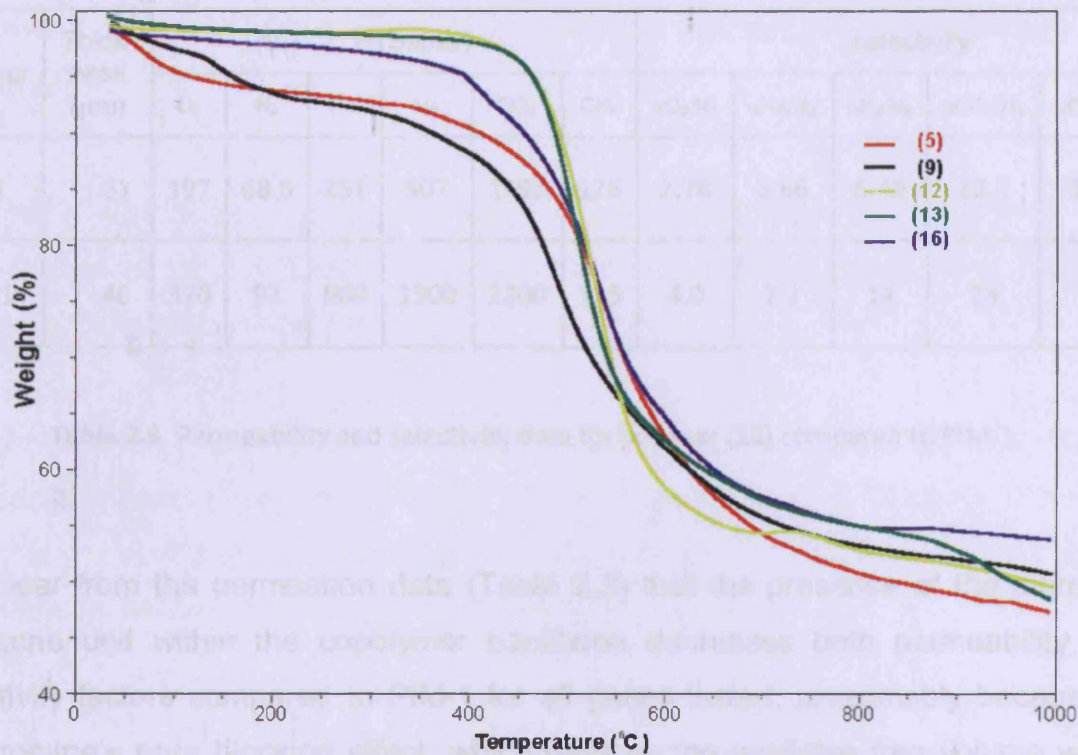
Figure 2.9. TGA profile for triptycene polymers (nitrogen)

It is noticeable from TGA curve that the greater the porosity of polymer the larger amount of solvents appears trapped within it.

2.8.3 Gas permeation measurements

Single-gas permeation experiments for polymer **(13)** were carried out by Dr. Detlev Fritsch, GKSS, Geesthacht, Germany. The results are given in Table **(2.3)**, which shows the gas permeability coefficient in Barrer (10^{-10} cm^3 [STP] cm cm^{-2} s^{-1} cmHg^{-1}) and ideal selectivity coefficient (P_x/P_{N2}) results for a solvent cast film of the polymer membrane. The order of permeability is CO_2 >H_2 >He >O_2 >CH_4 >N_2 which is the same as PIM-1.[26]

Polymer	Thickness (μm)	P (Barrer)						selectivity				
		O_2	N_2	He	H_2	CO_2	CH_4	$\alpha O_2/N_2$	$\alpha He/N_2$	$\alpha H_2/N_2$	$\alpha CO_2/N_2$	$\alpha CH_4/N_2$
(13)	61	197	68.6	251	507	1597	126	2.78	3.66	6.49	23.3	1.84
PIM-1	46	370	92	660	1300	2300	125	4.0	7.2	14	25	1.4

Table 2.3. Permeability and selectivity data for polymer **(13)** compared to PIM-1

It is clear from the permeation data (Table **2.3**) that the presence of the dibromo-triptycene unit within the copolymer backbone decreases both permeability and selectivity factors compared to PIM-1 for all gases tested, presumably because of the bromine's pore blocking effect, which reduces the available free volume within the structure.

Chapter 3. Synthesis and characterisation of biphenyl-based network polymers

The work described in this chapter is concerned with the synthesis and characterisation of substituted biphenyl-based network polymers using dioxane-forming polymerisation reaction.

The presence of substituents or a linkage on 2,2' positions restricts the free rotation between the phenyl rings and creates a site of contortion (*Fig. 3.1*), consequently reducing the ability of the materials from which they are composed to pack space efficiently, as will be demonstrated in this chapter.

Free rotation   Partially free   Restricted rotation
                      rotation

$R \neq H$
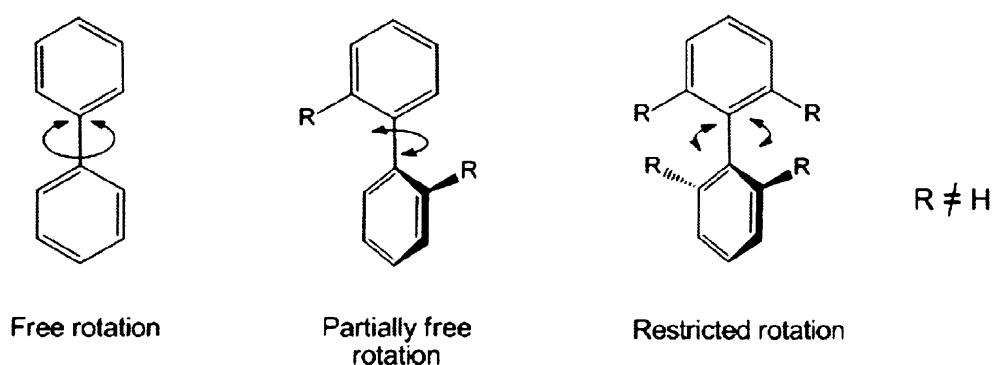
Figure 3.1. Substituent-rotation relationship of biphenyl unit.

The fused ring linking group is formed using an efficient double aromatic nucleophilic substitution reaction between linking monomer containing more than one catechol (1,2-dihydroxyaryl) and commercially available 2,2',3,3',5,5',6,6'-octafluoro-4,4'-dinitrilebiphenyl, in which, all fluorines are activated for nucleophilic aromatic substitution due to the presence of electron withdrawing groups on both phenyl rings.

A typical polymerisation procedure for the benzodioxane-forming reaction involves heating the reactants in DMF in the presence of K_2CO_3 at 70 °C for 48 hours. The crude product is isolated by addition of acidified water and simple filtration then washed with hot water then hot methanol, purification was accomplished by refluxing

in DMAc to remove unreacted starting materials and low molecular weight products then refluxing in THF then methanol to remove DMAc traces, drying in vacuum oven at 120 °C ensures the removal of most solvents traces.

3.1 Synthesis of biphenyl-based polymer (19)

The biphenyl-based polymer (19) was prepared using 3,3',4,4'-tetrahydroxy-biphenyl (17) as monomer, which could be readily synthesized as shown in Scheme (3.1). The coupling of 4-bromoveratrole (4-bromo-1,2-dimethoxybenzene) using n-buLi in THF at -78 °C gave 3,3',4,4'-tetramethoxy-biphenyl in 60 % yield following a literature procedure.[84] The corresponding 3,3',4,4'-tetrahydroxy-biphenyl (17) was obtained in high yield by demethylation using BBr3 in DCM.
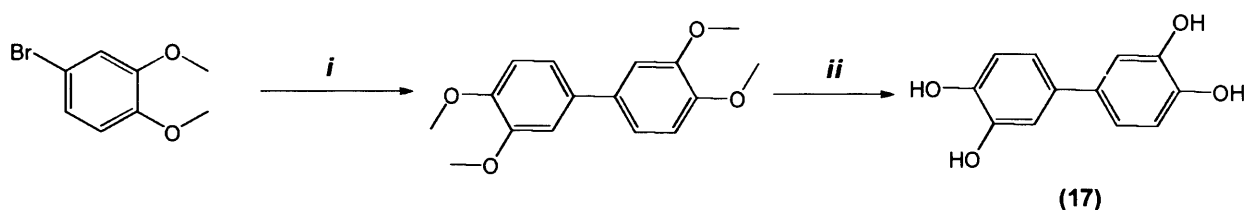
Scheme 3.1. Synthesis of 3,3',4,4'-tetrahydroxy-biphenyl. Reagents and conditions: (*i*) n-BuLi, THF, -78 °C. 12 hours (*ii*) BBr3, DCM, RT, 2h.

The reaction between 2,2',3,3',5,5',6,6'-octafluoro-4,4'-dinitrilebiphenyl (18) and two equivalents of 3,3',4,4'-tetrahydroxy-biphenyl (17) in DMF at 70 °C for 48 hours under anhydrous conditions afforded a network polymer in form of insoluble yellow powder (*Scheme 3.2*).
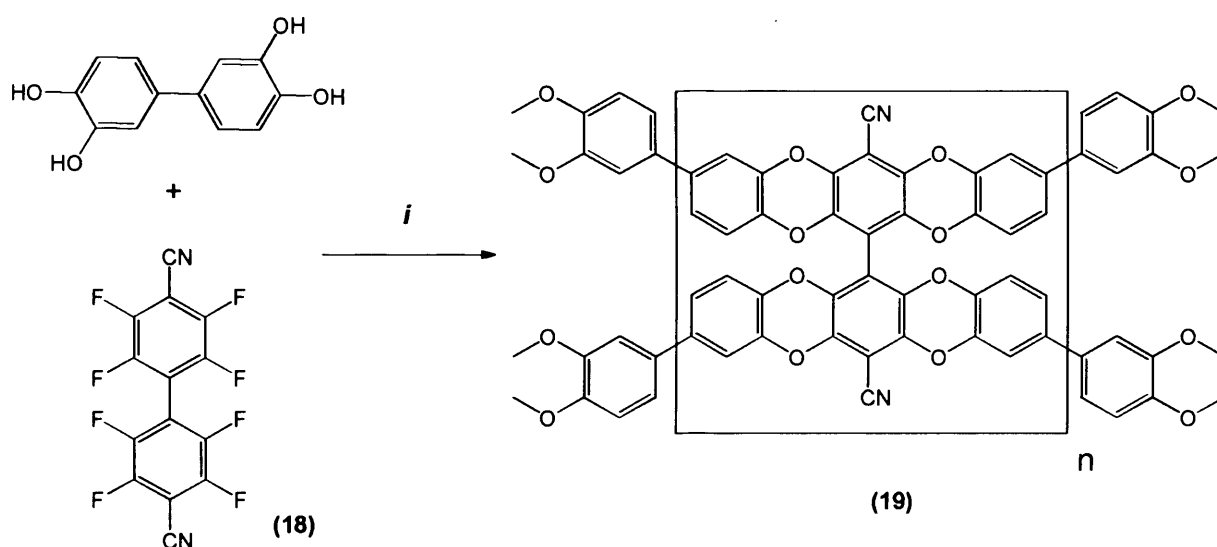
Scheme 3.2. Synthesis of polymer **(19)**. *Reagent and conditions*: (*i*) DMF, K₂CO₃, 70 °C, 48 hours.

Nitrogen sorption analysis at 77 K showed that the product has an apparent BET surface area of 920 $m^2 g^{-1}$.

3.2 Synthesis of biphenyl polymer (21) using anthracene monomer (20)

A substituted anthracene was used as the rigid linking group to prepare polymer **(21)**, the extended aromatic structure of anthracene was expected to provide additional free space within the polymer structure.

2,3,6,7-Tetramethoxy-9,10-dimethylanthracene was prepared by acid-catalysed condensation between acetaldehyde and veratrole at 0-5 °C in an average yield of 12%, demethylation of the methoxy groups using BBr₃ gave the corresponding 2,3,6,7-tetrahydroxy-9,10-dimethylanthracene **(20)** in 67 % yield (*Scheme 3.3*).
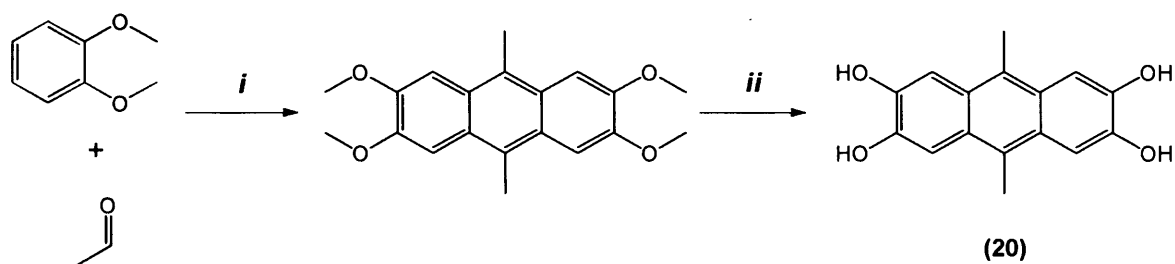
Scheme 3.3. Synthesis of 2,3,6,7-tetrahydroxy-9,10-dimethylanthracene. *Reagent and conditions*: (*i*) H₂SO₄, 0.5 hour. (*ii*) BBr₃, DCM, RT, 16h.

The reaction between 2,2',3,3',5,5',6,6'-octafluoro-4,4'-dinitrilebiphenyl and two equivalents of 9,10-dimethyl-2,3,6,7-tetrahydroxyanthracene **(20)** in DMF with an excess of K_2CO_3 under nitrogen at 70 °C for 48 hours afforded a network polymer **(21)** in the form of an insoluble yellow powder, which has an apparent BET surface area of 960 $m^2 g^{-1}$, (*Scheme 3.4*).
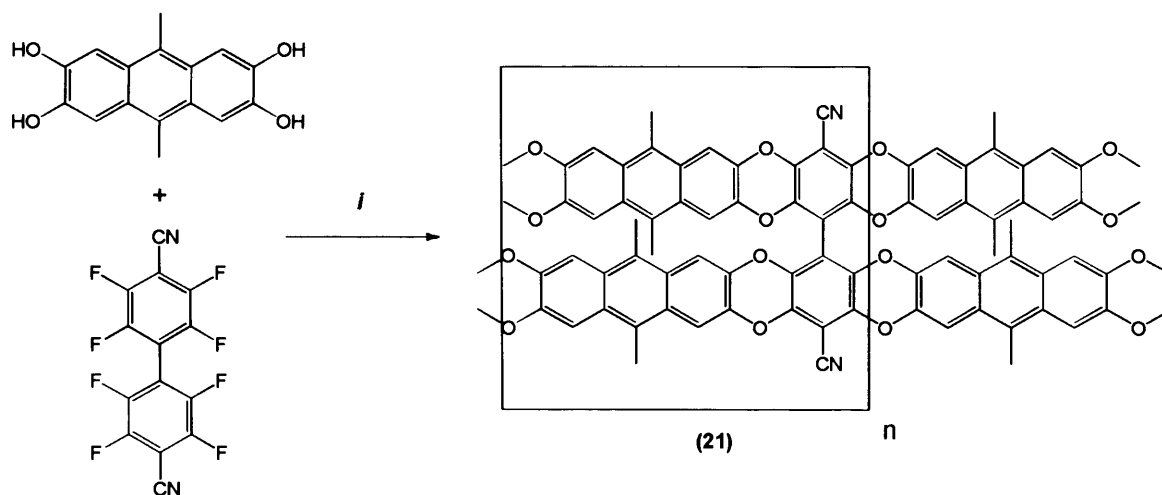
Scheme 3.4. Synthesis of polymer **(21)**. *Reagent and conditions*: (*i*) DMF, K_2CO_3, 70 °C, 48 hours.

3.3 Synthesis of biphenyl polymer (23) using 1,2,4,5-tetrahydroxy benzene (22)

Using a relatively small monomer with catechol end-groups such as 1,2,4,5-tetrahydroxybenzene as a bridging monomer to synthesis biphenyl-based polymer could lead to more defined structures with very small open cavities.

The monomer 1,2,4,5-tetrahydroxybenzene (22) was prepared by reduction of the commercially available 2,5-dihydroxy-1,4-benzoquinone using tin powder in concentrated HCl according to the literature[85], which was polymerised with 2,2',3,3',5,5',6,6'-octafluoro-4,4'-dinitrile-biphenyl in ratio of (2:1) in DMF and in excess of K_2CO_3 under nitrogen atmosphere at 70 °C to yield insoluble product consistent with the formation of a network polymer (Scheme 3.5).
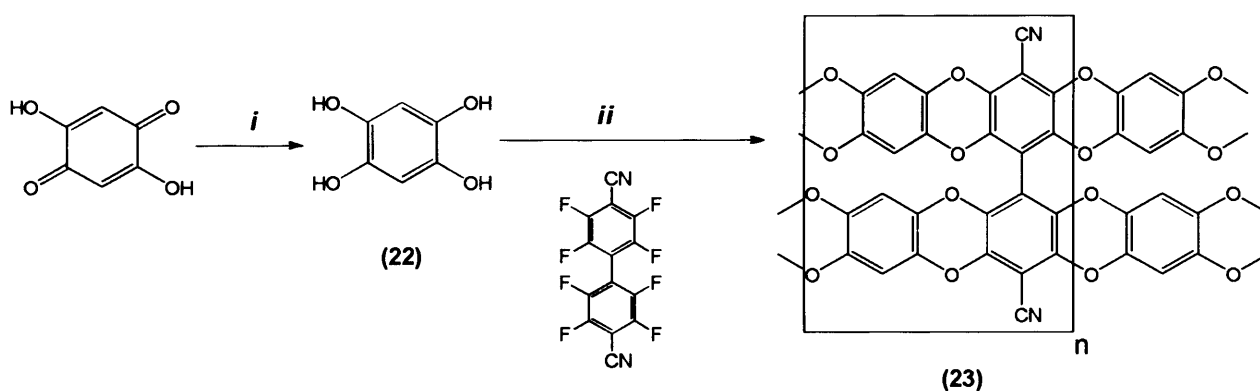
Scheme 3.5. Synthesis of polymer (23). Reagent and conditions: (i) Tin, HCl, reflux, 1 hour (ii) DMF, K_2CO_3, 70 °C, 48 hours.

Standard work-up and purification procedures has afforded (23) as insoluble brown powder, which found to has an apparent BET surface area of 887 $m^2 g^{-1}$.

3.4 Synthesis of polymer (25) using hexahydroxytriphenylene (24)

By incorporating the large flat triphenylene structure as the bridging monomer between the hindered rotation biphenyl unit, polymer (25) was synthesised by thermal polymerisation condensation between 2,2',3,3',5,5',6,6'-octafluoro-4,4'-

dinitrilebiphenyl   2,3,6,7,10,11-hexahydroxytriphenylene **(24)** in the ratio of 3:4 respectively in DMF and in excess of K_2CO_3 under nitrogen atmosphere at 70 °C for 48 hours (*Scheme 3.6*).
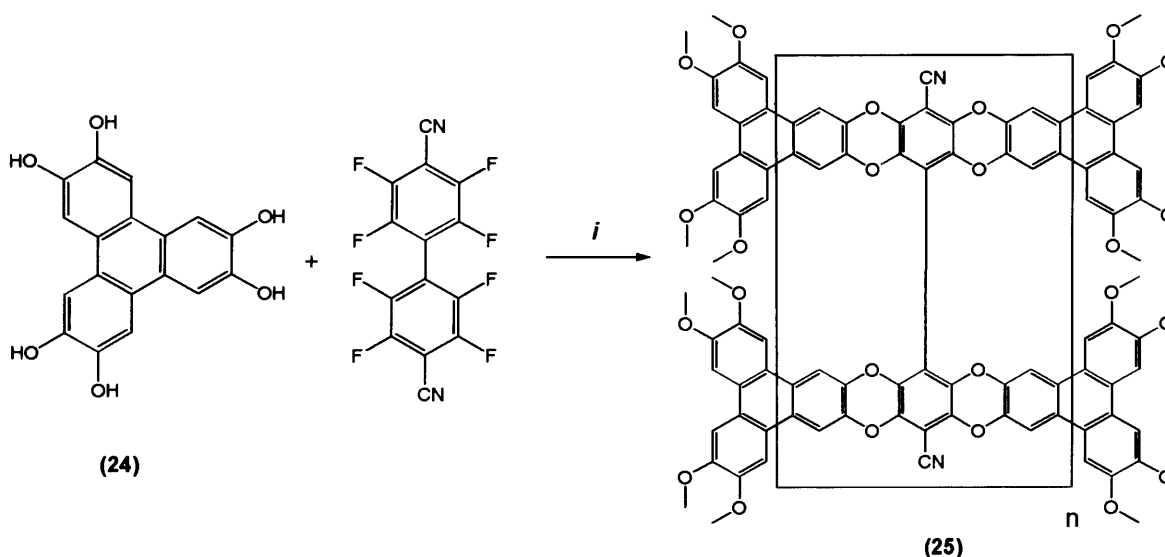
Scheme 3.6. Synthesis of polymer **(25)**. *Reagent and conditions*: (*i*) DMF, K_2CO_3, 70 °C, 48 hours.

Standard work-up and purification procedures gave **(25)** as insoluble dark brown powder, which was found to have an apparent BET surface area of 860 $m^2 g^{-1}$.

3.5 Synthesis of polymer (27)

The approach of synthesizing biphenyl-based polymers was extended by using a highly rigid and non-planar linking tetrol monomer, the presence of the ethylene bridge on 2,3,6,7-tetrahydroxy-9,10-dimethyl-9,10-ethanoanthracene forces the molecule to adapt a non-planar geometry. The required monomer was prepared in good yield by the acid-catalyzed condensation between 2,5-hexanedione and catechol according to a published procedure.[86]

Scheme 3.10. Synthesis of 2,3,6,7-tetrahydroxy-9,10-dimethyl-9,10-ethano-anthracene **(26)**. *Reagent and conditions*: (*i*) H_2SO_4 (70 %), RT, 7 days.

The polymerisation reaction between 2,3,6,7-tetrahydroxy-9,10-dimethyl-9,10-ethanoanthracene **(26)** and 2,2',3,3',5,5',6,6'-octafluoro-4,4'-dinitrilebiphenyl in (2:1) molar ratio was achieved using the standard conditions (*Scheme 3.11*).

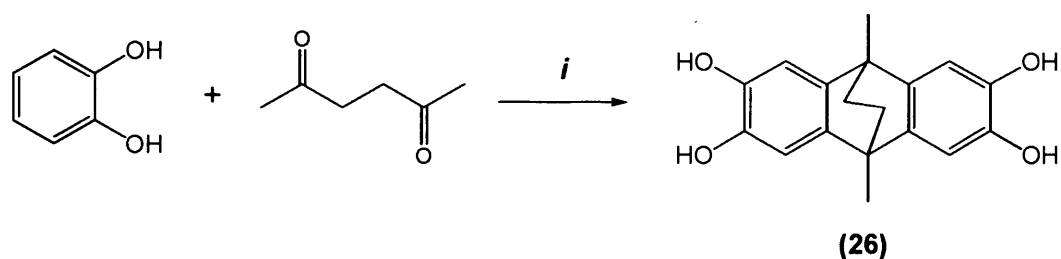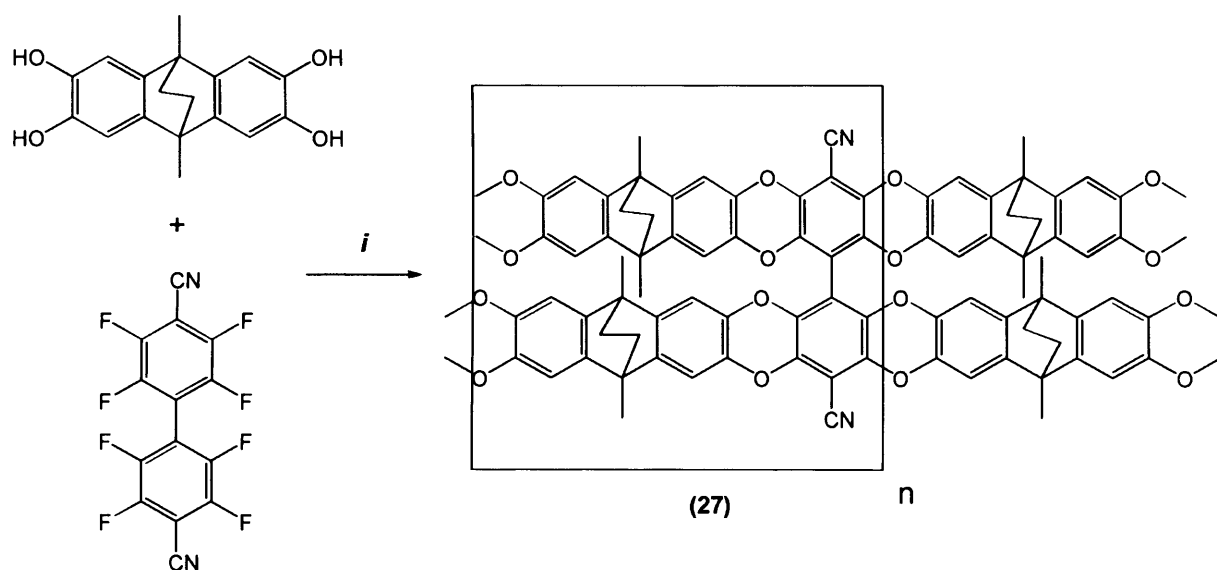**Scheme 3.11.** Synthesis of polymer **(27)**. *Reagent and conditions*: (*i*) DMF, K_2CO_3, 70 °C, 48 hours.

Typical work up and purification procedure afforded polymer **(27)** as a yellow powder, it appears that the bridged anthracene moiety within polymer structure has improved the overall porosity of **(27)** giving a BET surface area of 1309 m^2 g^{-1}.

3.6 Characterisation of biphenyl-based polymers

The chemical structures of the biphenyl-based network polymers were evaluated by their elemental analysis, which indicates the carbon percentage is significantly lower than the expected value based on the idealized polymer structures, H, and N elemental analysis values agreed to some extent with the expected values for the proposed repeat units of the network polymers (Table 2.4).

Polymer	Yield %	% C (Calc.) Found	% H (Calc.) Found	% N (Calc.) Found
(19)	94	(73.08) 66.18	(1.94) 2.21	(4.48) 4.55
(21)	88	(75.83) 70.94	(2.77) 2.77	(3.84) 3.98
(23)	90	(66.12) 63.34	(0.85) 1.09	(5.93) 6.22
(25)	78	(73.56) 69.64	(1.30) 2.85	(4.51) 3.45
(27)	79.5	(76.45) 70.61	(3.57) 3.41	(3.57) 4.14

Table 2.4. The elemental analyses results of biphenyl-based polymers.

The fluctuation of measured hydrogen and nitrogen percentage may be due to the tendency of the network polymers to hold water or solvent via intermolecular hydrogen bonding interactions as will be demonstrated in TGA profiling. Carbon analysis variations for all polymer adds to a growing body of evidence to suggest the microporous materials do not completely combust during analysis probably due to forming thermally stable carbides with foreign molecules trapped within deep cavities.

3.6.1 Nitrogen adsorption analysis

The porosity of powdered samples of the biphenyl-based polymers was assessed from their nitrogen sorption isotherms acquired at 77 K (Fig. **3.2**).
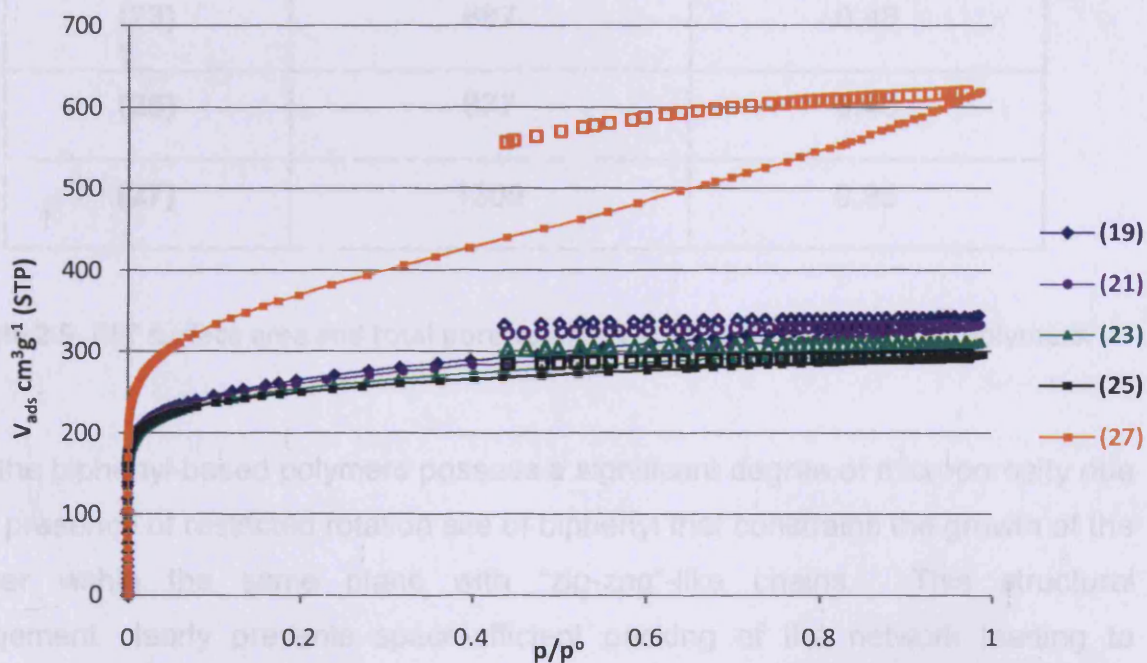
Figure 3.2. The nitrogen adsorption (solid line) /desorption (dashed line) isotherm for a powder sample of biphenyl-based polymers at 77 K.

All nitrogen adsorption isotherms demonstrate significant adsorption at low relative pressure (p/p^0 <0.01), this indicates the presence of a significant proportion of micropores (pore size < 2 nm). The apparent BET surface areas are within the range 660-1310 m^2 g^{-1} and their total pore volume was also determined and calculated from the amount of nitrogen adsorbed at a high relative pressure (p/p^o = 0.98) giving a range of 0.46-0.95 $cm^3 g^{-1}$ (*Table 2.5*).

Polymer	BET surface area (m² g⁻¹)	Pore volume (cm³ g⁻¹)
(19)	929	0.53
(21)	912	0.51
(23)	887	0.48
(25)	877	0.46
(27)	1309	0.95

Table 2.5. BET surface area and total pore volume values for biphenyl-based polymers.

All of the biphenyl-based polymers possess a significant degree of microporosity due to the presence of restricted rotation site of biphenyl that constrains the growth of the polymer within the same plane with "zig-zag"-like chains. This structural arrangement clearly prevents space-efficient packing of the network leading to substantial microporosity. Network polymers **19-25** demonstrate very similar nitrogen isotherms. Even using a monomer within which was an aryl-aryl bond with free rotation **(17)** to prepare a network **(19)** did not appear to compromise its microporosity. Polymer **(27)** clearly shows the highest surface area and pore volume among the series with the etheno-bridged anthracene unit providing additional intrinsic microporosity. This unit has structural features related to the triptycene unit for which polymers of even high microporosity were obtained previously (e.g. apparent BET surface area up to 1600 m² g⁻¹).

To prove that the porosity of these biphenyl-based polymers is mainly generated from hindered rotation on 2,2' position of biphenyl unit, 3,3',4,4'-tetrahydroxy-biphenyl **(17)** was polymerised with 2,3,5,6-tetrafluoroterephthalonitrile using the standard procedure to give a product with minimal surface area (Fig. **3.3**)
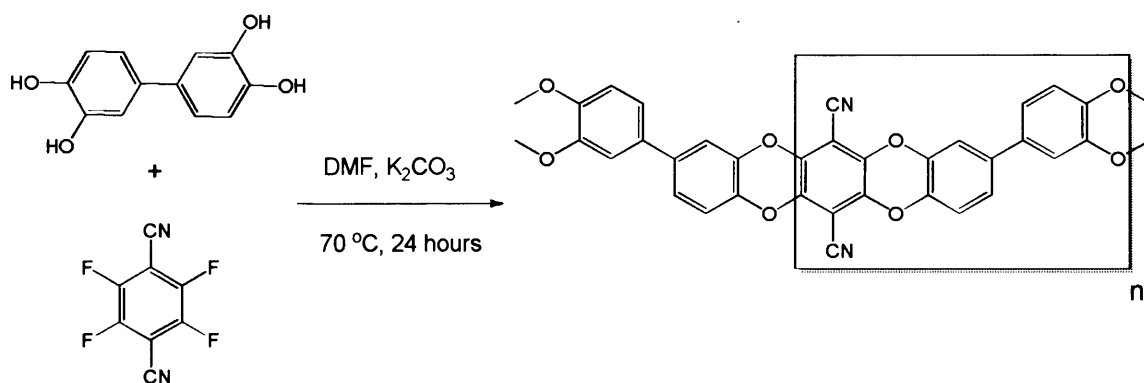
Figure 3.3. Non-porous biphenyl-based polymer

This result demonstrates the role of 2,2'-substituted biphenyl units to provide "awkward" and rigid macromolecular shapes that cannot pack space efficiently in which rotation is severely hindered creating highly rigid and contorted molecular structures.

3.6.2 Thermal stability

The thermal stability of the biphenyl-based polymers was evaluated by thermogravimetric analysis (TGA) under a nitrogen atmosphere at a heating rate of 10 °C per minute and up to 1000 °C. Generally, the weight loss due to thermal degradation for these polymers begins between 450-510 °C, the total weight loss before carbonisation was between 36-46 % of the stating weight.

All the polymers show a weight loss of between 1-4 % at low temperature up to 250 °C. This is probably due to loss of moisture and/or entrapped solvent, the TGA curve of prepared biphenyl polymers is shown in figure **(3.4)**.
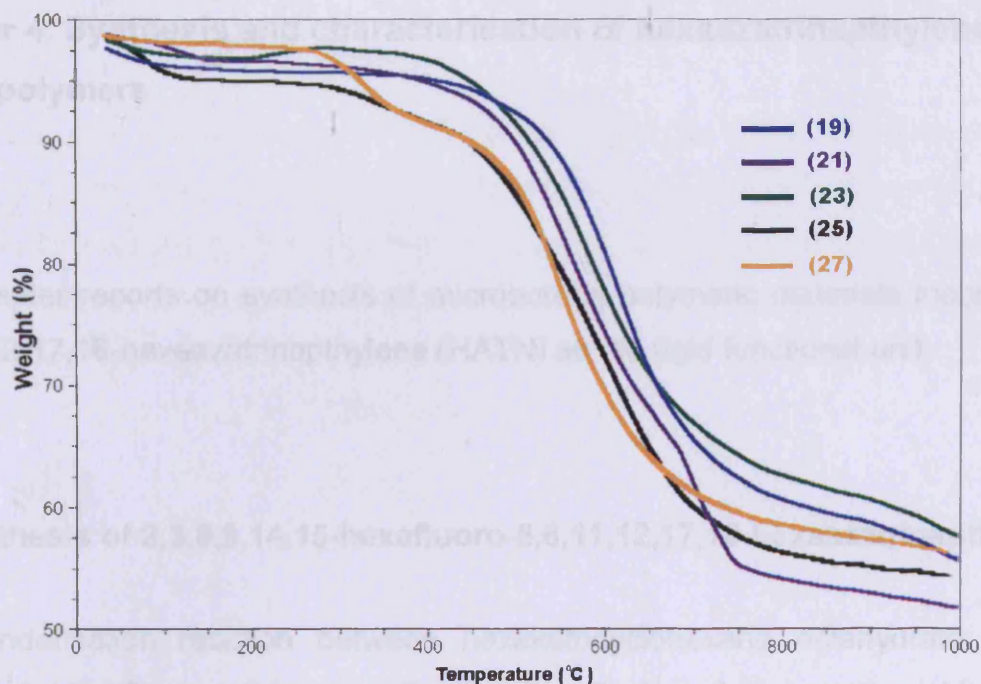
Figure 3.4. TGA analysis profile for biphenyl polymers (nitrogen atmosphere).

Polymer **(27)** shows a degradation peak around 300 °C presumably due to the loss of bridged ethane group first, the 8% weight loss at this temperature is consistent with percentage of ethane loss (~ 7.5 %) from the ideal structure. With the exception of polymer **(25), t**he similar temperature range for the degradation of the polymers is probably attributed to the similar structural features contained within the networks. In all cases, thermal degradation in nitrogen results in a loss of mass of only 40-50 % of original weight up to 1000 °C.

Chapter 4. Synthesis and characterisation of hexaazatrinapthylene-based polymers

This chapter reports on synthesis of microporous polymeric materials incorporating 5,6,11,12,17,18-hexaazatrinapthylene (HATN) as the rigid functional unit.

4.1 Synthesis of 2,3,8,9,14,15-hexafluoro-5,6,11,12,17,18-hexaazatrinapthylene

The condensation reaction between hexaketocyclohexane octahydrate and an excess of 4,5-difluoro-1,2-benzenediamine in refluxing glacial acetic acid afforded 2,3,8,9,14,15-hexafluoro-5,6,11,12,17,18- hexaazatrinapthylene (HATN(F)$_6$) **(28)** in high yield (78 %).
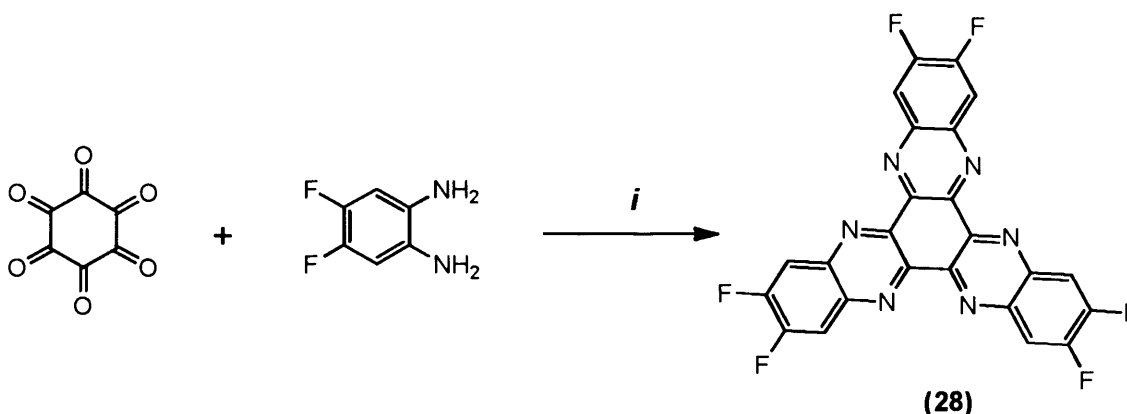
Scheme 4.1. Synthesis of *HATN(F)$_6$*. *Reagents and conditions:* (*i*) Acetic acid, reflux, 16 h.

The product **(28)** showed a little solubility in common organic solvents at room temperature, nevertheless, it was sufficiently soluble in chloroform to allow confirmation of the structure of **(28)** by ^{1}H NMR and ^{13}C NMR spectroscopy. High-Resolution Mass Spectrometry (HRMS) also confirmed the expected structure of **(28)**.

4.2 Synthesis of substituted tetrafluoro-HATN monomer

By blocking one active polymerisation site of HATN(F)$_6$ **(28)**, a suitable monomer **(29)** for forming ladder polymers (i.e. non-network polymers) and co-polymers is obtained. This was achieved by reacting 2,3,8,9,14,15-hexafluoro-5,6,11,12,17,18-hexaazatrinapthylene **(28)** with a molar equivalent of 3,5-di-tert-butylcatechol in DMF in presence of excess of K$_2$CO$_3$ (*Scheme 4.2*).
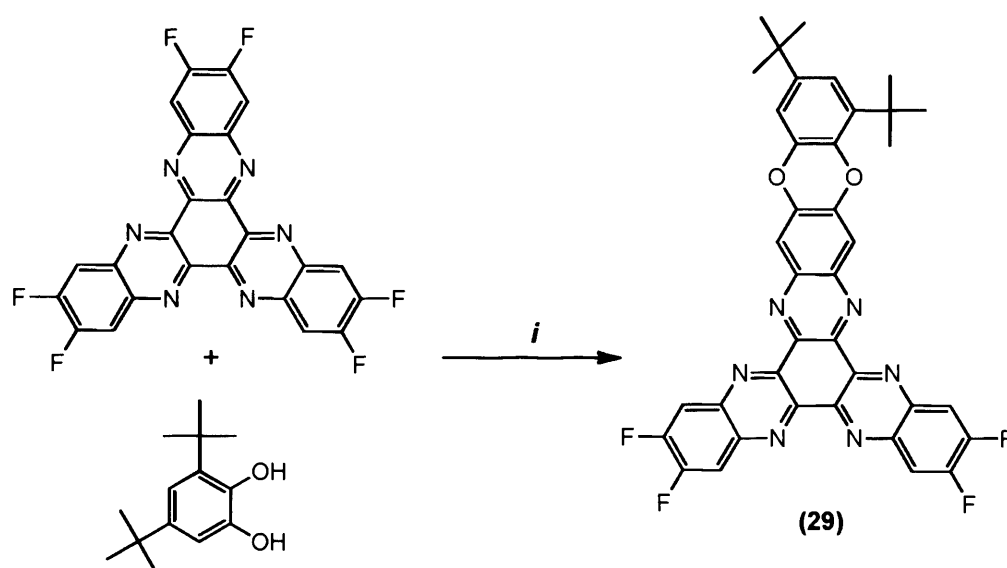
Scheme.4.2. Synthesis of tetrafluoro substituted HATN **(29)**. *Reagents and conditions:* (*i*) DMF, K$_2$CO$_3$, 130 °C, 2 hours.

This reaction was performed at different temperatures starting with slow addition of the catechol, but side products (di and tri-substituted HATN) always resulted in considerable yield. In order to optimize the yield of **(29)**, it was found that mixing the reactants at high temperature (130 °C) prior to the addition of base was required to achieve a controlled reaction with a reasonable 42 % yield. In contrast to HATN(F$_6$), compound **(29)** shows excellent solubility in various organic solvents at room temperature.

4.3 Model HATN reaction

In order to determine the feasibility of using monomers **(28)** and **(29)** in the aromatic nucleophilic reaction with catechol anions to form the dibenzo[1,4]dioxane linkages and to optimise the reaction conditions for polymerization, a model compound was prepared by reacting the monomers **(28, 29)** with excess of 3,5-di-tert-butylcatechol in anhydrous DMF and monitoring the reaction progress by TLC. It was found that any temperature above 70 °C was sufficient to convert **(28 or 29)** to fully substituted HATN compound **(30)**, (*Scheme 4.3*). This compares favourably to the equivalent with chlorine-containing monomer HATN(Cl₆) for which the model reaction was preformed at 120 °C.[27]
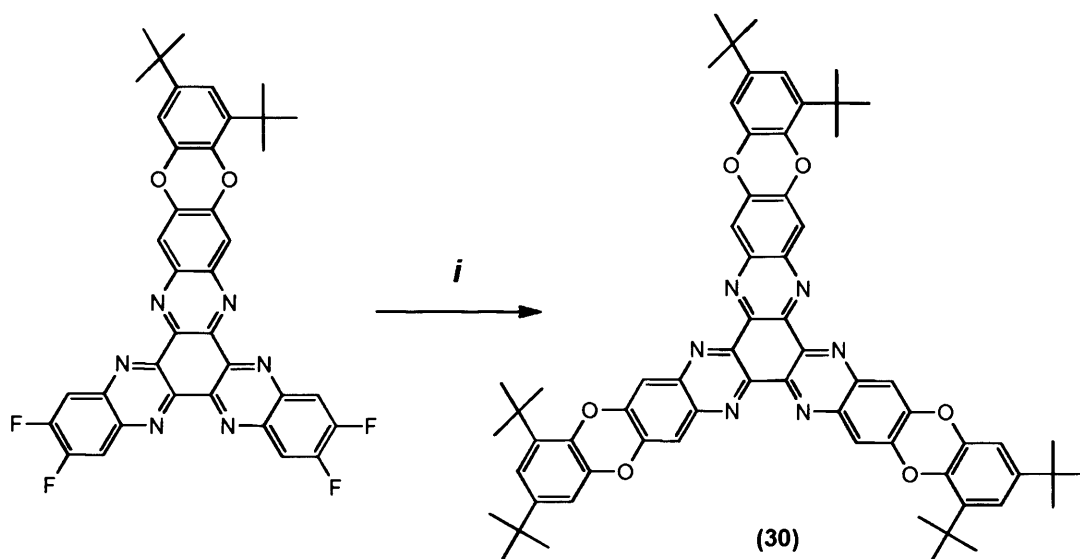
Scheme 4.3. Synthesis of HATN model compound. *Reagents and conditions:* (*i*) 3,5-di-tert-butylcatechol (excess), K₂CO₃, DMF, 70 °C.

4.4 Polymerisation of prepared fluorinated HATN monomers

The rigid, flat monomers **(28, 29)** were used to prepare microporous polymeric materials by employing benzo[1,4]dioxane formation reactions with different catechol monomers based on a double nucleophilic aromatic substitution (S_NAr) reaction of

the aryl fluorides with catecholate anions. As for the model compound described above, the general procedure involved heating molar equivalents of reactants in DMF in the presence of K_2CO_3 at 70 °C for 24 hours. Dry conditions were essential to avoid side reactions and all reactions were carried out under inert dry atmosphere using excess anhydrous potassium carbonate to ensure full catechol conversion into the more reactive catechol dianion. In each case, the crude product was isolated by the addition of acidified water and simple filtration. Purification was achieved by washing with hot water to remove any salts, followed by refluxing in different organic solvents to remove unreacted starting materials and low molecular weight products.

4.4.1 Synthesis of HATN-based network polymers

The hexaazatrinapthylene-based polymer (31) was prepared by thermal poly-condensation between equimolar amounts of 2,3,8,9,14,15-hexafluoro-5,6,11,12,17,18-hexaazatrinapthylene (28) and commercially available 2,3,6,7,10,11-hexahydroxy-triphenylene in DMF and in presence of K_2CO_3 at 70 °C (Scheme 4.4).
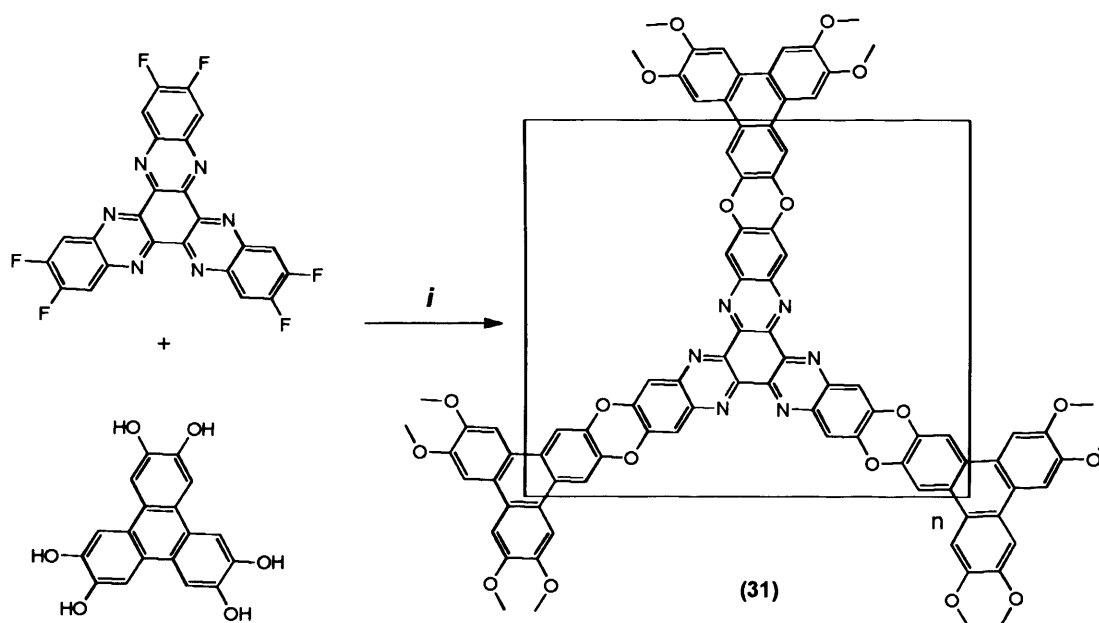
Scheme 4.4. Synthesis of polymer (31). Reagents and conditions: (i) K_2CO_3, DMF, 70 °C.

The resulting polymer was found to be insoluble in any organic solvent tested. Nitrogen sorption isotherms confirmed the presence of significant microporosity within the structure with an apparent BET surface area of 1180 m^2 g^{-1} and a very large total pore volume (1.74 mL g^{-1}).

To explore further the effect of the molecular structure of the bridging monomer on the microporosity of the HATN monomer, an anthracene unit was introduced. Polymer **(32)** was prepared high yield by the reaction between **(28)** with 2,3,6,7-tetrahydroxy-9-10-dimethylanthrace **(20)** in a molar ratio of (2:3), respectively (*Scheme 4.5*).
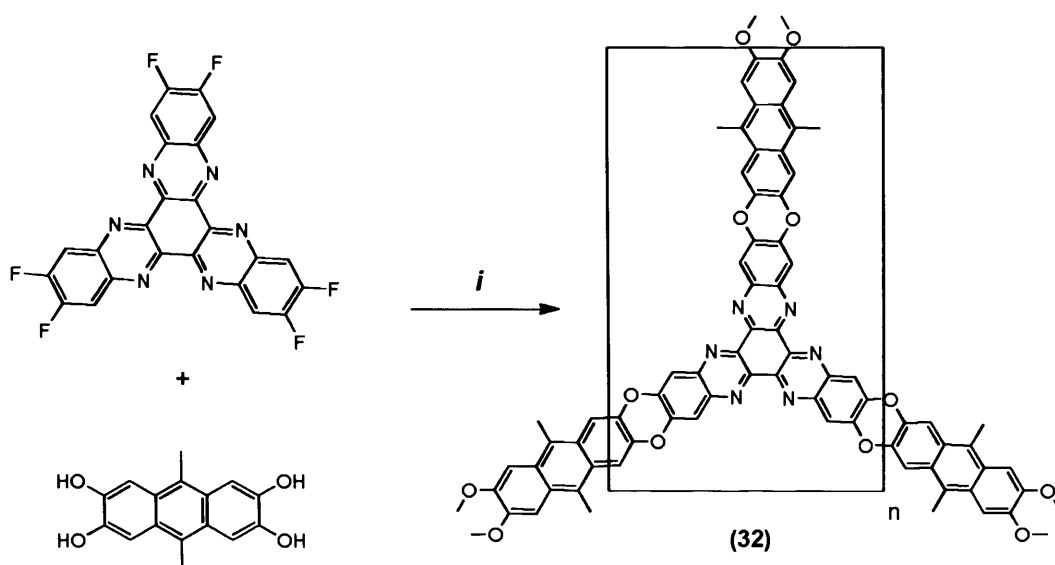
Scheme 4.5. Synthesis of polymer **(32)**. *Reagents and conditions:* (*i*) K$_2$CO$_3$, DMF, 70 °C

Using the same synthetic procedure, the smaller tetrol, 1,2,4,5-tetrahydroxybenzene **(22)** was used to prepare the network polymer **(33)** by its reaction with 2,3,8,9,14,15-hexafluoro-5,6,11,12,17,18-hexaazatrinapthylene **(28)** (*Scheme 4.6*).

71
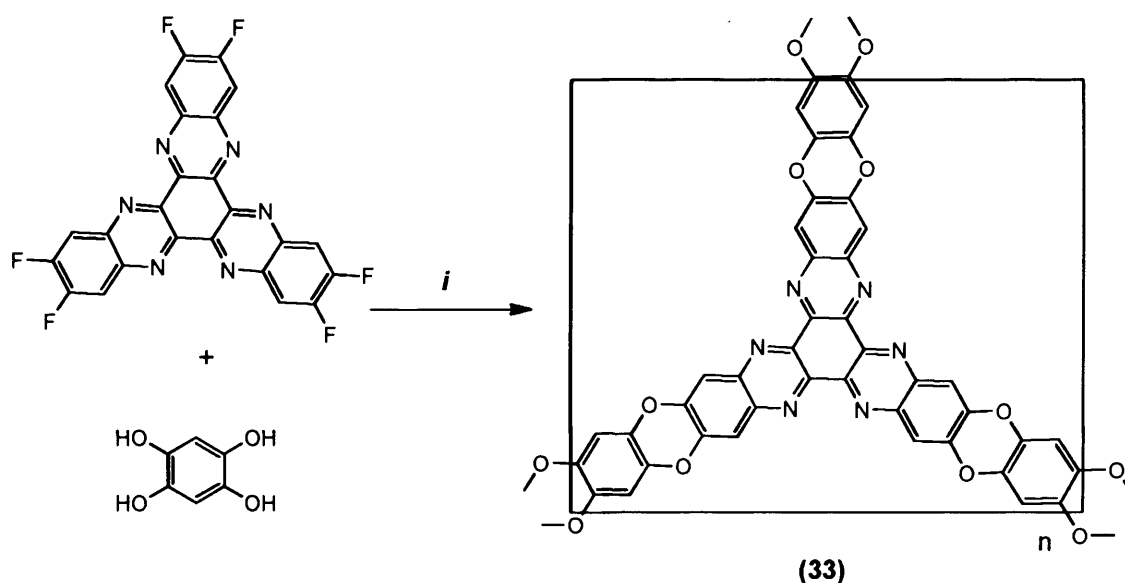
Scheme 4.6. Synthesis of polymer **(33)**. *Reagents and conditions:* (*i*) K₂CO₃, DMF, 70 °C.

Another HATN-based network was prepared using a monomer containing a spiro centre that would prevent the flat alignment of polymer chains. Thus, polymer **(34)** was prepared by the reaction between 2,3,6,7-tetrahydroxy-9,10-dimethyl-9,10-ethanoanthracene **(26)** and 2,3,8,9,14,15-hexafluoro-5,6,11,12,17,18-hexaazatri-phenylene **(28)** in DMF in presence of K₂CO₃ under nitrogen (Scheme **4.7**).
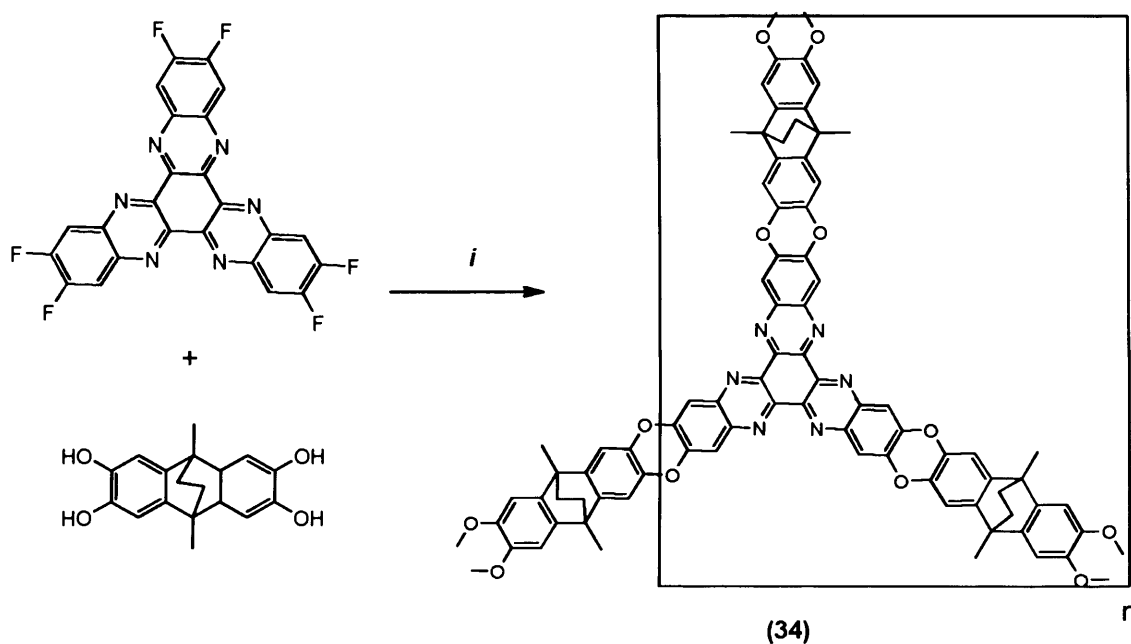
Scheme 4.7. Synthesis of polymer **(34)**. *Reagents and conditions:* (*i*) K₂CO₃, DMF, 70 °C.

4.4.2 Synthesis of HATN ladder polymer

By reacting the difunctional HATN monomer **(29)** with an aromatic tetrol containing a site of contortion, it was hoped to obtain a soluble microporous HATN-based ladder polymer. Hence, commercially available 5,5',6,6'-tetrahydroxy-3,3,3',3'-tetramethyl-1,1'-spirobisindane was used to prepare the HATn-based ladder polymer **(35)** in over 90 % yield (*Scheme 4.7*).
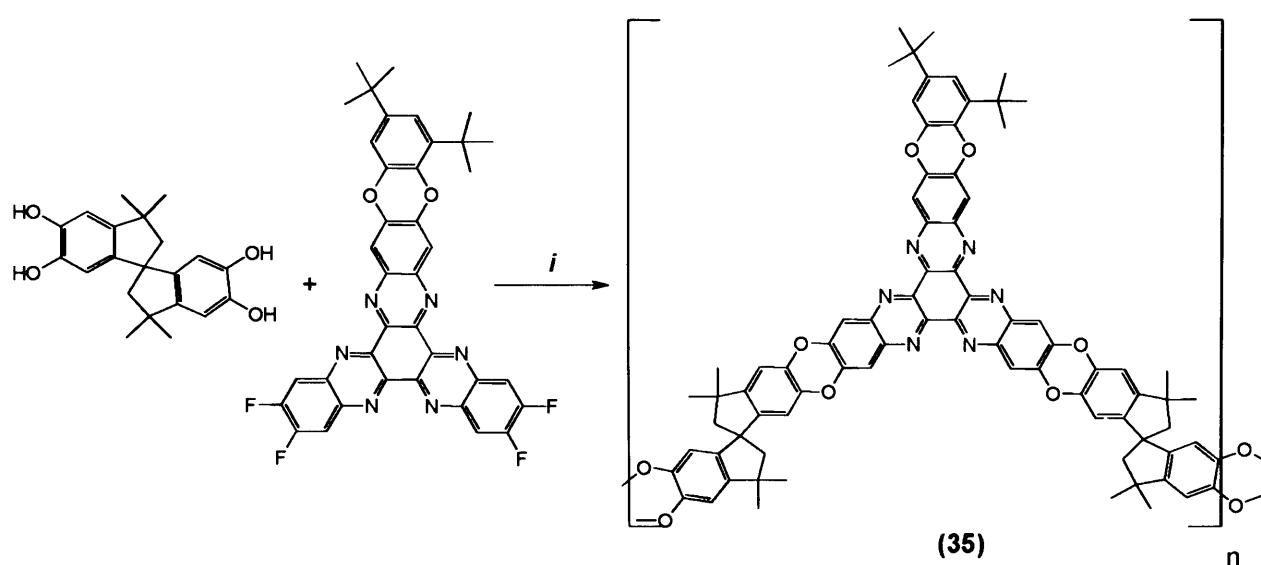
Scheme 4.7. Synthesis of polymer **(35)**. *Reagents and conditions:* (*i*) K$_2$CO$_3$, DMF, 70 °C.

The resulting orange product was found to be insoluble in any organic solvent but has an apparent BET surface area of 756 m^2 g^{-1} at 77 K.

Same procedure was employed for monomer **(29)** by reacting it with previous catechol compounds (2,3,6,7,10,11-hexahydroxytriphenylene, 2,3,6,7-tetrahydroxy-9-10-dimethylanthracene and 1,2,4,5-tetrahydroxbenzene) to give insoluble products with minimal apparent BET surface areas, which were not characterized further.

4.5 Characterisation of HATN-based polymers

As for previously described materials, the HATN-based polymers were evaluated by elemental analysis. In general, the percentage of carbon within the polymers is significantly lower than the expected values based on the idealized structures (Table *4.1*).

Polymer	Yield %	% C (Calc.) Found	% H (Calc.) Found	% N (Calc.) Found
(31)	96	(72.41) 63.63	(1.72) 3.67	(12.07) 9.96
(32)	97	(74.06) 66.13	(3.70) 3.45	(10.80) 11.30
(33)	93	(67.63) 60.13	(1.54) 2.20	(14.34) 15.03
(34)	90	(74.72) 66.78	(3.30) 3.66	(10.26) 9.29
(35)	93	(75.72) 64.14	(4.91) 5.37	(8.98) 7.10

Table 4.1. The elemental analyses results of HATN-based polymers.

In contrast, the elemental analysis data for hydrogen shows a greater amount than expected. This may be due to the tendency of the HATN unit to form hydrates *via* intermolecular hydrogen bonding interactions involving the aza-nitrogens, allowing for a water molecule to be associated with each of the three binding sites of the each HATN unit.[27]

4.5.1 Nitrogen adsorption analysis

The porosity of HATN-based polymers was assessed from their nitrogen sorption isotherms. The BET surface areas were found to be within the range 550-1180 $m^2 g^{-1}$. The total pore volume was also determined from the amount of nitrogen adsorbed at a relative pressure $p/p^° = 0.98$ and was found to be in the range of 0.4-1.74 $cm^3 g^{-1}$ (Table **4.2**).

Polymer	BET surface area ($m^2 g^{-1}$)	Pore volume ($cm^3 g^{-1}$)
(31)	1186	1.74
(32)	746	0.69
(33)	577	0.40
(34)	969	0.64
(35)	756	0.86

Table 4.2. BET surface area and pore volume values for HATN-based polymers.

Figure **(4.1)** represents the adsorption/desorption isotherms of prepared HATN-based polymers as a powder sample, the volume of nitrogen adsorbed (V_{ads}) in cm^3 per gram of the adsorbent is plotted versus relative pressure ($p/p^°$).
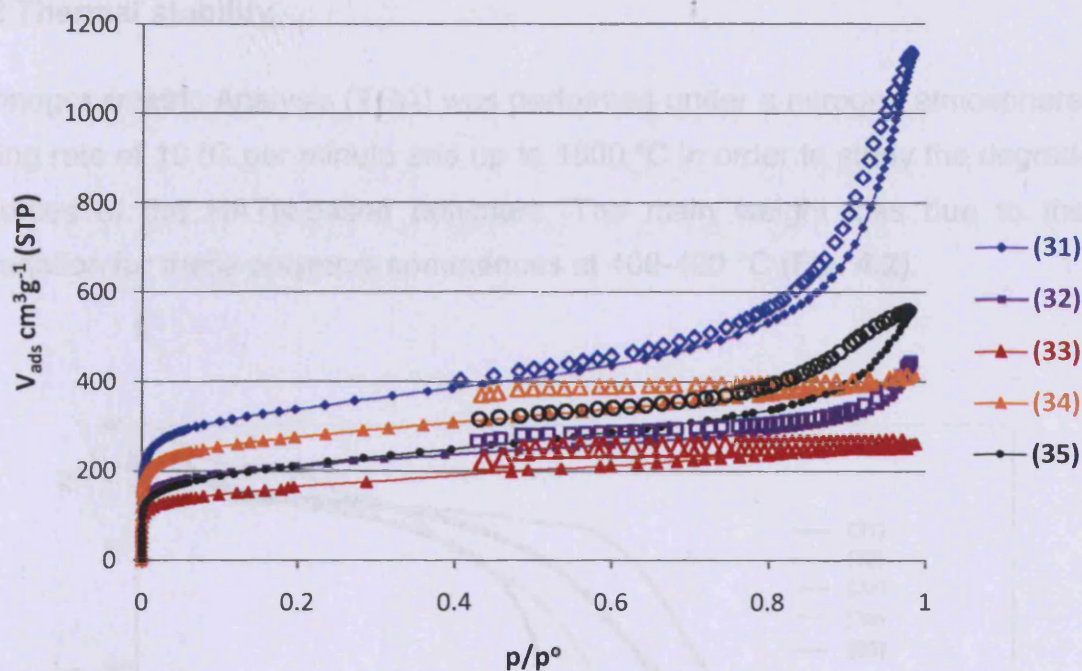
Figure 4.1. Nitrogen adsorption (solid lines)/desorption (dashed lines) isotherms at 77 K for HATN-based polymers.

All the isotherms for the HATN polymers obtained at 77 K exhibit significant uptake at low relative pressure (p/p^{o} < 0.1) typical for microporous materials. Generally, further adsorption occurs at higher relative pressure (p/p^{o} = 0.2-0.8) probably due to a combination of larger pores and swelling. Polymer **(31)** shows very high N_2 uptake (50 mmol g^{-1} at p/p^{o}= 0.98) due to additional adsorption between p/p^{o} = 0.8-1.0, which is usually associated with macroporosity. The total nitrogen adsorption of polymer **(31)** that exceeds the highest reported N_2 uptake for any PIM material.[28] For HATN-based polymers (**31, 32, 33**), it is likely that the porosity arises due to the formation of flat, porous sheets of polymer. Strong $\pi-\pi$ interactions between the extended aromatic triphenylene and HATN units may lead to a wider distribution of pore size than is generally found for PIMs. Arguably, the minimal surface areas of the network polymers derived from monomer **(29)** is due to the presence of the *tert*-butyl groups which prevent similar $\pi-\pi$ interactions between layers. In addition these groups may block microporosity.

4.5.2 Thermal stability

Thermogravimetric Analysis (TGA) was performed under a nitrogen atmosphere at a heating rate of 10 °C per minute and up to 1000 °C in order to study the degradation properties of the HATN-based polymers. The main weight loss due to thermal degradation for these polymers commences at 400-490 °C (Fig. **4.2**).
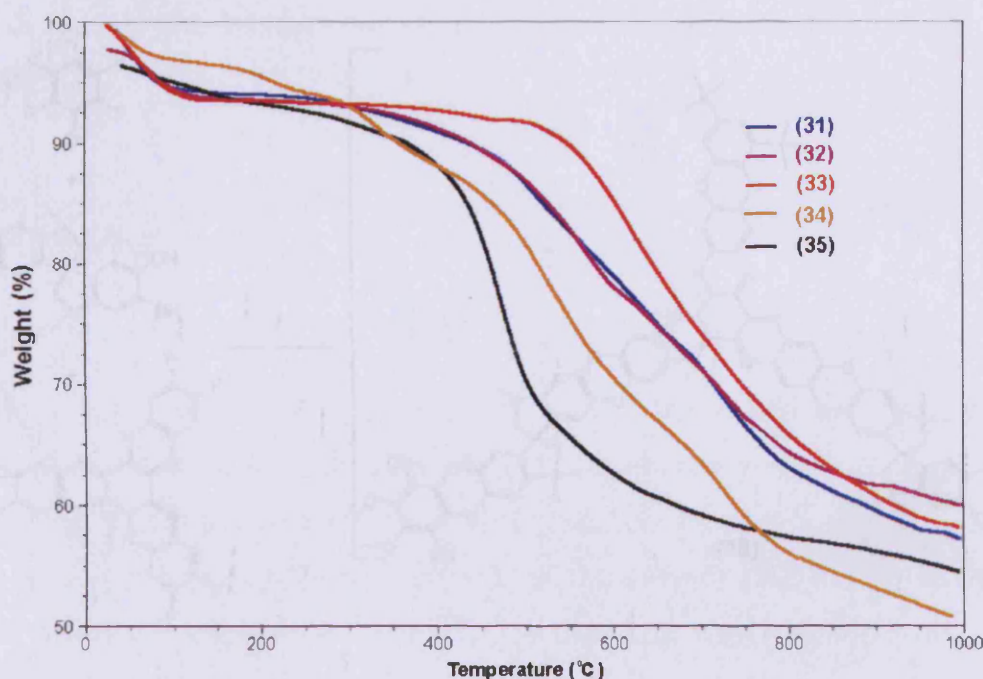
Figure 4.2. TGA analysis profile of HATN-based polymers (nitrogen atmosphere).

Although, all samples were vacuum degassed at high temperature (140 °C) prior to thermal stability analysis, the thermal gravimetric analysis (TGA) showed a small mass loss (4-5 %) for each polymer up to 200 °C which may be due to entrapped solvent or water molecules (i.e. hydrates of the HATN unit). Polymer **(34)** shows multistep degradation between 200-300 °C probably due to the loss of ethano-bridge *via* retro Diels-Alder. The ladder polymer **(32)** degrades at ~ 400 °C whereas the more stable networks starts to degrade only above 470 °C. In all cases, thermal degradation in nitrogen results in a loss of mass of about 45-50 % of starting weight at 1000 °C, indicating that carbonisation is occurring.

4.6 Synthesis of soluble HATN co-polymers

By incorporating various amounts of the HATN monomer **(29)** into the known flexible membrane forming PIM-1[26], a range of soluble ladder copolymer **(36)** for membrane studies was obtained in high yield with various percentage of monomer **(29)** up to 1:10 molar ratio.
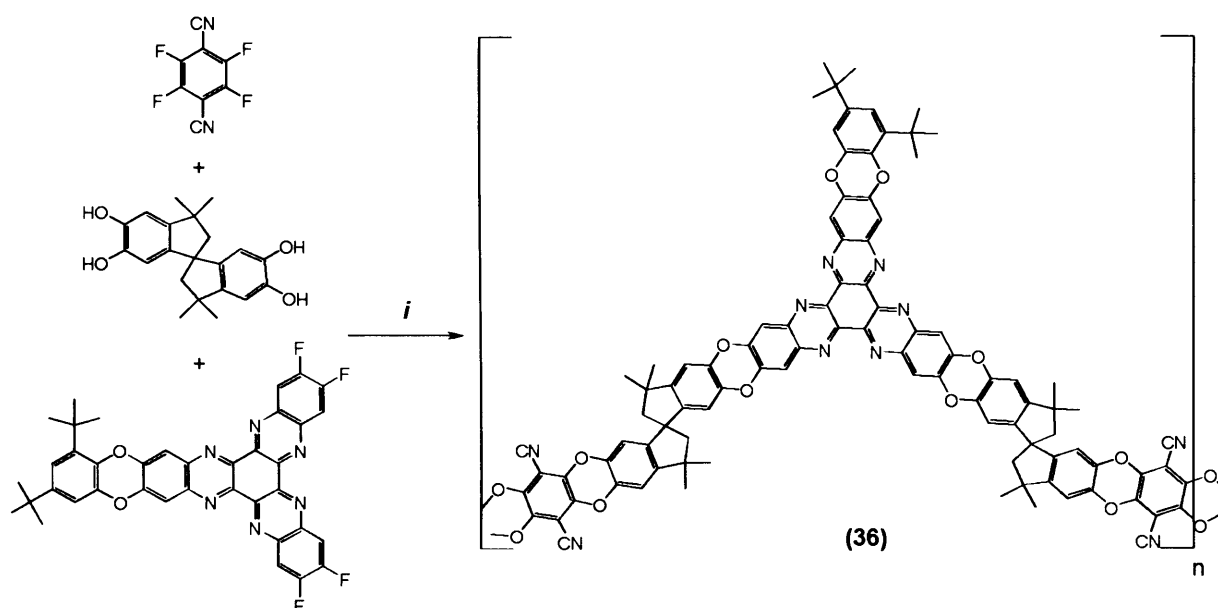
Scheme 2.26. Synthesis of copolymers **(36)**. *Reagents and conditions:* (*i*) K_2CO_3, DMF, 70 °C, 48 h.

The resulting copolymers were soluble in $CHCl_3$ and robust, flexible and transparent thin films were cast from $CHCl_3$ solutions of these polymers, some of physical properties of co-polymers prepared are shown in table **(4.3)**.

Polymer	HATN monomer (%)	M_w (g mol^{-1})	Polydispersity (M_w/M_n)	Surface area (m^2 g^{-1})	Solubility
36a	0.5	154x10^3	1.94	722	THF, CHCl$_3$
36b	1.0	168x10^3	3.17	708	THF, CHCl$_3$
36c	2.5	231x10^3	3.42	692	THF, CHCl$_3$
36d	10	106x10^3	4.82	687	CHCl$_3$

Table 4.3. Physical properties of co-polymers **(36a-d)** with different percentage of HATN monomer composition.

In general, a slight decrease of surface area value is observed with the increase of monomer **(29)** incorporated. Although, all sample batches were prepared under the same conditions (concentration, temperature, reaction time and purification), a small increase of polydispersity with the percentage increase of **(29)** is noticeable, which suggests that the presence of the HATN causes branching perhaps caused by a small degree of exchange of 3,5-di-*t*-butylcatechol.

Small amounts of HATN unit within the co-polymer **(36a-c)** were undetected by NMR spectroscopic analysis, however, ^{1}HNMR analysis for **(36d)** with 10 % HATN showed a broad peak characteristic of the aromatic HATN unit (Fig. **4.3**).
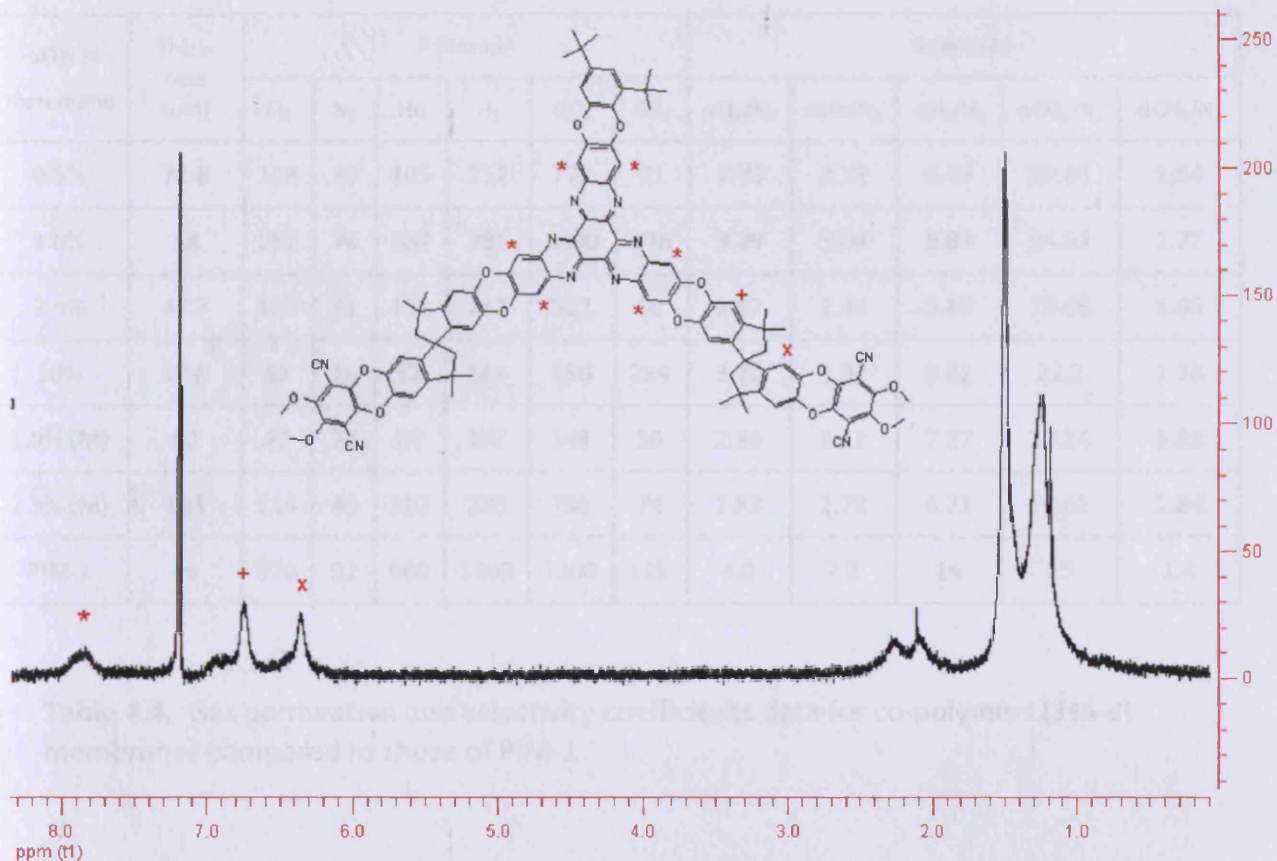
Figure 4.3. ^{1}HNMR spectra of co-polymer **(36d)** with 10 % of incorporated monomer **(29)**.

4.6.1 Gas permeation results

Polymer membranes of **(36a-d)** were prepared by casting from chloroform solution (5% wt) into a flat-bottomed glass dish and allowing the solvent to evaporate slowly. Gas permeation data were obtained at 30 °C with pure gases, using a pressure increase time-lag apparatus operated at low feed pressure, permeability coefficient (P) was calculated from the slope in the steady state region and apparent diffusion coefficient D, from the time-lag (θ) using D= l^2/6θ, where l is the membrane thickness. Permeability coefficient in Barrer (10^{-10} cm^3 [STP] cm cm^{-2} s^{-1} cmHg^{-1}) and ideal selectivity coefficient (P_x/P_{N2}) results for co-polymer **(36)** membrane are given in table **(4.4)** compared to PIM-1[26], (M) donates methanol treatment before measurement.

HATN % membrane	Thick-ness (μm)	P (Barrer)						Selectivity				
		O_2	N_2	He	H_2	CO_2	CH_4	$\alpha O_2/N_2$	$\alpha He/N_2$	$\alpha H_2/N_2$	$\alpha CO_2/N_2$	$\alpha CH_4/N_2$
0.5%	72.8	108	39	105	252	772	71	2.78	2.71	6.49	19.86	1.84
1.0%	58	252	76	387	756	1890	136	3.29	5.04	9.84	24.63	1.77
2.5%	47.7	110	41	101	243	812	80	2.67	2.44	5.88	19.66	1.96
10%	37.8	52	16	63	141	356	284	3.22	3.93	8.82	22.2	1.78
1.0% (M)	80	77	27	87	197	548	50	2.86	3.22	7.27	20.24	1.85
2.5% (M)	103	114	40	112	270	790	74	2.83	2.78	6.71	19.61	1.84
PIM-1	46	370	92	660	1300	2300	125	4.0	7.2	14	25	1.4

Table 4.4. Gas permeation and selectivity coefficients data for co-polymers (36a-d) membranes compared to those of PIM-1.

The selectivity order remained unchanged for most membranes, with the order of permeability of CO_2 >H_2 >He>O_2 >CH_4 >N_2 being the same for PIM-1, however, there are marked decreases in permeability coefficients for all co-polymer (36a-d) membranes compared to PIM-1. This is consistent with the reduction in microporosity measured by nitrogen adsorption. The selectivity for some gas pairs (e.g CH_4/N_2) is enhanced but not dramatically. In general, the transport properties of the HATN co-polymers are dependent on their processing history, in particular, methanol treatment, which is thought to help flush out residual solvent and allows relaxation of the polymer chains, can significantly enhance permeability.[87] However, for the HATN copolymers methanol treatment gave no significant enhancement of permeability or selectivity.

4.6.2 Binding metal ions with HATN co-polymer membranes

Hexaazatrinapthylene (HATN) behaves as a tridentate ligand that can bind with a range of metal ions to form complexes and coordination solids[27], this feature was

used to bind metal ions with polymer films of **(36)** that contains small percentage of the HATN unit (0.5 %, 1.0 %) for further study.

The presence of the HATN unit within co-polymers **(36b and c)** was indicated by chelating metal ions by immersing the films in a solution of the appropriate metal salt in methanol for few minutes following by washing with methanol several times to remove any deposited metal salt on the surface. Generally, the membrane changes colour as soon as it was dipped into the metal ion solution indicating that the chelation was instant (*Fig. 2.17*).
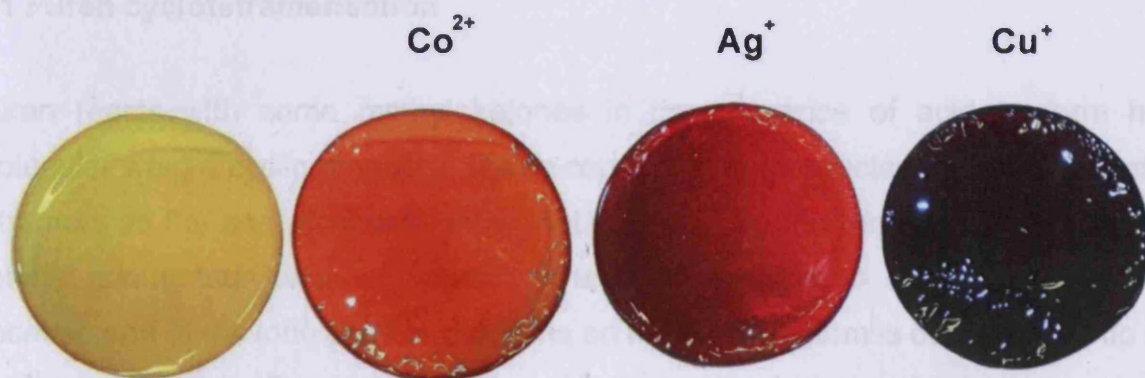

Figure 4.4. Polymer **(36c)** membranes with 0.5 % HATN loaded with different metal ions compared to the metal-free, as cast film (left).

Chapter 5. Synthesis and characterization of macrocycle-based network polymers

This chapter reports on the synthesis of macrocyclic compounds with catechol end-groups and their polymerisation reactions involving efficient dioxane-formation with fluorine–containing monomers.

5.1 Furan cyclotetramerisation

Furan reacts with some methyl ketones in the presence of acid to form high molecular weight cyclic products. These condensation products are called anhydro-tetramers as the analytical data show that they contain four units each of furan and ketone minus four units of water[88]. Furan is considered an aromatic system because one of the lone pairs of electrons on the oxygen atom is delocalized into the ring, creating a 4n+2 aromatic system. However, the heterocycle retains a strong diene character and successfully participates in Diels-Alder reactions.[89]

The condensation of acetone with furan is typical of the general reaction. From the proposed mechanism[88], the reaction starts with nucleophilic attack by the furan on protonated acetone followed by a loss of water to form the furan dimer (II), which condenses further to form the cyclic tetramer (V) in low yield (15%), (*Fig 5.1*).
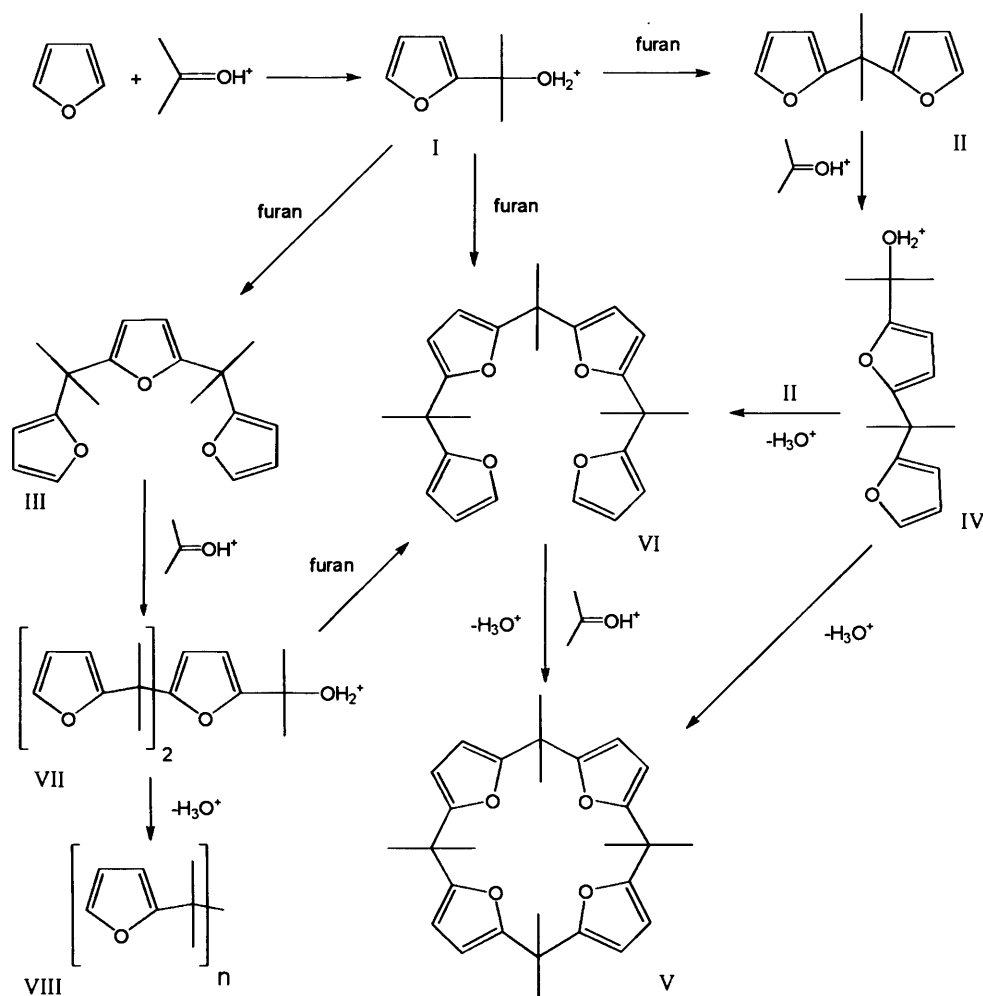
Figure 5.1. Proposed mechanism of furan-acetone anhydro-tetramer formation[88].

The low yields may be partly be accounted for by the formation of oligomeric and polymeric by-products.

5.2 Synthesis of dihydronaphthalene-1,4-endoxide tetramer

The cyclo-tetramer (**37**) was prepared in low yield from acetone condensation with furan in acidic media according to a literature procedure[90]. Since the furan structure is intact within the tetramer, treatment of cyclo-tetramer (**37**) with an excess of (1,2-dimethoxy benzyne) generated from 1,2-dimethoxy-benzenediazonium carboxylate hydrochloride (**1**) gave adduct (**38**) in 32% yield (*Scheme 5.1*).
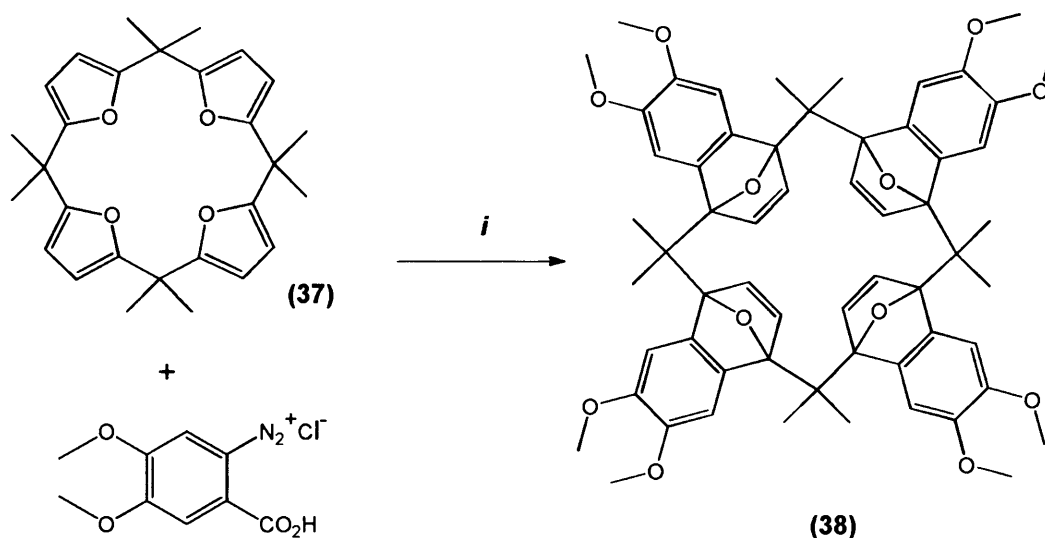
Scheme 5.1. Synthesis of the octamethoxy-dihydronaphthalene-1,4-endoxide tetramer **(38)**. *Reagent and conditions*: (*i*) 1,2-epoxypropane, dichloroethane, reflux, 12 h.

The D_{2d} symmetry is assigned to **(38)** on the basis of its NMR spectrum, which showed a single peak for all methyl groups (s, σ = 1.73). The ^{13}C NMR spectrum was consistent with the structure, showing only eight peaks for this C_{60} molecule.

The x-ray diffraction study of a single crystal of **(38)** obtained by slow evaporation from $CHCl_3$ solution shows that the exo-methylenes experience a substantial steric effect from the oxygen atoms of both adjacent dihydronaphthalene-1,4-endoxide moieties, as a result, all of the aryl rings are oriented to the outside of the structure centre plan with 18.7° angle in opposite alternating order with 90° apart to create a D_{2d} symmetry (*Fig. 5.2*).
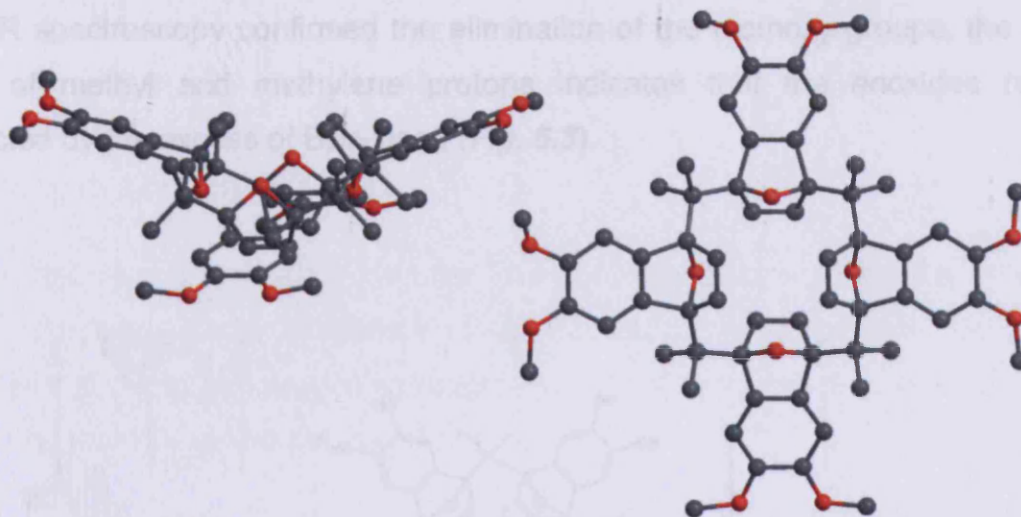
Figure 5.2. Solid state structure of **(38)**

Demethylation of compound **(38)** to obtain the catechol end-groups monomer has been carried out using the same procedure as described before[91] with the exception of adding extra four equivalent of BBr_3 to compensate for complexation with the lone pair on each bridged oxygen. Following the reaction progress by TLC showed that complete demethylation was achieved after 16 hours at room temperature (*Scheme 5.2*).
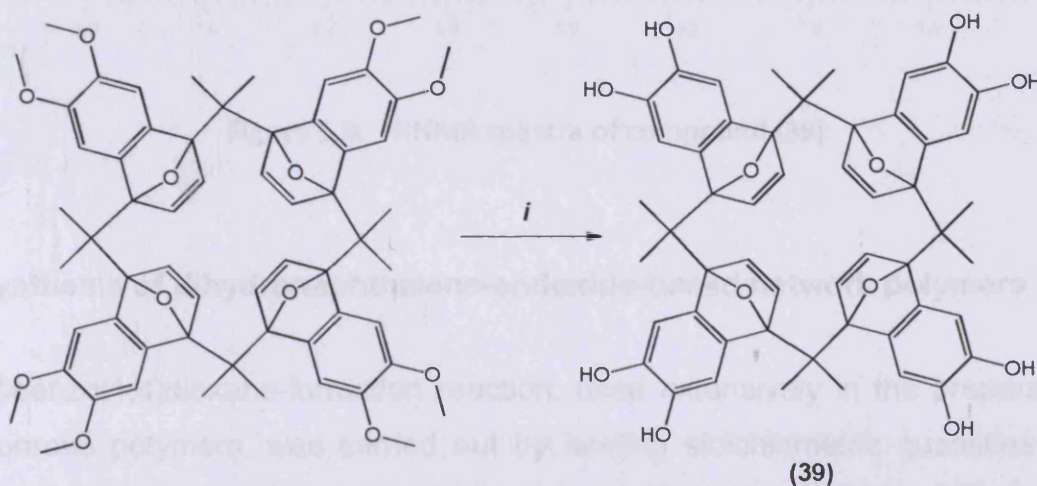
Scheme 5.2. Synthesis of the octahydroxy-dihydronaphthalene-1,4-endoxide tetramer. *Reagents and conditions*: (*i*) borontribromide, DCM, 16 hours, RT.

^{1}H NMR spectroscopy confirmed the elimination of the methoxy groups, the singlet peaks of methyl and methylene protons indicates that the enoxides remains unaffected by the excess of BBr$_3$ used (*Fig. 5.3*).

Figure 5.3. ^{1}HNMR spectra of compound **(39)**

5.3 Synthesis of dihydronaphthalene-endoxide-based network polymers

The dibenzo[1,4]dioxane-formation reaction, used extensively in the preparation of microporous polymers, was carried out by heating stoichiometric quantities of the activated fluoro-containing monomers and octahydroxy-dihydronaphthalene-1,4-endoxide tetramer **(39)** in anhydrous DMF under a nitrogen atmosphere. An excess of anhydrous potassium carbonate was added to the mixture during heating. In each case the polymeric material precipitated out of the solution and was isolated from the reaction mixture after 24 hours by addition of acidified distilled water, followed by

filtration. Purification was achieved by overnight washing of the crude product in various refluxing organic solvents then vacuum drying at 120 °C.

5.3.1 Synthesis of polymer (40)

The thermal polycondensation between catechol end-groups of tetramer (39) and 2,3,5,6- tetrafluoroterephthalonitrile in molar ratio of (1:2) respectively in DMF with an excess of K_2CO_3 under nitrogen atmosphere at 70 °C afforded the network polymer (40) as an insoluble yellow powder (Scheme 5.3).
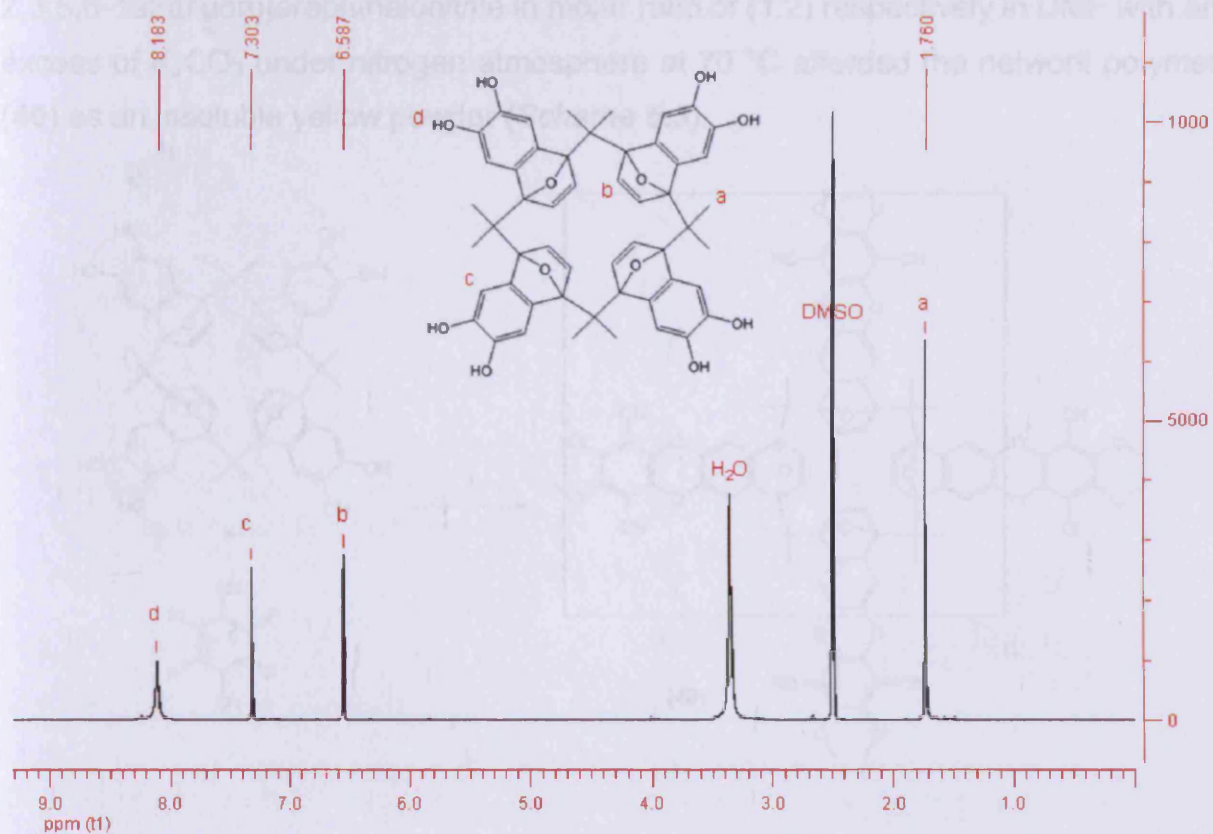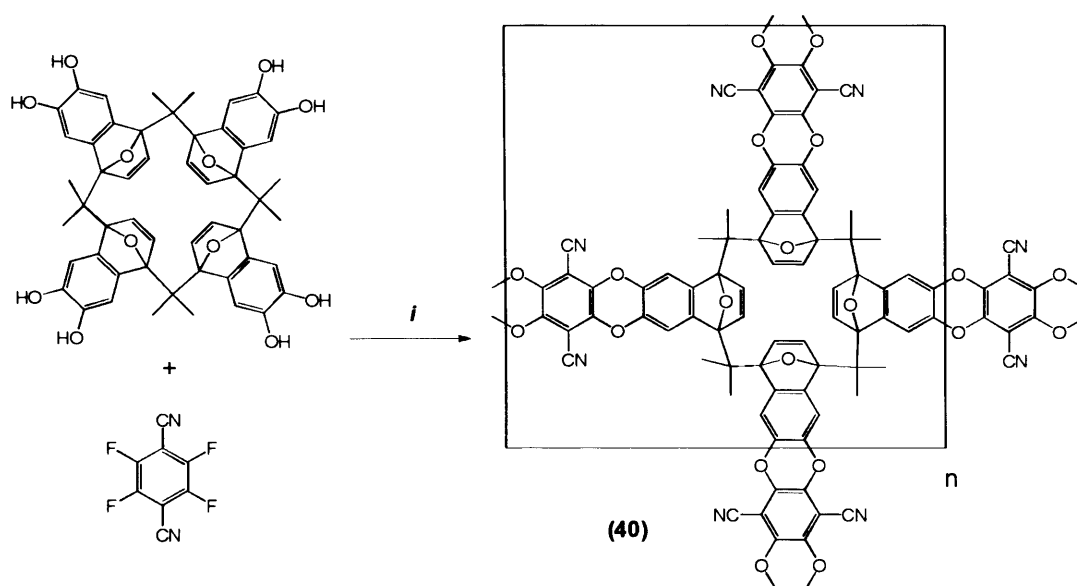
Scheme 5.3. Synthesis of the polymer (40). Reagents and conditions: (i) K_2CO_3, DMF, 70 °C, nitrogen atmosphere, 24 hours.

5.3.2 Synthesis of polymer (41)

Applying the same procedure with a larger fluorinated monomer, 2,3,8,9,14,15-hexafluoro-5,6,11,12,17,18-hexaazatrinapthylene (28) with monomer (39) in molar ratio of (4:3), respectively, produced the network polymer (41) (Scheme 5.4). Typical work up and purification procedure afforded (41) as insoluble brown powder
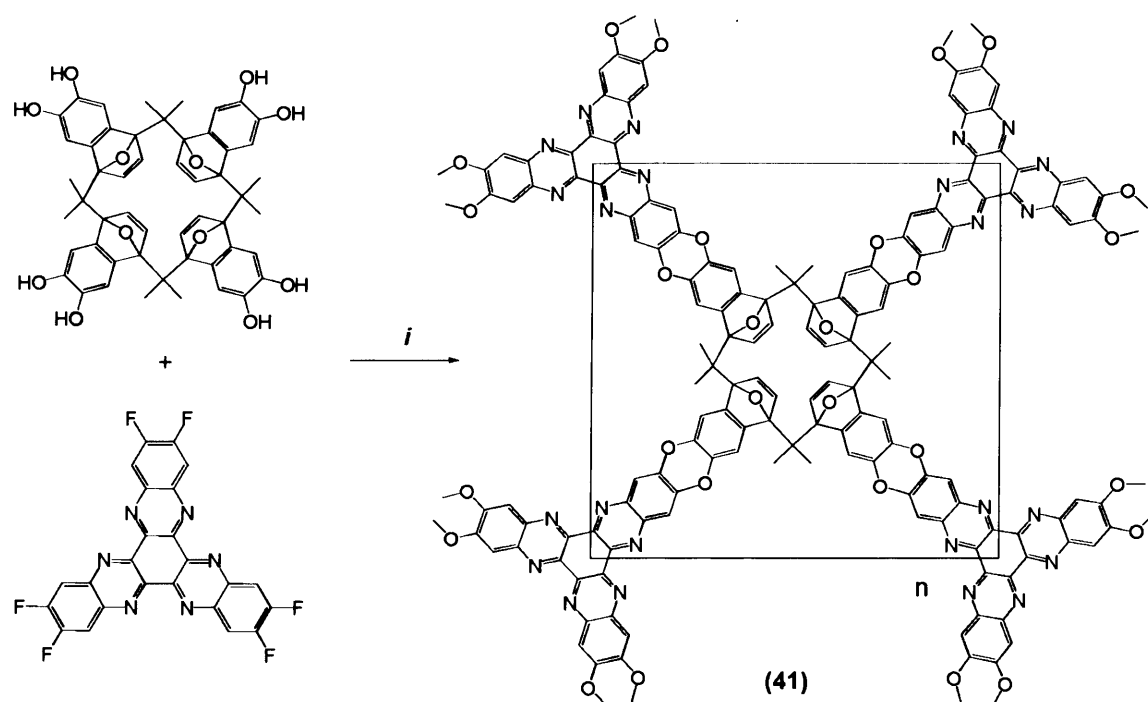
Scheme 5.4. Synthesis of polymer **(41)**. *Reagents and conditions*: (*i*) K₂CO₃, DMF, 70 °C, nitrogen atmosphere, 24 hours.

5.3.3 Synthesis of polymer (42)

The twisted structure of monomer **(39)** was exploited further by reacting it with molar equivalent of 2,2',3,3',5,5',6,6'-octafluoro-4,4'-dinitrilebiphenyl **(18)** using the standard synthetic procedure to prepare another macrocyclic-based polymer **(42)**, (*Scheme 5.5*).
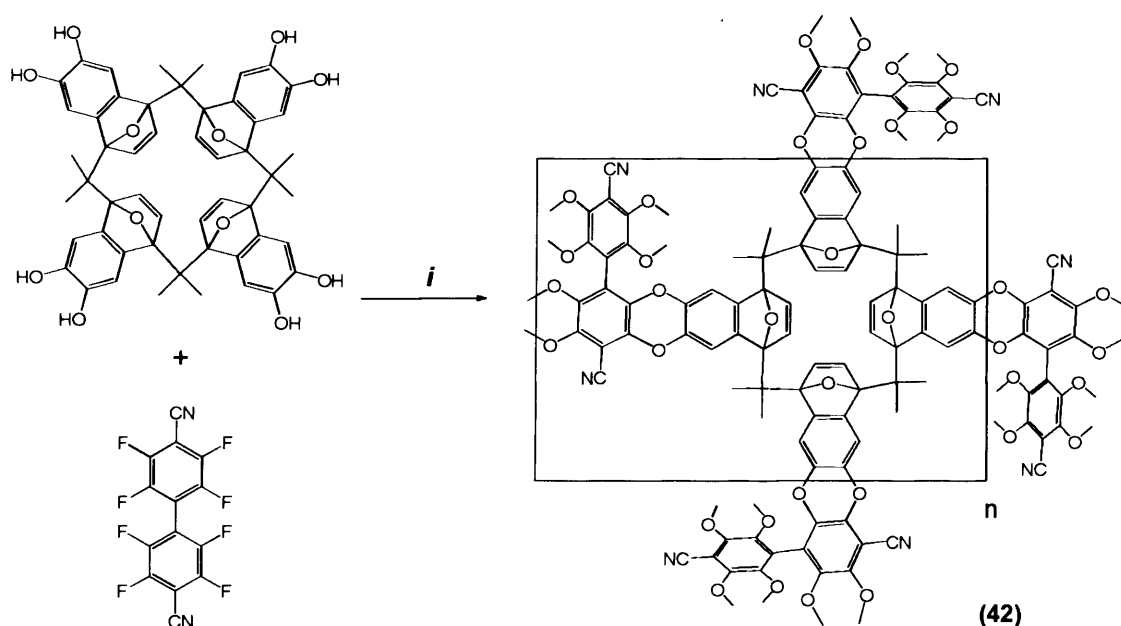
Scheme 5.5. Synthesis of polymer **(42)**. *Reagents and conditions*: (*i*) K₂CO₃, DMF, 70 °C, nitrogen atmosphere, 24 hours.

5.4 Resorcinarene-based network polymers

Resorcinol (1,3-dihydroxybenzene) undergoes acid-catalysed cyclocondensation with acetaldehyde to form a cyclotetramer,[92] with eight phenolic hydroxyl groups, called calixresorcarene, or simply, resorcinarene, The tetramer is obtained as a mixture of stereoisomers: C_{4v} (*boat shape*) in which all the hydroxyl groups oriented in same direction and C_{2v} (*saddle shape*) in which the hydroxyl groups on each phenyl ring have the opposite orientation to those on the adjacent ring (*Fig. 5.3*).
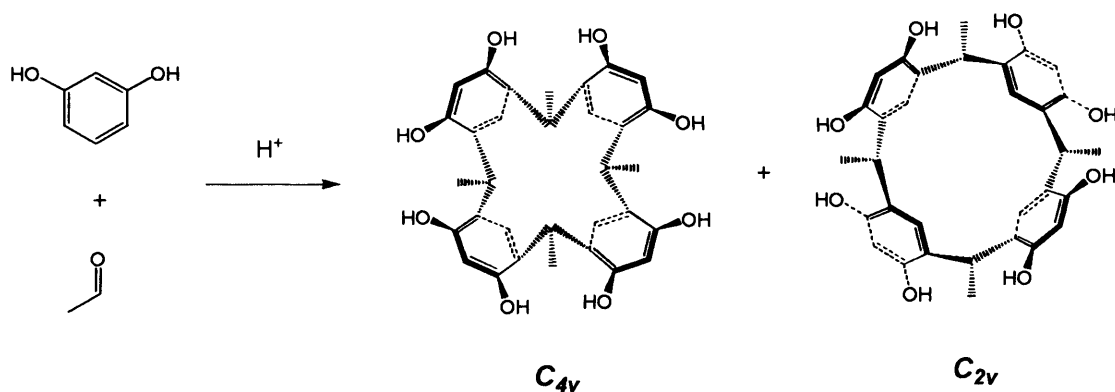
Figure 5.3. Main isomers of resorcinarene from the acetaldehyde-resorcinol cyclotetramerisation.

The C_{4v} isomer can be separated from other isomers with ease by simple crystallisation.[93] Recent studies shows that resorcinarene can react with 4,5-dichlorophthalonitrile by forming an aryl ether linkage between adjacent phenyl rings[94] (Fig. **5.4**). Although, resorcinarene isomer separation was not mentioned in the report, it is suspected that only C_{4v} isomer would be able to form such a linkage as the hydroxy groups have to be oriented in the same direction.
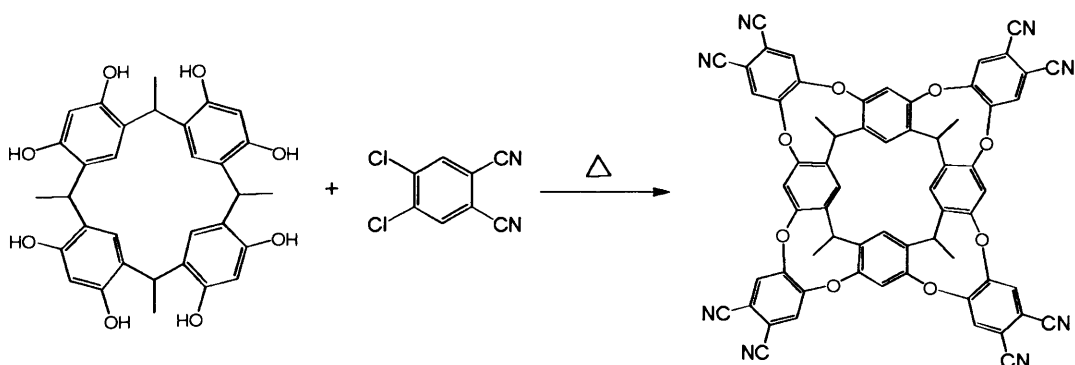
Figure 5.4. Dioxane linkage formation between resorcinarene and 4,5-dichloro-phthalonitrile.[94]

This reactivity makes resorcinarene an attractive monomer for the synthesis of microporous polymeric materials by using bridging compound with activated fluorine end-groups.

The resorcinarene-based network polymer **(43)** was prepared by the reaction between resorcinarene C_{4v} isomer and two molar equivalents of 2,3,5,6-tetrafluorophthalonitrile in DMF and in excess of K_2CO_3 under nitrogen atmosphere for 24 hours at 70 °C (*Scheme 5.6*). Standard work up and purification afforded **(43)** as insoluble orange powder,
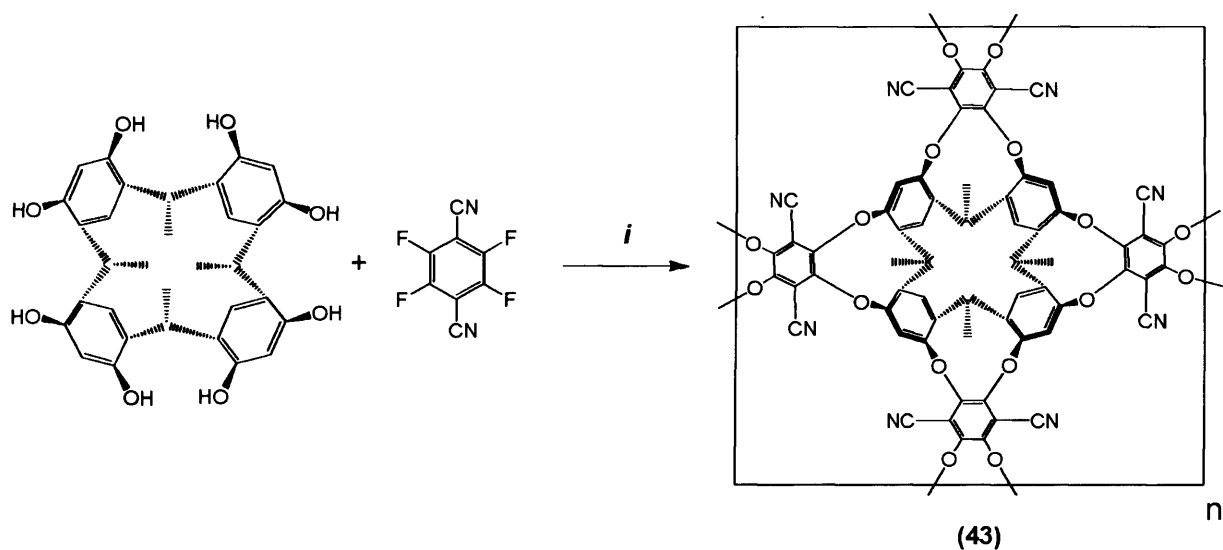
Scheme 5.6. Synthesis of polymer **(43)**. *Reagents and conditions*: (*i*) K₂CO₃, DMF, 70 °C, nitrogen atmosphere, 24 hours.

Another resorcinarene-based polymer was prepared by the reaction between 2,3,8,9,14,15-hexafluoro-5,6,11,12,17,18-hexaazatrinapthylene **(28)** and resorcinarene C_{4V} isomer in molar ratio of (4:3) under standard conditions (*Scheme 5.7*). Standard work up and purification procedure afforded **(44)** as insoluble light-brown powder.
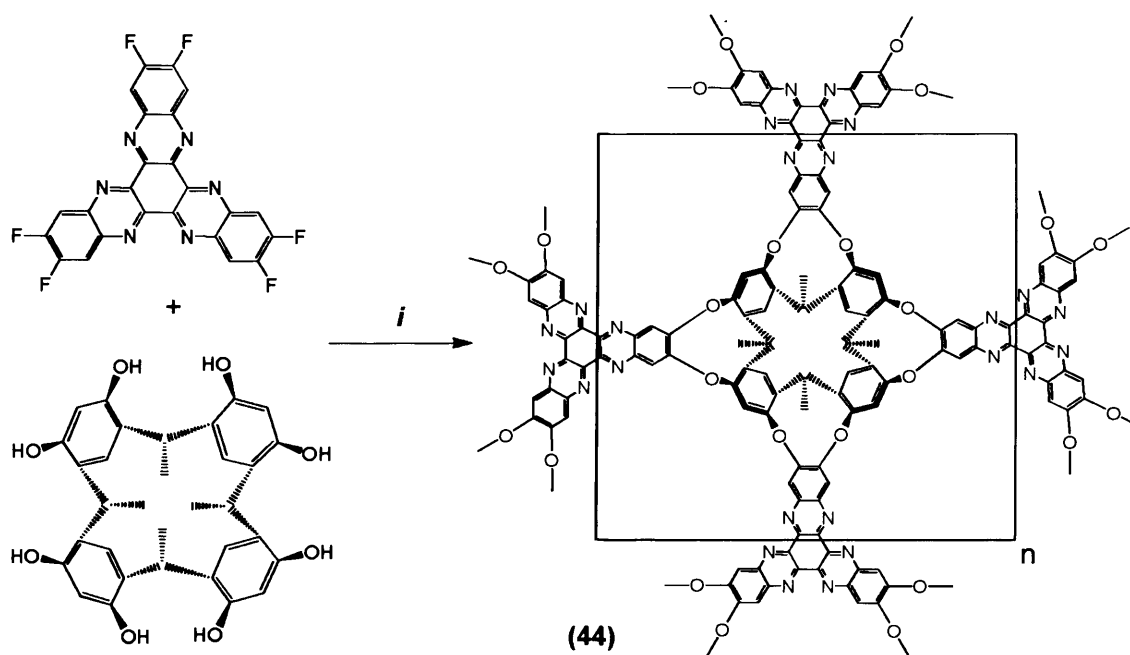
Scheme 5.7. Synthesis of polymer **(44)**. *Reagents and conditions*: (*i*) K₂CO₃, DMF, 70 °C, nitrogen atmosphere, 24 hours.

5.5 Triptycene-based phthalocyanine

The cyclotetramerisation formation reaction of phthalocyanine is a convenient synthetic route for the preparation of highly rigid cyclotetramer with appropriate end-groups suitable for use in polymerisation reactions. Of particular interest was the combination of triptycene and phthalocyanine units.

The phthalocyanine precursor was synthesised by the replacement of the bromines of **(10)** with cyano groups *via* copper-mediated nucleophilic aromatic substitution at elevated temperature, this was achieved by refluxing previously prepared 14,15-dibromo-9,10-di-ethyl-2,3,6,7-tetramethoxytriptycene **(10)** with excess copper cyanide in DMF, the corresponding phthalonitrile **(45)** was obtained in an average yield of 60% (*Scheme 5.8*).
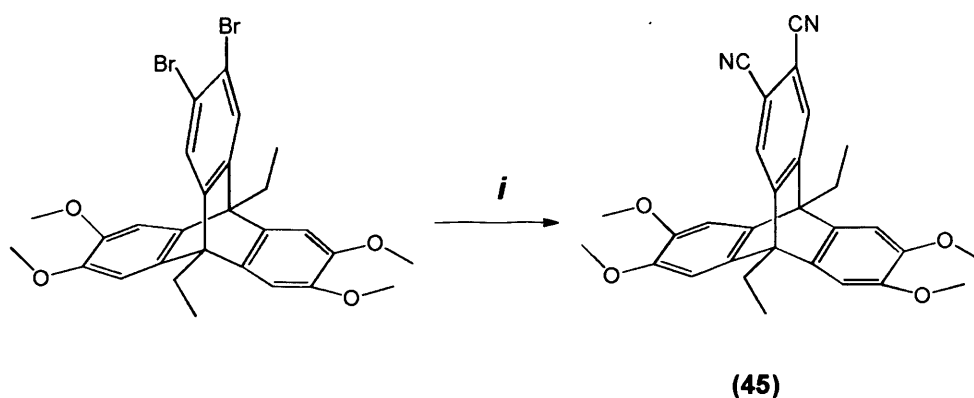
Scheme 5.8. Synthesis of 14,15-dicyano-9,10-di-ehtyl-2,3,6,7-tetramethoxytriptycene **(45)**. *Reagents and conditions:* (*i*) CuCN, DMF, reflux, 6 hours.

The compound **(45)** was used as the precursor to form the macrocyclic zinc phthalocyanine *via* thermal cyclotetramerisation by refluxing it with an excess of zinc(II) acetate in DMAc under dry conditions, the corresponding phthalocyanine **(46)** was obtained in an average yield of 80 % (*Scheme 5.9*).
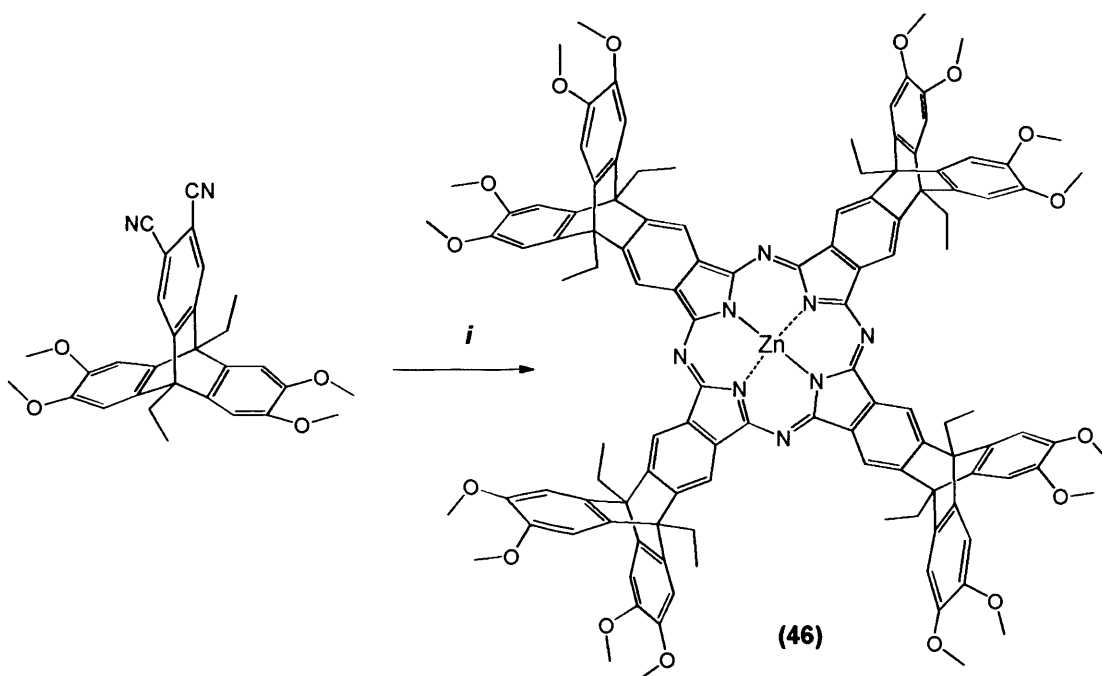
Scheme 5.9. Synthesis of methoxy phthalocyanine compound. *Reagents and conditions:* (*i*) Zn(CH₃COO)₂, DMAc, reflux, 48 hours.

The compound **(46)** was isolated purely by chromatography and found to be light sensitive in solution and stable in solid state. MALDI-MS spectroscopy detected a cluster of peaks at m/z = 1987 g mol^{-1}, which was consistent with the expected isotopic configuration for **(46)**.

The x-ray diffraction study of a single crystal of **(46)** obtained from CHCl$_3$/MeOH slow exchange mixture shows the C_{4h} symmetry of the molecule with the triptycenes protruding from the macromolecular plane of the phthalocyanine (*Fig. 5.5*). The zinc cation is pentacoordinate and has one methanol molecule as an axial ligand with disordered conformation.
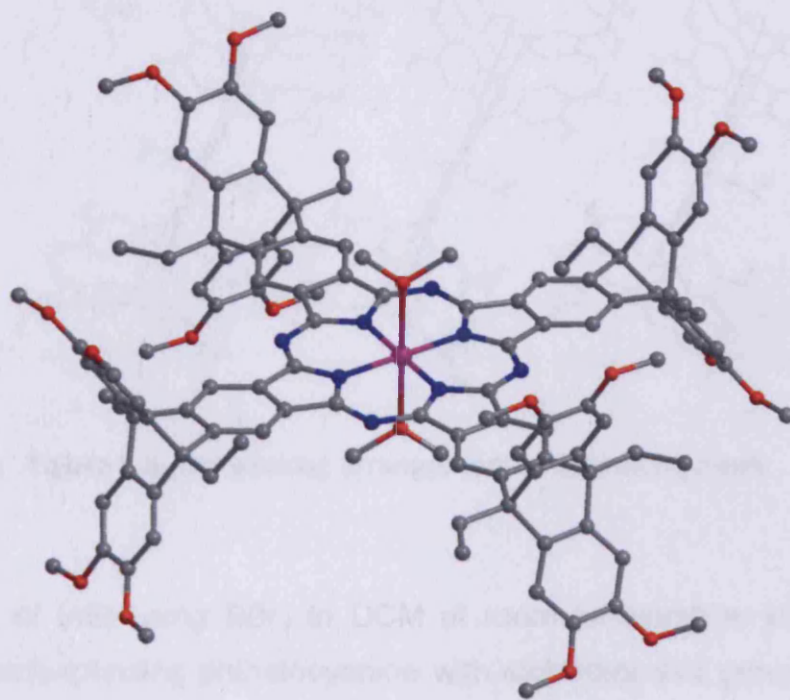
Figure 5.5. Solid state structure of **(46)**

As a result of the triptycene substitution, the packing arrangement of **(46)** shows an intermolecular distance between phthalocyanine central planes of 11 Å, thus no co-facial aggregation of compound **(46)** was observed unlike most metal phthalocyanines that tend to strongly stack together through π–π and other non-

covalent interactions.[65] The presence of the rigid triptycene also ensures the excellent solubility of **(46)** in wide range of organic solvents at room temperature.
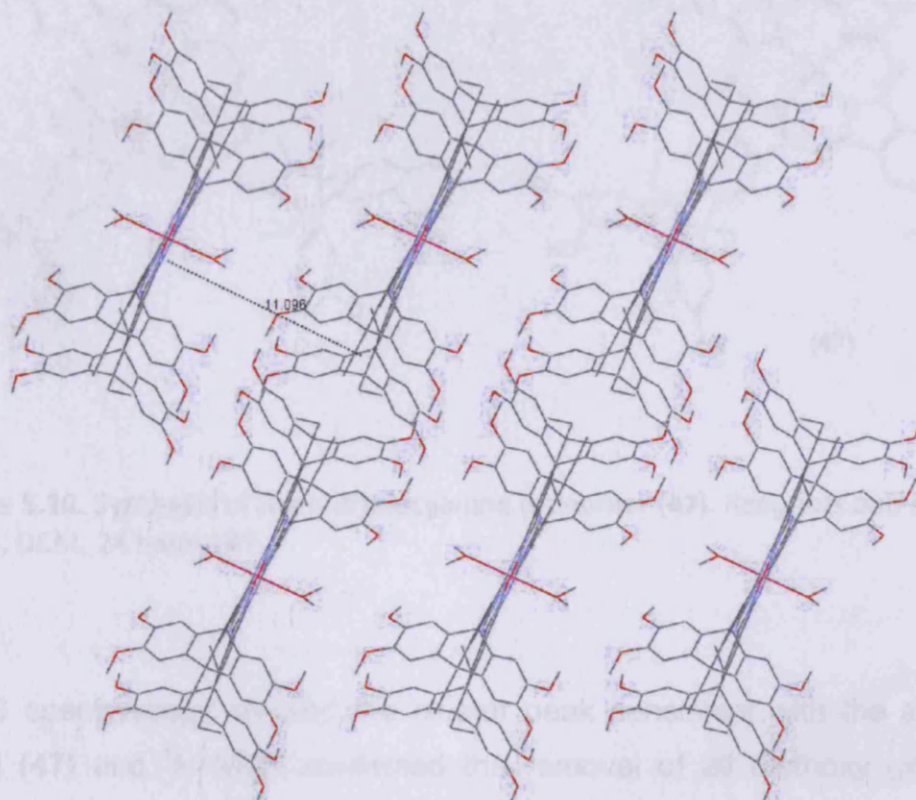
Figure 5.6. The packing arrangement of **(46)** along *c* axis.

Demethylation of **(46)** using BBr$_3$ in DCM at room temperature in dry conditions afforded the corresponding phthalocyanine with eight catechol groups **(47)** suitable for dioxane-forming polymerisation reactions (*Scheme 5.10*).
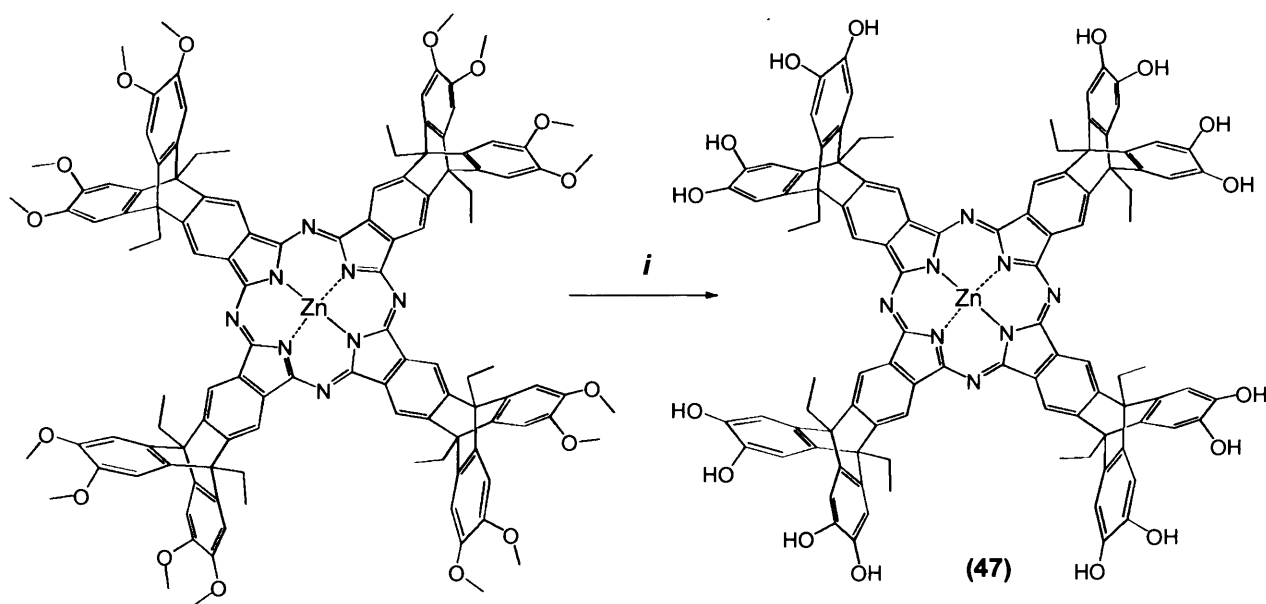
Scheme 5.10. Synthesis of the phthalocyanine monomer **(47)**. *Reagents and conditions:* (*i*) BBr₃, DCM, 24 hours, RT.

MALDI-MS spectroscopy showed the cluster peak consistent with the structure of compound **(47)** and ¹H NMR confirmed the removal of all methoxy groups. The increased molecular polarity of **(47)** due to the presence of 16 hydroxyl groups rendered it insoluble except for highly polar solvents (MeOH, DMSO and DMF).

5.5.1 Phthalocyanine-based polymer

The reaction of **(47)** with four molar equivalents of 2,3,5,6-tetrafluoroterephthalonitrile in DMF in the presence of K₂CO₃ under nitrogen atmosphere at 80 °C led to phthalocyanine-based network polymer **(48)**, (*Scheme 5.11*).
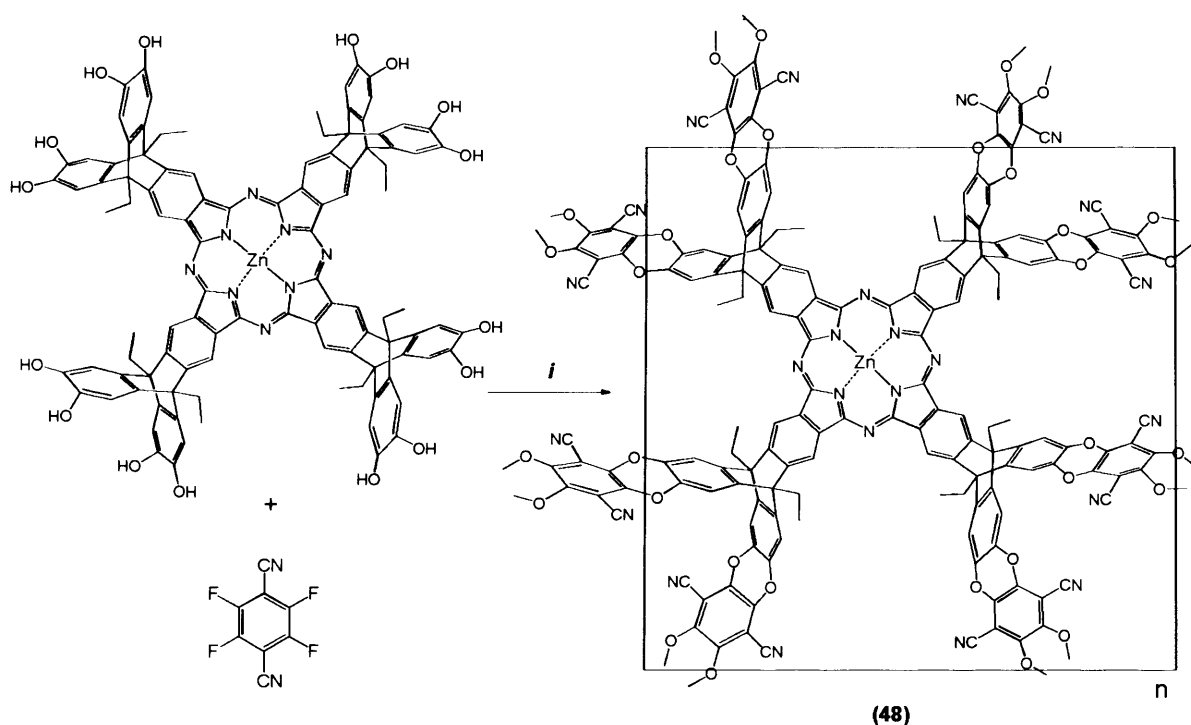
Scheme 5.11. Synthesis of phthalocyanine-based polymer. *Reagents and conditions*: (*i*) K_2CO_3, DMF, 80 °C, 48 hours, nitrogen atmosphere.

The resulting dark green product was found to be insoluble at any organic solvents tested. It was purified by overnight refluxing in various organic solvents then dried in a vacuum oven at 120 °C. The surface area measurement confirmed the presence of microporous architect in **(48)** with an apparent BET surface area of 800 m^2 g^{-1} at 77 K.

Monomer **(47)** was reacted with (2,3,8,9,14,15-hexafluoro-5,6,11,12,17,18-hexaazatrinapthylene **(28)** and 2,2',3,3',5,5',6,6'-octafluoro-4,4'-dinitrilebiphenyl **(18)** in same synthesis fashion to give products with minimal apparent BET surface areas, which were not characterized further.

5.10 Characterisation of the macrocyclic-based polymers

The network polymers were characterised by elemental analysis with the percentage of carbon within the polymers appearing to be significantly lower than the expected values based on the idealized structures, whereas nitrogen and hydrogen agrees more closely with the expected values (*Table 5.1*).

Polymer	Yield %	C % (Calc.) Found	H % (Calc.) Found	N % (Calc.) Found
(40)	96	(73.9) 63.58	(3.65) 4.24	(5.07) 5.12
(41)	90	(74.11) 65.34	(3.53) 3.95	(8.23) 8.83
(42)	88	(75.07) 66.97	(3.98) 4.79	(2.65) 3.68
(43)	91	(73.39) 65.84	(3.06) 3.07	(7.14) 7.83
(44)	83	(73.77) 64.74	(3.07) 3.46	(10.75) 11.19
(48)	93	(72.81) 68.22	(2.90) 4.15	(9.98) 8.08

Table 5.1. The elemental analyses of macrocyclic network polymers.

As for previously prepared PIMs, the low percentage of measured carbon is probably due to the combination of carbon formation, the presence of solvents and water traces trapped within the structure and incomplete functional group conversion. All cyclotetramer-based polymers were found to contain a significant amount of volatiles as demonstrated by TGA.

5.10.1 Nitrogen adsorption analysis

The porosity of these polymers was assessed from their nitrogen sorption isotherms. The BET surface areas of powdered sample of the macrocyclic-based polymers were determined using nitrogen adsorption (multi point BET calculation), which shows that these polymers are microporous materials with BET surface areas within the range 700- 1000 $m^2 g^{-1}$. The total pore volume was also determined and calculated from the amount of nitrogen adsorbed at a relative pressure of p/p^o = 0.98 and was found to be in the range of 0.4-0.59 $cm^3 g^{-1}$.

Polymer	BET surface area ($m^2 g^{-1}$)	Pore volume ($cm^3 g^{-1}$)
(40)	754	0.43
(41)	720	0.53
(42)	703	0.39
(43)	1032	0.55
(44)	1057	0.59
(48)	806	0.40

Table 5.2. BET surface area and pore volume values for macrocyclic-based polymers.

Figure (5.7) represents the adsorption/desorption isotherm of macrocyclic-based polymers as a powder sample, the volume of nitrogen adsorbed (V_{ads}) per gram of the adsorbent is plotted versus relative pressure (p/p^o).

450
400
350
300
250
200
150
100
50
0

V_{ads} cm^3 g^{-1} (STP)

0   0.2   0.4   0.6   0.8   1

p/p^o

—●—(40)
—▲—(41)
—◆—(42)
—●—(43)
—▲—(44)
—■—(48)
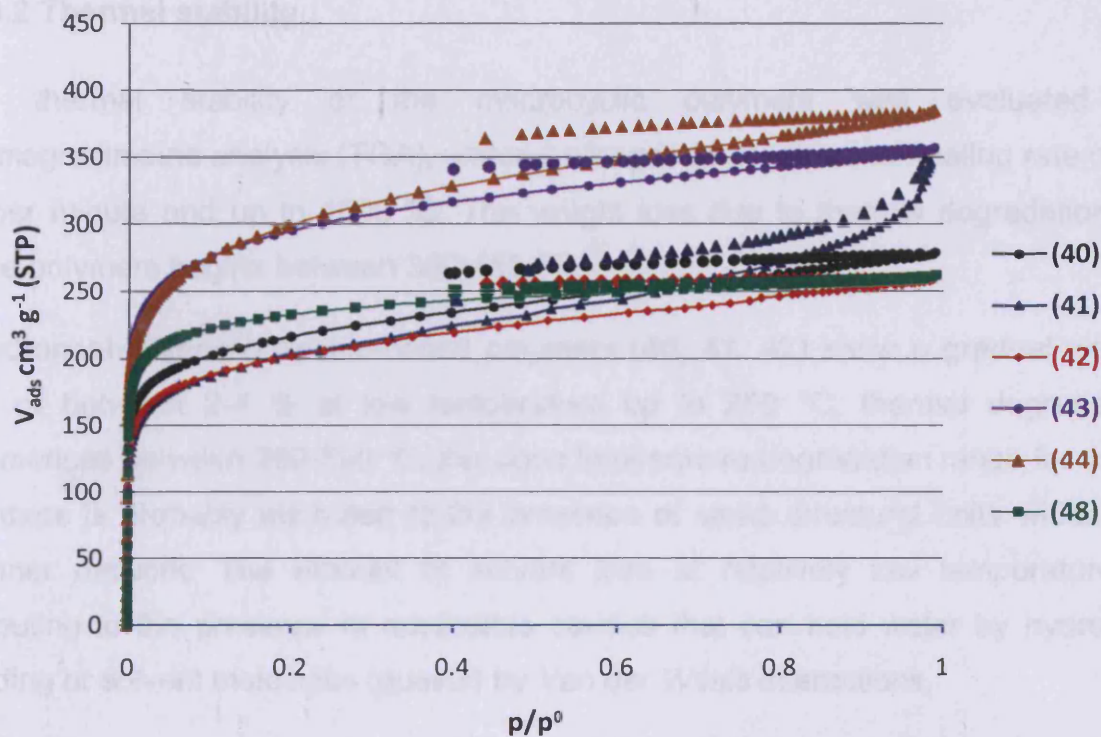
Figure 5.7. The nitrogen adsorption (solid line)/desorption (dashed line) isotherm for a powder sample of macrocyclic-based polymers at 77 K.

All powder samples of prepared polymers exhibit a typical (Type I) isotherm with relatively small amounts of hysteresis as compared to other PIMs. Indeed the lack of hysteresis and very flat adsorption isotherm within the range of p/p^o = 0.1-1.0 is unusual for this type of material and may be related to the very high functionality of the phthalocyanine monomer (i.e. eight catechol units) providing a more tightly cross-linked and rigid network which cannot swell at higher relative pressures of nitrogen. Despite the fact that larger more rigid monomers were used to prepare polymers (**41, 42**), the surface area are unremarkable. Resorcinarene-based polymers (**43, 44**) show the highest surface area among the series, with the bowl-like geometry of resorcinarene creating deep cavities within polymer structure.

5.10.2 Thermal stability

The thermal stability of the macrocyclic polymers was evaluated by thermogravimetric analysis (TGA), under a nitrogen atmosphere at heating rate of 10 °C per minute and up to 1000 °C. The weight loss due to thermal degradation for these polymers begins between 360-450 °C.

Dihydronaphthalene-endoxide-based polymers (**40, 41, 42**) show a gradual weight loss of between 2-4 % at low temperature up to 250 °C, thermal degradation commences between 360-390 °C, the close temperature degradation range for these polymers is probably attributed to the presence of same structural units within the polymer network. The amount of solvent loss at relatively low temperature is attributing to the presence of accessible cavities that can hold water by hydrogen bonding or solvent molecules (guests) by *Van der Waals* interactions.

Resorcinarene-based polymers (**43, 44**) show a relatively large 8 % of weight loss at ~ 100 °C with similar degradation profile, it seems the cage-like geometry of resorcinarene can trap considerable amount of solvent or water. Both polymer starts to degrade thermally at 410-430 °C. The TGA profile of phthalocyanine-based polymer (**48**) shows a weight loss of 6 % at low temperature consistent with the loss of water which is known to bind tightly to the axial sites of zinc phthalocyanine[39], thermal degradation commences at higher temperature around 450 °C probably due to the presence of more stable aromatic cyclic system. TGA profile for the polymers is shown in Figure (**5.8**).
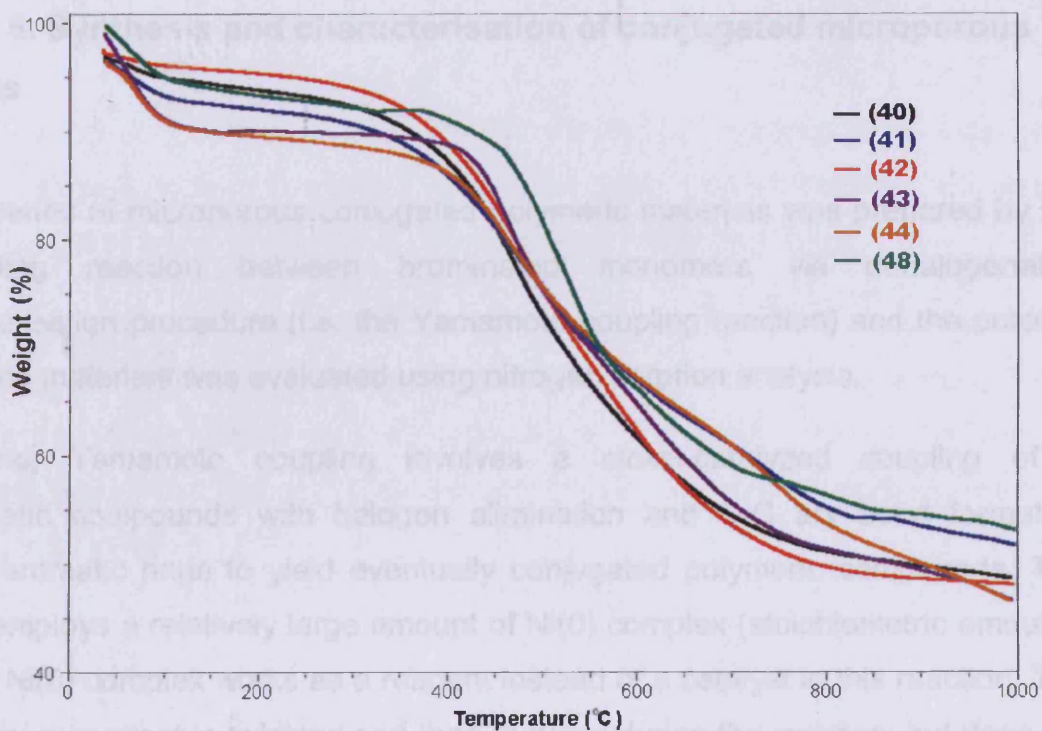
Figure 5.8. TGA profile of macrocyclic-based polymers (nitrogen atmosphere).

Chapter 6. Synthesis and characterisation of conjugated microporous polymers

A novel series of microporous conjugated polymeric materials was prepared by the self-coupling reaction between brominated monomers *via* dehalogenative polycondensation procedure (i.e. the Yamamoto coupling reaction) and the porosity of prepared materials was evaluated using nitrogen sorption analysis.

In general, Yamamoto coupling involves a nickel-catalyzed coupling of a haloaromatic compounds with halogen elimination and C-C ary bond formation between aromatic rings to yield eventually conjugated polymeric compounds. The reaction employs a relatively large amount of Ni(0) complex (stoichiometric amount), since the Ni(0) complex works as a reagent instead of a catalyst in this reaction. The Ni(0) complex reagent is oxidized and then reduced during the reaction, but does not return to the Ni(0) state, so it loses its reactivity after the reaction. In addition, the Ni(0) complex is extremely sensitive to ambient air and moisture, so the reaction has to be performed under a strictly inert atmosphere making it more cumbersome than dioxane polymerisation methods used for PIM synthesis.

The general polymerisation procedure involves heating stoichiometric amounts of aryl bromide compound, 1,5-cyclooctadiene, 2,2'-bipyridyl and bis(cyclooctadiene)Nickel(0) in DMF under nitrogen for a period of time depending of monomer solubility as the molecular weight of the π-conjugated polymers prepared by Yamamoto coupling seems to be dependant on the solubility and crystallinity of the polymers.[49] This is a trend that crystalline polymers have a lower molecular weight whereas less crystalline species propagate to form a higher molecular weight polymer.

Acidic workup is preferred by pouring the reaction mixture into a warm aqueous solution of ethylenediamine-tetraacetic acid, which also acts as chelating agent for nickel particles. The resulting crude materials have to be washed a few times with hot 10% NaOH solution to remove any acid traces then starting materials and low molecular weight materials are removed by refluxing in different organic solvents such as DMF, THF and methanol.

6.1 Synthesis of polytriptycene

The first attractive building blocks for Yamamoto polymerisation is triptycene, regardless of polymerisation method, it is anticipated that triptycenes will always have some void space present in the clefts between the phenyl rings.

Following the literature procedure[95] for triptycene bromination using iron as a catalyst, 2,3,6,7,14,15-hexabromo-triptycene was prepared in good yield (60 %). Polymerisation was carried out in anhydrous DMF with six equivalents of bis(cyclooctadiene)nickel(0), 2,2'-bipyridyl and 1,5-cyclooctadiene under dry nitrogen for 48 hours (*Scheme 6.1*).

(49) **(50)**
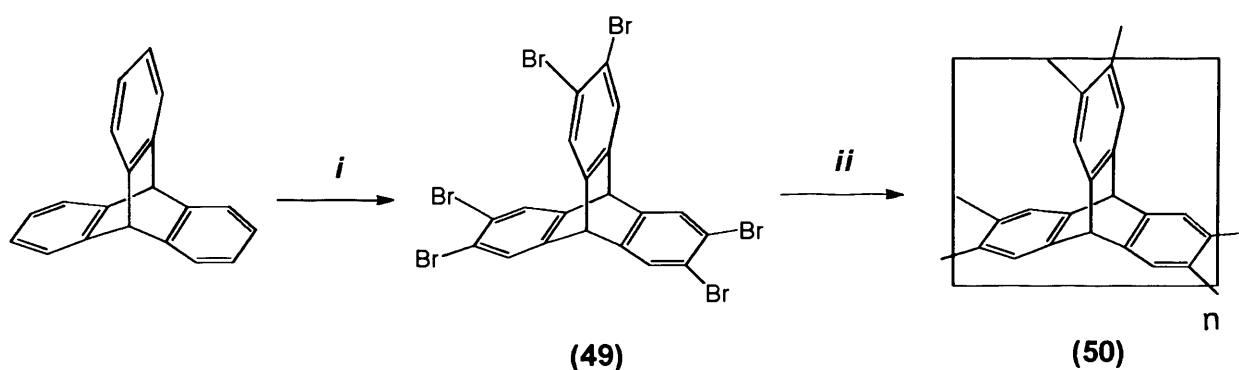
Scheme 6.1. Polytriptycene synthesis. *Reagents and condition*:(*i*) Br_2, $CHCl_3$, Fe, reflux, 1 hour; (*ii*) DMF, 1,5-cyclooctadiene, 2,2'-bipyridyl, bis(cyclooctadiene)nickel(0), 100 °C, 48 hours, nitrogen atmosphere.

The polytriptycene falls out of the solvent as a black precipitate. Following the standard work up and purification procedure afforded **(50)** as pale yellow product, which was found to be insoluble in any organic solvents or concentrated sulphuric acid, consistent with the formation of a network polymer.

Initially, BET surface area measurement of polytriptycene indicated significant microporosity giving a surface area of 690 m^2 g^{-1}. By repeating the reaction using a minimum amount of solvent and longer reaction time at higher temperature, a polymer network with higher surface area was achieved (>1000 m^2 g^{-1}) suggesting

that the polymerization proceeds even within the initial precipitate, as has been observed with related polymerisations.[49]

6.2 Triphenylmethane-based network polymer

Triphenylmethane was expected to be a suitable building block for microporous conjugated polymers as it is composed of three phenyl groups linked to sp^3 carbon with a rigid propeller-like configuration.[96] The bromination of triphenylmethane was anticipated to occur on the *para* positions similar to that found for the bromination of tetraphenylmethane.[97] Satisfactory results were obtained by the treatment of a dilute solution of triphenylmethane in CHCl$_3$ with three equivalents of bromine at 0 °C in the presence of FeBr$_3$ as a catalyst with the absence of light. The resulting tris(4-bromophenyl)methane (51) was obtain in good yield (62%) and isolated as viscous yellow liquid (*Scheme 6.2*).
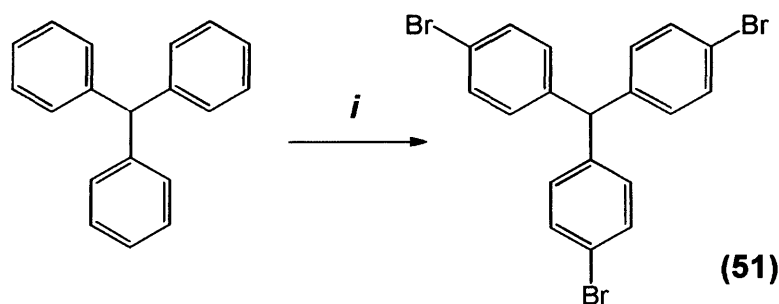
Scheme 6.2. Synthesis of tris(4-bromophenyl)methane. *Reagent and conditions:* (*i*) Br$_2$, CHCl$_3$, FeBr$_3$, 0 °C, 3 hours.

The polymerisation coupling reaction was performed in DMF with a three molar equivalent excess of of bis(cyclooctadiene)nickel(0) in the presence of 2,2'-bipyridyl and an excess of 1,5-cyclooctadiene under dry nitrogen and at 100 °C for 48 hours. Standard work up and purification procedure afforded (52) as off-yellow powder, which was was found to be insoluble in any organic solvent.
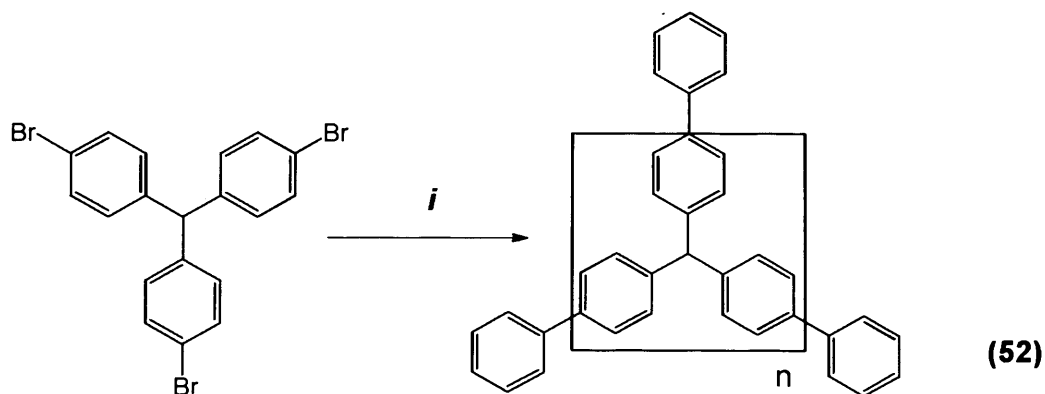
Scheme 6.3. Synthesis of triphenylmethane-based polymer. *Reagents and condition*:(*i*) DMF, 1,5-cyclooctadiene, 2,2'-bipyridyl, bis(cyclooctadiene)nickel(0), 100 °C, 48 hours, nitrogen atmosphere.

6.3 Synthesis of polypyrene

The flat structure of pyrene was thought to be of interest for incorporation within conjugated microporous polymers via Yamamoto coupling. The required tetrabromopyrene monomer was prepared according to a literature procedure[98] by refluxing pyrene with an excess of bromine in nitrobenzene to give a pale green product, which was insoluble in most organic solvents but partially soluble in hot DMF. LRMS confirmed and elemental analysis indicated the successful addition of four bromines onto the aromatic system.

The polymerisation of tetrabromopyrene using zero valance nickel compound was performed as before in DMF but reaction was left longer because of the reduced solubility of the monomer (Scheme **6.4**).

(53) **(54)**
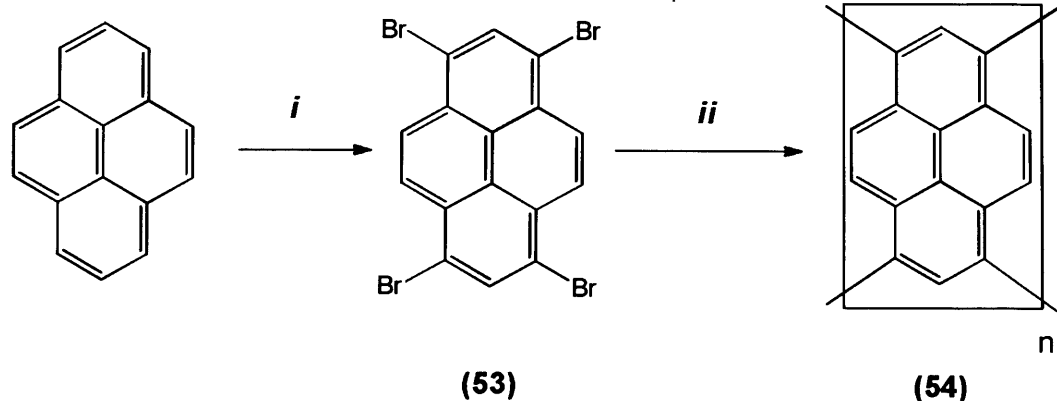
Scheme 6.4. Polypyrene synthesis. *Reagents and condition*:(*i*) Br$_2$, nitrobenzene, Fe, reflux, 24 hours; (*ii*) DMF, 1,5-cyclooctadiene, 2,2′-bipyridyl, bis(cyclooctadiene)nickel(0), 100 °C, 3 days, nitrogen atmosphere.

The reaction was quenched after three days. After work-up an orange precipitate was obtained that was insoluble in any organic solvent. The metal impurities and remaining starting materials were removed by refluxing several times in DMF then refluxing in THF, acetone and methanol.

6.4 Synthesis of polytriphenylene

A similar approach was taken to prepare another porous polymer derived from triphenylene, which can be brominated in six positions.[99] Bromination of triphenylene was carried out under harsh conditions by refluxing it in nitrobenzene with an excess of bromine in the presence of FeCl$_3$ as Lewis acid catalyst, giving the product 67% yield. The brominated triphenylene was found to be insoluble in any organic solvent; therefore NMR characterisation was not achieved. However elemental analysis gave the amount of bromine as 68% by weight, which is consistent with six added bromines. HRMS detected the corresponding mass of the product.

Polymerisation of hexabromotriphenylene was carried out in DMF under dry inert conditions using bis(cyclooctadiene)nickel(0) as a coupling reagent, since heaxbromotriphenylene is not soluble in the polymerization solvent, a minimum

amount of DMF was used with a longer reaction maintained at higher temperature. The resulting insoluble black product was purified by refluxing in DMF, THF, acetone and methanol to yield **(56)** as pale yellow powder,

Scheme 6.5. Polytriphenylene synthesis. *Reagents and condition*:(*i*) Br_2, nitrobenzene, Fe, reflux, 24 hours; (*ii*) DMF, 1,5-cyclooctadiene, 2,2'-bipyridyl, bis(cyclooctadiene)nickel(0), 100 °C, 3 days, nitrogen atmosphere.
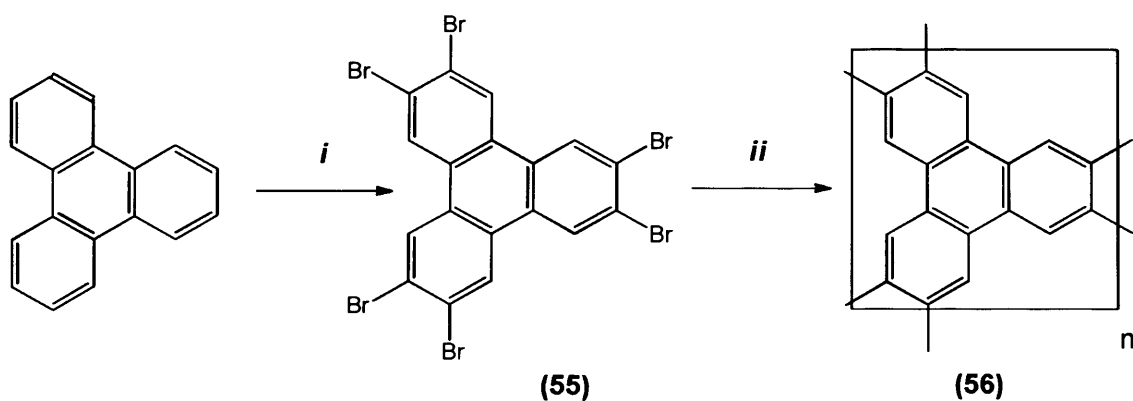
6.5 Synthesis of polypropellane

Hexabenzo[4.4.4]propellane is a relative of hexaphenyl-ethane in which the three phenyls on each aliphatic carbon are together linked at the ortho positions to form biphenyl linkages. The molecular symmetry of propellane is D_3 and features three biphenyl moieties lying orthogonal to each other in a helical arrangement around the aliphatic C-C bond.
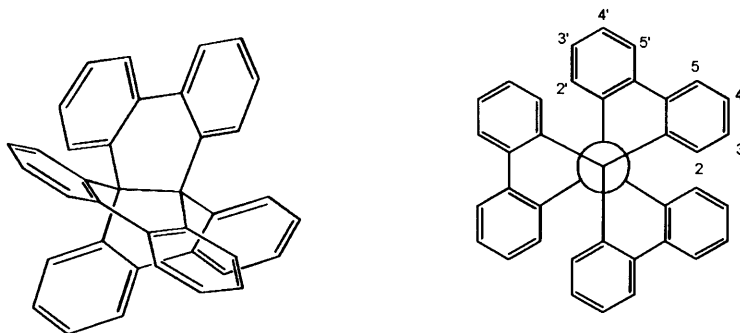

Figure 6.1. Hexabenzo[4.4.4]propellane structure.

Propellane is stable toward both reductive as well as oxidative cleavage of the central C-C bond and can be easily brominated at the 4,4'-positions of all three biphenyls[100], which makes it an attractive structural unit for for dehalogenative coupling polymerisation. Hence, hexabromopropellane was prepared via a multistep procedure: dimerisation of 9-fluorenone using zinc and $Zn(Cl)_2$ in a mixture of THF/H_2O gave 9,9'-bifluorene-9,9'-diol, which upon acid-catalysed rearrangement afforded a pinacolone.[101] Hexabenzo[4.4.4]propellane was obtained by coupling the pinacolone with biphenyl via lithium exchange mechanism followed by acid-catalysed rearrangement[100]. Bromination of propellane was carried out in $CHCl_3$ and in the presence of iron as a catalyst to afford the desired monomer (Scheme 6.6).
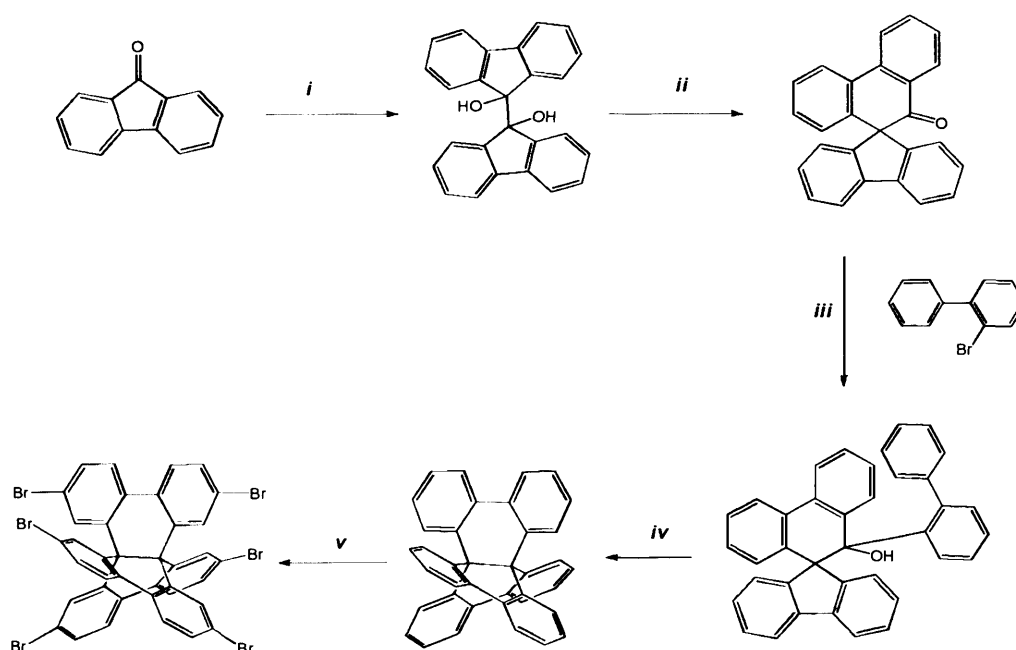
Scheme 6.6. Hexabromopropellane synthesis. *Reagents and Conditions:* (*i*) ZnCl, Zn (30 mesh), THF, H_2O, HCl (2 N); (*ii*) glacial acetic acid, conc. H_2SO_4, reflux; (*iii*) n-Butyllithium (2.5 M in hexane), anhydrous diethyl ether, -78 °C. (*iv*) glacial acetic acid, conc.H_2SO_4, 95 °C, 1 hour; (*v*) Br_2, $CHCl_3$, Fe, 40 °C, 4 hours.

The dehalogenative polycondensation of hexabromopropellane was carried out using an excess of 1,5-cyclooctadiene, 2,2'-bipyridyl and bis(cyclooctadiene)-nickel(0) in DMF at 100 °C for 48 hours under dry nitrogen atmosphere (Scheme 6.7).

(57)
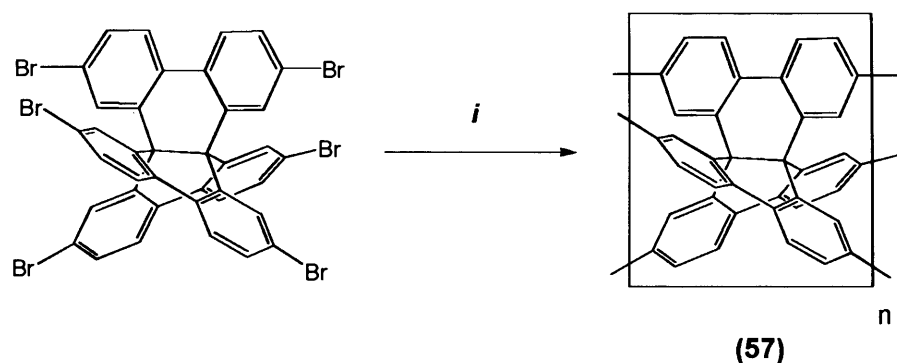
Scheme 6.7. Synthesis of triphenylmethane-based polymer. *Reagents and condition*: (*i*) DMF, 1,5-cyclooctadiene, 2,2'-bipyridyl, bis(cyclooctadiene) nickel(0), 100 °C, 48 hours, nitrogen atmosphere.

The resulting insoluble black product was purified by refluxing in DMF, THF, acetone and methanol several times to yield **(57)** as pale yellow powder.

6.6 Model Yamamoto reaction

To investigate the possible polymer conformation derived from using *o*-bromo monomers **(49, 55)**, a model reaction was preformed using monomer **(10)** in same synthesis procedure (Scheme **6.8**).

(58)
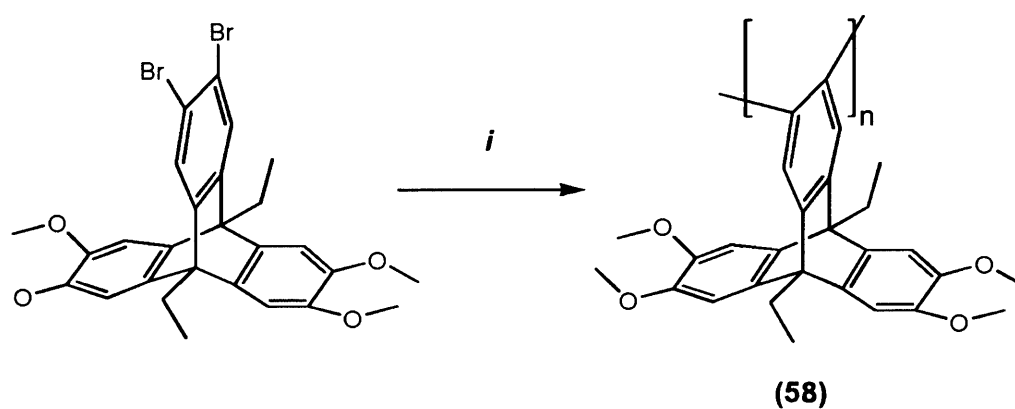
Scheme 6.8. Model Yamamoto reaction. *Reagents and condition*: (*i*) DMF, 1,5-cyclooctadiene, 2,2'-bipyridyl, bis(cyclooctadiene)nickel(0), 100 °C, 48 hours, nitrogen atmosphere.

Typical work-up procedure afforded single soluble product, which upon GPC analysis found to be an oligomeric materials with molecular weight average of (3 x 10^3 g mol^{-1}). ^{1}H NMR spectrum show broad peaks consistence with the repeat units and corresponds to **(58)** structure (Fig. **6.2**).
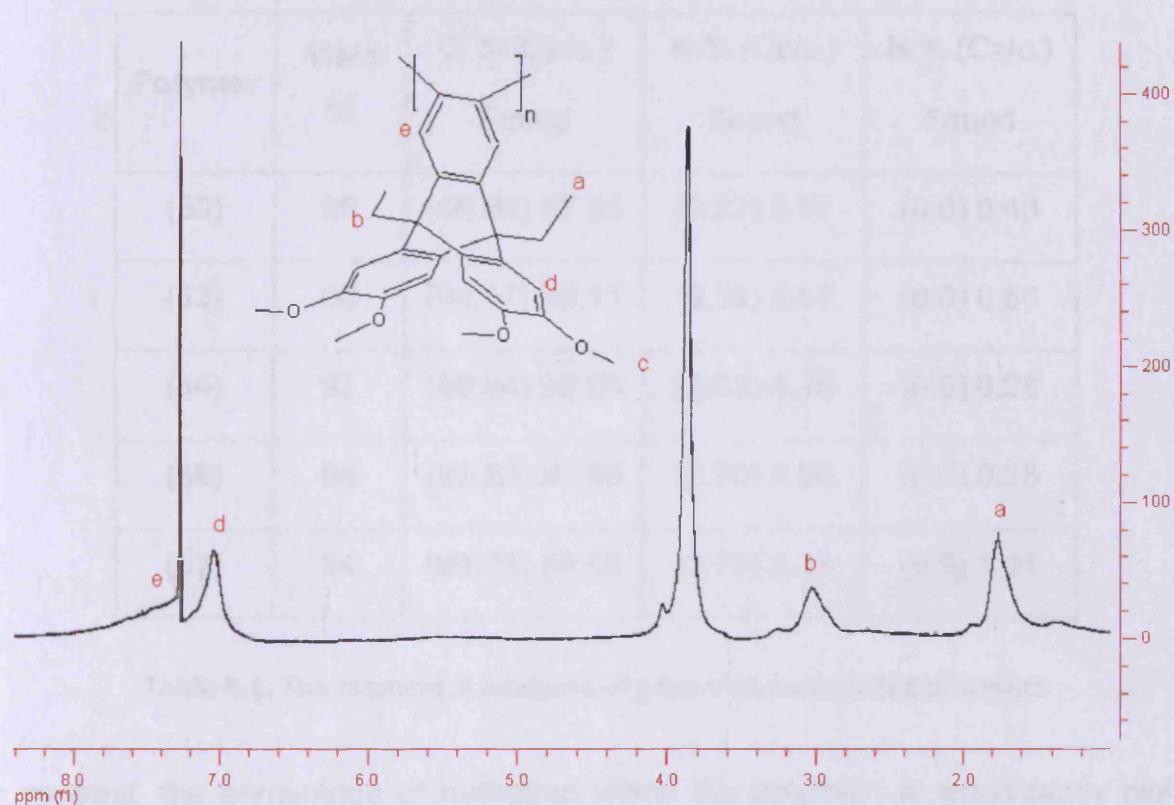
Figure 6.2. ^{1}HNMR spectra of **(58)** (CDCl$_3$).

MALDI-MS and mass spectroscopy analysis did not detect any products generated from coupling two or three molecules by forming biphenylene or triphenylene units. This result indicates the unlikely coupling of few o-dibromo monomers to form larger macrocyclic compounds.

6.8 Characterisation of coupled polymers

The chemical structures of the coupled polymers were confirmed by their elemental analysis. In general, the C values are lower than the expected values for the proposed repeat units of the network polymers (Table 6.1).

| Polymer	Yield %	C % (Calc.) Found	H % (Calc.) Found	N % (Calc.) Found
(50)	96	(96.64) 87.85	(3.22) 5.07	(0.0) 0.48
(52)	88	(94.47) 89.11	(5.38) 5.57	(0.0) 0.56
(54)	92	(96.84) 92.66	(3.03) 4.26	(0.0) 0.28
(56)	94	(97.29) 92.66	(2.70) 4.26	(0.0) 0.28
(57)	94	(96.08) 89.08	(3.79) 5.49	(0.0) 1.01

Table 6.1. The elemental analyses of prepared conjugated polymers

In contrast, the percentage of hydrogen within the polymers is significantly higher than the expected values based on the idealized structures despite the long drying time at elevated temperature under vacuum, this can be explained by trapped solvent or H-terminated end-groups that not accounted for in polymer repeat units. The nitrogen traces found in all samples defies a simple explanation but must originate from either trapped solvent or ligands.

6.8.1 Nitrogen adsorption analysis

The porosity of these polymers was assessed from the nitrogen sorption isotherm, The BET surface areas of powdered sample of prepared coupled polymer were determined using nitrogen adsorption (multi point BET calculation), which shows that

these polymers are microporous materials with BET surface areas of the range 500-1000 $m^2\,g^{-1}$. The total pore volume was also determined and calculated from the amount of nitrogen adsorbed at a relative pressure $p/p^0 = 0.98$ and was found to be in the range of 0.35-0.73 $cm^3\,g^{-1}$ (Table 6.2).

Polymer	BET surface area ($m^2\,g^{-1}$)	Pore volume ($cm^3\,g^{-1}$)
(50)	1058	0.73
(52)	598	0.35
(54)	970	0.68
(56)	635	0.47
(57)	543	0.43

Table 6.2. BET surface area and total pore volume of prepared conjugated polymers

Figure (6.3) represents the adsorption/desorption isotherms of prepared conjugated polymer as a powder sample at 77 K. The volume of nitrogen adsorbed (V_{ads}) per gram of the adsorbent is plotted versus relative pressure (p/p^0).
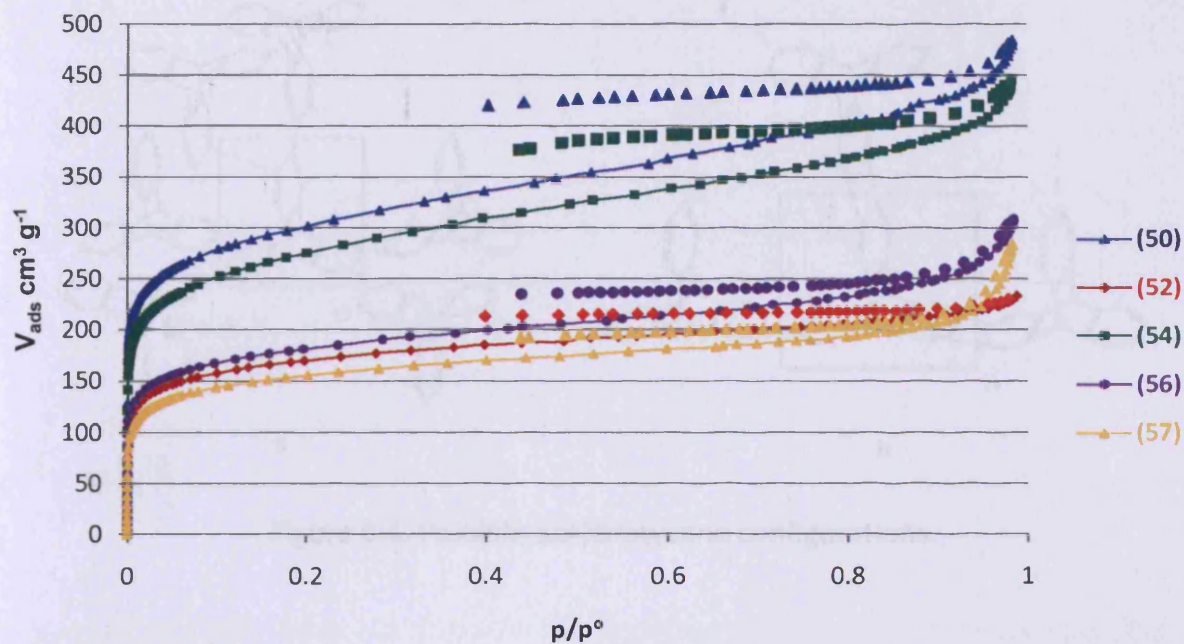
Figure 6.3. The nitrogen adsorption (solid line)/desorption (dashed line) isotherm for a powder sample of coupled polymers.

All polymer samples exhibit a (Type I) isotherm with a microporous character indicated by a large take-up of nitrogen at low relative pressure (p/p^o <0.01). Between relative pressures 0.20 and 0.98, there is further adsorption of nitrogen, which may indicate the presence of some mesopores sizes (pore size 2-50 nm). Alternatively, this further adsorption may be due to swelling of the structure during the adsorption experiment.

Polytriptycene **(50)** demonstrates the highest surface area compared to the other coupled polymers described in this chapter. The porosity of this polytriptycene is primarily attributed to the ability of individual triptycene units to express "internal molecular free volume" (IMFV), since each triptycene unit is potentially attached to six similar units (Fig. **6.3a**). This configuration is presumably favoured rather than forming a relatively unstable four-membered ring between triptycene units based on the model reaction product, (*Fig.* **6.4b**).[102]
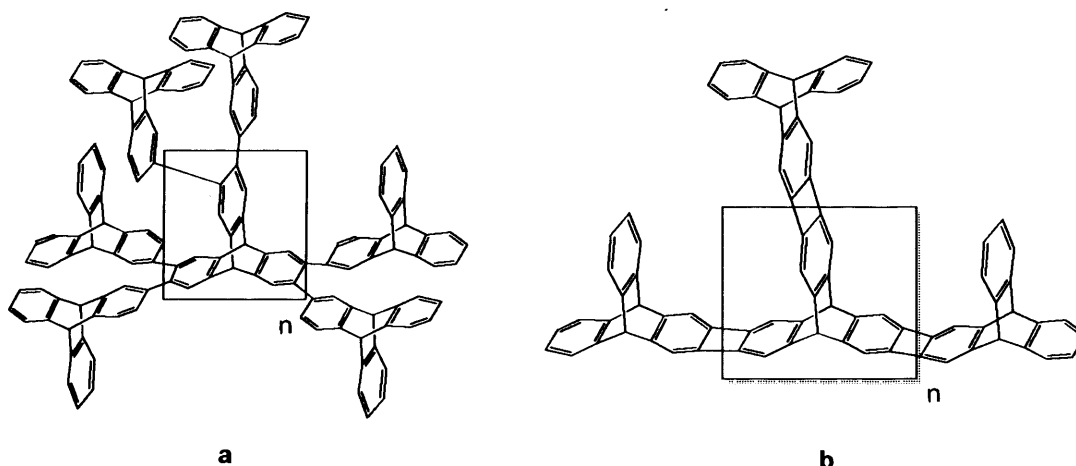
Figure 6.4. Possible polytriptycene configurations.

Triphenylmethane unit also expresses IMFV due to tetrahedral-like geometry but produced low porosity as a polymer **(52)** probably due to its relative flexibility of the resulting structure originated mainly from the presence of the small hydrogen on the sp^3 carbon.

Polypyrene **(54)** has a relatively high surface area and total pore volume despite the fact of its obvious flat geometry; this strongly indicates the pyrene motifs are oriented perpendicular to each other wherein local cavities are formed because of the inability for such structures to pack efficiently. In contrast, the low surface area and total pore volume of polytriphenylene **(56)** indicates a more efficient packing perhaps due to the the formation of triphenylene units to give a stable honey-comb structure (Fig **6.5a**), rather than the more open structure represented in Fig. **6.4b**.
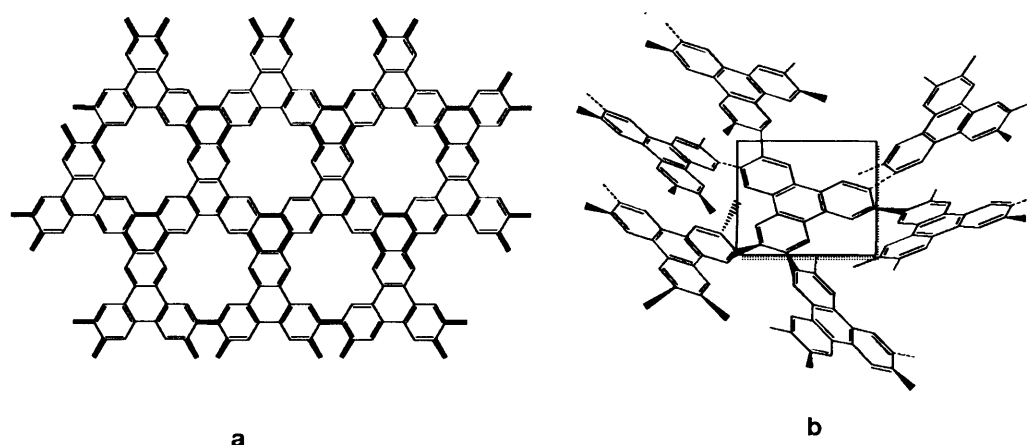
Figure 6.5. Possible polytriphenylene configurations.

Polypropellane **(57)** demonstrates low surface area despite the obvious large internal molecular free volume of the monomer. This is likely due to the compact packing of the near-spherical propellane units and a high degree of cross-linking.

6.8.2 Thermal stability

The thermal stability of conjugated polymers was evaluated by thermogravimetric analysis (TGA) under a nitrogen atmosphere at a heating rate of 10 °C per minute and up to 1000 °C. The initial weight loss due to thermal degradation for these polymers varies between 390-550 °C; the total weight loss is about 25-35 % of initial weight (Table **6.3**), which is low and reflects the high carbon content.

Polymer	Decomposition temperature (°C)	Total weight loss (%)
(50)	416	26
(52)	550	35
(54)	390	32
(56)	425	27
(57)	440	30

Table 6.2. TGA data of prepared conjugated polymers

The wide range of decomposition temperature is probably attributed to the different building blocks used in their synthesis. All the polymers show a weight loss of about 2-4 % at low temperature up to 250 °C; this is probably due to loss of moisture and/or entrapped solvent. Triphenylmethane polymer **(52)** thermally degrades at relatively high temperature presumably due to a uniform polymer structure, similar degradation temperature was reported for tetraphenylmethane polymer[51]. The TGA curves of prepared conjugated polymers are shown in Figure **(6.6)**.
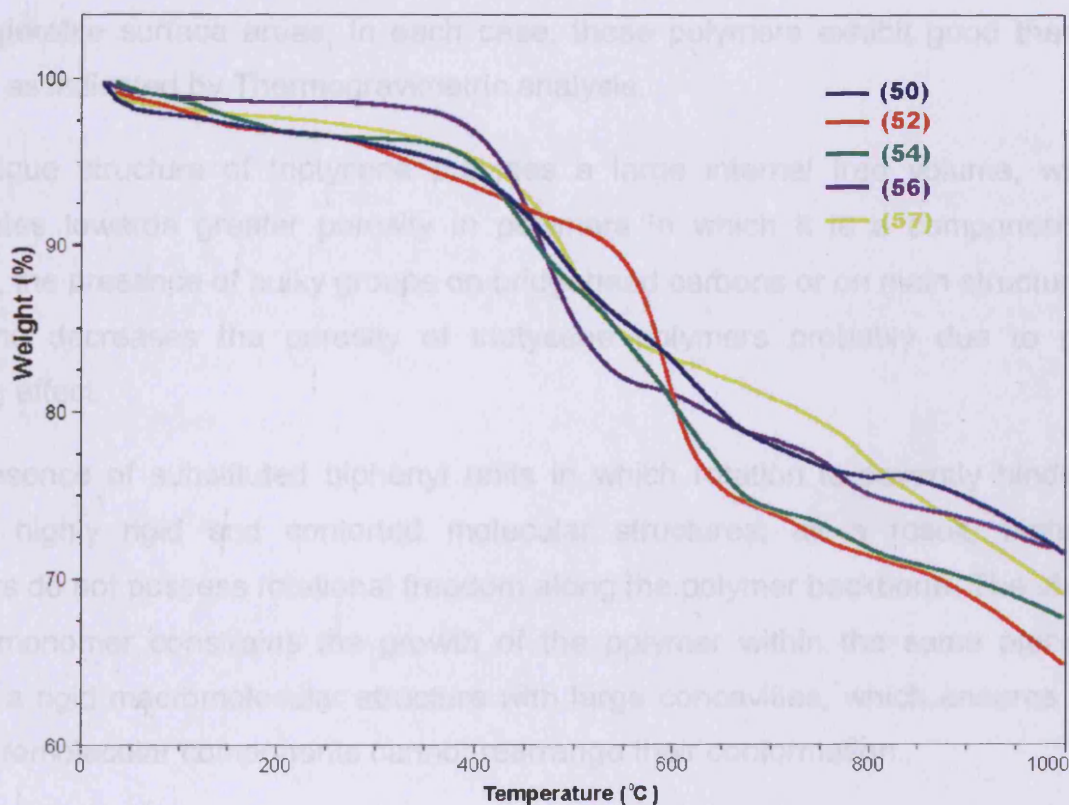

Figure 6.6. TGA profile of conjugated polymers (nitrogen atmosphere).

Chapter 7. Conclusion

Series of network and ladder microporous polymers were prepared by conventional nucleophilic aromatic substitution polycondensation reaction between catechol-containing compounds and activated o-flouro aryls monomers. The Yamamoto coupling reaction was also used to prepare microporous polymers by the self-coupling of various aryl bromide compounds. The resulting polymers were characterised by elemental analysis and nitrogen adsorption analysis, which showed a considerable surface areas. In each case, these polymers exhibit good thermal stability as indicated by Thermogravimetric analysis.

The unique structure of triptycene provides a large internal free volume, which contributes towards greater porosity in polymers in which it is a component. In general, the presence of bulky groups on bridgehead carbons or on main structure of triptycene decreases the porosity of triptycene polymers probably due to pore blocking effect.

The presence of substituted biphenyl units in which rotation is severely hindered creates highly rigid and contorted molecular structures; as a result, biphenyl polymers do not possess rotational freedom along the polymer backbone. The shape of this monomer constrains the growth of the polymer within the same plane to provide a rigid macromolecular structure with large concavities, which ensures that the macromolecular components cannot rearrange their conformation.

Polymers derived from flat aromatic monomers such as hexaazatrinapthylene, triphenylene and pyrene also possess a considerable degree of porosity; the presence of such structure creates an accessible free volume within the polymer chains.

Due to the highly rigid and contorted structure of polymeric chains, GPC analysis for soluble microporous polymers may not provide an accurate measurement of molecular mass, since there is a difference in their hydrodynamic volume compared with the more flexible polystyrene standards in solution.

Despite the geometry and functional groups of all the monomers used for polymerisation in this work, the distinct feature of all materials prepared in this study

is the rigidity of the resulting polymer architecture. To conclude, the polymers reported in this thesis possess considerable surface areas and may be considered as polymers of intrinsic microporosity in which the high rigidity and contorted structure of the polymer frustrates the efficient packing of the material in the solid state with the high nitrogen uptake at very low relative pressure may be taken as the primary indicator of microporosity in these materials.

7.1 Future work

The continuation of this work will focus on the utilisation of some of the prepared polymers that contains an active group or structure for a second reaction. For example, polymer (21) is a good candidate to perform Diels-Alder reaction on the anthracene structure using a strong dienophile such as malic anhydride or more bulky anhydride to create more twisted polymer structure that might enhance the porosity of the product.
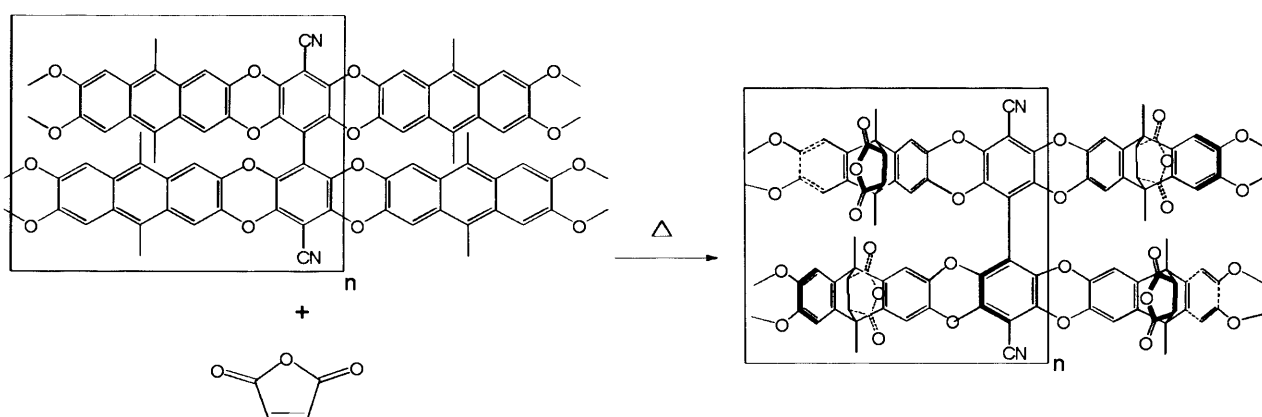
Scheme 7.1. Proposed reaction for polymer **(21)**. *Reagents and condition*: (*i*) xylene, reflux.

The anhydride groups on the expected polymer may be used for hypercrosslinking polymer chains *via* polyimide formation polycondensation using diamino-aryls as internal linkers. The polymeric chains of **(12)** may also be hypercrosslinked *via*

Yamamoto coupling of dibromo-triptycene units within polymer **(12)** as demonstrated by **(57)** formation.
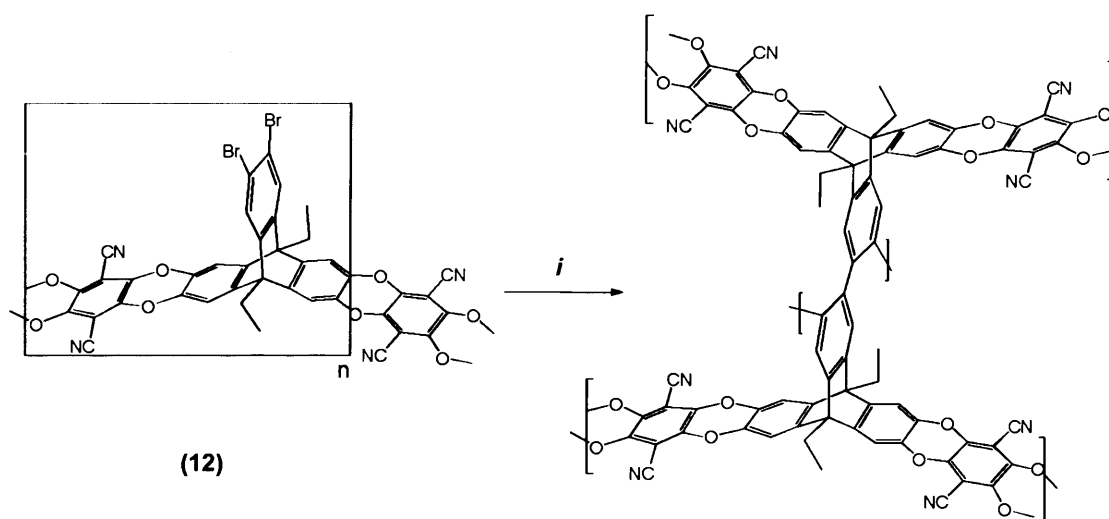
Scheme 7.2. Proposed hypercrosslinking of polymer **(12)**. *Reagents and condition*: (*i*) DMF, 1,5-cyclooctadiene, 2,2'-bipyridyl, bis(cyclooctadiene)nickel(0), heat, nitrogen atmosphere.

The advantage of such method besides creating new pore between the triptycene units on different chains is the elimination of heavy bromines from the final structure, which would increase gas adsorption per unit weight of adsorbent. Materials with the same ideal structure can be prepared using slightly different approach by demethylation of **(58)** then performing benzodioxane-forming reaction with different rigid fluorinated aromatic compounds.
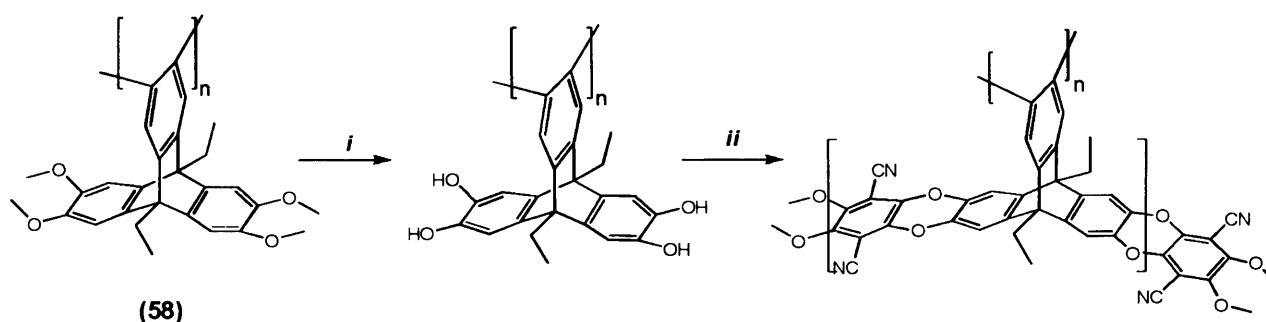
Scheme 7.3. Proposed hypercrosslinking of polymer **(58)**. *Reagents and condition*: (*i*) BBr₃, DCM. (*ii*) DMF, K₃CO₃, heat, nitrogen atmosphere.

EXPERIMENTAL

Chapter 8. Experimental

8.1 Experimental techniques

Starting materials and anhydrous solvents were purchased from Sigma-Aldrich, Acros, Alpha Aesar and TCI chemical companies and were used without further purification. Dry tetrahydrofuran was obtained by pre-drying commercially available tetrahydrofuran over sodium in presence of sodium benzophenone as indicator. Dry dichloromethane was obtained by drying commercially available dichloromethane over calcium chloride. All air/moisture sensitive reactions were performed under a nitrogen atmosphere.

Spectroscopic techniques

Nuclear magnetic resonance (NMR) spectra were recorded using Bruker Advance DPX 400 instrument, ^{1}H NMR spectra were recorded at 400 MHz, ^{13}C NMR spectra recorded at 100 MHz. All chemical shifts are reported as parts per million (δ) using tetramethylsilane (TMS) as internal standard. Signals are reported as singlet (s), doublet (d), triplet (t), quartet (q), multiplet (m) and broad (b). Infrared spectra were obtained either as solvent cast thin films on sodium chloride plates, or KBr discs and were recorded on Perkin-Elmer 1600 series FTIR spectrometer and absorptions are quoted in cm^{-1}. Mass spectra electron impact ionisation (**EI**) or chemical ionisation in the presence of ammonium ions (**CI**) were recorded on Fisons VG Platform II quadrupole instrument. High-resolution mass spectrometric data were obtained in electrospray (**ES**) or electron impact (**EI**) mode unless otherwise reported on a Waters Q-TOF micromass spectrometer. High mass measurements by matrix assisted laser desorption ionisation time of flight (MALDI-TOF) were recorded on a Micromass TofSpec 2E spectrometer with a nitrogen laser at 337 nm.

Gel permeation chromatography

GPC analyses were carried out on *Viscotek GPCmax* VE2001 with RI(VE3580)

detector, using chloroform as eluent; Columns: KF-805L SHODEX, Temperature: ambient; Flow rate of 1 mL/min; Calibration: a series of polystyrene standard up to Mw: 9.4 x10^5 with a narrow polydispersity.

Elemental analysis

Elemental analyses were obtained from Warwick Analytical Service using the CE440 Elemental Analyser (±0.15% accuracy with standard organic compounds) with embedded Ultra Micro balance and thermal conductivity detector.

Thermogravimetric analysis

Thermogravimetric analysis (TGA) measurements were obtained using SDT Q600 Analyser fitted with double beam microbalance (0.1μg sensitivity). All analyses were preformed at heating rate of 10 °C/min from 40 to 1000 °C.

BET surface area measurements

Adsorption/desorption isotherms of nitrogen were measured at low temperature using a Coulter SA3100 instrument with foreline filter and vacuum pump (10^{-3} mm Hg). The typical sample weight used in the measurement was less than 0.1 g; samples were degassed for at least 2 hours at 120 °C under high vacuum prior to analysis. Surface area calculated using multipoint BET data, pore size and pore size distribution analysis were done using BJH equation, sorption measurements were carried out under liquid nitrogen temperature and pure N_2 (99.999 %) was used as adsorbate.

Gas permeation measurements

Gas permeation data were measured by Dr. Detlev Fritsch (GKSS, Research Centre, Germany) at 30 °C with pure gases, using a pressure increase time-lag apparatus operated at low feed pressure (200-300 mbar) starting with an oil free vacuum (<10^{-4} mbar).

Other techniques

Melting points were determined using a Gallenkamp capillary melting point apparatus. Ultra violet/visible (UV/Vis) spectra were recorded on a shimadzu UV-260 spectrometer. TLC was carried out using plates precoated with Merck silica gel (60-254mesh). Visualisation was achieved by ultraviolet radiation at 254 nm. Column chromatography was carried out using Merck Silica gel 60 (230 – 400 mesh).

8.1 Experimental procedures

9,10-Dibenzyl-2,3,6,7-tetramethoxyanthracene (2)
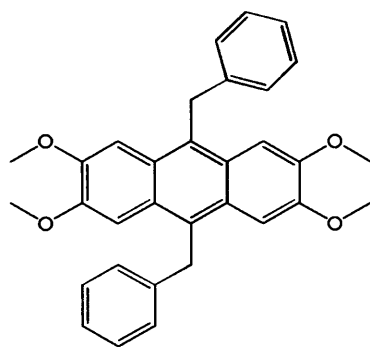
A mixture of veratrole (13.8 g, 0.1 mol), and phenylacetaldehyde (12.0g, 0.10 mol) was added dropwise at 0-5 °C over 0.5 hour with stirring to 50 mL of concentrated sulphuric acid In a 100 mL beaker. The reaction mixture was stirred for additional 0.5 hour then poured into 200 mL of water. The resulting precipitate was filtered, washed with water and dried in air. The crude product was recrystallised from methanol to give a pale yellow powder. Yield: 3.1 g, 69 mmol (12.9 %); Mp: >300 °C; ^{1}H NMR (400 MHz; CDCl$_3$) δ (ppm): 3.84 (s, 12H), 4.79 (s, 4H), 7.07-7.18 (m, 10H), 7.31 (s, 4H); ^{13}C NMR (100 MHz; CDCl$_3$) δ (ppm): 35.2, 56.1, 57.0, 103.1, 108.7, 126.5, 126.8, 128.0, 128.6, 129.1, 141.3, 149.5; LRMS, m/z, (CI): 478.7 [M$^+$].

9,10-Dibenzyl-2,3,6,7,14,15-hexamethoxytriptycene (3)
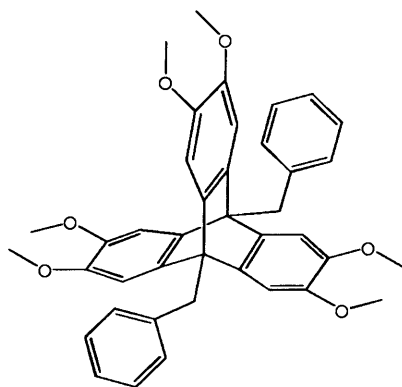
A mixture of 9,10-dibenzyl-2,3,6,7-tetramethoxyanthracene (1.5 g, 3.14 mmol) and 4,5-dimethoxybenzenediazonium-2-carboxylate[77]   (3.22 g,   13.18 mmol)   in dichloroethane (120 mL) and 1,2-epoxypropane (20 mL) was refluxed for 16 hours. After cooling to room temperature, the reaction mixture was concentrated under reduced pressure. The resulting oil was dissolved in DCM (15 mL) and purified by column chromatography (hexane/ethyl acetate 3:1) to give a white solid. Yield: 0.99 g, 1.62 mmol (51.5 %); Mp: 128-130°C; ^{1}H NMR (400 MHz; CDCl$_3$) δ (ppm): 3.46 (s, 18H), 4.46 (s, 4H), 6.84 (s, 6H), 7.2-7.4 (m, 10H); ^{13}C NMR (100 MHz; CDCl$_3$) δ (ppm): 33.1, 50.9, 55.9, 109.1, 125.9, 127.9, 130.8, 138.1, 141.2, 144.75; LRMS, m/z, (CI): 615.1 [M$^+$].

9,10-Dibezyl-2,3,6,7,14,15-hexahydroxytriptycene (4)
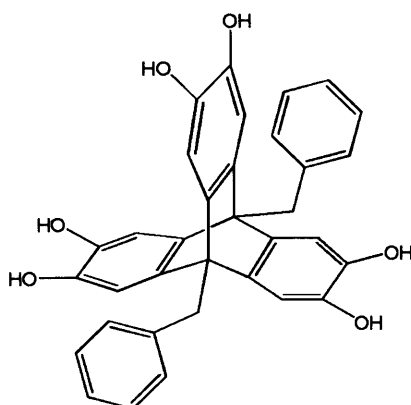
In a two-necked round bottom flask boron tribromide (3.40 mL, 19.81 mmol) was added dropwise to a stirred solution of 9,10-diethyl-2,3,6,7,14,15-hexamethoxytriptycene (0.82 g, 3.01 mmol) in dry dichloromethane (70 mL) at 0 °C under a nitrogen atmosphere. The reaction mixture was stirred at room temperature for 3 hours then poured into a mixture of ice and water, the precipitate was collected by filtration, washed with cold water and dried. The crude product was recrystallised from THF to give a purple solid. Yield: 0.69 g; 1.3 mmol (98 %); Mp: 110-112 °C (decomposition); ^{1}H NMR (400 MHz; DMSO-d$_6$) δ (ppm): 4.14 (s, 4H), 6.52 (s, 6H); 7.1-7.35 (m, 16H); ^{13}C NMR (100 MHz; DMSO-d$_6$) δ (ppm): 14.5, 19.2, 34.6, 55.9, 111.8, 120.5, 135.9, 137.2, 142.7; LRMS, m/z, (CI): 530.2 [M$^+$].

Di(benzyl)triptycene-based Polymer (5)
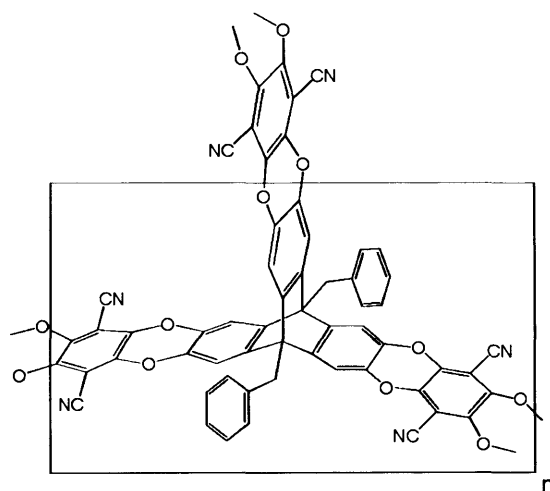
In a dry 100 mL round-bottom flask equipped with stirrer were added 9,10-Dibezyl-2,3,6,7,14,15-hexahydroxytriptycene (0.470 g, 0.88 mmol) and 2,3,5,6-tetrafluoroterephthalonitrile (0.266 g, 1.33 mmol) in anhydrous DMF (70 mL). To this stirred solution, a fine powder of anhydrous potassium carbonate (0.81 g, 5.87 mmol) was added and the reaction mixture was heated at 80 °C in an oil bath under nitrogen for 24 hours. On cooling, the reaction was poured into 150 mL of stirred acidified water; the resulting precipitate was then collected by suction filtration, washed with water and methanol. Purification was achieved by refluxing the product in THF, acetone, and methanol. The product was ground into a fine powder and dried in a vacuum oven at 120 °C for 24 hours to give an orange powder. Yield:

0.608 g (93 %); elemental analysis calc (%) for $C_{47}H_{20}N_3O_7$: C, 76.34; H, 2.71; N, 5.69; found: C, 63.68; H, 3.51; N, 5.94; IR (KBr cm^{-1}): =2239, 1601, 1496, 1448, 1272, 1147, 995, 874, 820, 755, 726; surface area (BET): 880 m^2 g^{-1}, total pore volume 0.58 mL g^{-1} at (p/p$^{\circ}$ = 0.98, adsorption); TGA (Nitrogen): Thermal degradation commences at ~ 460 °C.

9,10-Di(*sec*-butyl)-2,3,6,7-tetramethoxyanthracene (6)
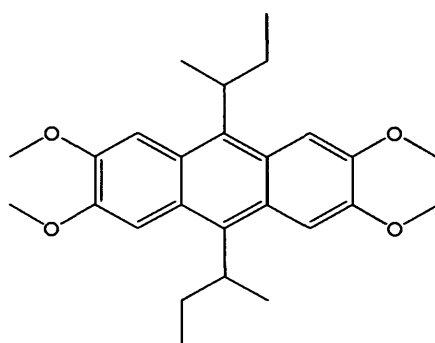
A mixture of 1,2-dimethoxybenzene (13.8 g, 0.10 mol) and 2-methylbutyraldehyde (8.6 g, 0.10 mol) was added dropwise to stirred concentrated sulphuric acid (40 mL) maintained at 0-5 °C over a period of 0.5 h. The reaction mixture was then stirred at this temperature for 2 hours and then poured into iced water. The resulting precipitate was filtered and washed with water then recrystallised from acetone to give a yellow powder. Yield: 2.99g, 7.3 mmol (14.6 %); Mp >300 °C; ^{1}H NMR (400 MHz; CDCl$_3$) δ (ppm): 0.82 (t, 6H, J_1=7.3 Hz, J_2=7.3 Hz), 1.65 (d, 6H, J=7.27 Hz), 2.08-2.16 (m, 4H), 3.92 (s, 12H), 4.05-4.14 (m, 2H), 7.56 (s, 4H); ^{13}C NMR (100 MHz; CDCl$_3$) δ (ppm): 13.81, 20.78, 29.64, 35.57, 55.49, 133.26; LRMS, *m/z*, (CI): 410.6 [M$^+$].

9,10-Di(*sec*-butyl)-2,3,6,7,14,15-hexamethoxytriptycene (7)
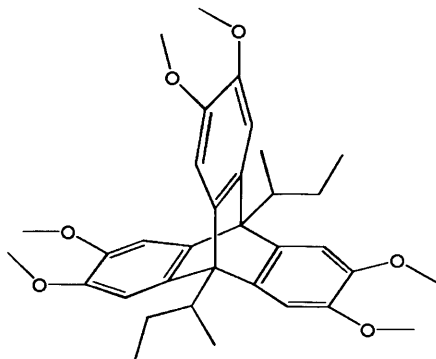
A mixture of 9,10-di(sec-butyl)-2,3,6,7-tetramethoxyanthracene (2.1 g, 5.12 mmol) and 4,5-dimethoxybenzenediazonium-2-carboxylate[77] (5 g, 20.44 mmol) in dichloroethane (120 mL) and 1,2-epoxypropane (20 mL) was refluxed for 12 hours. After cooling to room temperature the reaction mixture was concentrated under reduced pressure. The resulting oil was dissolved in DCM (15 mL) and purified by column chromatography using DCM as an eluent to give a pale yellow solid. Yield: 1.2 g, 2.21 mmol (43.1 %); Mp: 120-124°C; ^{1}H NMR (400 MHz; DMSO-d$_6$) δ (ppm): 1.45 (t, 6H, J_1=5.6 Hz, J_2=6.8 Hz), 1.79-1.91 (m, 6H), 2.1 (m, 2H), 2.33 (m, 2H), 2.95 (m, 1H), 3.05 (m, 1H), 3.75 (t, 6H, J_1= 2.8 Hz, J_2= 2.8 Hz), 3.82 (d, 12H, J= 2.8 Hz), 6.79-7.31(m, 6H); ^{13}C NMR (100 MHz; DMSO-d6) δ (ppm): 17.3, 21.1, 30.2, 37.1, 59.0, 113.3, 114.9, 142.6, 146.2; LRMS, *m/z*, (EI): 546.3 [M$^+$].

9,10-Di(sec-butyl)-2,3,6,7,14,15-hexahydroxytriptycene (8)
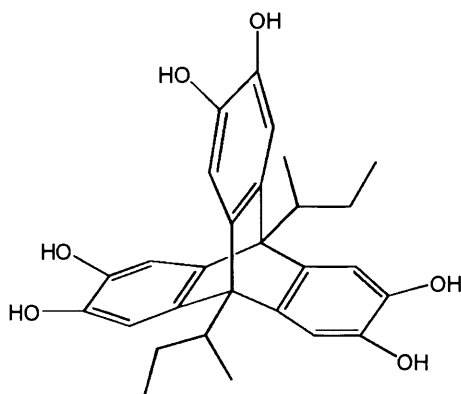
In a two-necked round bottom flask 9,10-di(sec-butyl)-2,3,6,7,14,15-hexamethoxytriptycene (1.10 g, 2.01 mmol) was dissolved in 50 mL dry dichloromethane. Under cooling in an ice bath, boron tribromide (1.3 mL, 13.52 mmol) was added dropwise. The reaction mixture was stirred overnight at room temperature, then poured into 50 mL distilled water and stirred for another 0.5 hour. After filtration, the precipitate was washed with water and dried under reduced pressure to give a purple solid. Yield: 0.89 g; 2.95 mmol; 96 % ; Mp: 110-114 °C (decomposition); ^{1}H NMR (400 MHz; DMSO-d$_6$) δ (ppm): .32 (t, 6H, J$_1$=6.8 Hz, J$_2$= 6.8 Hz); 1.60-1.67 (m, 6H), 1.67-1.99 (m, 4H), 2.12-2.19 (m, 2H), 6.64-7.12 (m, 6H); ^{13}C NMR (100 MHz; DMSO-d$_6$) δ (ppm): 15.0, 20.1, 26.9, 36.5, 58.8, 115.3, 141.2, 145.4; LRMS, m/z, (EI): 462.2 [M$^+$].

Di(sec-butyl)triptycene-based polymer (9)
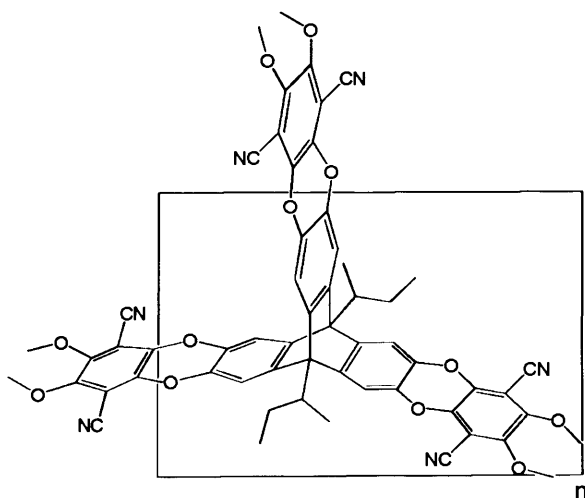
To a stirred solution of 9,10-di(sec-butyl)-2,3,6,7,14,15-hexahydroxytriptycene (0.495 g, 1.07 mmol) and 2,3,5,6-tetrafluoroterephthalonitrile (0.321 g, 1.6 mmol)) in anhydrous DMF (70 mL) was added anhydrous potassium carbonate (1.2 g, 8.7 mmol); the mixture was heated at 80 °C in an oil bath for 24 hours. On cooling, the mixture was poured into water (150 mL) and acidified with 2 N HCl. The crude product was collected by filtration and washed with water and methanol. Purification was achieved by stirring in refluxing THF and methanol. The resulting orange solid was ground into a fine powder and dried in a vacuum oven at 120 °C for 24 hours to give an orange powder. Yield: 0.696 g (97 %); elemental analysis calc (%) for

$C_{41}H_{24}N_3O_7$: C, 73.35; H, 3.58; N, 6.26; Found: C, 63.68; H, 3.51; N, 5.94; IR (KBr cm^{-1}): =2958, 1601, 1440, 1267, 1152, 1076, 1011, 871, 757, 735, 666; surface area (BET): 945 m^2 g^{-1}, total pore volume 0.58 mL g^{-1} at (p/p° = 0.98, adsorption); TGA (Nitrogen): Thermal degradation commences at 440 °C.
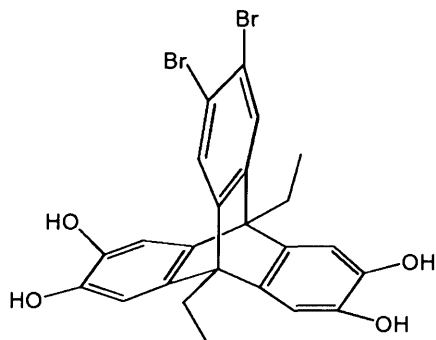
14,15-Dibromo-9,10-diethyl-2,3,6,7-tetramethoxytriptycene (10)
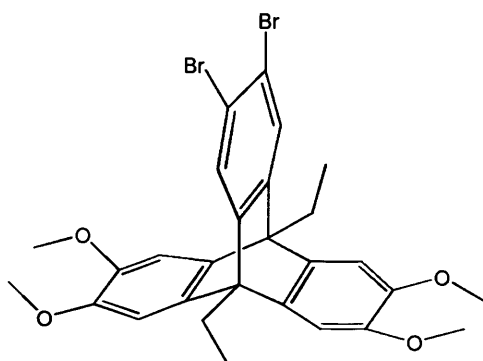
To a stirred solution of 9,10-diethylanthracene[28] (2g, 5.65 mmol) and 1,2,4,5-tetrabromobenzene (2.22 g, 5.65 mmol) in dry toluene (20 mL) at room temperature under nitrogen was added n-butyllithium (6 mmol) in hexane (30 mL) dropwise over 0.5 hour. The reaction mixture was stirred for additional 3 hours then methanol (10 mL) was added. The solvents were removed under reduced pressure and the resulting yellow oily solid was resolved by column chromatography using hexane:DCM (1:1) as an eluent to give an off-yellow powder. Yield: 0.485 g, 0.83 mmol (14.6%); Mp: 170-174 °C (decomposition); ^{1}H NMR (400 MHz; CDCl$_3$) δ (ppm): 1.63 (t, 6H, J= 7.2Hz), 2.84 (q, 4H, J= 7.2), 3.77 (s, 12H), 6.91 (s, 4H), 7.43 (b, 2H); ^{13}C NMR (100 MHz; CDCl$_3$) δ (ppm): 11.27, 20.24, 53.12, 56.73, 108.81, 120.45, 146.2; HRMS, m/z, (EI): 586.0335 [M$^+$], calulated for 28C 28H 4O 2 ^{79}Br: 586.0354.

14,15-Dibromo-9,10-diethyl-2,3,6,7-tetrahydroxytriptycene(11)

In a two-necked round bottom flask 14,15-dibromo-9,10-diethyl-2,3,6,7-tetramethoxytriptycene (1.42 g, 2.41 mmol) was dissolved in dry DCM (40 mL). Under cooling in an ice bath, boron tribromide (1.0 mL, 10.4 mmol) was added dropwise. The reaction mixture was stirred overnight at room temperature then poured into distilled water (50 mL) and stirred for another 0.5 hour. After filtration, the precipitate was washed with water, dissolved in ethyl acetate (50 mL), dried over $MgSO_4$ and filtered. Removing the organic solvents under reduced pressure gave an off-white solid. Yield: 1.11 g, 2.1 mmol (87 %); Mp: 174-178 (decomposition); ^{1}H NMR (400 MHz; Acetone-d$_6$) δ (ppm): 1.61 (t, 6H, J= 7.2 Hz), 2.84 (q, 4H, J= 7.2 Hz), 6.98 (s, 4H), 7.55 (s, 2H), 8.53 (s, 4H); ^{13}C NMR (100 MHz; Acetone-d$_6$) δ (ppm): 11.5, 20.9, 53.5, 55.9, 111.8, 120.5, 135.9, 137.2, 142.7; HRMS, m/z, (CI): 531.9713 [M$^+$], calc for C_{24} H_{20} O_4 ^{79}Br ^{81}Br: 531.9708

Dibromotriptycene-based polymer (12)
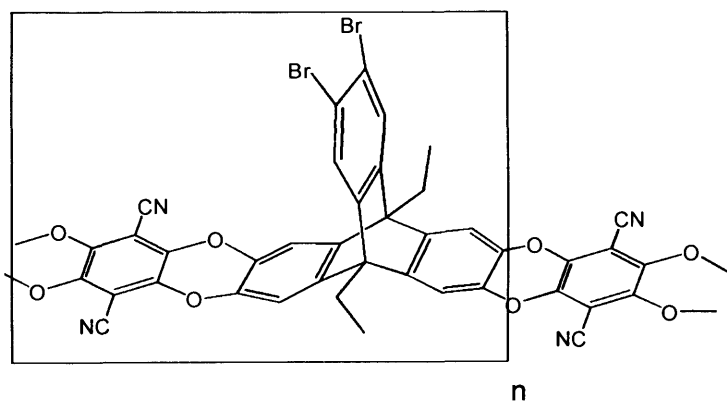
n

To a stirred solution of 14,15-dibromo-9,10-diethyl-2,3,6,7-tetrahydroxytriptycene (0.695 g, 1.31 mmol) and 2,3,5,6-tetrafluoroterephthalonitrile (0.261 g, 1.31 mmol) in anhydrous DMF (100 mL) was added anhydrous potassium carbonate (1.2 g, 8.7 mmol). The mixture was then heated at 60 °C for 48 hours under a nitrogen atmosphere. On cooling, the reaction mixture was poured into stirred aqueous HCl (1 %, 200 mL) and the resulting precipitate was collected by filtration, washed with distilled water, methanol and dried. The resulting precipitate was purified by dissolving in chloroform (20 mL), filtering the resulting solution through glass wool and reprecipitating by dropwise addition into methanol (200 mL). The product was finally collected by filtration and dried in a vacuum oven at 100 °C for 24 hours to give an orange powder. Yield: 0.75 g (88 %); elemental analysis calc (%) for $C_{32}H_{16}Br_2N_2O_4$: C, 58.92; H, 2.45; Br, 24.98, N, 4.29; found: C, 55.22; H, 2.64; Br, 24.84; N, 4.23; ^{1}H NMR (400 MHz; CDCl$_3$) δ (ppm): 1.53-1.6 (b, 6H), 2.67-2.8 (b, 4H), 6.88-6.98 (b, 4H), 7.43-7.49 (b, 2H); IR (thin film cm^{-1}): =2951, 2240, 1698, 1603, 1443, 1271, 1170, 1014, 968, 906, 865, 807, 753; surface area (BET): 511 m^2 g^{-1}, total pore volume 0.48 mL g^{-1} at (p/p$^\circ$ = 0.98, adsorption); TGA (Nitrogen): Thermal degradation commences at 470 °C; GPC (THF): Mw: 36860, Mn: 14433 relative to polystyrene.

Dibromotriptycene-based co-polymer (13)
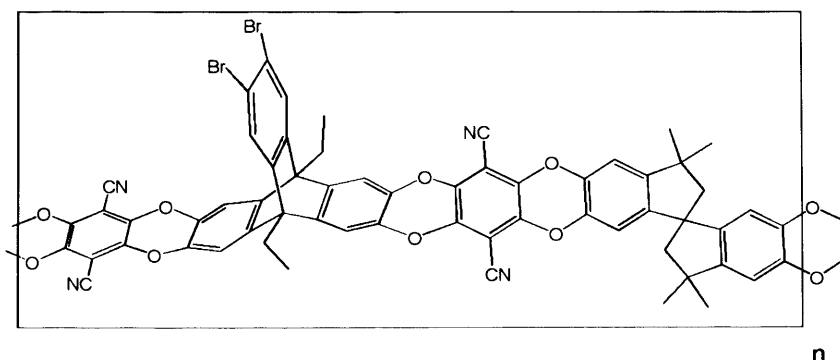
To a stirred solution of 14,15-dibromo-9,10-dithethyl-2,3,6,7-tetrahydroxytriptycene (0.541 g, 1.02 mmol), 2,3,5,6-tetrafluoroterephthalonitrile (0.407 g, 2.04 mmol) and 5,5',6,6'-tetrahydroxy-3,3,3',3'-tetramethyl-1,1'-spirobisindane (0.346 g, 1.02 mmol) in anhydrous DMF (90 mL) was added anhydrous potassium carbonate (1.8 g, 13

mmol) as a fine powder. The mixture was then heated at 60 °C for 48 hours under a nitrogen atmosphere. On cooling, the mixture was poured into water (200 mL) and acidified with 2 M HCl. The resulting precipitate was collected by filtration, washed with distilled water and methanol then dried. The product was purified by dissolving in chloroform (20 mL), filtering the resulting solution through glass wool and reprecipitating by dropwise addition into methanol (250 mL). The resulting precipitate was collected by filtration and dried in a vacuum oven at 100 °C for 24 hours to give an orange powder. Yield: 1.04 g (94 %); ^{1}H NMR (400 MHz; CDCl$_3$) δ (ppm): 1.2-1.3 (d, b, 12H), 1.56 (b, 12H), 2.07 (b, 2H), 2.26 (b, 2H), 2.74 (b, 4H), 6.34 (b, 2H), 6.74 (b, 2H), 6.93 (b, 4H), 7.47 (b, 2H); elemental analysis calc (%) for C$_{61}$H$_{36}$Br$_2$N$_4$O$_8$: C, 65.78; H, 3.26; Br, 14.37, N, 5.03; found: C, 62.45; H, 3.10; Br, 17.35; N, 4.91; IR (thin film cm^{-1}): =2954, 2927, 2869, 2239, 1606, 1442, 1363, 1268, 1212, 1172, 1108, 1012, 967, 874, 810, 753; GPC (THF): Mw: 69700 g mol^{-1}, Mn: 28912 relative to polystyrene; surface area (BET): 536 m^2 g^{-1}, total pore volume 0.42 mL g^{-1} at (p/p$^{\circ}$ = 0.98, adsorption); TGA (Nitrogen): Thermal degradation commences at 470 °C.

Tetramethoxy-bitriptycene (14)
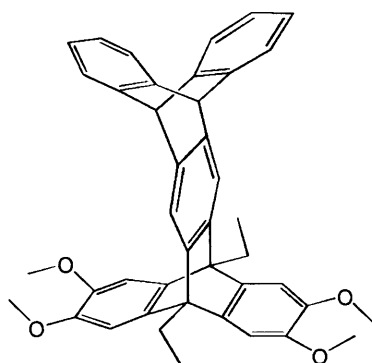
To a stirred suspension of anthracene (2.2 g, 12.35 mmol) and 14,15-dibromo-9,10-diethyl-2,3,6,7-tetramethoxytriptycene (1.68 g, 2.85 mmol) in dry THF (30 mL) at -78 °C under nitrogen was added n-butyllithium (3 mmol) in hexane (30 mL) dropwise over 0.5 hour. The reaction mixture was stirred for additional 3 hours and then methanol (10 mL) was added. The solvents were removed under reduced pressure and the resulting yellow oily solid was resolved by column chromatography using DCM as an eluent to give a white powder. Yield: 0.68 g, 1.12 mmol (39.3 %); Mp:

214-218 °C (decomposition); ^{1}H NMR (400 MHz; CDCl$_3$) δ (ppm): 1.75 (b, 6H), 3.01 (b, 4H), 3.86 (b, 12H), 5.51 (b, 2H), 6.91-7.7 (b); LRMS, m/z, (EI): 606.3 [M$^+$].

Tetrahydroxy-bitriptycene (15)
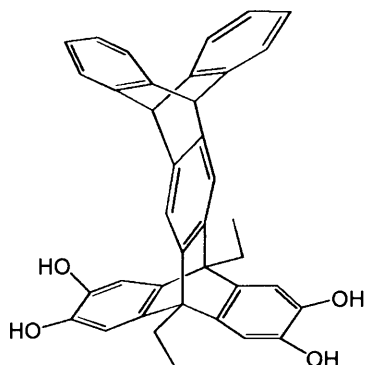
In a two-necked round bottom flask compound **(14)** (0.57 g, 0.94 mmol) was dissolved in 30 mL dry dichloromethane. Under cooling in an ice bath boron tribromide (0.4 mL, 3.76 mmol) was added dropwise. The reaction mixture was stirred overnight at room temperature then poured into water (50 mL) and stirred for another 0.5 hour. After filtration, the precipitate was washed with water and dried under reduced pressure to give a purple solid. Yield: 0.502 g; 0.91 mmol (97 %); Mp: 110-112 °C (decomposition); ^{1}H NMR (400 MHz; Acetone-d$_6$) δ (ppm): 1.64 (b, 6H); 2.9 (b, 4H), 5.68 (b, 2H), 6.9-7.63 (b, 14H); LRMS, m/z, (EI):550.2 [M$^+$].

Bitriptycene-based polymer (16)
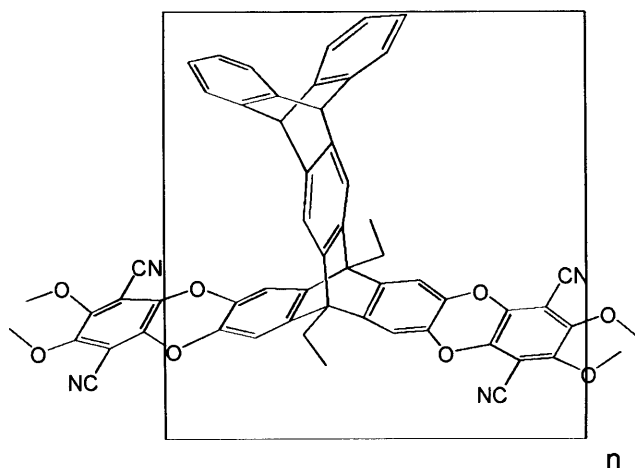
To a stirred solution of compound **(15)** (0.408 g, 0.74 mmol) and 2,3,5,6-tetrafluoroterephthalonitrile (0.0.148 g, 0.74 mmol) in anhydrous DMF (35 mL) was added anhydrous potassium carbonate (0.55 g, 3.99 mmol). The mixture was then heated at 60 °C for 48 hours under a nitrogen atmosphere. On cooling, the reaction mixture was poured into stirred aqueous HCl (1 %, 200 mL) and the resulting precipitate was collected by filtration, washed with distilled water, methanol and dried. Purification was achieved by refluxing the product in THF, acetone, and methanol. The resulting solid was ground into a fin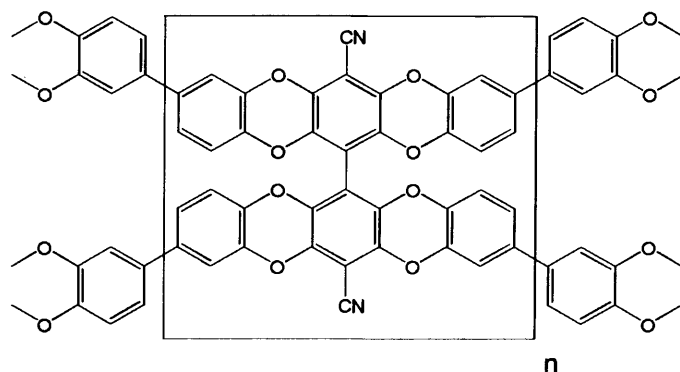e powder and dried in a vacuum oven at 120 °C for 24 hours to give a yellow powder. Yield: 0.453 g (91 %); elemental analysis calc (%) for $C_{46}H_{26}N_2O_4$: C, 82.29; H, 3.87; N, 4.18; found: C, 72.63; H, 3.47; N, 3.97; IR (KBr, cm^{-1}): 2341, 1599, 1442, 1267, 1125, 1088, 863, 730; surface area (BET): 726 m^2 g^{-1}, total pore volume 0.45 mL g^{-1} at (p/p$^{\circ}$ = 0.98, adsorption); TGA (Nitrogen): Thermal degradation commences at 440 °C.

3,3',4,4'-Tetrahydroxybiphenyl (17)
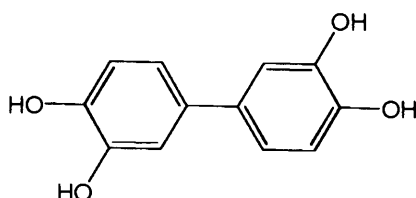
Boron tribromide (2.2 mL, 22.8 mmol) was added dropwise to a solution of 3,3',4,4'-tetramethoxybiphenyl[84] (1.55 g, 5.66 mmol) in dry DCM (35 mL) at 0 °C. The reaction mixture was stirred for 2 hours at room temperature, then poured into water (50 mL) and stirred for another 30 min. The precipitate was filtered and washed with water then dissolved in hot chloroform (80 mL), dried over MgSO$_4$ and filtered. Removing the organic solvents under reduced pressure gave a white powder. Yield: 0.99 g (81%); Mp: 228-232 °C; ^{1}H NMR (400 MHz; Acetone-d$_6$) δ (ppm): 6.86-6.93 (m, 4H), 7.06 (d, 2H); ^{13}C NMR (100 MHz; Acetone-d$_6$) δ (ppm): 114.79, 116.86, 119.19, 134.69, 145.38, 146.47, 207.31; HRMS, m/z, (EI): 218.0574 [M$^+$], calulated: 218.0579.

Biphenyl-based polymer (19)

A mixture of 2,2',3,3',5,5',6,6'-octafluoro-4,4'-dicarbonitrile-biphenyl (0.199 g, 0.57 mmol), 3,3',4,4'-tetrahydroxybiphenyl (0.249 g, 1.14 mmol) and anhydrous potassium carbonate (0.75 g, 54 mmol) in DMF (30 mL) was stirred at 70 °C under nitrogen atmosphere for 48 hours. Upon cooling, the mixture poured into stirred aqueous HCl (1%, 50 mL). The resulting precipitate was filtered and washed with water then purified by refluxing in DMAc, THF and methanol respectively. The product was then ground into a fine powder and dried in a vacuum oven at 120 °C for 24 hours to give a yellow powder. Yield: 0.335 g (94%); elemental analysis calc (%) for $C_{38}H_{12}N_2O_8$: C, 73.08; H, 1.94; N, 4.48. found: C, 66.18; H, 2.21; N, 4.55; IR (KBr, cm^{-1}): 2963, 2236, 1593, 1486, 1428, 1260, 1112, 1036, 987, 865, 807, 752; surface area (BET): 929 $m^2 g^{-1}$, total pore volume 0.53 mL g^{-1} at ($p/p° = 0.98$, adsorption); TGA (Nitrogen): Thermal degradation commences at 510 °C.
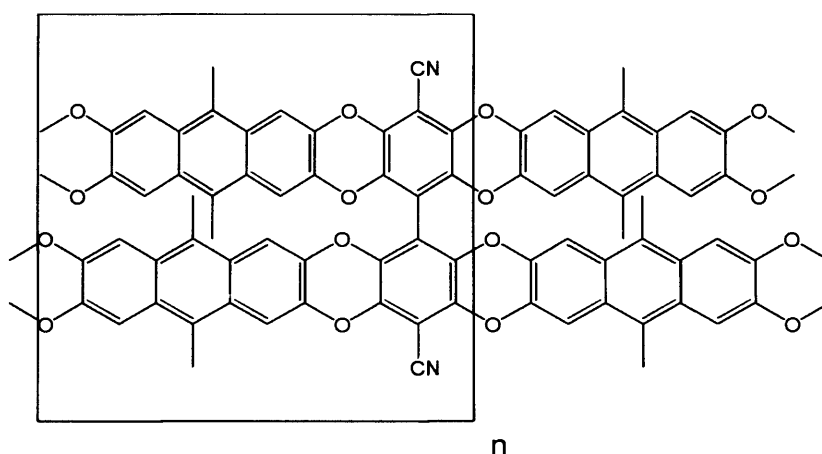
9,10-Dimethyl-2,3,6,7-tetrhydroxy-anthracene (20)
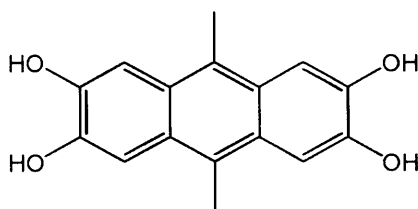
To a suspenstion of 9,10-dimethyl-2,3,6,7-tetramethoxy-anthracene[28] (1.8 g, 5.52 mmol) in dry DCM (60 mL) was added borontribromide (2.2 mL, 22.9 mmol) dropwise at 0 °C. The mixture stirred for 16 hours at room tempreture under nitrogen

then poured into water (50 mL) and stirred for additional 0.5 hour. The resulting precipitate was filtered and washed with water and dried under nitrogen flow for 24 hours to give a pale yellow powder. Yield: 0.99 g (67 %); Mp: >300 °C (decomposition); ^{1}H NMR (400 MHz; Acetone-d$_6$) δ (ppm): 2.79 (s, 6H), 7.51 (s, 4H), 8.39 (s, 4H); ^{13}C NMR (100 MHz; Acetone-d$_6$) δ (ppm): 15.02, 106.93, 127.36, 146.68, 206.73; HRMS, m/z, (EI): 270.0898 [M$^+$], calulated: 270.0892.

Biphenyl-based polymer (21)

n

A fine powder of anhydrous potassium carbonate (0.95 g, 7.24 mmol) was added at once to a stirred mixture of 9,10-dimethyl-2,3,6,7-tetrahydroxyanthracene (0.431 g, 1.59 mmol) and 2,2',3,3',5,5',6,6'-octafluoro-4,4'-dicarbonitrile biphenyl (0.277 g, 0.79 mmol) in anhydrous DMF (50 mL) and the reaction was stirred at 70 °C for 48 hours under nitrogen atmosphere. Upon cooling, the mixture poured into stirred aqueous HCl (1%, 120 mL) and the precipitate was filtered using suction filtration. Purification of the product was achieved by overnight refluxing in DMAc, THF and methanol respectively. The product was ground into a fine powder and dried in a vacuum oven at 120 °C for 24 hours to give a yellow powder. Yield: 0.51 g (88 %); elemental analysis calc (%) for C$_{46}$H$_{20}$N$_2$O$_8$: C, 75.83; H, 2.77; N, 3.84; Found: C, 65.94; H, 2.77; N, 3.98; IR (KBr, cm^{-1}): 2238, 1616, 1423, 1254, 1224, 1053, 989, 859, 738; surface area (BET): 912 m^2 g^{-1}, total pore volume 0.51 mL g^{-1} at (p/p^o = 0.98, adsorption); TGA (Nitrogen): Thermal degradation commences at 480 °C.

Biphenyl-based polymer (23)
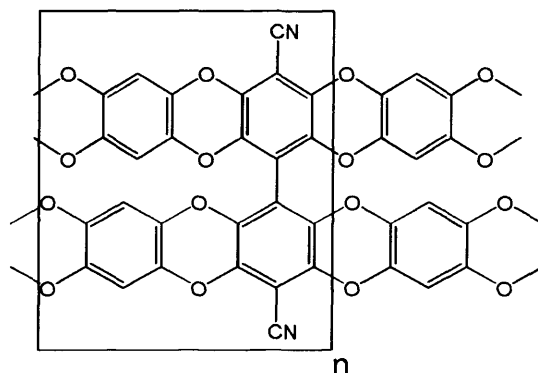
To a stirred mixture of 2,2',3,3',5,5',6,6'-octafluoro-4,4'-dinitrilebiphenyl (0.288 g, 0.83 mmol) and 1,2,4,5-tetrahydroxybenzene[85] (0.235 g, 1.65 mmol) in anhydrous DMF (45 mL) was added a fine powder of potassium carbonate (1.0 g, 7.25 mmol) at once. The mixture stirred at 70 °C under nitrogen for 48 hours then poured into stirred aqueous HCl (1%, 100 mL). The resulting precipitate was filtered and washed with water and methanol then purified by refluxing in DMAc, THF, acetone and methanol respectively. The product was ground into a fine powder and dried in a vacuum oven at 120 °C for 24 hours to give a brown powder. Yield: 0.351 (90 %); elemental analysis calc (%) for $C_{26}H_4N_2O_8$: C, 66.12; H, 0.85; N, 5.93. Found: C, 53.34; H, 1.69; N, 6.22; IR (KBr, cm^{-1}): v = 2238, 1627, 1509, 1425, 1262, 1161, 996, 865; surface area (BET): 887 m^2 g^{-1}, total pore volume 0.48 mL g^{-1} at (p/p^o = 0.98, adsorption); TGA (Nitrogen): Thermal degradation commences at 490 °C.

Biphenyl-based polymer (25)
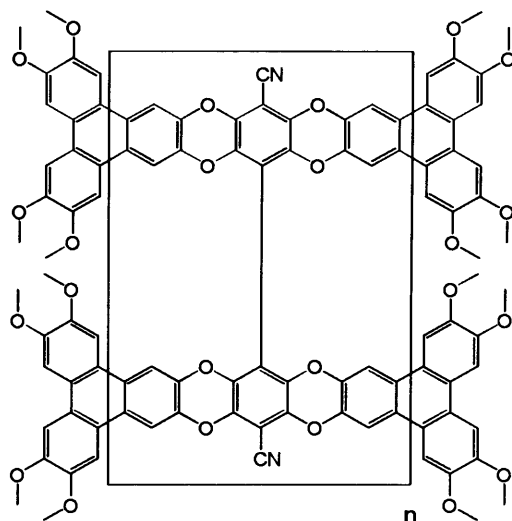
A mixture of 2,3,6,7,10,11-hexahydroxytriphenylene (0.371 g, 1.15 mmol) and 2,2',3,3',5,5',6,6'-octafluoro-4,4'-dinitrilebiphenyl (0.299 g, 0.86 mmol) was stirred in 50 mL of dry DMF in a Schlenk tube under nitrogen at 70 °C for 0.5 hour, then a fine powder of potassium carbonate (1.1 g, 8.02 mmol) was added at once. The reaction left stirring at same temperature for 48 hours then poured into stirred aqueous HCl (1%, 100 mL). The resulting precipitate was filtered and washed with water and methanol then purified by refluxing in DMAc, THF, acetone and methanol respectively. The product was ground into a fine powder and dried in a vacuum oven at 120 °C for 24 hours to give an off-brown powder. Yield: 0.463 g (78 %); elemental analysis calc (%) for the repeat unit $C_{38}H_8N_2O_8$: C, 73.56; H, 1.30; N, 4.51. Found: C, 69.64; H, 2.85; N, 3.45; IR (KBr, cm^{-1}): 2238, 1626, 1508, 1425, 1262, 1179, 1012, 972, 872; surface area (BET): 877 m^2 g^{-1}, total pore volume 0.46 mL g^{-1} at (p/p° = 0.98, adsorption); TGA (Nitrogen): Thermal degradation commences at 450 °C.
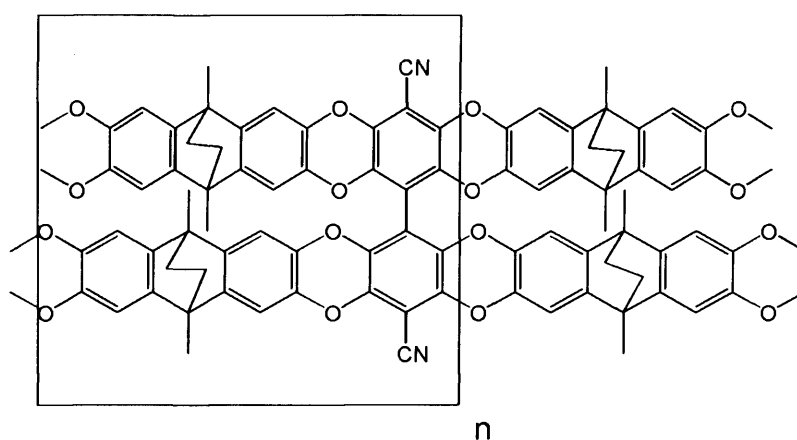
Biphenyl-based polymer (27)

A mixture of 3,6,7-tetrahydroxy-9,10-dimethyl-9,10-ethanoanthracene[86] (0.345 g, 1.15 mmol) and 2,2',3,3',5,5',6,6'-octafluoro-4,4'-dinitrilebiphenyl (0.2 g, 0.57 mmol) was stirred in 50 mL of dry DMF in a Schlenk tube under nitrogen at 70 °C for 0.5 hour, then a fine powder of potassium carbonate (0.75 g, 5.43 mmol) was added at once. The reaction left stirring at same temperature for 48 hours then poured into stirred aqueous HCl (1%, 100 mL). The resulting precipitate was filtered and washed with water and methanol then purified by refluxing in DMAc, THF, acetone and methanol respectively. The product was ground into a fine powder and dried in a vacuum oven at 120 °C for 24 hours to give a yellow powder. Yield: 0.36 g (79.5 %); elemental analysis calc (%) for $C_{50}H_{28}N_2O_8$: C, 76.45; H, 3.57; N, 3.57. Found: C, 70.61, H, 3.41, N, 4.14; IR (KBr, cm^{-1}): 2962, 2864, 2234, 1597, 1435, 1309, 1277, 1232, 1132, 992, 885, 799, 735; surface area (BET): 1309 m^2 g^{-1}, total pore volume 0.95 mL g^{-1} at (p/p° = 0.98, adsorption); TGA (Nitrogen): Thermal degradation commences at 480 °C.

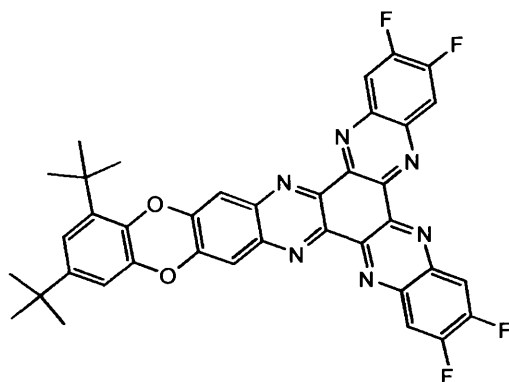## 2,3,8,9,14,15-Hexafluoro-5,6,11,12,17,18-hexaazatrinaphthylene (28)
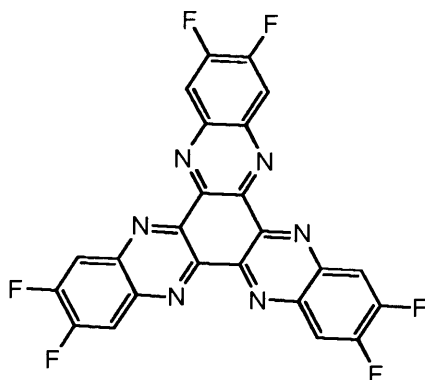
To a stirred solution of 4,5-difluorobenzene-1,2-diamine[103] (3.2g, 22.2 mmol) in glacial acetic acid (200 mL) was added hexaketocyclohexane octahydrate (2 g, 6.4 mmol). The reaction mixture was then heated under reflux for 16 hours and allowed to cool. The solid was collected by suction filtration, washed with hot acetic acid, water and ethanol. The product was then dried in vacuum oven at 120 °C to give a yellow powder. Yield: 2.46 g, 5 mmol (78%); Mp > 300 °C; ^{1}H NMR (400 MHz; CDCl$_3$) δ(ppm): 8.35 (m); ^{13}C NMR (100 MHz; CDCl$_3$) δ(ppm): 113.1, 115.3, 142.1, 161.8; HRMS, m/z, (EI): 492.0559 [M$^+$], calc: 492.0558.

HATN monomer (29)

A mixture of 2,3,8,9,14,15-hexafluoro-5,6,11,12,17,18-hexaazatrinaphthylene (1.0 g, 2 mmol) and 3,5-di-tert butyl catechol (0.45g, 2 mmol) were stirred in dry round bottom flask with anhydrous DMF (60 mL) at 130 °C for 0.5 hour then a fine powder
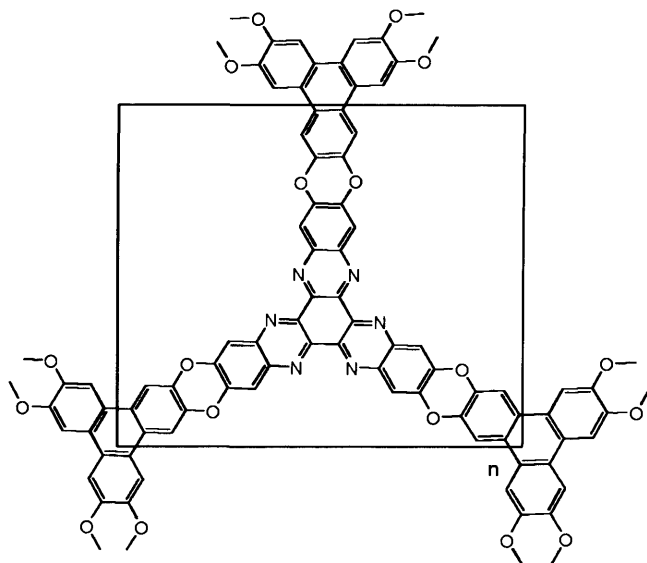
of anhydrous potassium carbonate (0.82 g, 6 mmol) was added. The reaction mixture was stirred in an oil bath for 2 hours at same temperature under a nitrogen atmosphere. On cooling, the reaction mixture was poured into 150 mL of distilled water. The orange solid was collected by suction filtration and washed with hot water. The crude product was purified by column chromatography using chloroform as eluent to give a deep orange powder. Yield: 0.575g, 0.85 mmol, 42%; Mp > 300 °C; ^{1}H NMR (400 MHz; CDCl$_3$) δ (ppm): 1.33 (9H, s), 1.45 (9H, s), 7.0 (1H, s), 7.1(1H, s), 7.25 (1H, s), 7.9(1H, s), 8.25-8.4 (4H, m); ^{13}C NMR (100 MHz; CDCl$_3$) δ (ppm): 30.34, 31.71, 35.18, 35.65, 112.57, 112.78, 113.02, 115.97, 119.86, 137.03, 138.08, 140.6. 141.82, 143.06, 147.79, 147.94, 148.25; LRMS, m/z, (CI): 674 [M$^+$].

Model HATN compound (30)
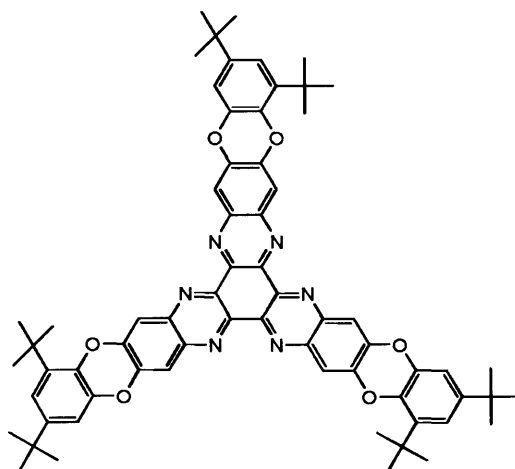
A mixture of compound (29) (0.4 g, 0.6 mmol), 3,5-di-tert-butyl catechol (0.52 g, 2.3 mmol) and anhydrous DMF (50 mL) was stirred for 0.5 hour at 70 °C then a fine powder of anhydrous potassium carbonate (0.74 g, 5.4 mmol) was added at once. The reaction mixture was stirred in an oil bath for 2 hours under a nitrogen atmosphere. On cooling, the reaction mixture was then poured into 100 mL of water. The orange solid was collected by suction filtration and washed with hot water and methanol. The crude product was recrystallised from hexane/chloroform to give a deep orange powder. Yield: 0.259 g, 0.25 mmol (42 %); Mp > 300 °C; ^{1}H NMR (400 MHz; CDCl$_3$) δ (ppm): 1.15-1.23 (m, 36H,), 1.4-1.46 (m, 36H,), 6.95-7.10 (m, 6H), 7.79-8.01 (m, 6H); LRMS, m/z, (CI): 1039 [M$^+$].

HATN-based network polymer (31)

To a stirred solution of 2,3,8,9,14,15-hexafluoro-5,6,11,12,17,18-hexaazatrinaphthylene (0.331 g, 0.67 mmol) and 2,3,6,7,10,11-hexahydroxy-triphenylene (0.218 g, 0.67 mmol) in dry DMF (50 mL) was added anhydrous potassium carbonate (0.7 g, 5 mmol) as a fine powder. The reaction mixture was then heated at 70 °C for 48 hours under nitrogen. On cooling, the reaction mixture was poured into stirred aqueous HCl (1%, 100 mL); the resulting precipitate was filtered and washed with water and methanol then purified by refluxing in DMAc, THF, acetone and methanol respectively. The product was ground into a fine powder and dried in a vacuum oven at 120 °C for 24 hours to give a red powder. Yield: 0.449 g (90 %); elemental analysis calc (%) for $C_{42}H_{12}N_6O_6$: C, 72.41; H, 1.71; N, 12.07; found: C, 63.63; H, 3.67; N, 9.96; IR (film, cm^{-1}): 3401, 1623, 1473, 1431, 1268, 1220, 1083, 995, 869; surface area (BET): 1189 m^{2}g^{-1}, total pore volume 1.74 mL g^{-1} at (p/p° = 0.98, adsorption); TGA (Nitrogen): Thermal degradation commences at 460 °C.

HATN-based network polymer (32)
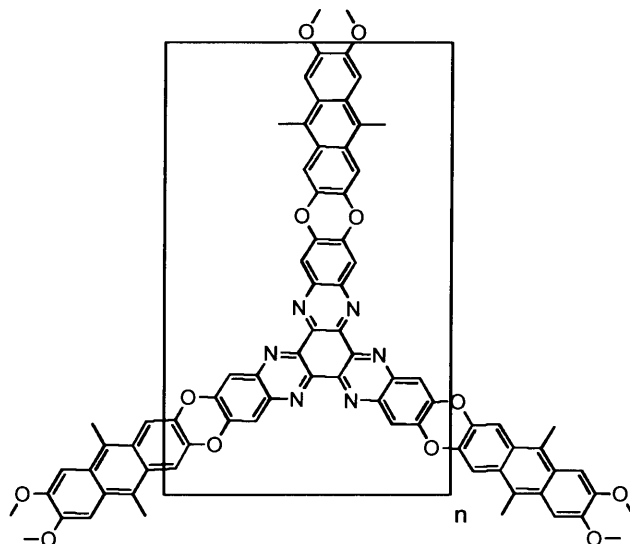
To a stirred solution of 2,3,8,9,14,15-hexafluoro-5,6,11,12,17,18-hexaazatrinaphthylene (0.261 g, 0.53 mmol) and 2,3,6,7-tetrahydroxy-9-10-dimethylanthracene (0.215 g, 0.8 mmol) in dry DMF (45 mL) was added anhydrous potassium carbonate (0.5 g, 3.6 mmol) as a fine powder. The reaction mixture was then heated at 70 °C for 48 hours under nitrogen. On cooling, the reaction mixture was poured into stirred aqueous HCl (1%, 100 mL); the resulting precipitate was filtered and washed with water and methanol then purified by refluxing in DMAc, THF, acetone and methanol respectively. The product was ground into a fine powder and dried in a vacuum oven at 120 °C for 24 hours to give a yellow powder. Yield: 0.4 g (97%); elemental analysis calc (%) for $C_{48}H_{21}N_2O_6$: C, 74.06; H, 3.70; N, 10.80; found: C, 66.13; H, 3.45; N, 11.30; IR (film, cm^{-1}): 2956, 1626, 1453, 1306, 1238, 1082, 984, 913, 870, 817, 777; surface area (BET): 746 m^2 g^{-1}, total pore volume 0.69 mL g^{-1} at (p/p° = 0.98, adsorption); TGA (Nitrogen): Thermal degradation commences at 450 °C.

HATN-based network polymer (33)
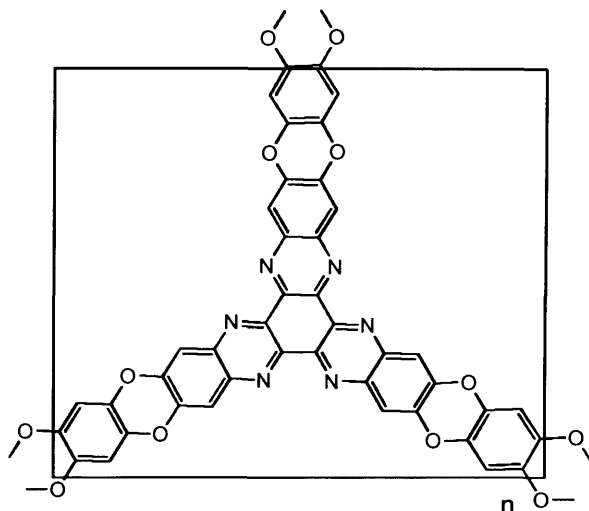
To a stirred solution of 2,3,8,9,14,15-hexafluoro-5,6,11,12,17,18-hexaazatrinaphthylene (0.405 g, 0.82 mmol) and 1,2,4,5-tetrahydroxybenzene (0.175 g, 1.2 mmol) in dry DMF (50 mL) was added anhydrous potassium carbonate (0.8 g, 5.8 mmol) as a fine powder. The reaction mixture was then heated at 70 °C for 48 hours under nitrogen. On cooling, the reaction mixture was poured into stirred aqueous HCl (1%, 100 mL); the resulting precipitate was filtered and washed with water and methanol then purified by refluxing in DMAc, THF, acetone and methanol respectively. The product was ground into a fine powder and dried in a vacuum oven at 120 °C for 24 hours to give a black powder. Yield: 0.449 g (93 %); elemental analysis calc (%) for $C_{33}H_9N_6O_6$: C, 67.63; H, 1.54; N, 14.34; found: C, 60.13; H, 2.20; N, 15.03; IR (film, cm^{-1}): 3043, 1632, 1500, 1468, 1303, 1226, 1143, 1082, 925, 876, 794; surface area (BET): 577 $m^2 g^{-1}$, total pore volume 0.40 mL g^{-1} at (p/p° = 0.98, adsorption); TGA (Nitrogen): Thermal degradation commences at 540 °C.
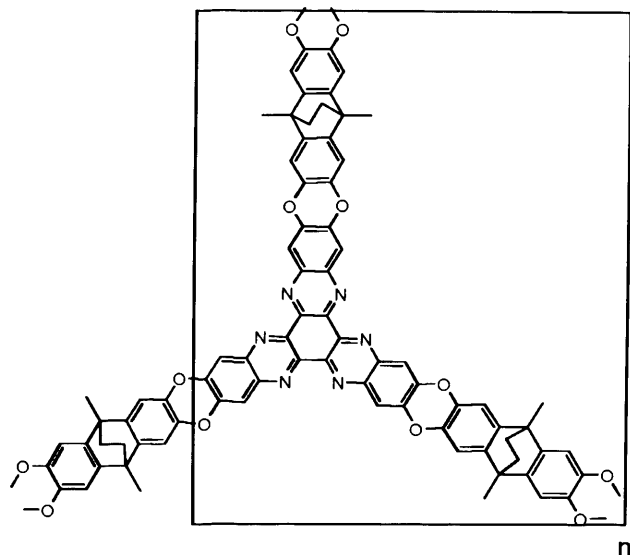
HATN-based network polymer (34)

A mixture of 3,6,7-tetrahydroxy-9,10-dimethyl-9,10-ethanoanthracene[86] (0.233 g, 0.78 mmol) and 2,3,8,9,14,15-hexafluoro-5,6,11,12,17,18-hexaazatrinaphthylene (0.255 g, 0.52 mmol) in DMF (30 mL) was stirred in a Schlenk tube under nitrogen at 70 °C for 0.5 hour, then a fine powder of potassium carbonate (0.55 g, 3.98 mmol) was added at once. The reaction left stirring at same temperature for 48 hours then poured into water (100 mL) and acidified with 2 N HCl. The resulting precipitate was filtered and washed with water and methanol then purified by refluxing in DMAc, THF, acetone and methanol respectively. The product was ground into a fine powder and dried in a vacuum oven at 120 °C for 24 hours to give an orange powder. Yield: 0.382 g (90 %); elemental analysis calc (%) for $C_{51}H_{27}N_6O_6$: C, 74.72; H, 3.30; N, 10.26. Found: C, 66.78; H, 3.66; N, 9.29; IR (KBr, cm^{-1}): 2962, 2925, 2856, 1609, 1455, 1376, 1316, 1268, 1243, 1207; surface area (BET): 969 m^2 g^{-1}, total pore volume 0.64 mL g^{-1} at (p/p° = 0.98, adsorption); TGA (Nitrogen): Thermal degradation commences at 480 °C.
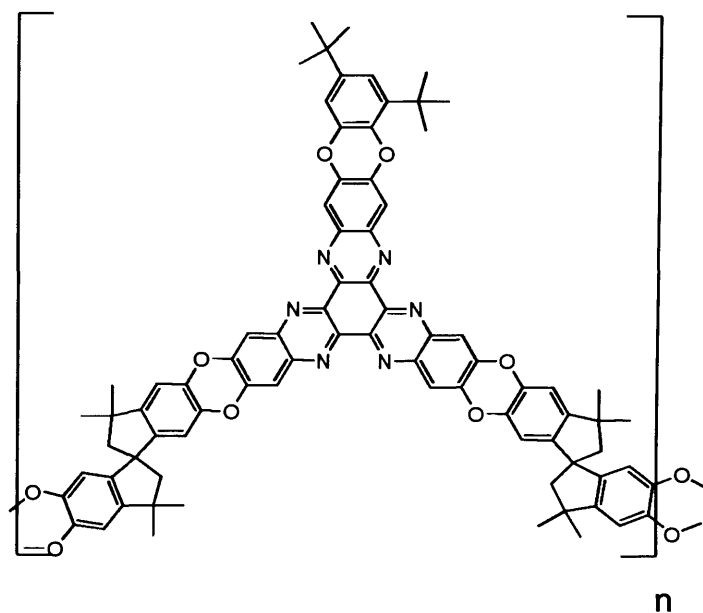
HATN-based ladder polymer (35)

A mixture of **(29)** (0.47 g, 0.7 mmol) and 5,5',6,6'-tetrahydroxy-3,3,3',3'-tetramethyl-1,1'-spirobisindane (0.237 g, 0.7 mmol) in anhydrous DMF (60 mL) was stirred in 100 mL round bottom flask under nitrogen at 70 °C for 0.5 hour, then a fine powder of potassium carbonate (0.58 g, 4 mmol) was added. The reaction left stirring at same temperature for 48 hours then poured into water (100 mL) and acidified with 2 N HCl. The resulting precipitate was filtered and washed with water and methanol then purified by refluxing in DMAc, THF, acetone and methanol respectively. The product was ground into a fine powder and dried in a vacuum oven at 120 °C for 24 hours to give an orange powder. Yield: 0.608 g, 93 %; elemental analysis calc (%) for $C_{59}H_{46}N_6O_6$: C, 75.72; H, 4.91; N, 8.98; found: C, 64.11; H, 5.37; N, 7.10; IR (KBr, cm^{-1}): 2950, 2862, 1609, 1471, 1438, 1414, 1362, 1310, 1236, 1078, 979, 869, 809; surface area (BET): 756 m^2 g^{-1}, total pore volume 0.86 mL g^{-1} at (p/p° = 0.98, adsorption); TGA (Nitrogen): Thermal degradation commences at 415 °C.
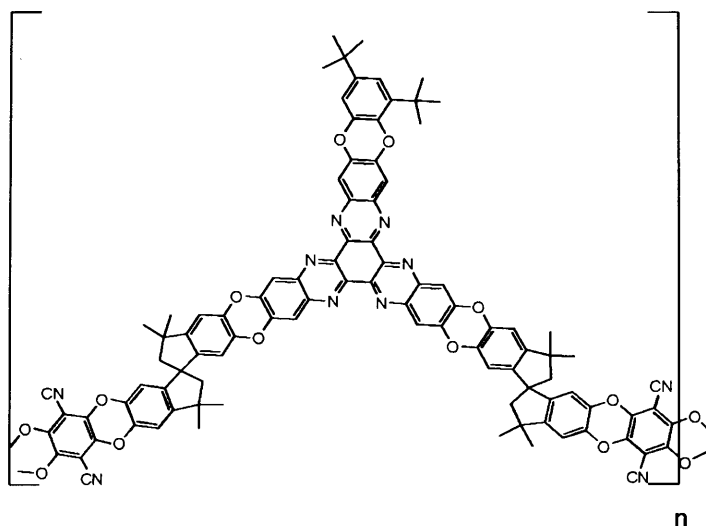
HATN-based copolymer (36)

General procedure for synthesis: to a mixture of 5,5',6,6'-tetrahydroxy-3,3,3',3'-tetramethyl-1,1'-spirobisindane, 2,3,5,6-tetrafluoroterephthalonitrile and HATn(F)$_4$ **(29)** stirred in anhydrous DMF (70 mL) under nitrogen at 70 °C, was added an excess of anhydrous potassium carbonate and the mixture left stirring for 48 hours at the same temperature. On cooling, the reaction mixture was poured into 150 mL of stirred acidified water and the precipitate collected by suction filtration, washed with water and methanol. Purification was achieved by dissolving the product in CHCl$_3$ (15 mL) then reprecipitating it by slow dropping into stirred methanol (250 mL). The product was collected by filtration and dried in vacuum oven at 120 °C for 24 hours. The table below shows the exact amount of monomers used.

Polymer	(29) %	(29) Weight (g)	2,3,5,6-tetrafluoro-terephthalonitrile weight (g)	Catechol weight (g)	Yield (g) (%)
36a	0.5	0.0143	0.419	0.721	0.88 (90)
36b	1.0	0.0278	0.4035	0.700	0.90 (93)
36c	2.5	0.0646	0.364	0.652	0.83 (91)
36d	10	0.2365	0.2807	0.5965	0.81 (85)

GPC (CHCl$_3$) **36a**: Mw: 154x10^3 g mol^{-1}, Mn: 79300; **36b**: Mw: 168x10^3 g mol^{-1}, Mn: 52900; **36c**: Mw: 231x10^3 g mol^{-1}, Mn: 67540; **36d**: Mw: 106x10^3 g mol^{-1}, Mn: 21990 relative to polystyrene. ^{1}H NMR (400 MHz; CDCl$_3$) δ (ppm): **36d**: 1.2-1.34 (b), 1.44-1.53 (b), 1.97-2.1 (b), 2.15-2.34 (b), 6.24-6.47 (b), 6.65-6.79 (b), 7.74-7.98 (b).

Dihydronaphthalene-1,4-endoxide tetramer (38)
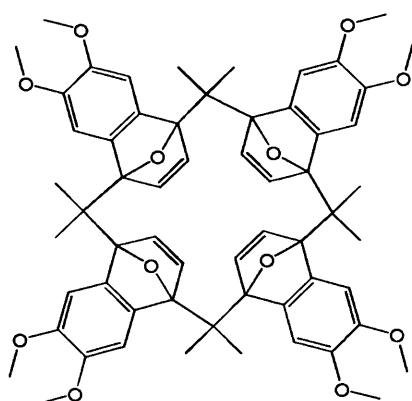
A solution of furan-acetone anhydro-tetramer **(37)**[90] (2.3 g, 5.32 mmol) and 4,5-dimethoxy benzenediazonium carboxylate hydrochloride (5.6 g, 22.9 mmol) in 200 mL of 1,2-dichloroethane containing, 20 mL of propylene oxide, was heated under reflux with stirring for 12 hours. The mixture was concentrated under reduced pressure and the remaining oil was chromatographed over silica gel using chloroform as eluent to give a pale red powder. Yield: 1.66 g (32%); Mp > 300 °C (decomposition); ^{1}H NMR (400 MHz; CDCl$_3$) δ (ppm): 1.73 (s, 24H), 3.84 (s, 24H), 6.57 (s, 8H), 7.07 (s, 8H); ^{13}C NMR (100 MHz; CDCl$_3$) δ (ppm): 22.1, 37.9, 57.1, 97.9, 108.9, 142.4, 144.6, 147.7; HRMS, m/z, (EI): 976.4405 [M$^+$], calc: 976.44.

Hydroxy-dihydronaphthalene-1,4-endoxide tetramer (39)
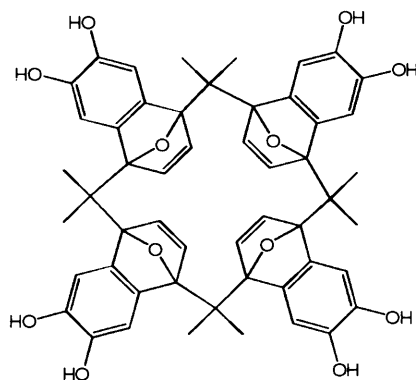
In 100 mL two-necked round bottom flask, compound (38) (1.15 g, 1.17 mmol) was dissolved in dry dichloromethane (45 mL). Under cooling in an ice bath, boron tribromide (1.4 mL, 14.1 mmol) was added dropwise; the reaction mixture was stirred for 16 hours at room temperature then poured into water (100 mL) and stirred for another 0.5 hour. After filtration, the precipitate washed with water then dried in vacuum oven at 60 °C for 24 hours to give a dark green powder. Yield: 0.92 g (91%); Mp > 300 °C (decomposition); ^{1}H NMR (400 MHz; Acetone-d$_6$) δ (ppm): 1.76 (s, 24H), 6.59 (s, 8H), 7.30 (s, 8H), 8.18 (b, 8H); ^{13}C NMR (100 MHz; Acetone-d$_6$) δ (ppm): 21.3, 38.1, 97.9, 109.5, 141.7, 145.1, 149.1; LRMS, *m/z*, (CI): 864. 5 [M$^+$].

Polymer (40)
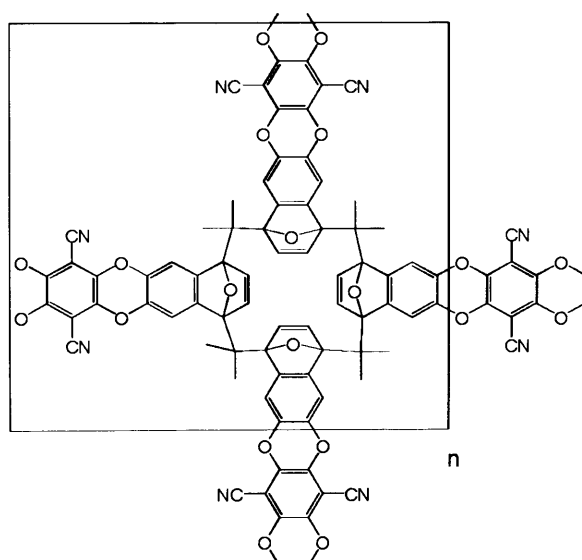
To a stirred mixture of **(39)** (0.624 g, 0.72 mmol) and 2,3,5,6-tetrafluoroterephthalonitrile (0.288 g, 0.88 mmol) in dry DMF (50 mL) was added a fine powder of anhydrous potassium carbonate (1.1 g, 7.97 mmol) under nitrogen atmosphere, the reaction was stirred at 70 °C for 24 hours then poured into water (100 mL) and acidified with 2 N HCl. The resulting precipitate was filtered and washed with water and methanol then purified by refluxing in DMAc, THF, acetone and methanol respectively. The product was ground into a fine powder and dried in a vacuum oven at 120 °C for 24 hours to give a dark yellow powder. Yield: 0.764 g (96%); elemental analysis calc (%) for $C_{68}H_{40}N_4O_{12}$: C, 73.9, H, 3.65; N, 5.07; found: C, 63.58, 3.24, 5.12; IR (KBr, cm^{-1}): 2956, 2239, 1699, 1615, 1515, 1446, 1273, 1012, 879; surface area (BET): 754 m^2 g^{-1}, total pore volume 0.43 mL g^{-1} at (p/p° = 0.98, adsorption); TGA (Nitrogen): Thermal degradation commences at 390 °C.

Polymer (41)
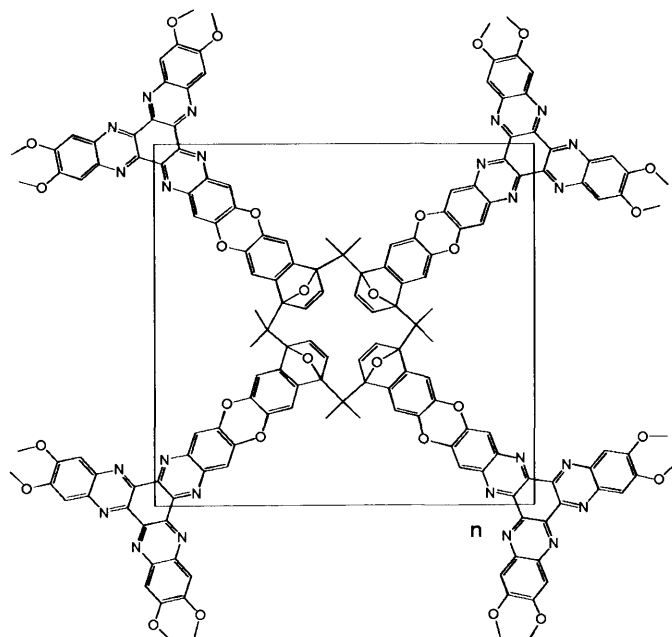
To a stirred mixture of **(39)** (0.410 g, 0.47 mmol) and 2,3,8,9,14,15-hexafluoro-5,6,11,12,17,18-hexaazatrinaphthylene (0.311g, 0.63 mmol) in dry DMF (45 mL) was added a fine powder of anhydrous potassium carbonate (0.65 g, 4.7 mmol) under

nitrogen atmosphere. The mixture was stirred at 70 °C for 24 hours then poured into acidified water (100 mL); the resulting precipitate was filtered and washed with water and methanol. Purification was achieved by refluxing the product in DMAc, THF and methanol respectively. The product was ground into a fine powder and dried in a vacuum oven at 120 °C for 24 hours to give a brown powder. Yield: 0.58 g (90%); elemental analysis calc (%) for $C_{84}H_{48}N_8O_{12}$: C, 74.11; H, 3.53; N, 8.23; Found: C, 65.34; H, 3.40; N, 8.83; IR (KBr, cm^{-1}): 2952, 1703, 1617, 1465, 1304,1259, 1217, 1080, 870; surface area (BET): 720 m^2 g^{-1}, total pore volume 0.53 mL g^{-1} at (p/p° = 0.98, adsorption); TGA (Nitrogen): Thermal degradation commences at 360 °C.

Polymer (42)
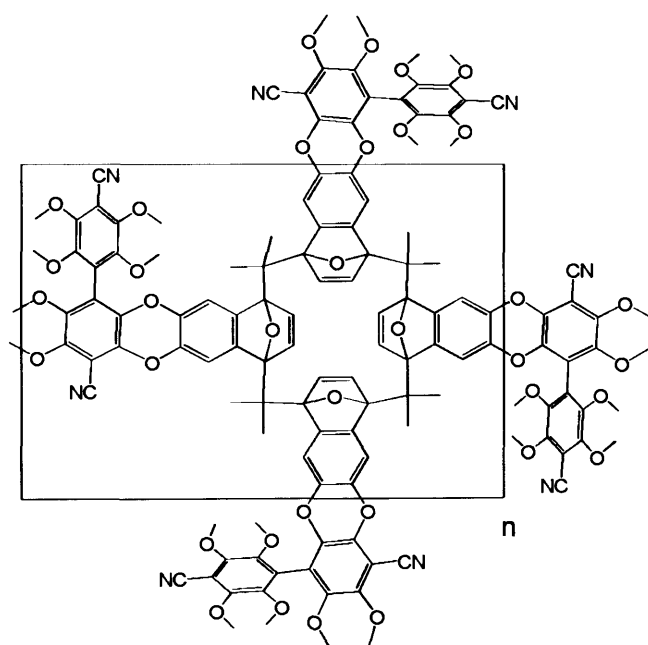
To a stirred mixture of **(39)** (0.457 g, 0.53 mmol) and 2,2',3,3',5,5',6,6'-octafluoro-4,4'-dicarbonitrile-biphenyl (0.184 g, 0.53 mmol) in DMF (40 mL) was added a fine powder of anhydrous potassium carbonate (0.75 g, 5.4 mmol) under nitrogen atmosphere. The mixture was stirred at 70 °C for 24 hours then poured into acidified water (100 mL); the resulting precipitate was filtered and washed with water and methanol. Purification was achieved by refluxing the product in DMAc, THF and methanol respectively. The product was ground into a fine powder and dried in a vacuum oven at 120 °C for 24 hours to give a brown powder. Yield: 0.493 g (88 %);

elemental analysis calc (%) for $C_{66}H_{42}N_2O_{12}$: C, 75.07; H, 3.98; N, 2.65; found: C, 66.97; H, 4.79; N, 3.68; IR (KBr, cm^{-1}): 2954, 2862, 2237, 1700, 1609, 1418, 1256, 1154,1005, 879; surface area (BET): 703 m^2 g^{-1}, total pore volume 0.40 mL g^{-1} at (p/p° = 0.98, adsorption); TGA (Nitrogen): Thermal degradation commences at 370 °C.
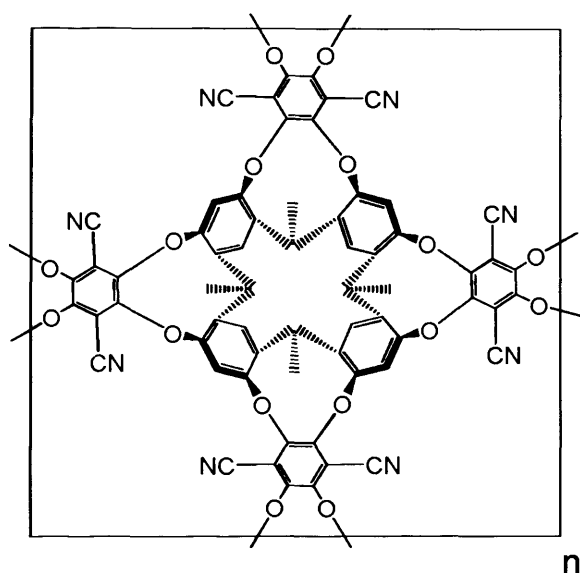
Polymer (43)

n

To a stirred mixture of resorcinarene C_{4V}[93] (0.374 g, 0.68 mmol) and 2,3,5,6-tetrafluoroterephthalonitrile (0.275 g, 1.37 mmol) in DMF (50 mL) was added a fine powder of anhydrous potassium carbonate (1.0 g, 7.24 mmol) under nitrogen atmosphere. The mixture was stirred at 70 °C for 24 hours then poured into acidified water (100 mL); the resulting precipitate was filtered and washed with water and methanol. Purification was achieved by refluxing the product in DMAc, THF and methanol respectively. The product was ground into a fine powder and dried in a vacuum oven at 120 °C for 24 hours to give an orange powder. Yield: (0.491 g (91.1 %); elemental analysis calc (%) for $C_{48}H_{24}N_4O_8$: C, 73.39; H, 3.06; N, 7.14; found: C, 65.84; H, 3.07; N, 7.83; IR (KBr, cm^{-1}): 2971, 2237, 1703, 1615, 1455, 1293, 1238, 1148, 1091, 1034, 1002, 895, 820; surface area (BET): 1032 m^2 g^{-1}, total pore volume 0.55 mL g^{-1} at (p/p° = 0.98, adsorption); TGA (Nitrogen): Thermal degradation commences at 420 °C.

Polymer (44)
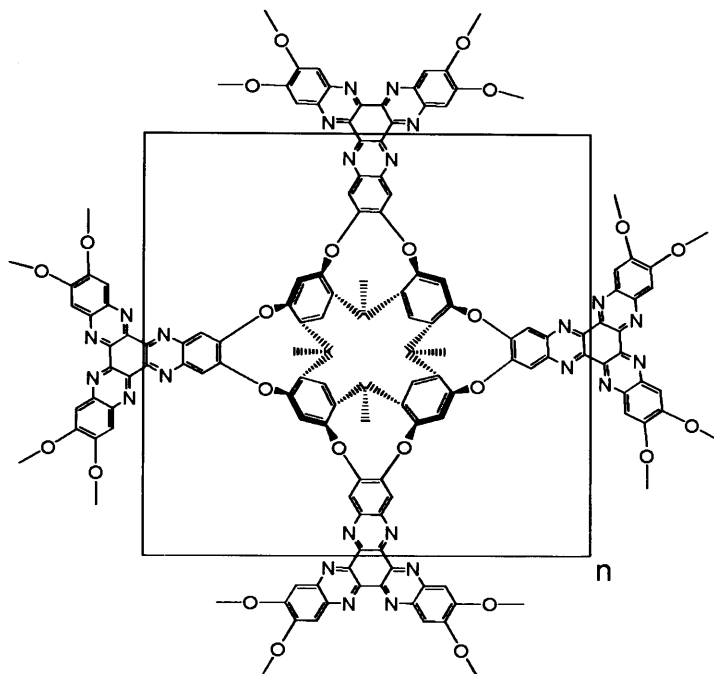
To a stirred mixture of resorcinarene C_{4v}[93] (0.305 g, 0.56 mmol) and 2,3,8,9,14,15-hexafluoro-5,6,11,12,17,18- hexaazatrinapthylene (0.368 g, 0.74 mmol) in DMF (50 mL) was added a fine powder of anhydrous potassium carbonate (1.0 g, 7.24 mmol) under nitrogen atmosphere, the mixture was stirred at 70 °C for 24 hours then poured into acidified water (100 mL), the resulting precipitate was filtered and washed with water and methanol. Purification was achieved by refluxing the product in DMAc, THF and methanol respectively. The product was ground into a fine powder and dried in a vacuum oven at 120 °C for 24 hours to give off-brown powder. Yield: 0.486 g (83.3 %); ; elemental analysis calc (%) for $C_{64}H_{32}N_8O_8$: C, 73.77; H, 3.07; N, 10.75; found: C, 64.74; H, 3.46; N, 11.19; IR (KBr, cm^{-1}): 2970, 1616, 1475, 1300, 1225, 1138, 1082, 1025, 987, 872; surface area (BET): 1059 m^2 g^{-1}, total pore volume 0.59 mL g^{-1} at (p/p° = 0.98, adsorption); TGA (Nitrogen): Thermal degradation commences at 410 °C.

14,15-Dicyano-9,10-di-ehtyl-2,3,6,7-tetramethoxy-9,10-[1',2']benzenoanthracene (45)
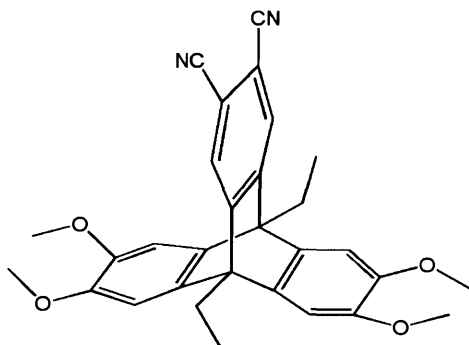
A mixture of 14,15-dibromo-9,10-diethyl-2,3,6,7-tetramethoxytriptycene (1.2 g, 2.04 mmol) and copper cyanide (3.73 g, 41.6 mmol) in dry DMF (40 mL) was refluxed for 6 hours. After cooling to room temperature, the reaction mixture was poured into concentrated ammonia (300 mL) and stirred for 2 hours. The resulting precipitate was filtered and dissolved in chloroform (15 mL) then chromatographed over silica gel using DCM as eluent to give a pale yellow powder. Yield: 0.67 g, 1.35 mmol (69 %); Mp: 128-132 °C (decomposition); ^{1}H NMR (400 MHz; CDCl$_3$) δ (ppm): 1.53 (t, 6H, J= 7.2, 7.2 Hz), 2.79 (q, 4H, J= 7.2, 7.2 Hz), 3.66 (s, 12H), 6.81 (s, 4H), 7.46 (b, 2H); ^{13}C NMR (100 MHz, CDCl3) δ (ppm): 11.29, 20.05, 53.91, 56.73, 108.21, 112.48, 116.41, 146.62, 150.02; LRMS, m/z, (EI): 480.2 [M]$^+$.

Phthalocyanine (46)
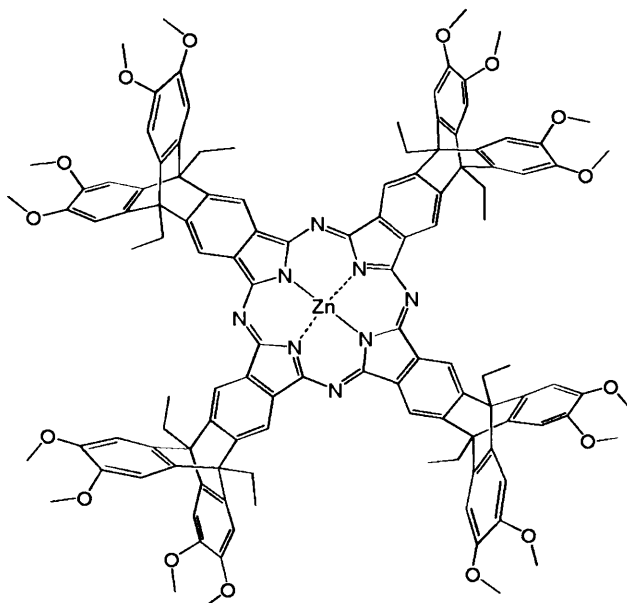
A mixture of 14,15-dicyano-9,10-diethyl-2,3,6,7-tetramethoxytriptycene (0.98g, 2.04 mmol) and zinc(II) acetate (0.52g, 2.84mmol) were refluxed in DMAc (30 mL) for 48 hours. After cooling, the mixture quenched with water (50 mL) and extracted with chloroform. The organic solvent removed and the green preciptate was purified by passing through a short column of silica using chloroform as an eluent to give a green powder. Yield: 0.82 g, 0.41 mmol (81%); Mp >300 °C; ^{1}H NMR (400 MHz; CDCl$_3$) δ (ppm): 1.67 (t, 24H, J= 7.2 Hz), 2.95 (q, 16H, J= 7.2 Hz), 3.77 (s, 48H), 6.94 (b, 16H), 7.67 (b, 8H); ^{13}C NMR (100 MHz, CDCl3) δ (ppm): 12.03, 21.23, 54.52, 56.8, 135.98, 146.2, 154.1; UV/vis (DCM): λ_{max} 685, 615, 348, 296, 229 nm; MS(*MALDI-TOF*): cluster centered at *m/z* 1987, calc: 1987 g mol^{-1}.

Phthalocyanine (47)
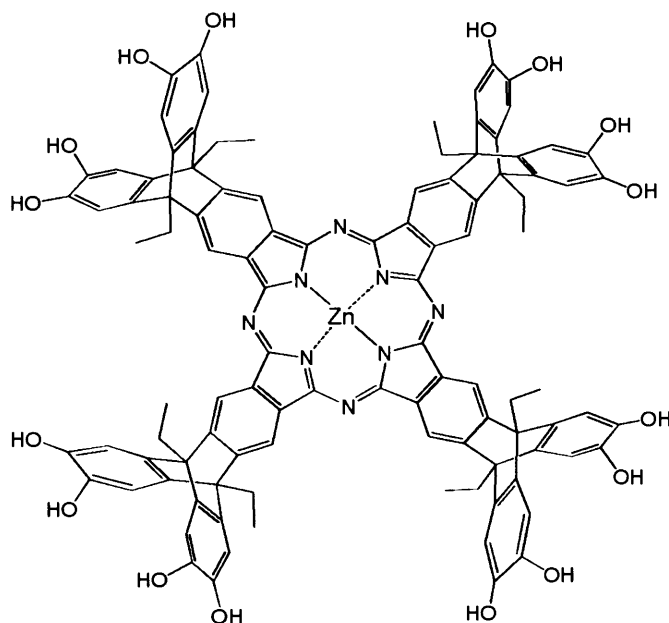
In a 100 mL two-necked round bottom flask, compound **(40)** (0.7 g, 0.35 mmol, 1.00 eq.) was dissolved in dry dichloromethane (40 mL). Upon cooling in an ice bath, boron tribromide (1.41 mL, 5.64 mmol, 16 eq.) was added dropwise and the reaction

mixture was stirred for 24 hours at room temperature. The mixture was poured into water (50 mL) and stirred for another 0.5 hour. After filtration, the precipitate was washed with water then recrystallised from a mixture of methanol/chloroform to give a green powder. Yield: 0.53 g, 2.95 mmol (86 %); Mp >300 °C (decomposition); ^{1}H NMR (400 MHz; DMSO-d$_6$) δ (ppm): 1.68 (t, 24H, J= 7.2, 7.2 Hz), 2.91 (q, 16H, J= 7.2, 7.2 Hz), 6.93 (b, 16H), 7.68 (b, 8H); UV/vis (MeOH): λ_{max} 684, 617, 359, 313, 225 nm; MS(*MALDI-TOF*): cluster cantered at *m/z*: 1764, calc: 1763 g mol^{-1}.

Phthalocyanine-based network polymer (48)
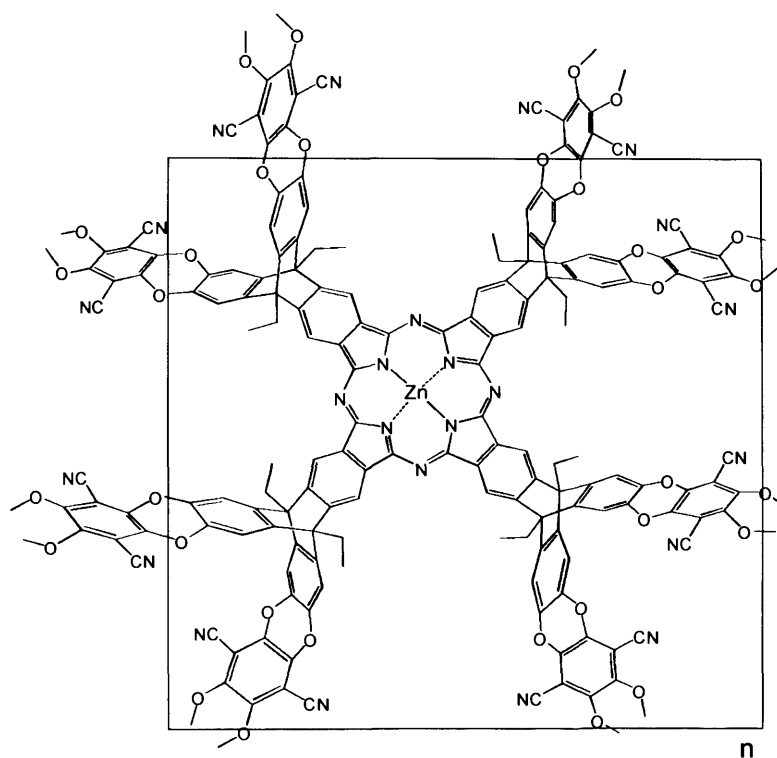
To a stirred mixture of compound **(47)** (0.4341 g, 0.246 mmol) and 2,3,5,6-tetrafluoroterephthalonitrile (0.1970 g, 0.984 mmol) in anhydrous DMF (50 mL) was added a fine powder of anhydrous potassium carbonate (0.68 g, 4.92 mmol) in one portion. The reaction mixture was then heated at 80 °C in an oil bath under nitrogen for 48 hours. On cooling, the reaction mixture was poured into 100 mL of stirred acidified water; the resulting precipitate was collected by suction filtration then washed with water and methanol. Purification was achieved by refluxing the product in DMAc, THF, acetone, and methanol respectively. The product was ground into a

fine powder and dried in a vacuum oven at 120 °C for 24 hours to give a deep green powder. Yield: 0.514 g (93%); elemental analysis calc (%) for $C_{136}H_{64}N_{16}O_{16}Zn$: C, 72.81; H, 2.90; N, 9.98; Found: C, 71.08; H, 5.83; N, 4.78; IR (KBr, cm^{-1}): 2883, 2240, 1768, 1725, 1601, 1441, 1355, 1268, 1156, 1010, 868, 744; surface area (BET): 806 $m^2 g^{-1}$, total pore volume 0.403 mL g^{-1} at (p/p° = 0.98, adsorption); TGA (Nitrogen): Thermal degradation commences at 450 °C.

Polytriptycene (50)
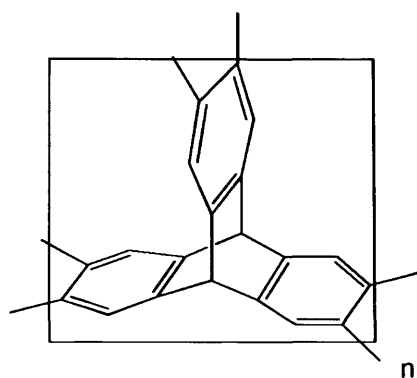
Bis(2,5-cyclooctadiene)nickel(0) (1.5 g, 5.45 mmol) was added in one portion to a stirred mixture of 2,3,6,7,14,15-hexabromotriptycene[95] (0.66 g, 0.908 mmol), 2,2'-dipyridyl (0.85 g, 5.5 mmol), 1,5-cyclooctadiene (0.58g, 5.5 mmol) and dry DMF (6 mL) in Schlenk tube under nitrogen. The solution was stirred for 48 hours at 100 °C under nitrogen then poured into a warm aqueous solution of ethylenediamine-tetraacetic acid (1 N, 150 mL). The resulting precipitate was filtered and washed with NaOH solution (10%; w/v), water and acetone. Purification was achieved by refluxing the product in DMF, THF and methanol respectively. The product was then ground and dried in vacuum oven at 140 °C for 24 hours to give a pale yellow powder (0.214 g, 95%); elemental analysis calc (%) for $C_{20}H_8$: C, 96.75; H, 3.25; N, 0.00; Found: C, 92.85; H, 4.06; N, 0.48; IR (KBr, cm^{-1}): 3020, 2955, 2863, 1700, 1607, 1461, 1184, 885, 829; surface area (BET): 1063 $m^2 g^{-1}$, total pore volume: 0.735 mL g^{-1} at (p/p° = 0.98) adsorption; TGA (Nitrogen): Thermal degradation commences at 420 °C.

Tris(4-bromophenyl)methane (51)
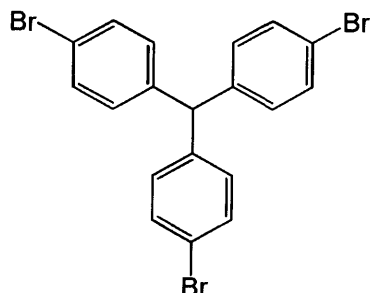
To a stirred solution of triphenylmethane (1.7 g, 6.96 mmol) and FeBr$_3$ (90 mg) in DCM (30 mL) was added a solution of bromine (1.1 mL, 21.4 mmol) in DCM (50 mL) dropwise over 0.5 hour at 0 °C, the mixture left stirring overnight and quenched with saturated solution of sodium thiosulfate. The organic layer was extracted and dried over MgSO$_4$, the solvents then were reduced under vacuum and the resulting oil was purified by short column using DCM as an eluent to give yellow oil. Yield: 2.07 g, 4.31 mmol (62 %); ^{1}HNMR (400 MHz; CDCl$_3$) δ (ppm): 5.43 (s, 1H), 6.95 (d, 6H, J= 8.4 Hz), 7.44 (d, 6H, J= 8.4 Hz); ^{13}C NMR (100 MHz; CDCl$_3$) δ (ppm): 55.45, 121.21, 131.36, 133.72, 142.16. HRMS, m/z, (EI): 477.8554 [M$^+$], calulated for C$_{19}$ H$_{13}$ ^{79}Br$_3$: 477.8567.

Triphenyl-methane polymer (52)
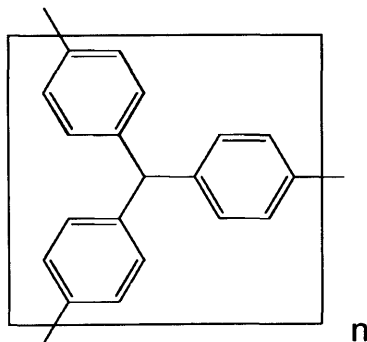
Bis(1,5-cyclooctadiene)nickel(0) (2 g, 7.27 mmol) was added in one portion to the stirred mixture of tris(4-bromophenyl)methane (1.16 g, 2.42 mmol), 2,2'-bipyridyl (1.14 g, 7.27 mmol), 1,5-cyclooctadiene (0.78 g, 7.32 mmol) and dry DMF (7 mL) in

a Schlenk tube at room temperature. The solution was stirred for 48 hours at 100 °C under nitrogen then poured into a warm aqueous solution of ethylenediamine-tetraacetic acid (1 N, 150 mL). The resulting precipitate was filtered and washed with NaOH solution (10% w/v), water and acetone. Purification was achieved by refluxing the product in DMF, THF and methanol respectively. The product was then ground and dried in vacuum oven at 140 °C for 24 hours to give an off-white powder. Yield: 0.511 g (88%); elemental analysis calc (%) for $C_{19}H_{13}$: C, 94.57; H, 5.43; N, 0.00; found: C, 89.11; H, 5.57; N, 0.56; IR (KBr, cm^{-1}): 3022, 2920, 1602, 1493, 1447, 1261, 1113, 1005; surface area (BET): 595 $m^2 g^{-1}$, total pore volume: 0.354 mL g^{-1}. TGA (Nitrogen): Thermal degradation commences at 550 °C.

1,3,6,8-Tetrabromopyrene (53)
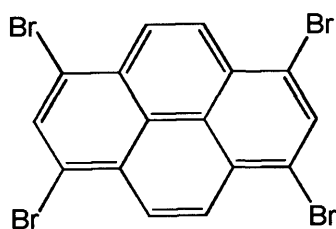
Bromine (1.5 mL, 29.7 mmol) was added dropwise to a stirred solution of pyrene (1.0 g, 4.95 mmol) in nitrobenzene (40 mL), a catalytic amount of $FeCl_3$ (20 mg) was added then the reaction was refluxed for 12 hours. Upon cooling, the resulting suspension was poured into methanol (100 mL) and the precipitate filtered using suction filtration and washed with methanol then dried in an oven at 120 °C to give pale green powder (2.48 g, 96%); Mp: >300 °C; elemental analysis calc (%) for $C_{16}H_6Br_4$: C, 37.11; H, 1.17; Br, 61.72; found: C, 37.24; H, 1.12; Br, 61.71; LRMS, m/z, (EI): 517.9 [M^+].

Polypyrene (54)

Bis(cyclooctadiene)nickel(0) (2 g, 7.27 mmol) was added in one portion to a mixture of 1,3,6,8-tetrabromopyrene (0.625 g, 1.21 mmol), 2,2'-bipyridine (1.14 g, 7.27 mmol), 1,5-cyclooctadie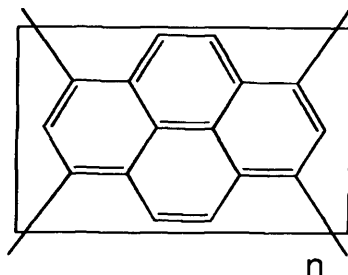ne (0.78 g, 7.32 mmol) and dry DMF (7 mL) in a Schlenk tube under nitrogen at room temperature. The solution was stirred for 72 hours at 100 °C under nitrogen then poured into a warm aqueous solution of ethylenediamine-tetraacetic acid (1 N, 150 mL). The resulting precipitate was filtered and washed with NaOH (10% w/v) solution, water and acetone. Purification was achieved by refluxing the product in DMF, THF and methanol respectively. The product was then ground into a fine powder and dried in a vacuum oven at 140 °C for 24 hours to give an orange powder. Yield: 0.22 g (92%); elemental analysis calc (%) for $C_{16}H_6$: C, 96.95; H, 3.05; Found: C, 92.66; H, 4.26; N, 0.28; IR (KBr, cm^{-1}): 3032, 1598, 1490, 1457, 845, 815; surface area (BET): 969 m^{2}g^{-1}, total pore volume: 0.68 mL g^{-1} at (p/p° = 0.98, adsorption). TGA (Nitrogen): Thermal degradation commences at 395 °C.

2,3,6,7,10,11-Hexabromotriphenylene (55)
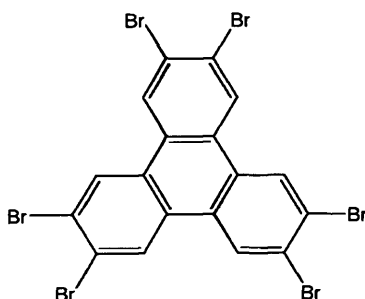
Triphenylene (1 g, 4.38 mmol) and FeCl₃ (100 mg) were stirred in nitrobenzene (25 mL) at 100 °C for 1 hour then bromine (2.3 mL, 44.84 mmol) was added dropwise over 0.5 hour. The reaction was heated under reflux for 12 hours then cooled to RT and poured into acetone (70 mL). The resulting precipitate was isolated using suction filtration and washed with acetone and methanol then dried in an oven at 100 °C to give a pale grey powder. Yield: 2.49 g, (80.2%); Mp: >300 °C; elemental analysis calc (%) for $C_{18}H_6Br_6$: C, 30.81; H, 0.86; Br, 68.33; found: C, 30.53; H, 0.87; N, 0.00; Br, 67.57; HRMS, m/z, (EI): 701.5520 [M⁺], caluated for 18C 6H 3 ^{79}Br 3 ^{81}Br: 701.5508.

Polytriphenylene (56)
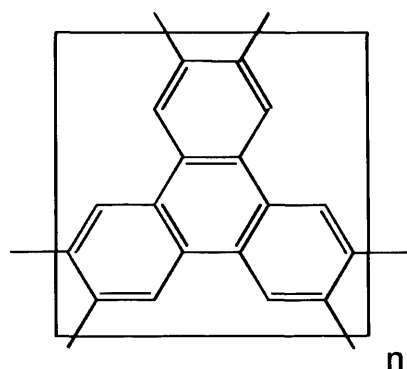
Bis(cyclooctadiene)nickel(0) (2 g, 7.27 mmol) was added in one portion to a stirred mixture of 2,3,6,7,10,11-hexabromo-triphenylene (0.85 g, 1.21 mmol) , 2,2'-bipyridine (1.14 g, 7.27 mmol), 1,5-cyclooctadiene (0.785 g, 7.27 mmol) and dry DMF (9 mL) in Schlenk tube under nitrogen. The solution was stirred for 72 hours at 100 °C under nitrogen then poured into a warm aqueous solution of ethylenediamine-tetraacetic acid (1 N, 150 mL); the precipitate was filtered and washed with %10 NaOH solution, water and acetone. Purification was achieved by refluxing the product in DMF, THF and methanol respectively. The product was then ground into a fine powder and dried in vacuum oven at 140 °C for 24 hours to give a yellow powder. Yield: 0.253 g, (94%); elemental analysis calc (%) for $C_{18}H_6$: C, 97.28; H, 2.72; Found: C, 89.79; H, 4.89; N, 0.35; IR (KBr, cm⁻¹): 3042, 2941, 1612, 1481, 1391, 876, 808; surface area (BET): 638 m² g⁻¹, total pore volume 0.47 mL g⁻¹ at (p/p° = 0.98, adsorption); TGA (Nitrogen): Thermal degradation commences at 425 °C.

Polypropellane (57)

n
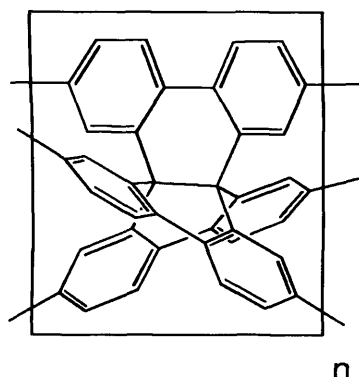
Bis(cyclooctadiene)nickel(0) (1.3 g, 4.27 mmol) was added in one portion to a stirred mixture of hexabromopropellane[100] (0.625 g, 0.66 mmol), 2,2'-bipyridine (0.74 g, 4.27 mmol), 1,5-cyclooctadiene (0.51 g, 4.27 mmol) and dry DMF (6 mL) in a Schlenk tube under nitrogen. The solution was stirred for 48 hours at 100 °C under nitrogen then poured into a warm aqueous solution of ethylenediamine-tetraacetic acid (1 N, 150 mL); the precipitate was filtered and washed with NaOH solution (10% w/v), water and acetone. Purification was achieved by refluxing the product in DMF, THF and methanol respectively. The product was then ground into a fine powder and dried in vacuum oven at 140 °C for 24 hours to give a pale yellow powder. Yield: 0.292 g (94 %); elemental analysis calc (%) for $C_{38}H_{18}$: C, 96.18; H, 3.82; N, 0.00; found: C, 89.08; H, 5.49; N, 1.01; IR (film cm^{-1}): 3052, 2931, 2864, 1683, 1602, 1471, 1446, 1005, 897, 816; surface area (BET): 543 $m^2 g^{-1}$, total pore volume 0.43 mL g^{-1} at (p/p° = 0.98, adsorption); TGA (Nitrogen): Thermal degradation commences at 440 °C.

9. References

1. Rouquerol, J.; Avnir, D.; Fairbridge, C.W.; Everett, D.H.; Haynes, J.M.; Pernicone, N.; Ramsay, J.D.F.; Sing, K.S.W.; Unger, K.K., *Pure & Appl. Chern*, 1994. **66**: p. 1739-1758.
2. Schüth, F.; Sing, K.S.W.; J.Weitkamp, *Handbook of Porous Solids*. Vol.3. 2002, Weinheim: Wiley-VCH: p. 293-295.
3. Broekhoff, J.; Van Dongen, R.H., *Physical and Chemical Aspects of Adsorbents and Catalysts*, Ed. Linsen, B.G. 1970, London: Academic Press.
4. Brunauer, S.; Deming, L.; Deming, W.; Teller, E., *J. Am. Chem. Soc*, 1940. **62**: p. 1723.
5. Sing, K.S.W., *Pure & Appl. Chem*, 1982. **54**: p. 2201-2218.
6. Langmuir, I., *J Am. Chem. Soc*, 1916. **38**: p. 2221-2295.
7. Brunauer, S.; Emmett, P.; Teller., E., *J Am. Chem. Soc*, 1938. **60**: p. 309-319.
8. Livingston, H.K., *J. Colloid. Interface Sci*, 1949. **4**: p. 447-458.
9. Duren, T.; Millange, F.; Ferey, G.; Walton, K.S.; Snurr, R.Q., *J. Phys.Chem*, 2007. **111**: p. 15350-15356.
10. Roberie, T.G.; Hildebrandt, D.; Creighton, J.; Gilson, J.P., *Preparation of Zeolite Catalysts*, in *Zeolites for Clean Technology*, M. Guisnet; J.P. Golson, Eds. 2001, Imperial College Press: London. p. 57-63.
11. Cundy, S.C.; Cox, A.P., *The hydrothermal synthesis of zeolites: Precursors, intermediates and reaction mechanism. Micro. Meso. Mat*, 2005. **82**: p. 1-78.
12. Long, J.R.; Yaghi, O.M., *Chem. Soc. Rev*, 2009. **38**: p. 1213-1214.
13. Eddaoudi, M.; Kim, J.; Rosi, N.; Vodak, D.; Wachter, J.; O'Keeffe, M.; Yaghi, O.M., *Science*, 2002. **295**: p. 469-472.
14. Lin, X.; Jia, J.; Zhao, X.; Thomas, K.M.; Blake, A.J.; Walker, G.S.; Champness, N.R.; Hubberstey, P.; Schroder, M., *Angew. Chem. Int. Ed*, 2006. **45**: p. 7358-7364.
15. Alaerts, L.; Kirschhock, C.E.A.; Maes, M.; Van der Veen, M.A.; Finsey, V.D., A.; Martens, J.A.; Baron, G.V.; Jacobs, P.A.; Denayer, J.F.M.; De Vos, D.E., *Angew. Chem., Int. Ed*, 2007. **46**: p. 4293-4297.
16. Farrusseng, D.; Aguado, S.; Pinel, C., *Angew. Chem., Int. Ed*, 2009. **48**: p. 7502-7513.
17. Horcajada, P.; Serre, C.; Vallet-Regi, M.; Sebban, M.; Taulelle, F.; Fe´rey, G., *Angew. Chem., Int. Ed*, 2006. **45**: p. 5974-5978.
18. Furukawa, H.; Ko, N.; Go, Y.B.; Aratani, N.; Choi, S.B.; Choi, E.; Yazaydin, A.O.; Snurr, R.Q.; O'Keeffe, M.; Kim, J.; Yaghi, O.M., *Science*, 2010. **239** p. 424 - 428.
19. Côté, A.P.; Benin, A.I.; Ockwig, N.W.; Matzger, A.J.; O'Keeffe, M.; Yaghi, O.M., *Science*, 2005. **310**: p. 1166-1170.
20. Smisek, M.; Cerny, S., *Active Carbon Manufacture, Properties and Aplications*. 1970, New York: Elsevier Pub: p. 115-116.
21. Davankov, V.A.; Tsyurupa, M.P., *React. Polym*, 1990. **13**: p. 27-42.
22. Davankov, V.A.; Pastukhov, A.V.; Tsyurupa, M.P., *J. Polym. Sci., Part B: Polym. Phys*, 2000. **38**: p. 1553.

23. Germain, J.; Frechet, J.; Svec, F., *J. Mater. Chem*, 2007. **17**: p. 4989-4997.
24. Germain, J.; Frechet, J.; Svec, F., *Chem. Commun*, 2009. **12**: p. 1526-1528.
25. Budd, P.M.; Makhseed, S.; Ghanem, B.S.; Msayib, K.; Tattershall, C.E.; McKeown, N.B., *Materials Today*, 2004. **7**: p. 40-46.
26. Budd, P.M.; Msayib, K.J.; Tattershall, C.E.; Ghanem, B.S.; Reynolds, K.J.; McKeown, N.B.; Fritsch, D., *Journal of Membrane Science*, 2005. **251**: p. 263-269.
27. Budd, P.M.; Ghanem, B.; Msayib, K.; McKeown, N.B.; Tattershall, C., *A nanoporous network polymer derived from hexaazatrinaphthylene. J. Mater. Chem*, 2003. **13**: p. 2721-2726.
28. Ghanem, B.; Hashem, M.; Harris, K.; Msayib, K.J.; Xu, M.; Budd, P.M.; Chaukura, N.; Book, D.; Tedds, S.; Walton, A.; McKeown, N.B., *Macromolecules*, 2010. **43**: p. 5287-5294.
29. McKeown, N.B.; Gahnem, B.; Msayib, K.J.; Budd, P.M.; Tattershall, C.E.; Mahmood, K.; Tan, S.; Book, D.; Langmi, H.W.; Walton, A., *Angew Chemi. Int Ed*, 2006. **45**: p. 1804–1807.
30. McKeown, N.B.; . *Phthalocyanine Materials*. 1998: Cambridge University Press. 1-3.
31. Leznoff, C.C., *Phthalocyanines: Properties and Applications*, Eds. A.B.P. Lever. Vol. 1-4. 1993: VCH publishers, New York.
32. Norris, D.J., *Phys. Rev. B. Condens. matter*, 1996. **53**: p. 16338-16346.
33. Day, P.N.; Wang, Z.Q.; Pachter, R., *J. Mol. Struct. (Theochem)*, 1998. **33**: p. 455-463.
34. Snow, A.W.; Griffith, J.R.; Marullo, N.P., *Macromolecules*, 1984. **17**: p. 1614-1624.
35. Wohrle, D.; Marose, U.; Knoop, R., *Makromol.Chem*, 1985. **186**: p. 2209-2228.
36. Gürek, A.G.; Bekaroglu, O.J., *Porphyrins Phthalocyanines*, 1997. **1**: p. 67-76.
37. Wörhle, D.; Benters, R.; Suvorova, O.; Schurpfeil, G.; Trombach, N.; Bogdahn-Rai, T., *J. Porphyrins Phthalocyanines*, 2000. **4**: p. 491-497.
38. McKeown, N.B., *J. Mater. Chem*, 2000. **10**: p. 1979-1995.
39. McKeown, N.B.; Makhseed, S.; Budd, P.M., *Chem. Commun*, 2002: p. 2780-2781.
40. Kovacic, P.; Wu, C., *Journal of Polymer Science*, 1960. **47**: p. 45-54.
41. Ohmori, Y.; Uchida, M.; Muro, K.; Yoshino, K., *Jpn. J. Appl. Phys*, 1991. **30**: p. 1941-1943.
42. Leclerc, M.; Diaz, F.M.; Wegner, G., *Macromolecular Chemistry and Physics*. **190**: p. 3105-3116.
43. Yamamoto, T.; Yamamoto, A., *Chem Lett*, 1977: p. 353-354.
44. Miyaura, N.; Suzuki, A., *Chem. Rev*, 1995. **95**(7): p. 2457-2483.
45. Braunsteiner, E.E.; Stille, J.K., *Macromolecules*, 1979. **12**: p. 1033-1038.
46. Jiang, J.X.; Su, F.; Trewin, A.; Wood, C.D.; Campbell, N.L.; Niu, H.; Dickinson, C.; Ganin, A.Y.; Rosseinsky, M.J.; Khimyak, Y.Z.; Cooper, A.I., *Angew. Chem. Int. Ed*, 2007. **46**: p. 8574 -8578.
47. Sonogashira, K.; Tohda, Y.; Hagihara, N., *Tetrahedron Lett*, 1975. **16**: p. 4467-4470.
48. Yamamoto, T., *Synlett*, 2003. **4**: p. 425-450.
49. Yamamoto, T.; Maruyama, J.T.; Zhout, Z.H.; Ito, T.; Fukuda, T.; Yoneda, Y.; Begum, F.; Ikeda, T.; Sasaki, S.; Takezoe, H.; Fukuda, A.; Kubotall, K., *J. Am. Chem. Soc*, 1994. **116**: p. 4832-4845.

50. Schmidt, J.; Werner, M.; Thomas, A., *Macromolecules*, 2009. **42**: p. 4426-4429.

51. Ben, T.; Ren, H.; Ma, S.; Cao, D.; Lan, J.; Jing, X.; Wang, W.; Xu, J.; Deng, F.; Simmons, J.M.; Qiu, S.; Zhu, G., *Angwe Chemi Int Edi*, 2009. **48**(50): p. 9457-9460.

52. Lu, W.; Yuan, D.; Zhao, D.; Schilling, C.I.; Plietzsch, O.; Muller, T.; Brse, S.; Guenther, J.; Blmel, J.; Krishna, R.; Li, Z.; Zhou, H.C., *Chem. Mater*, 2010. **22**: p. 5964-5972.

53. Mulder, M., *Basic Principles of Membrane Technology*. 2nd ed. 1996.

54. Robeson, L.M., *J. Mem. Sci*, 1991. **62**: p. 165-185.

55. Robeson, L.M., *J. Mem. Sci*, 2008. **320**: p. 390- 400.

56. Plate N, Y.s.Y., *Polymeric Gas Separation Membranes*. 1994, Baton Rouge: CRC Press. p. 115-208.

57. Stern, S.A., *J. Mem. Sci*, 1994. **94**: p. 1-65.

58. Hellums, M.W.; Koros, W.J.; Husk, G.R.; Paul, D.R., *J. Mem. Sci*, 1989. **46**: p. 93-112.

59. Phair, J.W.; Badwal, S.P.S., *Science and Technology of Advanced Materials*, 2006. **7**: p. 792-805.

60. Paul, D.; Yampolskii, Y., *Polymeric gas separation membranes.* . 1994: Baton rouge, CRC Press.

61. Fritzsche, A.; Kurz, J., *The separation of gases by membranes*, in *Handbook of industrial membrane technology*. 1990, William Andrew Publishing.

62. Hill, T., *J Chem. Phys*, 1956. **25**: p. 730-745.

63. Lee, K.H, Hwang, S.T., *J Colloid Interf. Sci*, 1986. **110**: p. 544-555.

64. Rhim, H.; Hwang, S. T., *J. Colloid Interf. Sci*, 1975. **52**: p. 174-181.

65. Budd, P.M.; McKeown, N.B.; Fritsch, D., *J. Mater. Chem*, 2005. **15**: p. 1977-1986.

66. Freeman, B.D., *Macromolecules*, 1999. **32**: p. 375 -380.

67. Moore, J.C., *J. Pol. Sci. Part A*, 1964. **2**: p. 835-843.

68. Allcock, H.R.; Lampe, F.W.; Mark, J.E., *Contemporary Polymer Chemistry*. 2003: Pearson Education, Inc.

69. Tant, M.R.; McManus, H.L.N.; Rogers, M.E., in *High-Temperature Properties and Applications of Polymeric Materials*. 1995, ACS Symposium Series. p. 1-20.

70. Daynes, H.A., *Proc. Roy. Soc. Lond*, 1920. Ser.A. **97**: p. 286-307.

71. Barrer, R.M., *Trans. Farad. Soc*, 1939. **35**: p. 628-643.

72. Crank, J., *Methods of measurement*, in *Diffusion in Polymers*, Eds Crank, J., Park, G.S. 1968, Academic Press: New York. p. 1-39.

73. Bartlett, P.D.; Ryan, M.J.; Cohen, S.G., *J. Am. Chem Soc*, 1942. **64**: p. 2649-2653.

74. Long, T.M.; Swager, T.M., *Adv. Mater*, 2001. **13**: p. 601-604.

75. Shi, G.Q.; Schlosser, M., *Tetrahedron*, 1993. **49**: p. 1445-1456.

76. Schlosser, M. H.; Keller, H., *Liebigs Ann*, 1995. **115**: p. 1587-1589.

77. Muellner, F.W.; Bauer, L., *J. Heterocyclic. Chem*, 1982. **20**: p. 1581-1586.

78. Ostaszewski, R., *Tetrahedron*, 1998. **54**: p. 6897-6902.

79. Hart, H.; Hi, C.; Nwokogu, G.; Sbamouilian, S.; Teuerstein, A., *J. Am. Chem. Soc*, 1980. **102**: p. 6649-6651

80. Hart, H.; Raju, N.; Meador, M.A.; Ward, D.L., *J. Org. Chem*, 1983. **48**: p. 4357-4360.

81. Griswold, I.J.; Dahlquist, F.W., *Nature Structural Biology* 2002. **9**: p. 567 - 568.
82. Burgess, C.G.V.; Everett, D.H., *J. Colloid Interface Sci*, 1970. **33** : p. 611-614.
83. Llinitch, O.M.; Fenelonov, V.B.; Lapkin, A.A.; Okkel, L.G.; Zamaraev, K.I., *Micro Meso Mater*, 1999. **31**: p. 97-110.
84. Sabine Laschat, *Synth*, 1999. **3**: p. 475-478.
85. Weider, P.R.; Hegedus, L. S.; Asada, H., *J. Org. Chem*, 1985. **50**: p. 4280-4282.
86. Niederl, J.B.; Nagel, R.H., *J. Am. Chem. Soc*, 1940. **62**: p. 3070-3072.
87. Budd, P.M.; McKeown, N.B.; Ghanem, B.S.; Msayib, K.J.; Fritsch, D.; Starannikova, L.; Belov, N.; Sanfirova, O.; Yampol'skii, Y.P.; Shantarovich, V., *J. Mem. Sci*, 2008. **325**: p. 851-860.
88. Ackman, R.G.; Brown, W.; Wright, G.F., *J. Org. Chem*, 1955. **20**: p. 1147-1158.
89. Diels, O.; Alder, K.J., *Liebigs Ann. Chem*, 1931. **490**: p. 243-257.
90. Beals, R. E; Brown, W. H., *J. Org. Chem*, 1956. **21**: p. 447-448.
91. McOmie, J.F.W.; Watts, M.L.; West, D.E., *Tetrahedron*, 1967. **24**: p. 2289-2292.
92. Hogberg, A.G., *J. Am. Chem. Soc*, 1980. **102**: p. 6046-6050.
93. Tunstad, L.M.; Tucker, J.A.; Dalcanale, E.; Weiser, J.; Bryant, J.A.; Sherman, J.C.; Helgeson, R.C.; Knobler, C.B.; Cram, D.J., *J. Org. Chem*, 1989. **54**: p. 1305-1312.
94. Kantar, C.; Aˇgar, E.; Sasmaz, S., *Dyes and Pigments*, 2008. **77**: p. 487-492.
95. Hilton, C.L.; Jamison, C.R.; Zane, H.K.; King, B.T., *J. Org. Chem*, 2009. **74**: p. 405-407.
96. Riche, P.; Pascard-Billy, C., *Acta Cryst*, 1974. **B30**: p. 1874-1876.
97. Robson, R.. Hoskins, B.F., *J. Am. Chem. Soc*, 1990. **112**: p. 1546-1554.
98. Venkataramana, G.; Sankararaman, S., *Eur. J. Org. Chem*, 2005. **19**: p. 4162-4166.
99. Tanaka Yuuji, S.T., US7183435 (B2), 2007.
100. Debroy, P.; Lindeman, S.V.; Rathore, R., *Org. Lett*, 2007. 9(21): p. 4091-4094.
101. Lee-Ruff, E., *J. Org. Chem*. 1998. **63**: p. 7168-7171.
102. Tsui, N.T.; Paraskos, A.J.; Torun, L.; Swager, T.M.; Thomas, E.L., *Macromolecules*, 2006. **39**: p. 3350-3358.
103. Uchida, M., Chihiro, M., Kanbe, T., *Bull Chem Pharm Bull* (Tokyo), 1989. **37**(6): p. 1517-1523.